DEVELOPMENT OF NOVEL NMR PULSE SEQUENCES

VOLUME 1

PAUL CHRISTOPHER DOUGLAS

Doctor of Philosophy

ASTON UNIVERSITY

September 2003

Aston University

Development of Novel NMR Pulse Sequences

Paul Christopher Douglas

Doctor of Philosophy

September 2003

To elucidate the structures of organic molecules in solution using pulse FT NMR, heteronuclear pulse sequence experiments to probe carbon-13 (^{13}C) and proton (^{1}H) spin systems are invaluable.

The one-dimensional insensitive nucleus detected PENDANT experiment finds popular use for structure determination via one-bond ^{13}C-^{1}H scalar couplings. PENDANT facilitates the desired increase in ^{13}C signal-to-noise ratio, and unlike many other pulse sequence experiments (e.g., refocused INEPT and DEPT), allows the simultaneous detection of ^{13}C quaternary nuclei. The first chapter herein details the characterisation of PENDANT and the successful rectification of spectral anomalies that occur when it is used without proton broadband decoupling.

Multiple-bond (long-range) ^{13}C-^{1}H scalar coupling correlations can yield important bonding information. When the molecule under scrutiny is devoid of proton spectral crowding, and more sensitive 'inverse' pulse sequence experiments are not available, one may use insensitive nucleus detected long-range selective one-dimensional correlation methods, rather than more time consuming and insensitive multidimensional analogues. To this end a novel long-range selective one-dimensional correlation pulse sequence experiment has been invented. Based on PENDANT, the new experiment is shown to rival the popular selective INEPT technique because it can determine the same correlations while simultaneously detecting isolated ^{13}C quaternary nuclei. INEPT cannot facilitate this, potentially leaving other important quaternary nuclei undetected.

The novel sequence has been modified further to yield a second novel experiment that simultaneously yields selective ^{13}C transient nOe data. Consequently, the need to perform the two experiments back-to-back is conveniently removed, and the experimental time reduced.

Finally, the SNARE pulse sequence was further developed. SNARE facilitates the reduction of experimental time by accelerating the relaxation of protons upon which pulse sequences, to which SNARE is appended, relies. It is shown, contrary to the original publication, that relaxation time savings can be derived from negative nOes.

Keywords: PENDANT, Long-range Heteronuclear Scalar Coupling, 1-D Heteronuclear Correlation experiments, Selective Transient nOe, SNARE

Dedicated to my parents Christopher and Sandra, my brother Christopher, my uncle Jeff, my grandfather Stanley, and in loving memory of my grandparents, Ellen, Elizabeth and William.

Acknowledgements

I would like to thank Professor Emeritus John Homer for his continued support, guidance and expertise throughout the research as well as the occasional jaunt on the badminton court. I am indebted to Dr Michael Perry who has provided his considerable expertise in NMR applications, not to mention an amazing array of puns for every conceivable situation! I would like to thank Dr Martin Beevers for his continued support.

Thank you to all the guys at Bruker UK especially Dr Andrew Gibbs and Dr Timothy Horne who have provided me with first-rate training in the use of recently acquired hardware.

My thanks extend to all my friends who have kept me sane (well at least in part) with much needed social outlets. Thanks in particular to Chris and Kath whose recent hospitality has made the completion of this thesis less of a burden.

Finally, thanks to my family who have stood by me all the way.

Table of Contents

Table of Figures

Chapter 1

Chapter 2

Chapter 3

Chapter 4

Table of Contents of Volume 2

Preface

This thesis is concerned with both theoretical and experimental investigations into the development of existing and novel NMR pulse sequences, with particular emphasis on those sequences that involve long-range scalar couplings, and long-range transient nOes between ^{13}C and ^{1}H.

In view of the theoretical implications due to the diversity of topics covered, relevant aspects of fundamental theory are overviewed to provide a readily accessible base for the development of novel ideas and evaluations of existing concepts. This approach, having very little place in theses concerned with analytical uses of NMR, is hopefully justified to provide a 'guide' for readers. In order to make more stimulating reading for those who are well versed with the detailed theory underlying NMR, these overviews are deferred to a set of appendices so as not to cause unnecessary lengthening of the main text. The appendices have been arranged to be as continuous as possible so that one may read the appendices almost as a separate entity. Within the main body of the thesis, including the general introduction, references to the appendices will be made in the normal way so that one may immediately pursue those concepts if so required.

Introduction

This introduction serves to establish the general concepts underlying the work reported in this thesis. Due to the varied nature of the work, each chapter has a separate introduction in which the thrust, context and associated references are given in more detail. This method of reporting has been chosen in an attempt to prevent an overall loss of continuity, which may have occurred had a more traditional detailed introduction been positioned at the beginning of the thesis. Indeed, the traditional introduction is replaced by a corresponding coherent set of appendices to which essential cross-reference is made.

Liquid-state pulse Fourier transform nuclear magnetic resonance spectroscopy (pulse FT NMR) (Appendix A1 and A2) is without doubt one of the most powerful spectroscopic tools available for the confirmation and elucidation of molecular structure in solution.

Modern NMR experiments invariably rely on sequences of pulses (Appendix A1.7) that are arranged with varying degrees of complexity. Pulse sequences, (Appendix A2) as they are generically named, consist of a number of radio frequency (*r.f.*) pulses, sandwiched between fixed or variable delays, which enable the precise manipulation of the nuclear spin system of magnetic nuclei (Appendix A1). It is the very precision of pulse sequence experiments that enable specific properties of the molecule to be probed and aid in structure determination.

Arguably, the most intensive use of pulse NMR experiments is for the confirmation of molecular structure, whereby one sets out to determine chemical changes that have occurred as a result, of for example, synthesis or molecular interactions. Therefore, only a few appropriate pulse NMR experiments will probably need to be used to determine those changes. On the other hand, structure elucidation may necessitate reliance on a much larger array and more complex set of NMR pulse experiments, in order to probe the bonding and conformation of the molecule in detail.

Whether seeking confirmation or detailed structure elucidation, the exact type of pulse sequence experiments employed obviously depends upon the specific questions asked of the molecule. However, excluding studies of chemical exchange, the experiments will generally utilise and investigate one or more of the following properties:

- through-bond interactions, namely scalar couplings (Appendix A3): which can yield

information regarding the bonding structure, proximity of nuclei and molecular geometry.

- Through-space interactions, namely intramolecular dipolar interactions via the nuclear Overhauser effect (nOe) (Appendix A7): Nuclear Overhauser enhancements can yield internuclear distances between coupling dipoles, and so aid in the confirmation of structure and the elucidation of structural conformation.

Arguably, the study of "small" to "medium" molecular weight organic molecules in solution are the most routinely probed by NMR spectroscopy. For these, heteronuclear pulse sequence experiments are invariably performed to investigate the interactions named above between, for example, carbon-13 (^{13}C) and protons (^{1}H). The unique power of NMR spectroscopy, in comparison to other branches of spectroscopy, is that pulse sequence experiments make possible the direct through-bond and through-space dispositional correlations of such nuclei within molecules, provided they mutually exhibit the properties referred to above. This makes it possible to piece together molecular structure more easily. Therefore, strategies are designed to this end, and may involve the analysis of more than one experiment or the analysis of one (and perhaps more) *correlation experiments*.

Heteronuclear correlations in small to medium molecular weight organic molecules may be determined using a number of experimental methods. Of particular importance are multidimensional correlation experiments (Appendix A5.2 and Appendix A8.3), which may be employed to "map" the correlated nuclei in a multidimensional frequency spectrum (AppendixA5). The advantages of, for example, using multidimensional correlation experiments for the correlation of e.g., ^{13}C-^{1}H scalar couplings are:

- heteronuclei, ((insensitive nuclei) and in the case of ^{13}C, also isotopically dilute) often benefit from polarisation transfer (Appendix A8.3 and Appendix A8.3.1) as a result of coherence (polarisation) transfer, which is implicit in many multidimensional experiments probing scalar couplings.
- Correlations are determined simultaneously and from one experiment.
- ^{1}H chemical shifts (Appendix A3) of those crowded spectral regions are separated as a function of the chemical shift of the correlated heteronucleus, therefore, facilitating easier analysis of crowded spectral regions.

However, the disadvantages of multidimensional experiments utilising direct detection of the

heteronucleus are:

- lack of sensitivity, even though the insensitive heteronucleus benefits from polarisation transfer.
- High concentrations of the molecule under scrutiny are required.
- Long experimental times as a consequence of:
    - the generally large number of transients that are required in order to achieve an adequate signal-to-noise ratio (Appendix A2) and complete the phase cycle.

Despite the considerable value of multidimensional experiments, one-dimensional experiments, such as PENDANT, INEPT (Appendix A8.3) and DEPT, can also be extremely valuable for nuclear positional correlations.

As a result of the relatively recent advent of so-called 'inverse' spectroscopy, it is now possible to perform correlation experiments that yield information comparable to that derived from multidimensional experiments, by the detection of the more sensitive ^{1}H. Consequently, experiment times for a given signal-to-noise ratio are greatly reduced in comparison to heteronuclear detected analogues. Indeed, many one-dimensional (1-D) heteronuclear detected experiments like e.g., PENDANT, INEPT and DEPT, which are often routinely employed regardless of the structural problem, will no doubt inevitably be replaced by analogous inverse correlation experiments.

Unfortunately, inverse experiments are not always available to NMR users as they require specialist hardware, which may also include special NMR probes to obtain optimum sensitivity. Consequently, some researchers may be limited to experiments that employ direct detection of the heteronucleus for the elucidation and confirmation of molecular structure. In this case, to address the inherent disadvantages of heteronuclear detected multidimensional correlation experiments mentioned above, these workers may have no alternative but to turn to 1-D experiments to deduce the required correlations.

For example, in the simplest way, one may establish short-range (one-bond) heteronuclear scalar coupling correlations between e.g., ^{13}C and ^{1}H, by the analysis of two 1-D pulse NMR experiments. A single pulse ('direct-detect' ('pulse and collect')) (Appendix A2.1) ^{1}H experiment provides a suitable ^{1}H spectrum, from which the ^{13}C-^{1}H short-range scalar

coupling constant, $^{1}J_{CH}$, and coupling multiplicity can be determined from the ^{13}C proton satellites (Appendix A3.2.7). It is then possible to correlate the ^{13}C and ^{1}H nuclei by simple inspection of coupling multiplicities and J-values in a proton coupled ^{13}C spectrum. To obtain the ^{13}C spectrum, a proton coupled, INEPT, DEPT or PENDANT experiment may be performed. Importantly, each of these experiments increases the signal-to-noise ratio of the spectral signals of the insensitive ^{13}C nuclei via polarisation transfer, or in the case of PENDANT, polarisation exchange (Chapter 1).

Similarly, for example, it is possible to perform a selective 1-D polarisation transfer experiment that utilises selective perturbation of one of the ^{13}C proton satellites. Consequently, only those ^{13}C nuclei that exhibit short-range scalar coupling to the selected proton appear in the ^{13}C spectrum, thus automatically correlating the nuclei. The selective experiment is particularly useful since it derives correlations from one experiment that also facilitates an increase in spectral signal-to-noise ratio of the insensitive heteronucleus.

The pre-requisites for both 1-D correlation methods described above are; a well-resolved proton spectrum that is devoid of spectral overcrowding and also the unambiguous assignment of either the ^{1}H or ^{13}C spectra. The former is necessary so that ^{13}C proton satellites can be observed and the selectivity of perturbation and hence the correlation power is maintained. Therefore, generally selective pulse methods are only suitable for molecules having a small to medium molecular weight. However, in circumstances when only a select few correlations may be required to solve a structural problem, selective methods can be viable in larger molecules, despite inherently exhibiting greater proton spectral crowding.

The main thrust of work detailed in this thesis is concerned with the development of novel 1-D heteronuclear correlation (selective) pulse sequence experiments that utilise direct detection of the heteronucleus. Specifically, the pulse sequence experiments are designed to probe the following properties for molecules in the extreme narrowing limit (Appendix A6.4.3) that are in general, although not exclusively, devoid of proton spectral crowding:

- long-range (typically 2 and 3 intervening bonds) ^{13}C-^{1}H scalar couplings (Appendix A3.2.7) with simultaneous detection of quaternary nuclei.
- Long-range ^{13}C-^{1}H dipolar couplings via 1-D transient nuclear Overhauser effects (Appendix A7.3),

with a view to:

- reducing experimental time.
- Increasing convenience on the part of the user, by removing the need to perform extra pulse sequence experiments for the "complete" characterisation of the heteronuclear spin system.

The latter criterion is intended to establish the novel pulse sequence experiments as techniques that can be implemented "routinely" for relevant aspects of structure confirmation and/or elucidation.

In addition to novel work, the further characterisation and development of existing pulse sequence experiments invented at Aston University, namely PENDANT and SNARE have been undertaken.

The thesis is presented with the characterisation and development of PENDANT given first, as this provides the grounding upon which the novel pulse sequences in the following two chapters are based. Therefore, elements of these two chapters rely upon the reader being familiarised with the concepts developed in the preceding chapter(s). This is to maintain a contiguous and logical structure with the added intention of making more stimulating reading of the thesis overall. Finally, the development of SNARE is reported, which involves a different aspect of one of the global aims of this thesis, i.e., decreasing experimental time in heteronuclear polarisation transfer experiments.

Chapter 1 Extended characterisation and development of the PENDANT pulse sequence experiment

The early stages of elucidation or confirmation of organic molecular structure by liquid state NMR, often necessitates the determination of short-range (one bond) heteronuclear scalar coupling multiplicities, e.g., $^{13}C - {}^{1}H$. To this end, the one-dimensional pulse sequences, SEFT, APT [1], SEMUT [2, 3], refocused INEPT [1,4], and DEPT [1,4-5], and more recently, PENDANT [6] and DEPTQ [7] are performed for the direct detection of insensitive (X), and usually dilute nuclei, e.g., ^{13}C.

When the determination of short-range scalar coupling (Appendix A3) correlations (via the combined analysis of the scalar coupling constants (J) and multiplicity) is unimportant, all the experiments named above are routinely performed using broadband decoupling of the sensitive nuclei (^{1}H) during acquisition (Appendix A3.2.8). Proton broadband decoupling facilitates a further increase in the signal-to-noise ratio (S/N) in the insensitive nuclear spectrum but collapses the scalar coupling multiplets due to ^{1}H. However, each of the techniques employs a form of *spectral editing* (Appendix A8.3.1.1), which allows the assignment of the ^{1}H-X short-range scalar coupling multiplicities. Of course when correlations are sought via J and the scalar coupling multiplicities, each of the experiments named above can be performed without proton broadband decoupling during acquisition.

SEFT, APT and SEMUT, enable the detection of all types of insensitive nuclei, i.e., those, which exhibit short-range scalar coupling and those that do not, e.g., quaternary ^{13}C nuclei. The S/N of SEFT, APT and SEMUT, depends upon the magnitudes of the nuclear Overhauser enhancements (nOe) (Appendix A7.2.6), which have built-up at the insensitive nucleus from proton broadband decoupling during acquisition, and/or a preparation period.

In comparison to SEFT, APT and SEMUT, the increased sensitivity of INEPT and DEPT, which exploit polarisation transfer (Appendix A8.3.1) from protons to insensitive nuclei, affords them greater popularity. However, INEPT and DEPT unlike the less sensitive SEFT, APT and SEMUT experiments, are disadvantaged by their inability to simultaneously detect quaternary nuclei. Therefore INEPT and DEPT experiments must be supplemented (usually with one of the other experiments named above) with techniques that enable the detection of quaternary nuclei in order to fully characterise the spin system of insensitive nuclei.

The more recently proposed PENDANT [6] pulse sequence experiment, enables the spectral edited detection of heteronuclear short-range scalar coupling multiplicities, common to INEPT and DEPT, with the added advantage of simultaneously detecting quaternary nuclei. The sensitivity of the quaternary nuclei in analogy to SEFT, APT and SEMUT, benefit from nuclear Overhauser enhancement when the spectrum is acquired under proton broadband decoupling. Furthermore, it has also been shown that quaternary nuclei benefit from small amounts of polarisation transfer from long-range scalar coupling with protons should it exist [8].

PENDANT is virtually identical to INEPT in its pulse sequence construction. The exception is the presence of an additional $\pi/2$ pulse, which is applied to the insensitive nuclei at the beginning of the PENDANT pulse sequence, and has a phase that is parallel to the receiver phase. Rather misleadingly, some articles in the literature (of which the popular reference [1] is an example) have likened PENDANT to INEPT, by what appears to be a trivial inclusion of an extra pulse, which facilitates the detection of quaternary nuclei. However, the pulse also serves to completely change the spin-population dynamics of the heteronuclear spin system, resulting in polarisation exchange rather than polarisation transfer, which is implicit to INEPT and DEPT.

Polarisation exchange is manifested in the spectrum as an even distribution of population enhancement across the entire range of insensitive nuclear multiplets: After an ideal PENDANT transfer, a CH doublet is observed with two anti-phase lines with 8 : -8 units of intensity, in contrast to the familiar anti-phase 10 : -6 unit intensity distribution across the same doublet after an ideal INEPT transfer [4]. PENDANT polarisation exchange has been described elsewhere in terms of the spin-energy level population perturbations [9] and is not discussed further here.

Furthermore, the final evolution delay of 5/4J in PENDANT as opposed to 3/4J used in INEPT, decreases the sensitivity of some scalar coupling multiplicities to the average <J> value used, therefore, increasing signal-to-noise ratio and achieving more efficient spectral editing [6,8]. The 5/4J evolution delay facilitates the refocusing of single quantum coherences towards the hypothetical detection axis, while the 3/8J evolution delay causes single quantum coherences to evolve away from the hypothetical detection axis.

More recently, the DEPTQ pulse sequence has been proposed and enables the detection of quaternary nuclei, which similarly benefit from nuclear Overhauser enhancement when the spectrum is acquired under proton broadband decoupling. Based upon the classical DEPT experiment, DEPTQ also benefits from the comparatively better insensitivity to <J> values than INEPT and PENDANT experiments for spectral editing.

Proton detected (inverse) 2-D heteronuclear correlation experiments, e.g., HSQC, HMQC, and their derivatives [1, 10-11] are becoming increasingly popular, due to their increased sensitivity in comparison to those that employ detection of insensitive nuclei. However, for *routine* analysis of heteronuclear short-range scalar couplings, they have not yet completely superseded the 1-D techniques that employ detection of insensitive nuclei. This is probably because of the familiarity of 1-D experiments, their ease of implementation, and the fact that inverse experiments generally rely upon the availability of modern NMR spectrometers.

Therefore, it is envisaged that all of the 1-D pulse sequences mentioned thus far will continue to receive routine use for the analysis of heteronuclear short-range scalar couplings, and PENDANT and DEPTQ will no doubt continue to increase in popularity due to their ability to simultaneously detect quaternary nuclei.

The nature of polarisation exchange has been sufficiently described in terms of idealised spin-energy population diagrams for CH spin systems [9], similar to that utilised for the description of INEPT [4]. The evolution of single quantum coherence in the rotating frame has been schematised using simplistic classical vector models characterising quaternary nuclei and short-range coupled insensitive nuclei of doublet multiplicity [6]. Unfortunately, the short-comings of the simplistic vector description, which was intended to give an explanation of the PENDANT experiment that could be universally understood, has led to a few misinterpretations of the PENDANT experiment.

More detailed analysis of the evolution of coherences using the well-known product operator formalism [12] (Appendix A8) have revealed certain properties that impact upon the observable signals and traits of the PENDANT spectrum that have not yet been characterised. Moreover, some small errors and ambiguous comments have been made in a more recent publication, with respect to recent adaptations to the PENDANT pulse sequence for the suppression of multiplet and phase anomalies [8].

Therefore, it has been the aim of this chapter to analyse the PENDANT experiment using the product operator formalism and to rectify the errors in the said publication and establish a more appropriate theoretical interpretation. Furthermore, by analogy with INEPT and DEPT, the full characterisation of the PENDANT experiment is useful when PENDANT is used as a *building block* in more complex pulse sequences. Indeed the novel work detailed in chapters 2 and 3 depends upon it.

1.1 Further analysis of the PENDANT experiment

The PENDANT pulse sequence is given in figure 1.1. The phase of each pulse, P_n, is given in parentheses, which corresponds to the first phase in the phase cycle. The various numbered stages, σ_n, refer to the stages at which the product operator analysis is given later.

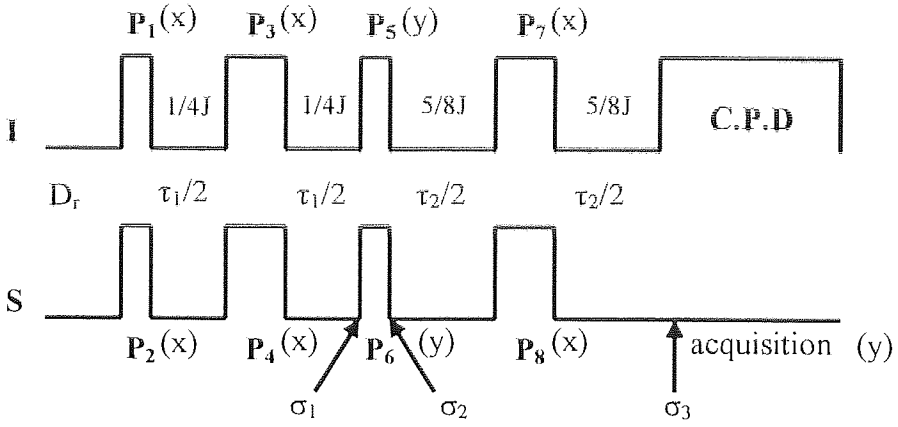

Figure 1.1 **PENDANT pulse sequence. By analogy with accepted convention for the depiction of pulse sequences [1], small open rectangles depict $\pi/2$ pulses and those which are twice as wide depict π pulses. C.P.D = Composite Pulse Decoupling (Appendix A3.2.8) and D_r = inter-pulse sequence relaxation delay (Appendix A2.2)**

The presence of P_2 applied to the insensitive nuclei, (S = e.g., ^{13}C) at the beginning of PENDANT, with its phase orthogonal to the polarisation transfer pulse, P_6, is implicit to the simultaneous detection of quaternary nuclei. With the exception of the length of the final evolution delay, τ_2, = 5/4J, the remainder of the PENDANT pulse sequence is identical in construction to INEPT and is solely responsible for polarisation exchange between protons and insensitive nuclei and subsequent spectral editing during τ_2.

A property of the PENDANT pulse sequence that has not been previously acknowledged is a result of its completely symmetric structure with respect to the pulses applied to both sensitive (I = ^1H) and insensitive (S) nuclei: As well as acting as a polarisation transfer

experiment in the normal *forward* sense, i.e., from protons to insensitive nuclei, PENDANT also simultaneously causes polarisation transfer in the *reverse* sense, i.e., from insensitive nuclei to protons, by analogy with that implicit to proton detected (inverse) experiments like HSQC. Indeed, it is this property that gives rise to the polarisation exchange phenomenon of PENDANT, i.e., the simultaneous polarisation transfer between protons and insensitive nuclei.

The concept of PENDANT simultaneously causing polarisation transfer in the forward and reverse sense is easily demonstrated by comparing the structure of PENDANT with the refocused INEPT and refocused reverse INEPT pulse sequences [1, 10-11] (figure 1.2). It is evident that the PENDANT pulse sequence can be considered to be an amalgamation of the forward and reverse refocused INEPT pulse sequences. Therefore, the PENDANT pulse sequence must, by default, simultaneously give rise to polarisation transfer in the forward and reverse sense.

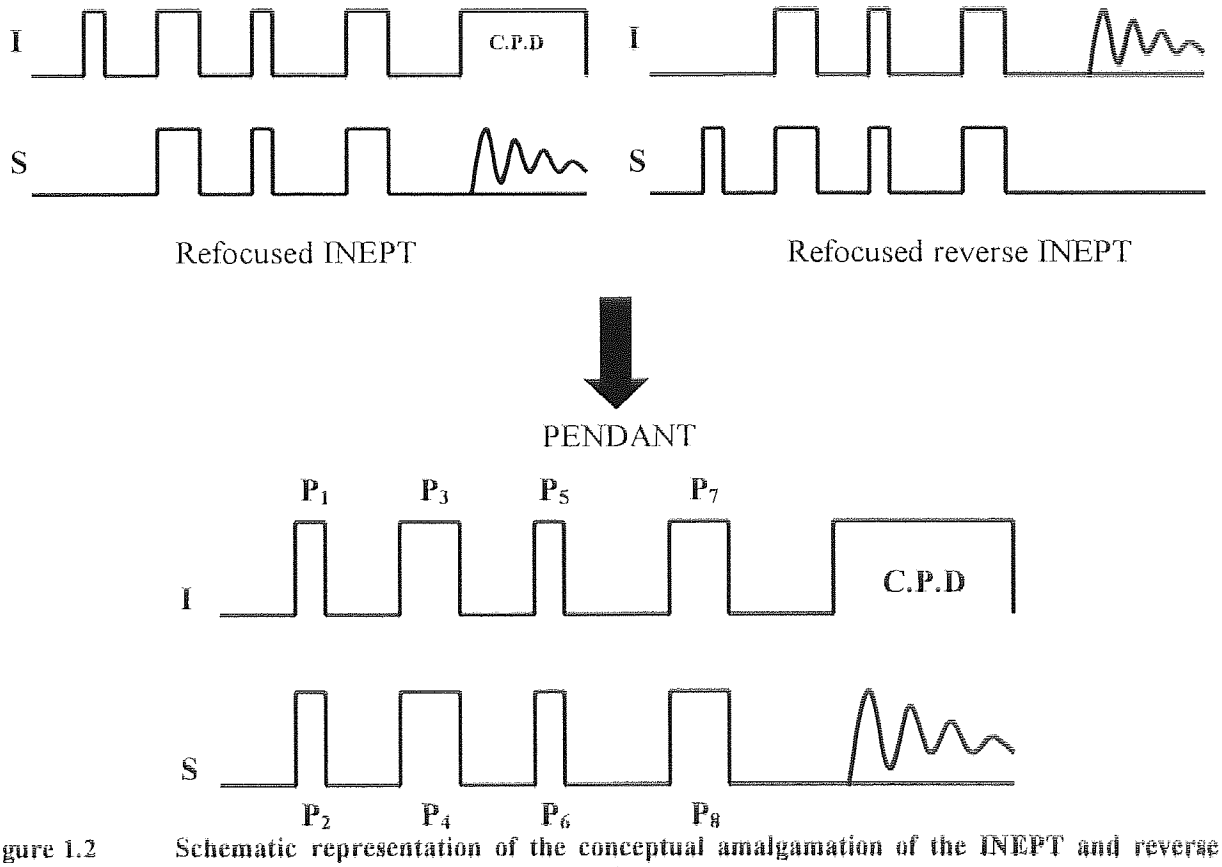

Figure 1.2 **Schematic representation of the conceptual amalgamation of the INEPT and reverse INEPT pulse sequence to give PENDANT.**

Of course, the effects of the reverse transfer in PENDANT can be neglected because the resulting proton coherences cannot contribute toward observable signals in the insensitive

nuclear spectrum. However, the same cannot be said of insensitive nuclear coherences, (residual coherences) that are not transferred in the reverse sense.

The efficiency of polarisation transfer in PENDANT, is largely dependent upon attaining the optimum evolution of coherence due to short-range heteronuclear scalar coupling (I-S) during τ_1, i.e., the condition 1/2J. If this condition is achieved, optimum reverse polarisation transfer takes place and all insensitive nuclear coherence is converted to proton coherence. However, in reality the value of J differs for each scalar coupling, and the average value of <J> used to set τ_1 will invoke different inverse polarisation transfer efficiencies for each insensitive nucleus. Consequently, insensitive nuclear coherence, hereafter called *residual* coherence, that was not transferred to protons in the reverse sense, exists after the polarisation exchange step, caused by pulses, P_5 and P_6. As the residual coherences were excited by the pulse P_2, they exhibit the same phases as quaternary coherences and hence contribute to the PENDANT spectrum.

Thus far the effect of residual coherences upon the PENDANT spectrum have been overlooked. Investigative work reported here has shown that for a typical range of J-values for ^{13}C-^{1}H short-range scalar coupling, found in typical organic molecules, the effect of residual coherences contribute little to the PENDANT spectrum. However, the characterisation of the residual coherences has proved useful for the amendment of errors in the publication named previously.

The following section provides a detailed analysis of the PENDANT experiment using product operator formalism, which has been overviewed in appendix A8.

1.2 Product operator description of PENDANT

The effect of the PENDANT pulse sequence upon, sensitive (I) and insensitive (S) nuclei are treated separately for reasons of consistency and clarity. A qualitative description of the transformations caused by the pulse sequence and their depiction by the product operators is given at each numbered stage, σ_n, in the pulse sequence of figure 1.1. Finally, all observable coherences are illustrated.

To maintain simplicity and clarity the following assumptions have been made:

- all spins I involved in short-range coupling to S are magnetically equivalent

(Appendix A3.2.3.2).

- All pulses are assumed to be perfect, i.e., on-resonance, of correct length (hence causing correct nutation angles), of the correct phase and do not suffer from the adverse effects of *r.f.* inhomogeneity (Appendix A9).
- Off-resonance effects are not considered (see above).

To save unnecessary lengthening of the product operator terms the following notations are used to describe the various product operator coefficients:

$$c_{Jn} = \cos \pi J_{IS} \tau_n$$
$$s_{Jn} = \sin \pi J_{IS} \tau_n$$

The cosine (cos) and sine (sin) terms above do not discriminate between the magnetically equivalent I spins involved in the coupling multiplicity SI_n, e.g., $^{13}CH_2$.

In order to convey the relevant points, it is assumed that the average value of <J> used invokes the condition $\tau_1 \neq 1/2J$ for all heteronuclear short-range scalar coupling multiplicities.

1.2.1 Coherences that originate from I nuclei

The PENDANT experiment with respect to the behaviour of coherence, which has originated from I, is identical to that of the well-documented INEPT experiment [4] and has already been given in appendix A8.3.1. Therefore, only the product operator representation of coherence that exists after polarisation exchange, i.e., σ_2, for SI_n terms are given. The product operator transformation valid up until σ_2 is given by

$$I_Z \xrightarrow{(\pi/2_I)_x \, \pi J_{IS} \tau_1 \, 2I_z S_z (\pi_{I+S})_x} \sigma_1 \xrightarrow{(\pi/2_{I+S})_y} \sigma_2 \qquad 1.1$$

Coherences of I are excited from longitudinal magnetisation and evolve during τ_1 due to short-range scalar coupling while chemical shifts are refocused. Application of the polarisation exchange pulses P_5 and P_6 initiates polarisation transfer from I to S for all coherences anti-phase with respect to scalar coupling with S. In-phase I coherences, i.e., those that did not develop scalar coupling remain invariant to P_5 and continue to be

unobservable for the remainder of the experiment. Therefore, only observable S coherences, which originate from polarisation transfer from I are given:

σ_2 SI $2S_x I_z s_{J1}$

SI$_2$ $2\left(S_x I_{1z} + S_x I_{2z}\right)s_{J1}$

SI$_3$ $2\left(S_x I_{1z} + S_x I_{2z} + S_x I_{3z}\right)s_{J1}$ 1.2

The final evolution period, τ_2, until σ_3, serves to refocus chemical shift evolution while short-range scalar coupling continues to evolve.

$$\sigma_2 \xrightarrow{\pi J_{IS}\tau_2 2I_z S_z (\pi_{1+S})_x} \sigma_3 \qquad 1.3$$

The observable single quantum coherence which is present during detection, without broadband decoupling of I nuclei, i.e., protons, is given by

σ_3 SI $\left\{\left(-2S_x I_z c_{J2} - \overset{(a)}{S_y s_{J2}}\right)s_{J1}\right\}\xi_1$

SI$_2$ $\left\{\left[\begin{array}{l}\left(-2S_x I_{1z} c^2{}_{J2} - 4S_y I_{1z} I_{2z} c_{J2} s_{J2} - \overset{(a)}{S_y s_{J2} c_{J2}} + 2S_x I_{2z} s^2{}_{J2}\right) + \\ \left(-2S_x I_{2z} c^2{}_{J2} - 4S_y I_{1z} I_{2z} c_{J2} s_{J2} - \overset{(a)}{S_y s_{J2} c_{J2}} + 2S_x I_{1z} s^2{}_{J2}\right)\end{array}\right]s_{J1}\right\}\xi_1$

SI$_3$ See Overleaf

$$\left\{\left[\begin{array}{l}\left(\begin{array}{l}-2S_xI_{1z}c^3{}_{J2}-4S_yI_{1z}I_{2z}c^2{}_{J2}s_{J2}+8S_xI_{1z}I_{2z}I_{3z}c_{J2}s^2{}_{J2}-\overset{(a)}{S_ys_{J2}}c^2{}_{J2}\\+2S_xI_{2z}c_{J2}s^2{}_{J2}-4S_yI_{2z}I_{3z}s^3{}_{J2}\end{array}\right)+\\\left(\begin{array}{l}-2S_xI_{2z}c^3{}_{J2}-4S_yI_{2z}I_{3z}c^2{}_{J2}s_{J2}+8S_xI_{1z}I_{2z}I_{3z}c_{J2}s^2{}_{J2}-\overset{(a)}{S_ys_{J2}}c^2{}_{J2}\\+2S_xI_{3z}c_{J2}s^2{}_{J2}-4S_yI_{3z}I_{1z}s^3{}_{J2}\end{array}\right)+\\\left(\begin{array}{l}-2S_xI_{3z}c^3{}_{J2}-4S_yI_{2z}I_{3z}c^2{}_{J2}s_{J2}+8S_xI_{1z}I_{2z}I_{3z}c_{J2}s^2{}_{J2}-\overset{(a)}{S_ys_{J2}}c^2{}_{J2}\\+2S_xI_{1z}c_{J2}s^2{}_{J2}-4S_yI_{1z}I_{2z}s^3{}_{J2}\end{array}\right)\end{array}\right]s_{J1}\right\}\xi_1$$

1.4

Where ξ_1 represents a proportionality constant depicting the enhancement factor indicative of polarisation transfer from I to S, i.e., γ_I/γ_S and the dependence of the magnitudes of the coherences on:

- the longitudinal relaxation of I between transients (Appendix A2) during acquisition and the relaxation delay (D_r).
- T_2 relaxation of I nuclei during τ_1.
- T_2 relaxation of S nuclei during τ_2.

The in-phase S coherences illustrated by terms (a) in expression 1.4, indicate those coherences that would be observable when the PENDANT spectrum is acquired with broadband decoupling of I nuclei. All anti-phase S coherences with respect to coupling with I are cancelled as a result of broadband decoupling. In common with INEPT, (Appendix A8.3.1) the coherences depicted by terms (a) exhibit the same transfer function allowing spectral editing:

$$\begin{array}{ll}\sigma_3(IS) & -S_y \sin \pi J_{IS}\tau_1 \sin \pi J_{IS}\tau_2\\ \sigma_3(I_2S) & -2S_y \sin \pi J_{IS}\tau_1 \sin \pi J_{IS}\tau_2 \cos \pi J_{IS}\tau_2\\ \sigma_3(I_3S) & -4S_y \sin \pi J_{IS}\tau_1 \sin \pi J_{IS}\tau_2 \cos^2 \pi J_{IS}\tau_2\end{array} \qquad 1.5$$

The cosine terms modulate the sign of the coherence according to the coupling multiplicity during τ_2 giving rise to spectral editing.

1.2.2 Coherences that originate from S nuclei

The overall transformation of the pulse and delay cascade up until σ_1, is to refocus chemical shift evolution due to τ_1, and to cause evolution of scalar coupling.

$$S_Z \xrightarrow{(\pi/2_{I+S})_x \pi J_{IS} \tau_1 2I_z S_z (\pi_{I+S})_x} \qquad 1.6$$

σ_1 S $+S_y$ Quaternary coherence

SI $+S_y c_{J1} - 2S_x I_z s_{J1}$

SI_2 $+S_y c^2_{J1} - 2\left(S_x I_{1z} c_{J1} s_{J1} + S_x I_{2z} c_{J1} s_{J1}\right) - 4S_y I_z I_z s^2_{J1}$

SI_3 $+S_y c^3_{J1} - 2\left(S_x I_{1z} c^2_{J1} s_{J1} + S_x I_{2z} c^2_{J1} s_{J1} + S_x I_{3z} c^2_{J1} s_{J1}\right)$
$-4\left(S_y I_{1z} I_{2z} c_{J1} s^2_{J1} + S_y I_{1z} I_{3z} c_{J1} s^2_{J1} + S_y I_{2z} I_{3z} c_{J1} s^2_{J1}\right) + 8S_x I_{1z} I_{2z} I_{3z} s^3_{J1}$

1.7

Single quantum coherence of S has evolved due to short-range scalar coupling during the evolution delay τ_1.

The effect of the polarisation transfer pulses P_5 and P_6 upon the coherences is given by

$$\sigma_1 \xrightarrow{(\pi/2_{1,S})_y} \sigma_2 \qquad 1.8$$

σ_2 S $+S_y^{(1)}$

SI $+S_y^{(1)} c_{J1} - 2S_z^{(2)} I_x s_{J1}$

SI_2 $+S_y^{(1)} c^2_{J1} - 2\left(S_z^{(2)} I_{1x} c_{J1} s_{J1} + S_z^{(2)} I_{2x} c_{J1} s_{J1}\right) + 4S_y^{(3)} I_{1x} I_{2x} s^2_{J1}$

$$
\begin{aligned}
SI_3 \quad & \overset{(1)}{+ S_y c^3{}_{J1}} - 2\Big(S_z I_{1x} c^2{}_{J1} s_{J1} + \overset{(2)}{S_z I_{2x}} c^2{}_{J1} s_{J1} + S_z I_{3x} c^2{}_{J1} s_{J1}\Big) \\
& + 4\Big(S_y I_{1x} I_{2x} c_{J1} s^2{}_{J1} + \overset{(3)}{S_y I_{1x} I_{3x}} c_{J1} s^2{}_{J1} + S_y I_{2x} I_{3x} c_{J1} s^2{}_{J1}\Big) \\
& + 8 \overset{(4)}{S_z I_{1x} I_{2x} I_{3x}} s^3{}_{J1}
\end{aligned}
\qquad 1.9
$$

Two-spin S single quantum coherence is transferred to I single quantum coherence e.g., terms (2) shown above, which is consistent with the effect of reverse coherence transfer as mentioned previously. These coherences do not contribute to observable signals in the S spectrum.

Triple heteronuclear quantum coherence, e.g., terms (3) and triple homonuclear quantum coherence anti-phase to S, e.g., term (4), which are superposition's of pure multiple quantum coherences (Appendix A8.2.1), are created from SI_n coherence, where $n > 1$. The former is created due to the fact that the S_y operator is invariant to the pulse, P_6 of phase y, in contrast to the latter where SI and SI_3 coherences with phase, S_x, do not remain invariant to P_6.

During τ_2, heteronuclear triple quantum coherence of S nuclei (terms (3)) for SI_3 couplings evolve further due to passive short-range scalar coupling to the remaining I spin. However, S coherence for SI_2 couplings, do not evolve further due to short-range heteronuclear scalar coupling, since the maximum number of active couplings is involved in the multiple quantum coherence.

Similarly, homonuclear triple quantum coherences anti-phase to S (terms (4)), evolve due to short-range scalar coupling with S during τ_2. However, due to the fact that the evolution delays in PENDANT are optimised for short-range heteronuclear scalar coupling, it is considered that evolution due to homonuclear scalar coupling and heteronuclear long-range scalar couplings are ineffective.

All heteronuclear and homonuclear multiple quantum coherences described above are refocused due to chemical shift during the final τ_2 evolution delay and are not reconverted to observable single quantum coherence.

The pulses, P_5 and P_6, have purged the spin system of anti-phase single quantum coherence of S. Therefore, the only observable coherences to survive the polarisation exchange step that originates from S magnetisation at the start of PENDANT, are:

- in-phase S coherences, i.e., *residual* coherences, which exhibit short-range scalar coupling, (terms (1)) and,
- quaternary coherence.

The remaining pulse and delay cascade up until σ_3 causes the evolution of scalar coupling and refocusing of chemical shift during τ_2.

$$\sigma_2 \xrightarrow{(\pi_{1+S})_x \pi J_{IS} \tau_2 2I_z S_z} \sigma_3 \qquad 1.10$$

The observable residual coherences present during detection without broadband decoupling of I nuclei is given by:

σ_3 S $\quad \{-S_y\}\xi_2$

SI $\quad \{[-S_y c_{J2} - 2S_x I_z c_{J2} s_{J2}]c_{J1}\}\xi_2$

SI_2 $\quad \{[-S_y c^2_{J2} - 2(S_x I_{1z} c_{J2} s_{J2} + S_x I_{2z} c_{J2} s_{J2}) - 4S_y I_z I_z s^2_{J2}]c^2_{J1}\}\xi_2$

SI_3 $\quad \left\{\left[\begin{array}{l} +S_y c^3_{J2} - 2(S_x I_{1z} c^2_{J2} s_{J2} + S_x I_{2z} c^2_{J2} s_{J2} + S_x I_{3z} c^2_{J2} s_{J2}) \\ -4(S_y I_{1z} I_{2z} c_{J2} s^2_{J2} + S_y I_{1z} I_{3z} c_{J2} s^2_{J2} + S_y I_{2z} I_{3z} c_{J2} s^2_{J2}) \\ +8S_x I_{1z} I_{2z} I_{3z} s^3_{J1} \end{array}\right] c^3_{J1}\right\}\xi_2$

1.11

Where ξ_2 represents a proportionality constant depicting the dependence of the magnitude of the coherences on γ_S and:

- longitudinal relaxation of S during acquisition and the relaxation delay (D_r)
- T_2 relaxation (Appendix A6) of S during the pulse sequence.

The magnitudes of the residual coherences are attenuated, according to c^n_{J1}. The evolution

delay, τ_1, is set to an average compromise value of <J> indicative of the J-range of the molecule. For routine implementation of PENDANT, the <J> value often used is 145Hz, therefore, the magnitude of residual coherences can vary markedly between different coupling multiplicities and different molecules. In addition, the signs may also vary according to the function c^n_{J1}, in analogy to spectral editing caused by c^n_{J2}.

1.2.3 Observable coherences in PENDANT spectra

The PENDANT spectrum of short-range scalar coupled S nuclei are, therefore, comprised of a superposition of residual S coherences and S coherences that have originated from polarisation transfer. This property is unique to PENDANT spectra due to the symmetric structure of the pulse sequence and the requirement of the phase cycling to maintain detection of quaternary nuclei. In contrast, INEPT and DEPT spectra are composed purely from S coherences that have originated from polarisation transfer from protons.

The effect of this superposition of coherences may be two fold:

1. The intensity of S signals is different from that expected purely from polarisation transfer from I to S.
2. Phase and multiplet distortions inherent to all polarisation transfer experiments of this type, i.e., INEPT and DEPT [13-14] are different for PENDANT spectra (See Section 1.6 later).

The effect of residual coherence in terms of both points highlighted above is unlikely to be important in most PENDANT spectra due to the efficiency of purging by the polarisation exchange pulses. For example, the typical J-range of $^{13}C - {}^{1}H$ multiplicities in organic compounds is of the order, 120-200Hz. Therefore, for a coupling of e.g., J = 180Hz, which corresponds to a typical CH doublet J-value, a simple calculation, using the corresponding product operator in expression 1.9, suggests that 18% of the total intensity of S coherence present after P_2 exists at σ_3. When scaled with the intensity factor, ξ_2, the magnitude of the residual coherence in comparison to that which originates from polarisation transfer is likely to be minimal, due to the comparatively larger intensity factor ξ_1:

- residual coherences are derived from dilute insensitive nuclei in comparison to S coherence that originates from polarisation transfer, which is polarisation enhanced by the factor γ_I/γ_S.
- The magnitudes of T_1 values for S nuclei are larger than the T_1 values for I nuclei.

Since the latter dictate the magnitude of the relaxation delay in order to optimise polarisation transfer from I to S, the magnitude of residual coherences are comparatively small.

1.2.4 Proton decoupled PENDANT spectra

PENDANT experiments are most often performed using proton broadband decoupling. In this case the longitudinal relaxation of S during the acquisition time is also subject to nuclear Overhauser enhancement. Therefore, the magnitudes of residual coherences in comparison to non-broadband decoupled spectra are larger.

One further point concerns the additive or subtractive nature of the superposition of residual coherences and coherences that have originated from polarisation transfer from I. By analogy with the modulation utilised for spectral editing, residual coherences exhibit an extra modulation as a function of multiplicity and the evolution period τ_1, (c^n_{J1}). As the values of τ_1 and τ_2 are not equivalent, i.e., 1/2J and 5/4J, the residual coherences may be modulated such that they are anti-phase to coherences that have originated from polarisation transfer from I. The latter exhibit phases (signs) attributed to only one cosine function, c^n_{J2}.

Superposition of residual coherence in anti-phase causes the partial cancellation of signals in the PENDANT spectrum, the magnitude of which depends on the factors given above. This may only become significant when S nuclei exhibit extreme J-values in comparison to the value of <J> used for τ_1 and τ_2 and which have benefited from nuclear Overhauser enhancement. The converse argument must also be considered, i.e., fortuitous enhancement of the signal may occur from a positive superposition of coherences.

A brief experimental investigation into the effect of residual coherences on PENDANT spectra is given in the following section.

1.3 Experimental investigation into the presence and effect of residual S coherences upon PENDANT spectra

In order to determine the level of residual coherences that exist during acquisition of PENDANT spectra, two PENDANT pulse sequences were modified in the following manner:

1. The initial proton pulse, P_1, in PENDANT was removed, which is tantamount to a reverse INEPT experiment, which utilises detection of the insensitive nucleus.

Therefore, only observable residual S coherence contributes to the signals in the spectrum, due to the fact that polarisation transfer from I to S is no longer possible.

2. A 'direct-detect' analogue of PENDANT was manufactured by the removal of all proton pulses such that the spectrum consists purely of S coherence that originates from S magnetisation prior to the beginning of all PENDANT experiments.

The spectrum obtained via PENDANT without the first proton pulse was compared to the spectrum of the 'direct-detect' analogue of the PENDANT pulse sequence. Consequently, the magnitudes of residual coherences, which survive the purging effect of the polarisation exchange pulses was determined. Finally, comparison to a normal PENDANT spectrum was made.

Appendix A3 and A4 describes the standard experimental procedures for the preparation, acquisition of and processing of NMR spectra, which are valid for all experimental work undertaken. Appendix A4.5 provides information regarding pulse program language and spectrum acquisition parameters.

1.3.1 Materials and Equipment

Experiments were performed using a sample of 60/40, vol/vol., ethyl-5-(chloromethyl)-2-furan-carboxylate and duetero chloroform respectively, the latter providing field –frequency locking (Appendix A4.3). Experiments were performed using a Bruker Avance 300MHz NMR spectrometer with a 5mm $^{13}C - {}^{1}H$ dual probe.

Ethyl-5-(chloromethyl)-2-furan-carboxylate compound was chosen because it exhibits an appropriate variety of $^{13}C - {}^{1}H$ short-range scalar coupling multiplicities with J-value ranges indicative of most common organic molecules (Figure 1.3).

1.3.2 Acquisition parameters

All PENDANT experiments were performed in the standard way as recommended for routine analysis, i.e., to achieve nominal spectral editing with τ_1 and τ_2 set to 1/2J and 5/4J respectively for $\langle J \rangle$ = 145Hz. 16 transients were collected for each experiment and a 3 second relaxation delay (D_r) was used.

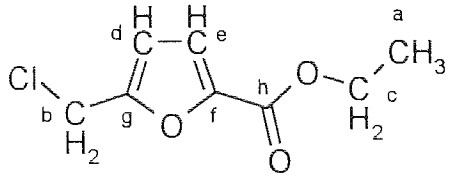

CH group	J (Hz)
a	128
b	153
c	151
d	178
e	180

Figure 1.3 **Structural diagram ethyl-5-(chloromethyl)-2-furan-carboxylate and table of short-range ^{13}C-^{1}H J values.**

SW was set to encompass the entire chemical shift range of the solute using TD = SI = 32K, providing adequate digital resolution of 0.37Hz (Appendix A2.4), to ensure correct representation of signal intensity and multiplet structure. ^{13}C spectra were acquired at 300K with proton broadband decoupling of protons using composite pulse decoupling (C.P.D) (Appendix A3.2.8). The carrier frequency for both ^{1}H and ^{13}C was set at the centre of the solute chemical shift range of each.

1.3.3 Spectrum processing

All ^{13}C spectra were processed using line broadening of 1Hz (Appendix A2.5.2). All spectra were phase corrected to the same parameters. All spectra are presented in absolute intensity scaling mode for comparison purposes.

1.4 Results and discussion

Figures 1.4, 1.5 and 1.6 overleaf illustrate the spectra of the direct-detect analogue of PENDANT, PENDANT without the first proton pulse and normal PENDANT respectively. The intensity of figure 1.5 has been multiplied by a factor of 8 for ease of comparison.

Signals for **a**, **b** and **c** of figure 1.5 are largely suppressed from the spectrum due to the purging effect of the I and S polarisation exchange pulses, P_5 and P_6 which have converted residual S coherence that is anti-phase with respect to scalar coupling, to various orders of unobservable multiple quantum coherence. The high efficiency of the purging of signals **b** and **c** (**c** appears in partial dispersion) is due to the close matching of their individual J-values, 153Hz and 151Hz respectively, as compared to <J> = 145Hz.

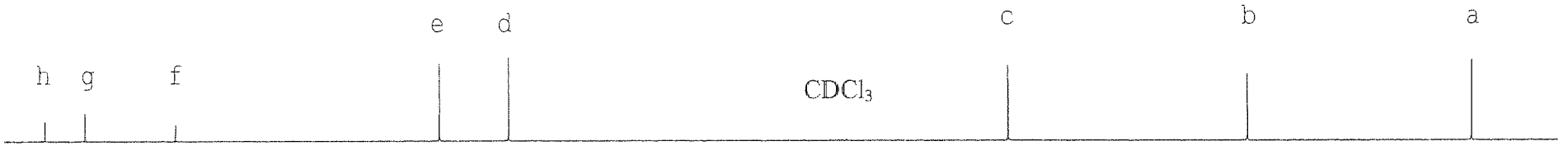

Figure 1.4 - 'direct detect' analogue of PENDANT

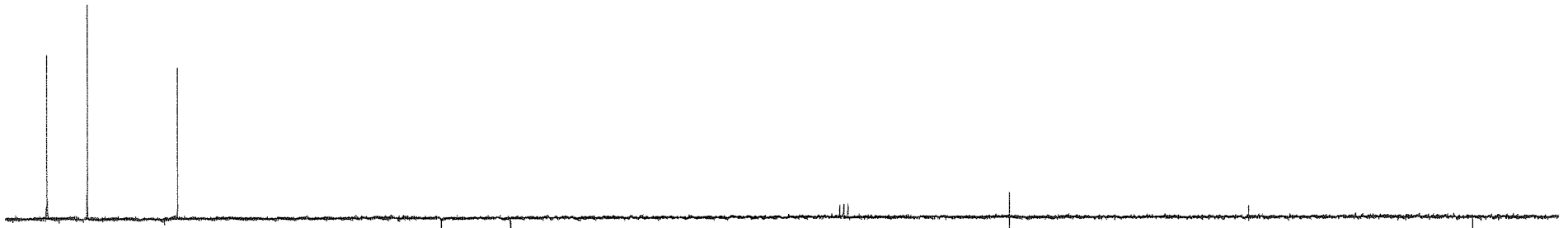

Figure 1.5 - PENDANT without first proton pulse (P_1) at × 8 intensity scaling

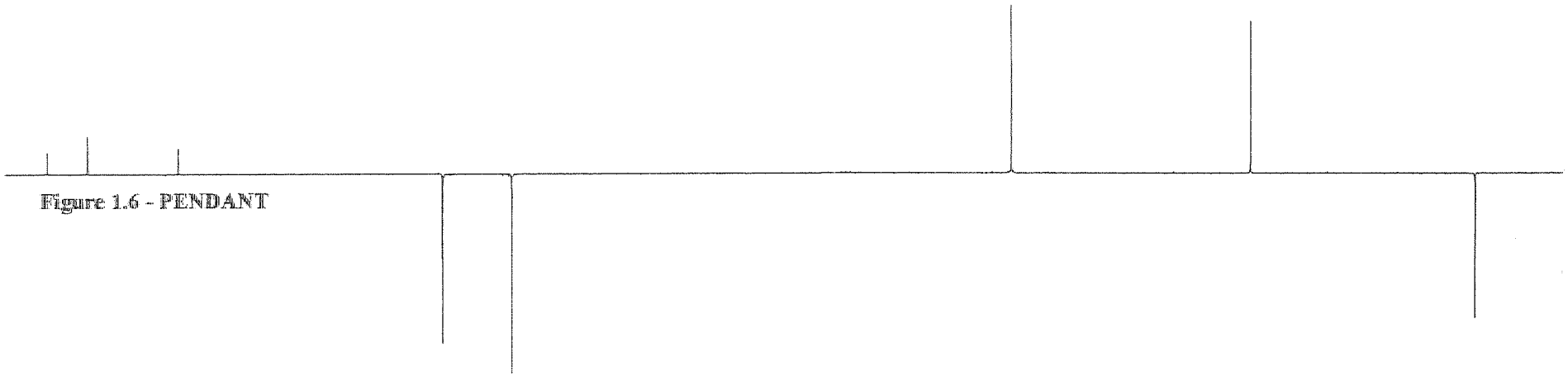

Figure 1.6 - PENDANT

Short-range scalar coupling of these multiplicities evolve during τ_1 to an anti-phase condition that closely approaches unity, i.e., 1/2J, such that near optimum purging occurs.

The suppression of signals **a**, **d** and **e** is less due in part to the greater mismatch between their individual J-values of 128Hz, 178Hz and 180Hz respectively and <J> = 145Hz. By comparison of the integrals of the **e** signals between figure 1.4 and figure 1.5, the level of suppression is calculated to be 90%. This is approximately 8% more than that predicted by the simple trigonometric calculation given previously, when it was predicted that 18% of the total intensity of the S coherence would be present during acquisition. The discrepancy between the predicted value and that attained via experiment may be attributed to off-resonance effects and/or *r.f.* inhomogeneity, associated with both S and I pulses. The impact of off-resonance effects and/or *r.f.* inhomogeneity, has not been considered in this rudimentary analysis, since the PENDANT experiment, in common with refocused INEPT, is routinely performed in this way.

It is evident that the residual coherences for all multiplicities give rise to signals of the same phase as those in PENDANT shown in figure 1.6. Therefore, an additive superposition of residual S coherence and that which originates from polarisation transfer from I occurs. For the **e** signal, the additive superposition of the residual signal represents 4% of the total integrated intensity of the **e** signal in the PENDANT spectrum of figure 1.6. Therefore, in comparison to INEPT, where the intensity of signals is entirely dependent on polarisation transfer from I, PENDANT spectra benefit, albeit trivially, from the additive superposition of residual coherence.

Finally it is noted that the intensities of the quaternary signals, **f**, **g** and **h** in figure 1.6 are not exactly 1/8th of those in figure 1.5. It is likely that the explanation of the intensity 'discrepancy' is due to the quaternaries having received partial polarisation transfer from ^{1}H. Indeed, this phenomenon (which was mentioned previously) is consistent with observations reported in a publication on PENDANT, and is probably attributed to small amounts of long-range scalar coupling evolution during the short-range coupling optimised delays, τ_1 and τ_2.

1.5 Conclusion

In PENDANT spectra of ^{13}C nuclei, which exhibit a range of short-range J-values indicative of commonly studied organic ^{13}C-^{1}H spin systems, the superposition of residual S coherences

with S coherences that originate from polarisation transfer from I has been proven to be reasonably inconsequential. The polarisation exchange pulses purge the majority of residual observable single quantum coherence by conversion to various orders of unobservable coherence. The superposition of the residual coherences is additive, albeit rather trivial, and benefits the development of signal-to-noise ratio. These observations are based upon the use of PENDANT in the way recommended for routine use, i.e., for <J> = 145Hz with τ_1 and τ_2 set to 1/2J and 5/4J respectively.

For the study of ^{13}C in organic molecules exhibiting short-range $^{13}C - {}^{1}H$ scalar coupling, the signal-to-noise ratio of PENDANT spectra compared to INEPT should be slightly better due to the additive nature of residual S coherences. For ^{13}C nuclei with higher intensity scaling factors, ξ_2, i.e., that exhibit large nOe enhancements during acquisition, the signal enhancement could reach appreciable values.

1.6 Phase and multiplet anomalies in PENDANT spectra

When PENDANT and INEPT experiments are performed without proton broadband decoupling during acquisition, short-range scalar coupling multiplets do not possess the usual binomial intensity distribution of the component lines but instead exhibit multiplet and phase anomalies. Sorensen and Ernst have usefully categorised both types of anomaly according to the following definitions [13]:

- multiplet anomalies are considered to be intensity variations of component lines of a multiplet from those of a normal binomial distribution, disregarding phase.
- Phase anomalies are defined as dispersive contributions to otherwise absorptive multiplet lineshapes.

Multiplet anomalies can affect the intensity of peaks in decoupled spectra but the effect of phase anomalies are restricted to the observation of coupled spectra. Figure 1.8, given overleaf, illustrates a PENDANT spectrum obtained without proton broadband decoupling, of the same sample of ethyl-5-(chloromethyl)-2-furan-carboxylate as used in the work described previously. Multiplet and phase anomalies are exhibited by the signals **a** and **b**, which correspond to CH_3 and CH_2 multiplicities respectively, while signal **c**, which corresponds to another CH_2 multiplicity, exhibits only multiplet anomalies.

INEPT spectra exhibit multiplet anomalies, due to uneven polarisation transfer across the

destination spin multiplets, a property inherent to the spin dynamics of INEPT style polarisation transfer [4, 13]. The unique spin dynamics of the PENDANT experiment utilising polarisation exchange [9] does not inherently cause multiplet anomalies in this way, however, multiplet and phase anomalies are created by a property shared by both experiments: the final refocusing period in PENDANT and INEPT serves to achieve both spectral editing and maximise in-phase coherence to have originated from polarisation transfer, should it be required for decoupling. Only partial refocusing of signals can occur during the final fixed evolution period due to the compromise value of <J> used, and the evolution of further passive I spin couplings. Therefore, a superposition of in-phase and anti-phase single quantum coherences occurs, the latter causing phase and multiplet anomalies. Of course the explanation given above neglects the effect of off-resonance effects (Appendix A1.8.3), which may invoke phase anomalies.

Specifically, even-coupling orders (n = 2, 4 for SI_n) of single quantum coherences, which correspond to product operators, e.g., $4S_{x,y}I_zI_z$, are responsible for multiplet anomalies, while odd coupling orders (n =1,3 for SI_n), of single quantum coherences, which correspond to product operators, e.g., $2S_{x,y}I_z$, are responsible for phase anomalies (Appendix A8.2.2). (Figure 1.7)

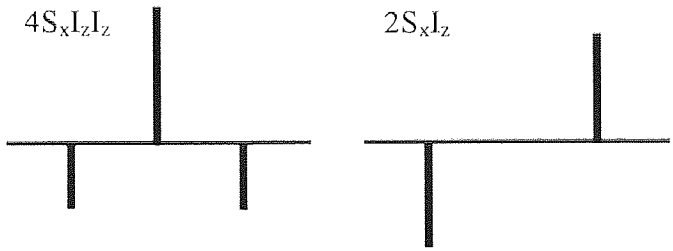

Figure 1.7 **Spectral depictions of multiplet and phase anomaly coherences for SI scalar couplings for magnetically equivalent I nuclei.**

During acquisition of PENDANT spectra without broadband decoupling of protons, it has been shown in expressions 1.4 and 1.11 that an array of multiplet and phase anomaly-causing coherences exist for both residual coherences and coherences, which have originated from polarisation transfer. The magnitudes of these coherences depend upon the J-value of the scalar couplings and, τ_1 and τ_2. In contrast, INEPT and DEPT exhibit phase and multiplet anomalies which originate purely from polarisation transfer from I to S.

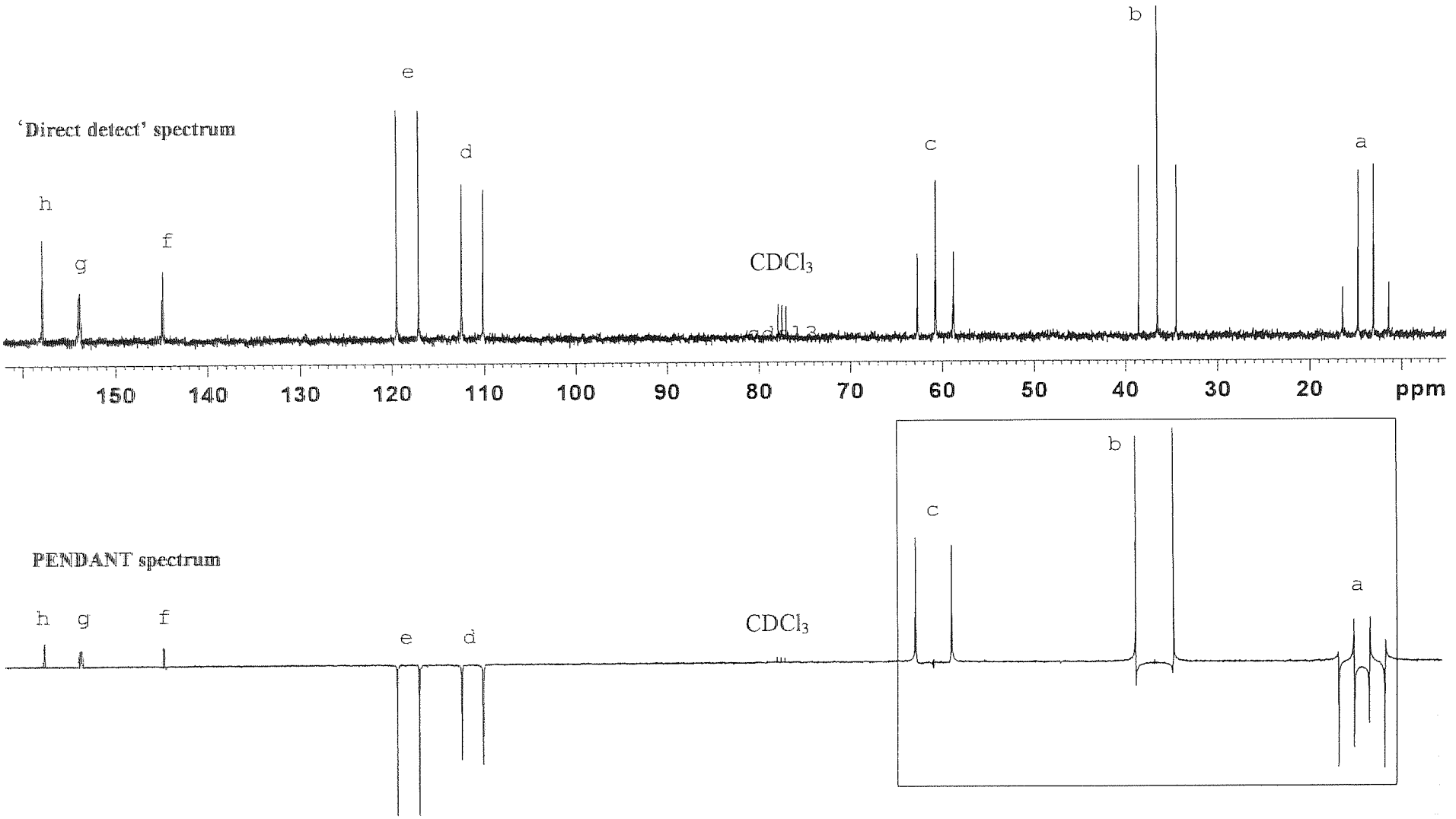

Figure 1.8 Multiplet and phase anomalies in a typical non-proton broadband decoupled PENDANT spectrum.

Furthermore, the phase and multiplet anomalies in PENDANT that originate from the two sources of coherence are not simply additive. This is due to the fact that the phase of residual coherences differ from those that originate from polarisation transfer: specifically, residual coherences exhibit a c^n_{J1} function while those that originate from polarisation transfer exhibit a s^n_{J1} function. The effect is to cause a mismatch in phase between the two types of coherence, which attributes another phase anomaly upon their superposition. Realisation of this difference between PENDANT and INEPT and DEPT is purely academic, since the magnitudes of the residual signals have already been shown to be trivial.

Before, progressing to describe the amendments made, a brief synopsis of the methods introduced by Sorensen and Ernst, upon which the methods employed by Homer and Perry are based, is given here.

1.6.1 Removing phase and multiplet anomalies from PENDANT spectra

The removal of phase and multiplet anomalies from proton coupled spectra are sometimes required in order to make measurements of J-values easier. Methods for the removal of phase and multiplet anomalies were originally proposed by Sorensen and Ernst [13] and were applied to refocused INEPT and DEPT experiments. From these methods, Homer and Perry [8] derived similar approaches for the removal of phase and multiplet anomalies from proton coupled PENDANT spectra. However, it has been revealed, from the analysis of coherences that originate from S nuclei given previously, that the methods utilised by Homer and Perry for the removal of phase and multiplet anomalies from proton coupled PENDANT spectra require amendment.

Homer and Perry proposed the use of two types of purging method based upon the methods proposed by Sorensen and Ernst [13, 14]:

- the application of a total of three π pulses of specific phase applied to both I and S nuclei in order to selectively purge only phase anomalies from the proton coupled PENDANT spectrum. This method was based upon a single π pulse method utilised by Sorensen and Ernst for the purging of phase anomalies in DEPT spectra, dubbed the DEPT$^+$ pulse sequence [13].

- The application of a hard (Appendix A1.7) $\pi/2$ proton 'purge' pulse, of unspecified phase, prior to acquisition, in order to remove phase and multiplet anomaly-causing

signals from the proton coupled PENDANT spectrum. Employing a $\pi/2$ proton 'purge' pulse in order to remove phase and multiplet anomaly-causing signals was originally applied to the refocused INEPT pulse sequence, dubbed the $INEPT^{+}$ pulse sequence [13].

It is shown here that the overall transformation of the purging method achieved by the three π pulses described by Homer and Perry, can be achieved by one π pulse applied to protons (I).

It is also shown here that in contrast to $INEPT^{+}$, only one specific phase of $\pi/2$ purge pulse can be used for the elimination of multiplet and phase anomalies in PENDANT spectra.

1.6.2 Removing phase anomalies from PENDANT spectra using π pulses: A review of work presented in the original publication by Homer and Perry

Sorensen and Ernst [13] proposed a method of removing phase anomaly-causing coherences in DEPT spectra, by applying a π pulse to protons prior to acquisition on every other transient. The application of a proton π pulse inverts the sign of phase anomaly-causing coherences, i.e., those with odd numbers of I_z operators, e.g., $2S_{x,y}I_z$ and $8S_{x,y}I_zI_zI_z$. The sign of the phase anomaly coherences on the second transient, when the proton π pulse is not applied, are opposite and cancel with respect to a constant receiver phase. On the other hand, the sign of multiplet anomaly-causing coherences remain invariant to the proton π pulse since they contain even numbers of I_z operators. Therefore, over the course of two transients, the phase anomaly coherences cancel leaving only multiplet-anomaly coherences and in-phase coherence present during acquisition.

The modified PENDANT pulse sequence proposed in the original publication [8] utilising the three π proton pulses, A, B and C is given below.

^{1}H (I) $\quad (\pi/2)_x - \tau_1 - (\pi)_x - \tau_1 - (\pi/2)_y\ [A] - \tau_2 - (\pi)_x - \tau_2 -$

$\qquad\qquad\qquad\qquad\qquad\qquad\qquad \sigma_2 \qquad\qquad\qquad \sigma_3$

^{13}C (S) $\quad (\pi/2)_x - \tau_1 - (\pi)_x - \tau_1 - (\pi/2)_y\ [B] - \tau_2 - (\pi)_x - \tau_2 - [C] -$ **Acquire (y)**

where $[A] = [B] = [C] = \pi_y$

The point at which pulses A and B occur corresponds to the stage σ_2 in the product operator description of PENDANT given previously, i.e., directly after polarisation exchange (expressions 1.2 and1.9).

As described previously, with reference to expression 1.8, coherences that originate from S that were anti-phase with respect to short-range scalar coupling, i.e., phase and multiplet anomaly-causing coherences, are purged by the effect of the polarisation exchange pulses. Therefore, only in-phase S_y coherence that originates from S exists during application of A and B and remains invariant to the y-phase pulse B.

The only other S coherence that exists during application of A and B, is that which has originated from I, due to polarisation transfer, given in expression 1.2. For simplicity only the SI_2 multiplicity, from expression 1.2 is considered as it becomes composed of both phase and multiplet anomaly coherences, which facilitate discussion of the relevant points:

$$\sigma_2 \qquad SI_2 \qquad \left[\begin{matrix}\left(-2S_xI_{1z}c^2{}_{J2}\right)+\\ \left(-2S_xI_{2z}c^2{}_{J2}\right)\end{matrix}\right]s_{J1} \qquad 1.12$$

Application of A and B (y phase) causes simultaneous inversions of S_x and I_z, the overall effect of which, is to cause a 2π radians rotation in sign of the operators, i.e., the sign of the coherence remains invariant. Therefore, there is no collective effect of A and B upon all S coherences.

Prior to the application of the final pulse C, S coherences that exist, which originate from polarisation transfer from I and residual coherence of S are given earlier in expressions 1.4 and 1.11 respectively. The S coherences for a SI_2 multiplicity given in expressions 1.4 and 1.11 are given below in expressions 1.13 and 1.14 respectively.

$$\left\{\left[\begin{matrix}\left(-2S_xI_{1z}c^2{}_{J2}-4S_yI_{1z}I_{2z}c_{J2}s_{J2}-S_ys_{J2}c_{J2}+2S_xI_{2z}s^2{}_{J2}\right)+\\ \left(-2S_xI_{2z}c^2{}_{J2}-4S_yI_{1z}I_{2z}c_{J2}s_{J2}-S_ys_{J2}c_{J2}+2S_xI_{1z}s^2{}_{J2}\right)\end{matrix}\right]s_{J1}\right\}\xi_1 \qquad 1.13$$

$$\left\{\left[-S_y c^2{}_{J2} - 2\left(S_x I_{1z} c_{J2} s_{J2} + S_x I_{2z} c_{J2} s_{J2}\right) - 4 S_y I_{1z} I_{2z} s^2{}_{J2}\right] c^2{}_{J1}\right\} \xi_2 \qquad 1.14$$

It is apparent that application of pulse C causes the sign inversion of coherences, with odd numbers of I_z operators, i.e., phase anomaly coherences, $2S_{x,y}I_z$, which is precisely what occurs for DEPT$^+$. As implied in the original publication by Homer and Perry, when pulses A, B and C are applied on every other transient with respect to a constant receiver phase, the phase anomaly coherences are cancelled after every second transient. Therefore, S signals of short-range scalar coupling multiplicities, SI_2 and SI_3, only exhibit multiplet anomalies, due to the superposition of the remaining multiplet anomaly coherence and in-phase coherence. This result is depicted in figure 1.9 for the ^{13}C PENDANT spectrum of a CH_3 group in ethylbenzene, which has been reproduced from the original publication.

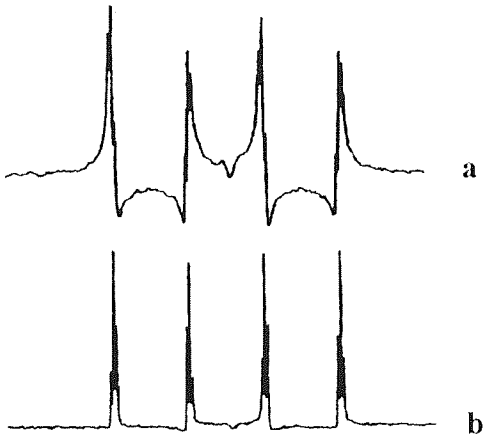

Figure 1.9 **Proton coupled ^{13}C PENDANT spectra of the CH_3 group of ethylbenzene, (a) PENDANT and (b) PENDANT$^+$. Reproduced with permission from the authors.**

1.7 Conclusion

It has been shown theoretically that pulses A and B, situated after the polarisation exchange pulses in a modified PENDANT experiment by Homer and Perry, do not effect the removal of phase anomaly-causing coherence. However, the sole action of a π pulse of y-phase, i.e., pulse C, which in analogy to DEPT$^+$ is situated just prior to acquisition, effects the removal of phase anomaly coherence on every second transient. Moreover, as the proton π pulse acts upon z-magnetisation, i.e., I_z, the proton pulse can be of arbitrary phase, contrary to the specification of a y-phase pulse in the original publication.

1.8 Removing phase and multiplet anomalies from PENDANT spectra using a $\pi/2$ proton 'purging' pulse.

In the original publication by Homer and Perry, it was proposed that in common with INEPT[+], applying a $\pi/2$ proton 'purging' pulse immediately before acquisition, hereafter referred to simply as a 'purge' pulse, should facilitate the purging of multiplet and phase anomalies. However, the publication neglected to specify the necessary phase of the purge pulse.

Prior to acquisition, i.e., σ_3, observable single quantum coherences that originate from polarisation transfer from I and from residual S coherence have been given in expressions 1.4.and 1.11 respectively. For simplicity, the S coherence of only the SI_2 multiplicity is considered, since it is composed of both phase and multiplet anomaly coherences, which facilitate discussion of the relevant points. The S coherences at σ_3 that originate from polarisation transfer from I and from residual S coherence are given by expressions 1.15 and 1.16 respectively.

$$\sigma_3 \qquad SI_2 \qquad \left\{\left[\begin{array}{l}\left(-2S_xI_{1z}c^2{}_{J2}-4S_yI_{1z}I_{2z}c_{J2}s_{J2}-S_ys_{J2}c_{J2}+2S_xI_{2z}s^2{}_{J2}\right)+\\ \left(-2S_xI_{2z}c^2{}_{J2}-4S_yI_{1z}I_{2z}c_{J2}s_{J2}-S_ys_{J2}c_{J2}+2S_xI_{1z}s^2{}_{J2}\right)\end{array}\right]s_{J1}\right\}\xi_1 \qquad 1.15$$

$$\sigma_3 \qquad SI_2 \qquad \left\{-S_yc^2{}_{J2}-2\left(S_xI_{1z}c_{J2}s_{J2}+S_xI_{2z}c_{J2}s_{J2}\right)-4S_yI_zI_zs^2{}_{J2}\right]c^2{}_{J1}\Big\}\xi_2 \qquad 1.16$$

It is evident that an arbitrarily phased purge pulse (e.g., x or y) is sufficient to convert all anti-phase coherences, i.e., phase and multiplet anomaly-causing coherences to unobservable heteronuclear multiple quantum coherence leaving only in-phase coherence. The latter exhibiting multiplet lines with a binomial intensity distribution. For example, a purge pulse of y phase or x phase converts I_z operators to I_x and I_y respectively.

It is evident that the application of an arbitrarily phased purge pulse causes the purging of all

multiplet and phase anomaly coherences as in INEPT, since expression1.15 describes the S coherences that originate from polarisation transfer from I which are implicit to INEPT.

However, it was shown previously in expression 1.9 that residual S coherence for SI, SI_2 and SI_3 is converted to single quantum coherence of I, heteronuclear triple quantum coherence and homonuclear triple quantum coherence respectively due to the purging effect of the polarisation exchange pulses. Expression 1.9 is reproduced here for convenience:

$$
\begin{aligned}
SI \quad & +S_y c_{J1} - 2\overset{(a)}{S_z I_x} s_{J1} \\
SI_2 \quad & +S_y c^2{}_{J1} - 2\overset{(a)}{\left(S_z I_{1x} c_{J1} s_{J1} + S_z I_{2x} c_{J1} s_{J1}\right)} + 4 S_y I_{1x} I_{2x} s^2{}_{J1} \\
SI_3 \quad & +S_y c^3{}_{J1} - 2\overset{(a)}{\left(S_z I_{1x} c^2{}_{J1} s_{J1} + S_z I_{2x} c^2{}_{J1} s_{J1} + S_z I_{3x} c^2{}_{J1} s_{J1}\right)} \\
& +4\overset{(b)}{\left(S_y I_{1x} I_{2x} c_{J1} s^2{}_{J1} + S_y I_{1x} I_{3x} c_{J1} s^2{}_{J1} + S_y I_{2x} I_{3x} c_{J1} s^2{}_{J1}\right)} \\
& +8 S_z I_{1x} I_{2x} I_{3x} s^3{}_{J1}
\end{aligned}
\qquad 1.17
$$

In the product operator description of a normal PENDANT experiment, these residual multiple quantum coherences were neglected since they remain unobservable for the rest of the PENDANT experiment.

Immediately prior to acquisition, the chemical shifts of these coherences that evolved during τ_2 is refocused. The residual single quantum coherences of S, evolve due to short-range scalar coupling as described previously in expression 1.9, and are omitted from these expressions hereafter. Single quantum coherence of I, i.e., terms (a) above evolve as normal due to scalar coupling during τ_2. Similarly, multiple a SI_2 quantum coherences that do not exhibit their maximum number of active I coherences, i.e., terms (b) in expression 1.17 for SI_3, evolve during τ_2 due to passive spin couplings with the remaining I nuclei.

The situation prior to acquisition, i.e., σ_3, for coherences SI_2 and SI_3 respectively is given by:

$$
\begin{aligned}
SI_2 \quad & \left\{ \overbrace{-2\left(S_z I_{1x} c_{J1} s_{J1} + S_z I_{2x} c_{J1} s_{J1}\right)}^{(a)} \right\} c_{J2} + I_y c_{J1} s_{J1} s_{J2} + \overbrace{4 S_y I_{1x} I_{2x} s^2_{J1}}^{(e)} \\
& \left\{ \begin{array}{l} \overbrace{-2\left(S_z I_{1x} c^2_{J1} s_{J1} + S_z I_{2x} c^2_{J1} s_{J1} + S_z I_{3x} c^2_{J1} s_{J1}\right)}^{(a)} \\ \overbrace{+4\left(S_y I_{1x} I_{2x} c_{J1} s^2_{J1} + S_y I_{1x} I_{3x} c_{J1} s^2_{J1} + S_y I_{2x} I_{3x} c_{J1} s^2_{J1}\right)}^{(b)} \end{array} \right\} c_{J2} \\
SI_3 \quad & + 3 I_y c^2_{J1} s_{J1} s_{J2} \\
& \overbrace{\begin{array}{l} -8 S_x I_{1x} I_{2x} I_{3z} c_{J1} s^2_{J1} s_{J2} - 8 S_x I_{1x} I_{3x} I_{2z} c_{J1} s^2_{J1} s_{J2} - 8 S_x I_{2x} I_{3x} I_{1z} c_{J1} s^2_{J1} s_{J2} \\ \overbrace{+8 S_z I_{1x} I_{2x} I_{3x} s^3_{J1} c_{J2}}^{(c)} \end{array}}^{(d)}
\end{aligned}
$$

1.18

Evolution due to scalar coupling to the passive I spin for SI_3 in terms (b) in expression 1.17 creates terms (d) in expression 1.18. Evolution of homonuclear triple quantum coherence to the remaining anti-phase S spin, i.e., term (c) has been neglected, since it will be shown not to contribute to observable coherence.

Application of a y-phase purge pulse applied to I nuclei prior to acquisition causes the following transformations of coherences:

- the excitation of longitudinal two-spin order ($2S_zI_z$) from coherences (terms (a)), which are unobservable in the PENDANT spectrum.
- In-phase I coherence remains invariant to the y-phase purge pulse and is unobservable in the PENDANT spectrum.
- Heteronuclear triple quantum coherences of SI_3, i.e., terms (d) are converted to double heteronuclear quantum coherences, e.g., $8S_xI_zI_zI_x$, which remain unobservable.
- Triple homonuclear quantum coherence of SI_3, i.e., terms (c) is converted to longitudinal four-spin order ($8S_zI_zI_zI_z$), which remains unobservable.
- However, application of a y-phase purge pulse, causes the re-conversion of heteronuclear triple quantum coherence, i.e., terms (b) ($4S_yI_xI_x$) for SI_3 and term (e) for SI_2, to observable multiplet anomaly single quantum coherence, $4S_yI_zI_z$ for both

SI_2 and SI_3 multiplicities. The magnitude of the multiplet anomaly coherence, $4S_yI_zI_z$ for SI_3 is proportional to a further c_{J2} function.

Observable S coherence during non-proton broadband decoupled acquisition is given by:

$$
\begin{aligned}
S \quad & \left\{ \overset{(a)}{-S_y} \right\} \xi_2 + \\
SI \quad & \left\{ \left[\overset{(a)}{-S_y c_{J2}} \right] c_{J1} \right\} \xi_2 + \left\{ \left(\overset{(b)}{-S_y s_{J2}} \right) s_{J1} \right\} \xi_1 \\
SI_2 \quad & \left\{ \left[\overset{(a)}{-S_y c^2_{J2}} \right] c^2_{J1} - 4S_y I_z I_z s^2_{J1} c_{J2} \right\} \xi_2 + \left\{ \left(\overset{(b)}{-2S_y s_{J2} c_{J2}} \right) s_{J1} \right\} \xi_1 \\
SI_3 \quad & \left\{ \begin{array}{l} \left[\overset{(a)}{+S_y c^3_{J2}} \right] c^3_{J1} + \\ \left[-4\left(S_y I_{1z} I_{2z} c_{J1} s^2_{J1} + S_y I_{1z} I_{3z} c_{J1} s^2_{J1} + S_y I_{2z} I_{3z} c_{J1} s^2_{J1} \right) \right] c_{J2} \end{array} \right\} \xi_2 + \\
& \left\{ \left(\overset{(b)}{-3S_y s_{J2} c^2_{J2}} \right) s_{J1} \right\} \xi_1
\end{aligned}
$$

1.19

where terms (a) represent coherence that has originated from S and terms (b) represent coherence that has originated from polarisation transfer. Multiple quantum coherence T_2 relaxation [4] during τ_2 has not been considered so that the intensity factor ξ_2 is still relevant to the multiplet anomaly coherences that were created by the y-phase purge pulse.

Using a y-phase purge pulse in PENDANT experiments is unsuitable for the effective purging of all anomaly-causing coherences for SI_2 and SI_3 multiplicities. Application of an x-phase purge pulse is suitable because it does not cause the re-conversion of heteronuclear multiple quantum coherences back into multiplet anomaly-causing coherences. This is due to the fact that the I_x coherences, which were created by the proton polarisation transfer pulse, P_5, remain invariant to the x-phase pulse. Therefore, in contrast to INEPT$^+$, and contrary to that implied in the original publication, the specification of the phase of the purge pulse

appended to PENDANT is critical.

The purged version of PENDANT utilising an x-phase purge pulse, hereafter referred to as PENDANT^{+}-x, gives rise to spectra with multiplets displaying a binomial distribution of intensities of their component lines. Observable coherence is a superposition of residual in-phase coherence and in-phase coherence originating from polarisation transfer.

1.8.1 Experimental proof for the use of an x-phase purge pulse in PENDANT

In order to justify the theoretical comments made above for the prescription of an x-phase purge pulse for use in PENDANT, the following experimental methodology was employed.

A basic PENDANT pulse sequence was modified by the inclusion of a purge pulse immediately prior to acquisition with either x or y-phase, i.e., PENDANT^{+}-x and PENDANT^{+}-y respectively (Figure 1.10).

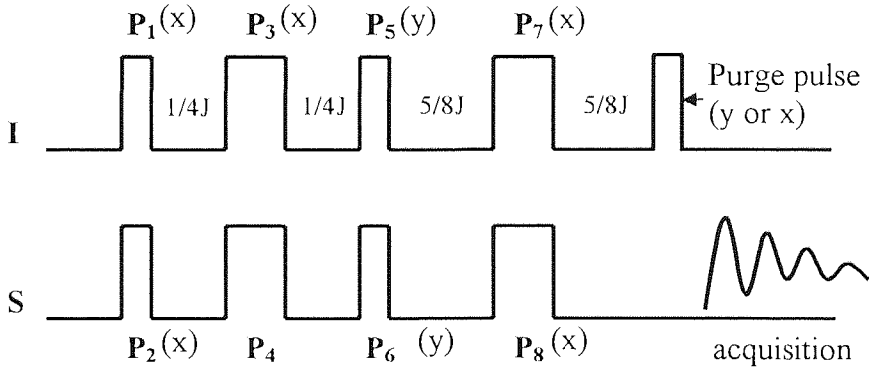

Figure 1.10 **PENDANT^{+}-(x and y)**

PENDANT^{+}-x and PENDANT^{+}-y experiments were performed and their spectra compared to a normal PENDANT and direct detect ^{13}C spectrum. All PENDANT experiments were performed using identical parameters. The direct detect ^{13}C spectrum acts as a control spectrum, since by definition, it is devoid of multiplet and phase anomalies and exhibits a binomial distribution of intensities of the component lines.

Appendix A3 and A4 describes the standard experimental procedures for the preparation, acquisition of and processing of NMR spectra, which are valid for all experimental work undertaken. Appendix A4.5 provides information regarding pulse program language and spectrum acquisition parameters.

1.8.2 Materials and Equipment

Experiments were performed using a sample of 60/40, vol/vol., ethyl-5-(chloromethyl)-2-furan-carboxylate and duetero chloroform respectively, the latter providing field –frequency locking. Experiments were performed using a Bruker Avance 300MHz NMR spectrometer with 5mm $^{13}C - {}^{1}H$ dual probe.

1.8.3 Acquisition parameters

All PENDANT experiments were performed in the standard way as recommended for routine analysis, i.e., to achieve nominal spectral editing with τ_1 and τ_2 set to 1/2J and 5/4J respectively for <J> = 145Hz. 16 transients were collected for each experiment and a 3 second relaxation delay (D_r) was used.

SW was set to encompass the entire chemical shift range of the solute using TD = SI = 32K, providing adequate digital resolution of 0.37Hz, to ensure correct representation of signal intensity and multiplet structure. ^{13}C spectra were acquired at 300K and the carrier frequency for both ^{1}H and ^{13}C was set at the centre of the solute chemical shift range of each.

1.8.4 Spectrum processing

All ^{13}C spectra were processed using line broadening of 1Hz. All spectra were phase corrected to the same parameters. All spectra are presented in absolute intensity scaling mode for comparison purposes.

1.9 Results and Discussion

For convenience figure 1.11, overleaf displays the spectra of figure 1.8 again for means of comparison. Figures 1.12 and 1.13 on the next page illustrate the PENDANT^{+}-y and PENDANT^{+}-x spectra respectively.

The enclosed region containing the CH_3 multiplet and CH_2 multiplets (a, b and c) in figure 1.11, adequately illustrate the phase and multiplet anomalies inherent to all multiplets. Therefore figures 1.12 and 1.13 specify only these regions for means of simple comparison.

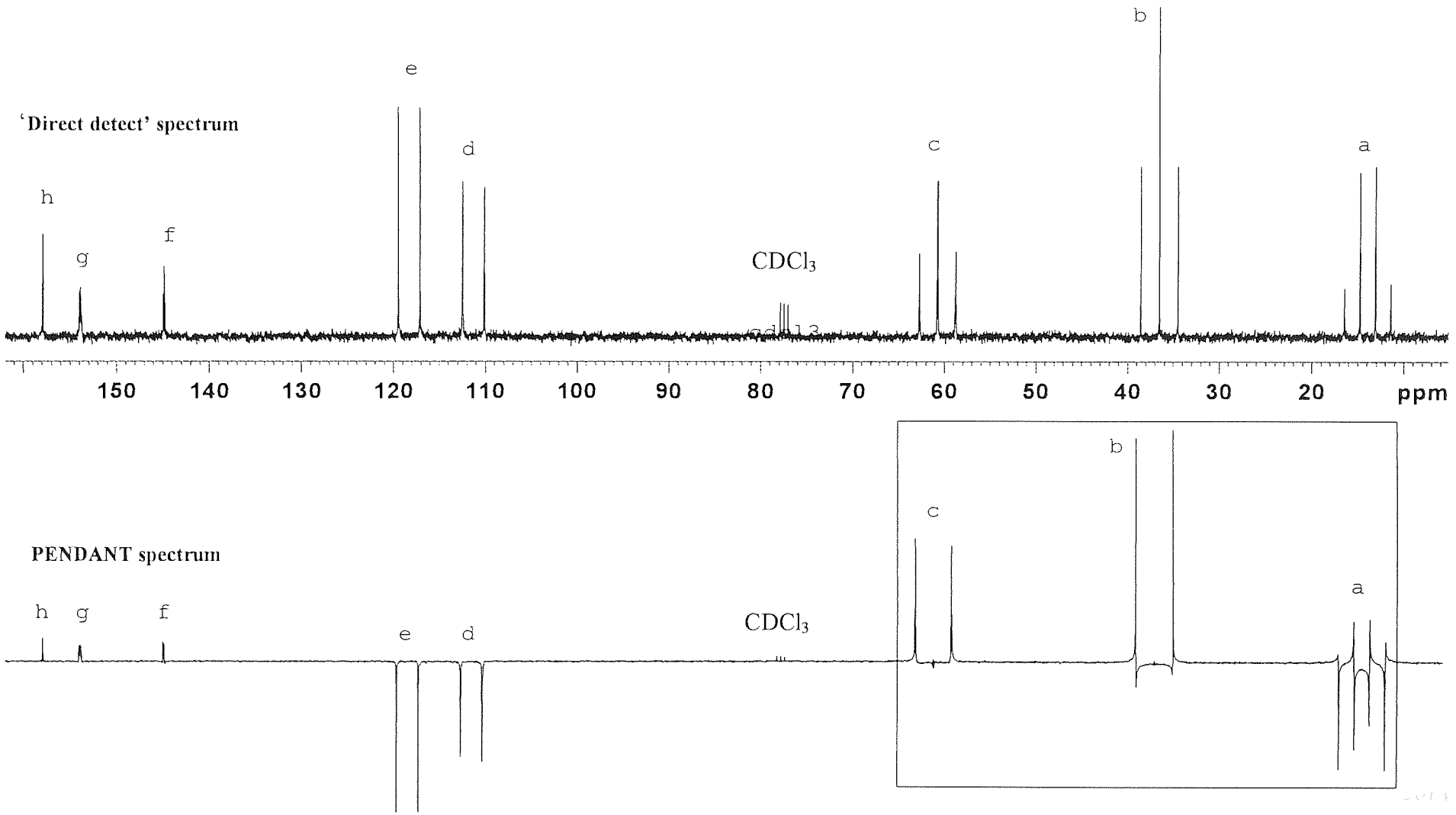

Figure 1.11 Multiplet and phase anomalies in a typical non-proton broadband decoupled PENDANT spectrum.

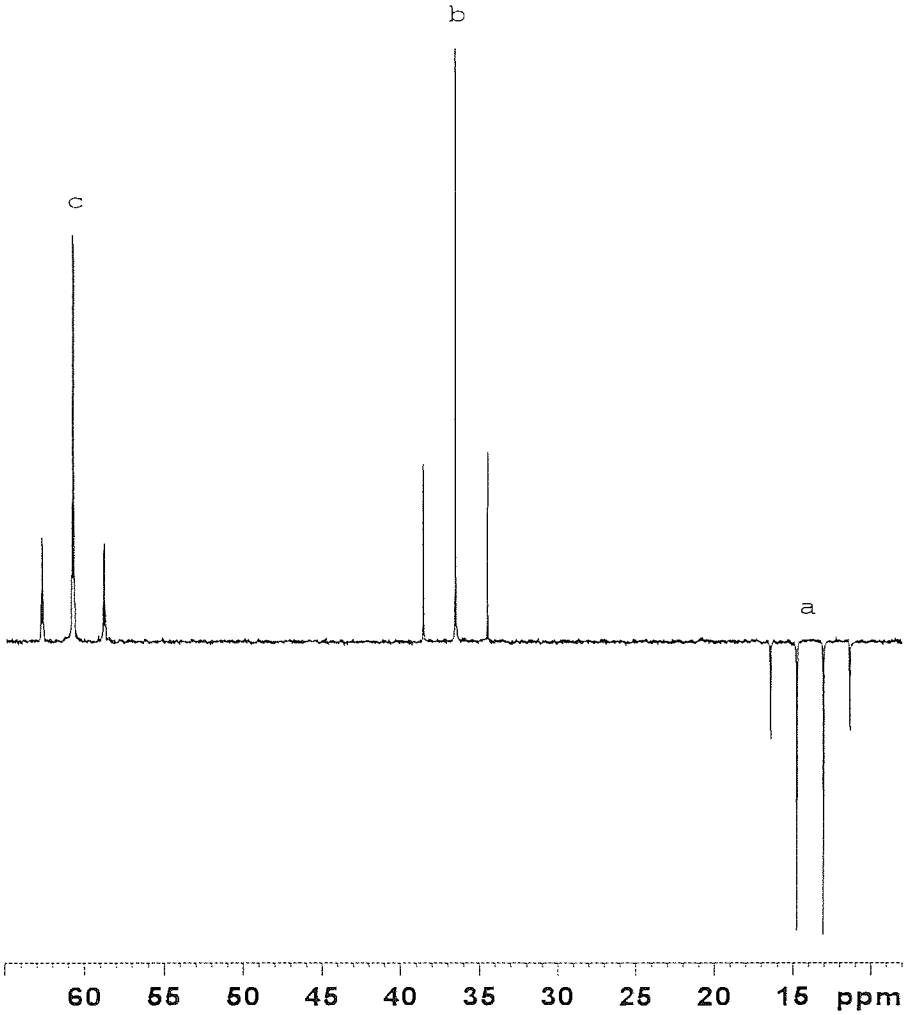

Figure 1.12 – PENDANT^{+}-y. Phase anomalies of multiplets a and b have been successfully purged. However, multiplets a, b and c exhibit multiplet anomalies as predicted.

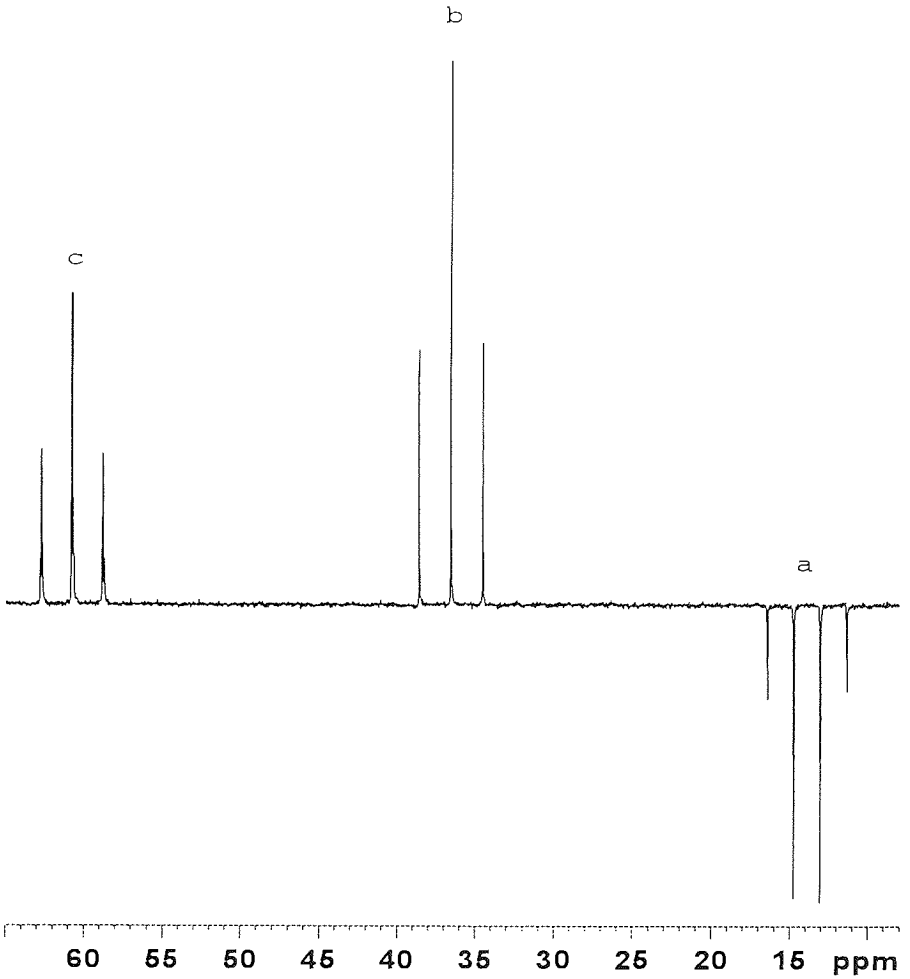

Figure 1.13 – PENDANT^{+}-x. Phase and multiplet anomalies have been successfully purged for a, b and c as predicted.

It is clearly visible in figure 1.11 the characteristic multiplet anomalies indicative of polarisation transfer and phase anomalies, giving rise to the dispersive line-shapes. Figure 1.12 clearly illustrates the utility of the y-phase purge pulse to purge the spectrum of phase anomaly-causing coherences, since all dispersive contributions to lines-shapes have been removed. However, upon inspection of the relative intensities of the component lines of the CH_2 multiplicities, it is evident that by comparison to figure 1.11, that a binomial (or near binomial) intensity distribution has not been restored.

As predicted, the y-phase purge pulse has indeed reconverted residual S phase heteronuclear triple quantum coherence into multiplet anomaly-causing single quantum coherence. The anomaly-causing coherence is superimposed upon both in-phase residual coherence and S coherence that originates from polarisation transfer from I.

Figure 1.13 clearly demonstrates the necessity of using a x-phase purge pulse. Both phase and multiplet anomalies have been purged from the spectrum, restoring binomial intensities of the CH_2 and CH_3 multiplicities.

Three further experiments were performed, using two modified PENDANT$^+$-y pulse sequences and a modified PENDANT experiment, to prove that the y-phase purge pulse does indeed excite multiplet anomaly-causing coherence from heteronuclear multiple quantum coherence:

1. A PENDANT pulse sequence without the first proton pulse, P_1.
2. A PENDANT$^+$-y pulse sequence without the first proton pulse, P_1.
3. PENDANT$^+$-y pulse sequence with the first S pulse, P_2, phase cycled (phase inverted) such that detectable carbon coherence cancels with respect to the nominal constant receiver phase cycling.

- Experiment (1), in common with the previous section, facilitates detection of residual S coherences only, since polarisation transfer from I to S is no longer achieved due to the removal of the first proton pulse.
- Experiment (2) facilitates the detection of the superposition of residual in-phase S coherence and residual multiplet anomaly coherence only, the latter being excited by the y-phase purge pulse.

- Experiment (3) facilitates the detection of S coherence that originates only from polarisation transfer from I.

Figures 1.14, 1.15 and 1.16 overleaf illustrate the spectra of experiments (1), (2) and (3) respectively, focusing on multiplets **a**, **b** and **c**. Figure 1.14 clearly demonstrates once more the efficiency of the purging of residual coherence by the polarisation exchange pulses in PENDANT as described in the previous section. Figure 1.15 clearly demonstrates the presence of multiplet anomaly-causing coherence during detection, i.e., the anti-phase multiplet pattern indicative of $4S_yI_zI_z$, given previously in figure 1.7 that has been excited due to the y-phase purge pulse.

Figure1.16 clearly demonstrates the efficient purging of phase and multiplet anomaly-causing coherences by the y-phase purge pulse which acts upon S coherence, which originates from polarisation transfer from I only.

PENDANT spectra of S nuclei, which exhibit short-range scalar coupling, are the superposition of coherences that originate from residual coherence and that, which originates from polarisation transfer from I. Therefore, the addition of the spectra in figures 1.15, and 1.16 gives rise to the PENDANT$^+$-y spectrum of figure 1.12. Indeed, this is the case, and by inspection of figures 1.14, and 1.15 it can be easily envisaged that the outer lines of the CH_2 multiplet would appear with significantly attenuated intensity with respect to the enhanced centre line. This is exactly the same as figure 1.12.

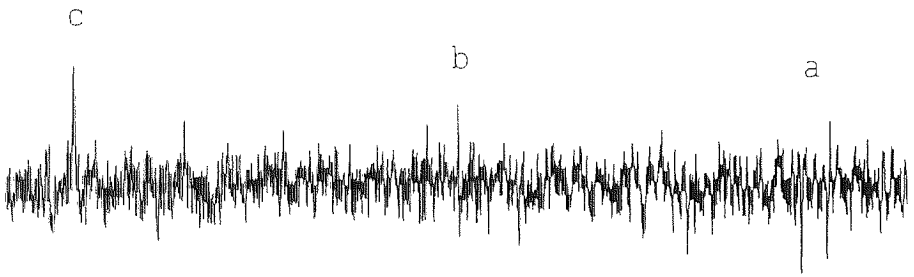

Fig 1.14 - PENDANT without first proton pulse

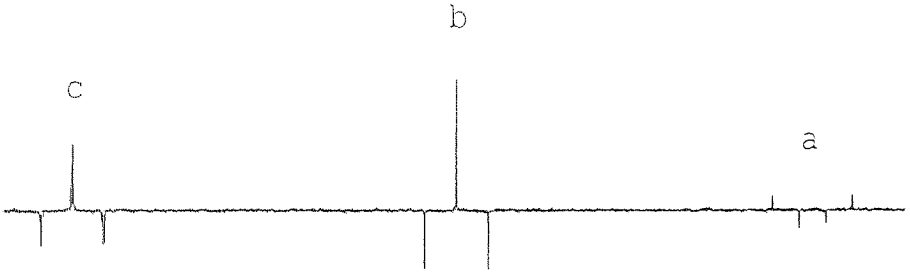

Figure 1.15 - PENDANT^{+}-y without first proton pulse

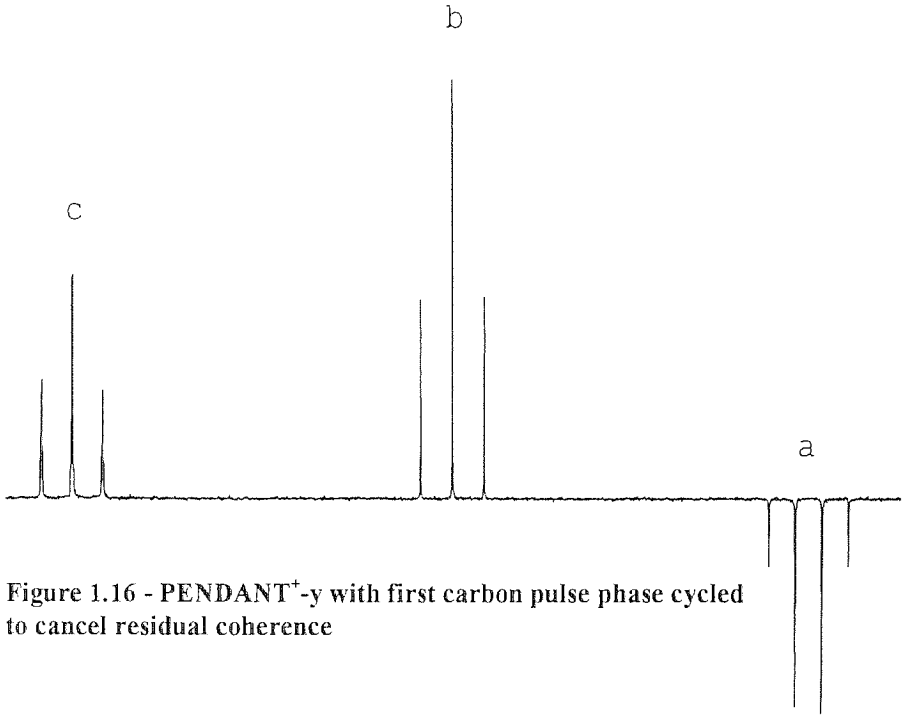

Figure 1.16 - PENDANT^{+}-y with first carbon pulse phase cycled to cancel residual coherence

1.10 Conclusion

It has been shown that the specification of an x-phase purge pulse applied to I nuclei in PENDANT^{+} (PENDANT^{+}-x) is critical to the removal of both phase and muliplet anomaly-causing coherences for the acquisition of proton coupled spectra. The requirement for the specification of a x-phase pulse in contrast to e.g., INEPT^{+}, is due to the unique symmetric structure of the PENDANT pulse sequence and its subsequent phase cycling, which enables the simultaneous detection of quaternary nuclei. This feature of the PENDANT experiment necessitates the excitation of heteronucelar triple quantum coherence that originates from residual S coherences, by the polarisation exchange pulses. The unique phase of this coherence necessitates the use of a x-phase purge pulse to prevent its subsequent re-conversion to multiplet anomaly-causing coherence prior to acquisition.

Therefore, the original publication by Homer and Perry is slightly misleading by not defining a specific phase of purge pulse for which the correct performance of the PENDANT^{+} experiment is critical.

Chapter 2 Development of selective PENDANT for the identification of long-range heteronuclear scalar couplings and observation of the complete quaternary spin-system

Further to the basic analysis of short-range heteronuclear scalar couplings, the analysis of heteronuclear long-range scalar couplings is often central to the complete elucidation of molecular structure. The analysis of heteronuclear long-range scalar couplings is particularly useful for the assignment of quaternary nuclei, e.g., ^{13}C. Quaternary nuclei are often the hub of important chemical functional groups, e.g., chiral centres, acid and ester functions, etc, and the analysis of their long-range scalar couplings to protons proves useful for the characterisation of carbon backbones in organic molecules.

When modern NMR spectrometers are available, inverse (^{1}H detected) 2-D techniques like HMBC [1, 10-11], can be used to correlate insensitive nuclei, e.g., ^{13}C, to sensitive nuclei, e.g., protons that exhibit mutual long-range scalar coupling. HMBC experiments are routinely performed in less than one hour due to the high sensitivity of inverse techniques. Furthermore only small concentrations of the molecule in solution is required, making these experiments highly attractive to synthetic chemists.

A vast number of NMR users possess older spectrometers, which are not amenable to inverse techniques, and have to rely upon less sensitive experiments, which utilise direct detection of the insensitive nucleus. For example, the 2-D techniques, COLOC, HETCOR, and their many derivatives [1, 10-11, 15,16], routinely require acquisition of spectra over several hours to obtain adequate signal-to-noise ratios (S/N). Furthermore, greater concentrations of the molecules under scrutiny are required. Selective 1-D analogues of these 2-D techniques are particularly attractive when only a few selected correlations are required for analysis, thus considerably reducing the experimental time.

Of course, the pre-requisites for the implementation of selective techniques must be amenable to the molecule under scrutiny, i.e., well resolved proton spectra devoid of spectral crowding and resonance overlap. In molecules where these pre-requisites are satisfied,

selective polarisation transfer techniques like selective INEPT [16] (a modified refocused INEPT experiment, whereby all hard proton pulses are replaced by selective pulses) provide fast and sensitive means for determining unambiguously, insensitive nuclei that are long-range scalar coupled to selected proton(s). This is because the selective proton pulses (Appendix A10) manipulate only those protons in molecules that are bonded to ^{12}C (Appendix A3.2.7). Therefore, polarisation transfer only occurs to those ^{13}C nuclei that exhibit long-range scalar coupling to the selected proton. Consequently the resulting spectrum only displays signals for ^{13}C nuclei that exhibit long-range scalar coupling to the selected proton, hence automatically providing the correlation.

Selective INEPT (hereafter referred to as INAPT, which is the popularly adopted alternative acronym [1]) has received wide spread use in for example the characterisation of natural products via structurally interesting long-range scalar couplings over three bonds [17 and multiple references therein]. Such extensive use of INAPT confirms the importance of selective one-dimensional long-range correlation techniques. However, one significant disadvantage with all INEPT-like experiments is their inability to directly detect quaternary nuclei. INAPT only identifies quaternary nuclei that exhibit long-range scalar coupling to the selected proton, while all other quaternary nuclei remain unobservable.

Although still of particular use, INAPT fails to identify quaternary nuclei that may not share scalar coupling with the selected protons or are devoid of scalar couplings. This necessitates another experiment be performed for the identification of all quaternary nuclei in the sample, e.g., PENDANT, DEPTQ, SEMUT $GL^{+}(q)$ [3] or pulsed field gradient (PFG) selected experiments [18].

It is apparent that it would be of particular use to develop a technique that shares the properties of INAPT, with the added advantage of simultaneously identifying all quaternary nuclei, which do not exhibit scalar coupling to the selected proton, or are devoid of scalar couplings. This type of experimental method would establish the technique as a tool for routine analysis; the experimenter would no longer require further experiments to identify other quaternary nuclei that may exist. The experimenter would then be in a position to decide whether to proceed with further selective experiments in order to identify their scalar couplings, should they exist. Such an experimental technique would reduce overall experiment time and be ultimately more convenient, since a separate experiment to determine

all quaternary nuclei would no longer be required.

To this end a long-range selective PENDANT pulse sequence was invented: the PENDANT experiment inherently detects all quaternary nuclei, while simultaneously causing polarisation transfer from the selected proton(s) (as a part of polarisation exchange) to insensitive nuclei and hence identifying their long-range scalar couplings.

Usually, the selective analogues of polarisation transfer techniques, such as INAPT, are identical to their non-selective analogues, with the exception of the replacement of all hard pulses applied to the sensitive nucleus, with selective pulses. However, in the case of a selective PENDANT experiment this simple modification is not sufficient: the detection of quaternary nuclei by PENDANT necessitates the propagation of residual coherences originating from the insensitive nuclei, i.e., those that exhibit short-range scalar coupling to protons.

It has been shown previously that these residual signals do not usually constitute significant problems in PENDANT spectra. However, the effect of residual signals becomes a more important factor when converting PENDANT to a selective analogue. This is because residual coherences that do not exhibit long-range coupling to the selected proton, i.e., coherences that exhibit short-range scalar coupling only, will be visible in the spectrum, since they are not superimposed upon signals that have originated from polarisation transfer. This may potentially falsify assignments and certainly lead to a cosmetic degradation of the spectrum.

Therefore, as well as converting the PENDANT experiment to its selective analogue, by the inclusion of selective pulses applied to the sensitive nucleus, an additional pulse sequence element is also incorporated to suppress the residual coherences inherent to PENDANT experiments.

2.1 The suppression of residual coherences in a selective PENDANT experiment

The significant difference in magnitudes of heteronuclear long-range scalar couplings and heteronuclear short-range scalar couplings provides a basis for their separation, the latter

being at least one order of magnitude greater than the former.

Low pass J-filtering elements for heteronuclear spin systems have been invented for this purpose [10-11]. They are so called for their selective filtering of long-range coupled coherences, which exhibit low J-values, while suppressing coherences, which exhibit short-range coupling with higher J-values. The spectra of experiments containing low-pass J-filters contain the signals of the former, i.e., those that are due to quaternary nuclei, while the latter are largely suppressed. Similarly, quaternaries that do not exhibit scalar coupling pass the J-filter and are also observed in the spectrum.

The pulse sequence SEMUT $GL^{+}(q)$ [3, 19] (subspectral editing using a multiple quantum trap) for quaternaries (q), is an example of a low-pass J-filter for the detection of ^{13}C quaternary nuclei. The filter converts ^{13}C coherence, which exhibits short-range scalar to protons coupled to unobservable multiple quantum coherences, which are subsequently trapped and can no longer contribute to observable signals in the spectrum. Only quaternary nuclei, which exhibit long-range scalar coupling, or are devoid of scalar coupling, pass the filter, and are detected in the spectrum.

The SEMUT $GL^{+}(q)$ pulse sequence is shown in figure 2.1 and a qualitative description of its function is given here.

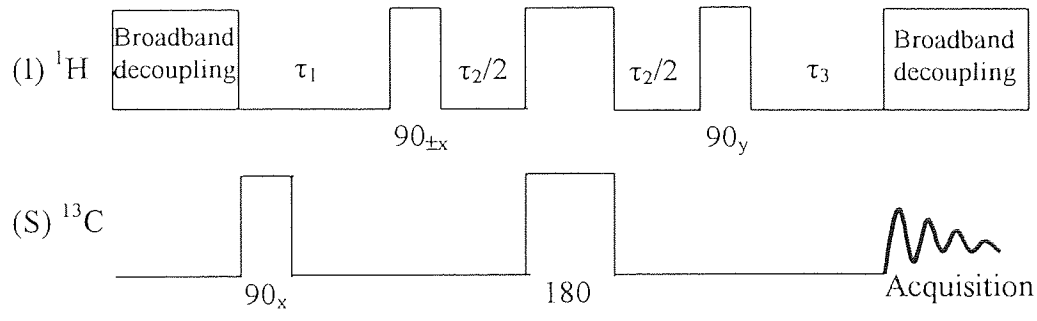

Figure 2.1 SEMUT GL^{+} (q) pulse sequence.

^{13}C coherence is excited by the first S pulse (90_x). All evolution delays, τ_1, τ_2 and τ_3 are different and take values which are optimised according to a recipe [3] for a typical range of short-range scalar coupling constants for ^{13}C-^{1}H. The evolution delays are set to 1/2J in order to maximise the evolution of short-range scalar coupling such that it approaches the maximum anti-phase condition, i.e., $2S_{x,y}I_z$. The two proton purge pulses with orthogonal

phases, separated by the evolution delay τ_2, convert ^{13}C single quantum coherence that is anti-phase with respect to the short-range coupling with ^{1}H, to unobservable multiple quantum coherence. The latter is subsequently trapped, since the orthogonal phases of the purging pulses prevent its subsequent re-conversion to observable single quantum coherence. All ^{13}C quaternary nuclei that exhibit long-range scalar couplings or are devoid of coupling, pass the J-filtering scheme relatively unaffected.

The efficiency of suppression of short-range coupled ^{13}C signals is largely dependent upon the judicious choice of the three evolution delays, which are designed to encompass the J range present in the molecule and hence maximise the evolution of all short-range scalar coupling multiplicities. SEMUT $GL^{+}(q)$ nominally achieves a high degree of suppression, c.a. 98% for a typical range of ^{13}C-^{1}H coupling constants found in most organic molecules.

A multiple quantum trap method of similar structure to SEMUT $GL^{+}(q)$ was deemed sufficient for the suppression of residual insensitive nuclear coherences in selective PENDANT and the propagation of quaternary coherence for detection.

The selective PENDANT pulse sequence is given in figure 2.2 overleaf, where the integrated J-filter element is indicated. Pulse phases relative to the first transient in the phase cycle are given in parentheses adjacent to the pulses. The labels σ_n indicate the various points at which the pulse sequence is analysed in subsequent sections.

2.2 Synopsis of the selective PENDANT experiment

A synopsis of the function of the selective PENDANT experiment is given here. Later on, a more thorough description is given using the product operator formalism in order to track the fate of insensitive (^{13}C) and sensitive (^{1}H) nuclear coherences during the experiment.

Unlike the multiple quantum trap utilised in SEMUT $GL^{+}(q)$, the structure of the low-pass J-filter and its integration into the selective PENDANT pulse sequence, is designed to give rise to maximum suppression, while not interfering with long-range polarisation transfer from the selected proton(s). The latter property was not required in the SEMUT $GL^{+}(q)$ experiment since it was designed merely to provide direct-detect quaternary-only spectra. Indeed, the low-pass J-filter in the selective PENDANT experiment is designed to yield a secondary function, namely the polarisation exchange step.

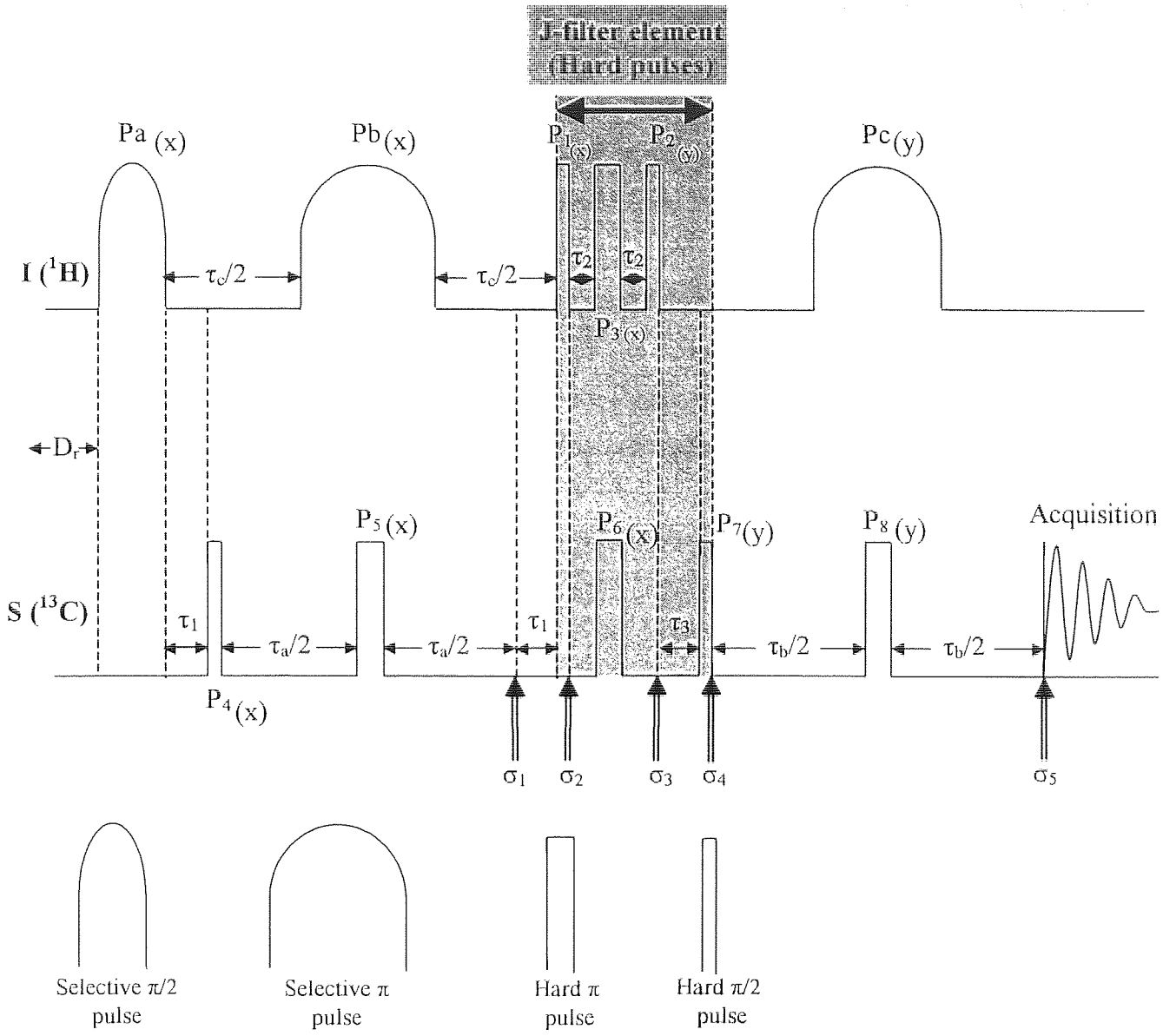

Figure 2.2 **Selective PENDANT pulse sequence.**

The positioning of the J-filter at the centre of the selective PENDANT pulse sequence, to simultaneously invoke the polarisation exchange step, is also implicit to the maintenance of suppression efficiency of the residual coherences. This is because, the number of S refocusing (π) pulses subsequent to the J-filter is minimised to one, in contrast to being positioned at the beginning of the pulse sequence. This is important, since refocusing pulses are a primary source of extraneous coherences, due to off-resonance effects, *r.f.* inhomogeneity and pulse nutation angle imperfections (Appendix A1.8.3) [20, 21, 22,]. It follows that, if less refocusing pulses are after the J-filter, the better the efficiency of suppression.

The structure of the low-pass J-filter differs from that of SEMUT $GL^+(q)$ in two important ways:

- the J-filter is comprised of three evolution delays τ_1, τ_2 and τ_3, however, in contrast to SEMUT $GL^+(q)$, $\tau_1 = \tau_3$. The equalisation of τ_1 and τ_3 is necessary to refocus the quaternary chemical shift prior to the application of pulse, P_7.

- The pulse P_7 is the ^{13}C polarisation exchange pulse. P_7 has the secondary function of purging ^{13}C coherences, which has a specific coupling order, which have evolved due to short-range coupling during τ_3. This property is demonstrated in the product operator analysis of the pulse sequence in subsequent sections.

By comparison with the J-filter element in SEMUT $GL^+(q)$ experiment, the differences in the J-filter element in selective PENDANT impacts slightly upon the efficiency of suppression of residual coherence. Firstly, the requirement that $\tau_1 = \tau_3$ in selective PENDANT, limits slightly the utility of the J-filter to suppress a larger range of short-range J-values. The strategy of the choice of τ_1 and τ_2 is less sophisticated as a result and is described later on. However, it is shown that the order selective purging effect caused by P_7, not only provides further suppression, which is missing in SEMUT $GL^+(q)$, but also provides a convenient method of discriminating the breakthrough of residual ^{13}C coherences that pass the J-filter and are present in the spectrum.

Selective PENDANT is inherently longer than SEMUT $GL^+(q)$, due to the fact that it is designed to yield long-range polarisation transfer. Consequently, the potential for recovery of ^{13}C magnetisation between refocusing pulses is increased. It follows that off-resonance effects etc, caused by the ^{13}C refocusing pulses, can lead to more drastic excitations of ^{13}C coherence. Subsequently, these coherences, which may exhibit short-range coupling, can potentially breakthrough into the spectrum and decrease the efficiency of suppression. Indeed, it has been proven that off-resonance effects are the primary source of breakthrough of residual coherences.

The pulse sequence elements prior to and after the J-filter element are, the excitation, scalar coupling evolution, and chemical shift refocusing elements, implicit with polarisation transfer and detection via PENDANT. Upon inspection of figure 2.2, it is evident that the first ^{13}C

pulse, P_4, is staggered in time with respect to the first proton pulse, P_a, by the amount τ_1, the reasons for which are explained later on in the product operator description. As the staggering of the ^{13}C pulse does not affect the spin-population dynamics, polarisation exchange, which is inherent to PENDANT, is also inherent to the selective PENDANT experiment.

2.3 Analysis of the Selective PENDANT experiment

Analysis of the experiment is facilitated using the product operator formalism [12] (Appendix A8) for the description of coherences present at the key numbered stages (σ_n) in the pulse sequence. The results of the transformations of the product operators according to the effect of the pulse sequence have been illustrated. However, their derivations have been omitted to prevent unnecessary lengthening of the analysis, which will only serve to protract the explanation. The overall effects of these various elements are generally well-known (Appendix A8) and so the transformations have been restricted to a qualitative description.

To ensure clarity, the fate of the insensitive (S) nuclei coherence is treated separately, i.e., quaternary coherence, residual short-range coupled coherence and residual coherence, which exhibits short-range coupling and also long-range coupling to the selected proton.

The product operator representation of coherence that originates from polarisation transfer from ^1H to ^{13}C, i.e., I to S, is illustrated separately later on. This is because it is identical to that already given for the PENDANT experiment in the previous chapter. Finally, all coherences contributing to observable signals are illustrated at the end. Computation of the product operators have been based upon the following assumptions, which will be fully addressed later:

- all selective pulses (Appendix A10) are pure-phase pulses acting over the entire proton multiplet, i.e., encompassing long-range heteronuclear couplings and proton homonuclear couplings, with uniform phase and intensity.
- All selective pulses are phase-coherent with hard pulses, i.e., a selective x-phase pulse corresponds exactly to an x-phase hard pulse.
- Relaxation during the selective pulse is assumed to be negligible and evolution due to scalar coupling during this time is also assumed zero.

The proton selective pulses are set on-resonance to cause excitation of coherence that exhibit

long-range heteronuclear scalar coupling and proton homonuclear coupling only, while leaving the short-range couplings unaffected. This is achieved by ensuring the selectivity of the selective pulse, or the excitation bandwidth, (Appendix A10) encompasses only the proton multiplet indicative of this coupling. This is achieved by setting the proton carrier frequency at the resonance frequency of the protons that are attached to ^{12}C, leaving the protons attached to ^{13}C, i.e., at the satellite frequencies, unaffected (Appendix A3.2.7).

2.4 Product operator description of the selective-PENDANT experiment

For reasons of clarity the following notations will be used to describe the various product operator coefficients:

$c_{Jn} = \cos \pi J_{IS} \tau_n$
$s_{Jn} = \sin \pi J_{IS} \tau_n$
$c_{\Omega 1} = \cos \pi \Omega \tau_n$
$s_{\Omega 1} = \sin \pi \Omega \tau_n$

S = insensitive nuclei = ^{13}C
I = sensitive nuclei = ^{1}H.

As it is assumed that all spins involved in short-range coupling are magnetically equivalent, the cosine (cos) and sine (sin) terms above do not discriminate between the spins involved, to save unnecessary lengthening of the terms.

2.4.1 Residual S coherences that exhibit short-range scalar coupling only and no long-range coupling to the selected proton

The density operator representing initial S magnetisation and the effective transformation up until σ_1 is given by:

$$S_Z \xrightarrow{(\pi/2+\pi_s)_x} +S_y . \qquad 2.1$$

The overall transformation caused by the pulse and delay cascade up until σ_1 causes excitation of in-phase S coherence as chemical shift and short-range scalar coupling evolution is refocused by the S inversion pulse at the centre of τ_a. The evolution of short-

range scalar coupling is prevented, as the selective proton inversion pulse is ineffective to coherences that do not exhibit long-range scalar coupling to the selected proton(s).

σ_1 signifies the start of the low-pass J-filter scheme. In order to maximise the conversion of short-range coupled single quantum coherence to unobservable multiple quantum coherence, the delay τ_1 is set to $\tau_1 = 2J_{SR}^{-1}$, where J_{SR} is the value chosen to encompass the typical short-range J-values of the ^{13}C-^{1}H couplings in the molecule. The optimisation of the J-filter delays is discussed later on. It will be assumed for completeness that $\tau_1 \neq 2J_{SR}^{-1}$ for all couplings.

During τ_1, short-range heteronuclear scalar coupling and chemical shift evolves. P_1 causes the excitation of heteronuclear multiple quantum coherence of orders determined by the number n of I_z operators present in the product operators. The effective transformation is given by:

$$\sigma_1 \xrightarrow{\Omega S_z \tau_1 + \pi J_{IS} \tau_1 2I_z S_z + (\pi/2_1)_x} \sigma_2 \qquad 2.2$$

$$\sigma_2 \quad SI \quad + S_y c_{\Omega 1} \overbrace{c_{J1}}^{(a)} - S_x s_{\Omega 1} c_{J1} + 2\left(S_x I_y c_{\Omega 1} s_{J1} + S_y I_y s_{\Omega 1} s_{J1}\right)$$

$$SI_2 \quad \overbrace{+ S_y c_{\Omega 1} \overbrace{c^2_{J1}}^{(a)} - S_x s_{\Omega 1} c^2_{J1}}^{(b)} + 2\left(S_x I_{1y} c_{\Omega 1} c_{J1} s_{J1} + S_y I_{1y} s_{\Omega 1} c_{J1} s_{J1} + S_x I_{2y} c_{\Omega 1} c_{J1} s_{J1} + S_y I_{2y} s_{\Omega 1} c_{J1} s_{J1}\right) \overbrace{- 4S_y I_{1y} I_{2y} c_{\Omega 1} s^2_{J1} + 4S_x I_{1y} I_{2y} s_{\Omega 1} s^2_{J1}}^{(b)}$$

SI_3 See overleaf

$$SI_3 \quad \overbrace{+S_y c_{\Omega 1} c^3{}_{J1} + S_x s_{\Omega 1} c^3{}_{J1}}^{(a)} \quad \overbrace{+2\begin{pmatrix} S_x I_{1y} c_{\Omega 1} c^2{}_{J1} s_{J1} + S_y I_{1y} c^2{}_{J1} s_{\Omega 1} s_{J1} + S_x I_{2y} c_{\Omega 1} c^2{}_{J1} s_{J1} + S_y I_{2y} s_{\Omega 1} c^2{}_{J1} s_{J1} \\ S_x I_{3y} c_{\Omega 1} c^2{}_{J1} s_{J1} + S_y I_{3y} s_{\Omega 1} c^2{}_{J1} s_{J1} \end{pmatrix}}^{(b)}$$

$$\overbrace{-4\begin{pmatrix} S_y I_{1y} I_{2y} c_{\Omega 1} c_{J1} s^2{}_{J1} - S_x I_{1y} I_{2y} s_{\Omega 1} c_{J1} s^2{}_{J1} + S_y I_{2y} I_{3y} c_{\Omega 1} c_{J1} s^2{}_{J1} - \\ S_x I_{2y} I_{3y} s_{\Omega 1} c_{J1} s^2{}_{J1} + S_y I_{2y} I_{3y} c_{\Omega 1} c_{J1} s^2{}_{J1} - S_x I_{2y} I_{3y} s_{\Omega 1} c_{J1} s^2{}_{J1} \end{pmatrix}}^{(b)}$$

$$\overbrace{-8S_x I_{1y} I_{2y} I_{3y} c_{\Omega 1} s^3{}_{J1} + S_y I_{1y} I_{2y} I_{3y} s_1 s^3{}_{J1}}^{(b)} \qquad 2.3$$

Multiple quantum coherences (terms (b)), i.e., product operators with more than one transverse operator, e.g., S_xI_y, remain trapped for the remainder of the experiment and are unobservable during acquisition due to the following reasons.

- Single quantum coherences that were converted to multiple quantum coherences, which had not evolved to the maximum coupling order, e.g., (terms (b)) SI_2 and $2S_xI_{1y}$, subsequently evolve due to passive couplings to the remaining I spins during τ_2. These coherences are converted into higher order multiple quantum coherences by P_2:

$$2S_x I_{1y} c_{\Omega 1} c_{J1} s_{J1} \xrightarrow{\pi J_{IS} \tau_2 2I_z S_z + (\pi/2_1)_y + (\pi_{I+S})_x} 2S_x I_{1y} c_{\Omega 1} c_{J1} s_{J1} c_{J2} - 4S_y I_{1y} I_{2x} c_{\Omega 1} c_{J1} s_{J1} s_{J2}. \qquad 2.4$$

Thient with the 'rules' governing the evolution of multiple quantum coherences using the product operator formalism (Appendix A8.2), whereby active spins do not evolve due to scalar coupling.

- Chemical shift is refocused over the τ_2 period. Therefore, coherences that have not evolved, due to passive short-range scalar couplings, i.e., I_y coherences, remain invariant to the P_2 y-phase pulse and are not re-converted to observable single quantum coherence.

In-phase residual single quantum coherences (terms (a)), which survived the first element of the J-filter, continue to evolve due to short-range scalar coupling during τ_2, while chemical shift is refocused. P_2 causes the excitation of multiple quantum coherence of orders determined by the number n of I_z operators present in the product operators, in the same manner as described above.

$$\sigma_2 \xrightarrow{\pi J_{IS}\tau_2 2I_zS_z + (\pi/2_1)_y + (\pi_{1+S})_x} \sigma_3$$

$$\sigma_3 \quad SI \quad \left[\overbrace{-S_y c_{\Omega 1} c_{J2} - S_x s_{\Omega 1} c_{J2}}^{(a)} + 2\left(S_x I_x c_{\Omega 1} s_{J2} - S_y I_x s_{\Omega 1} s_{J2}\right) \right] c_{J1}$$

$$SI_2 \quad \left[\begin{array}{l} \overbrace{-S_y c_{\Omega 1} c^2_{J2} - S_x s_{\Omega 1} c^2_{J2}}^{(a)} \\ +2\left(S_x I_{1x} c_{\Omega 1} c_{J2} s_{J2} - S_y I_{1x} s_{\Omega 1} c_{J2} s_{J2} + S_x I_{2x} c_{\Omega 1} c_{J2} s_{J2} - S_y I_{2x} s_{\Omega 1} c_{J2} s_{J2}\right) \\ -4S_y I_{1x} I_{2x} c_{\Omega 1} s^2_{J2} + 4S_x I_{1x} I_{2x} s_{\Omega 1} s^2_{J2} \end{array} \right] c^2_{J1}$$

$$SI_3 \quad \left[\begin{array}{l} \overbrace{-S_y c_{\Omega 1} c^3_{J2} - S_x s_{\Omega 1} c^3_{J2}}^{(a)} \\ +2\left(\begin{array}{l} S_x I_{1x} c_{\Omega 1} c^2_{J2} s_{J2} - S_y I_{1x} s_{\Omega 1} c^2_{J2} s_{J2} + S_x I_{2x} c_{\Omega 1} c^2_{J2} s_{J2} \\ -S_y I_{2x} s_{\Omega 1} c^2_{J2} s_{J2} + S_x I_{3x} c_{\Omega 1} c^2_{J2} s_{J2} - S_y I_{3x} s_{\Omega 1} c^2_{J2} s_{J2} \end{array} \right) \\ -4\left(\begin{array}{l} S_y I_{1x} I_{2x} c_{\Omega 1} c_{J2} s^2_{J2} - S_x I_{1x} I_{2x} s_{\Omega 1} c_{J2} s^2_{J2} + S_y I_{2x} I_{3x} c_{\Omega 1} c_{J2} s^2_{J2} - \\ S_x I_{2x} I_{3x} s_{\Omega 1} c_{J2} s^2_{J2} + S_y I_{2x} I_{3x} c_{\Omega 1} c_{J2} s^2_{J2} - S_x I_{2x} I_{3x} s_{\Omega 1} c_{J2} s^2_{J2} \end{array} \right) \\ +8S_x I_{1x} I_{2x} I_{3x} c_{\Omega 1} s^3_{J2} - S_y I_{1x} I_{2x} I_{3x} s_{\Omega 1} s^3_{J2} \end{array} \right] c^3_{J1}$$

2.5

In-phase coherences (terms (a)), which have survived the entire low pass J-filter evolve due to short-range scalar coupling during τ_3, while evolution due to chemical shift during τ_1 has been refocused prior to P_7, since $\tau_1 = \tau_3$. As mentioned previously, P_7 is the ^{13}C polarisation

exchange pulse.

$$\sigma_3 \xrightarrow{\pi J_{IS}\tau_3 2I_zS_z+(\pi/2_S)_y} \sigma_4 \qquad 2.6$$

$$\sigma_4 \quad SI \quad \left[-S_y \overset{(a)}{c_{J3}} - 2S_z \overset{(b)}{I_z} s_{J3} \right] c_{J1} c_{J2}$$

$$SI_2 \quad \left[-S_y \overset{(a)}{c^2_{J3}} \overbrace{-2\left(S_z I_{1z} c_{J3} s_{J3} + S_z I_{2z} c_{J3} s_{J3}\right)}^{(b)} + 4S_y I_{1z} \overset{(c)}{I_{2z}} s^2_{J3} \right] c^2_{J1} c^2_{J2}$$

$$SI_3 \quad \left[\begin{array}{l} \overbrace{-S_y \overset{(a)}{c^3_{J3}} - 2\left(S_z I_{1z} c^2_{J3} s_{J3} + S_z I_{2z} c^2_{J3} s_{J3} + S_z I_{3z} c^2_{J3} s_{J3}\right)}^{(b)} \\ \overbrace{+4\left(S_y I_{1z} I_{2z} c_{J3} s^2_{J3} + S_y I_{1z} I_{3z} c_{J3} s^2_{J3} + S_y I_{2z} I_{3z} c_{J3} s^2_{J3}\right)}^{(c)} \\ -8S_z I_{1z} \overset{(d)}{I_{2z}} I_{3z} s^3_{J3} \end{array} \right] c^3_{J1} c^3_{J2}$$

2.7

The y-phase pulse, P_7, causes odd coupling-order purging, i.e., coherences with S_x phase, terms (b and d), which correspond to odd numbers of I_z operators in the product operator, e.g., $2S_xI_z$ and $8S_xI_zI_zI_z$ for SI and SI_3.

In-phase S_y coherence, terms (a) and multiplet anomaly coherence, terms (c) remain invariant to the y-phase pulse, P_7. Therefore, residual coherence that passes the J-filter of short-range scalar coupling multiplicities SI_n where, $n > 1$ is a superposition of in-phase and multiplet anomaly-causing coherences. All observable residual coherences are significantly attenuated by the low pass J-filter. The level of attenuation/suppression is dependent upon the judicious choice of the durations of τ_1 and τ_2.

Observable residual in-phase and multiplet anomaly-causing coherence, terms (a) and (c), respectively, survive until acquisition; as evolution due to chemical shift and short-range scalar coupling is refocused during the final period τ_b. The observable residual signals in the final spectrum are represented thus.

$$\sigma_4 \xrightarrow{(\pi/2+\pi_s)_y} \sigma_5 \qquad 2.8$$

$$\sigma_5 \qquad SI \qquad \left\{\left[-S_y^{(a)} c_{J3}\right] c_{J1} c_{J2}\right\}\xi_2$$

$$SI_2 \qquad \left\{\left[-S_y^{(a)} c^2_{J3} + 4S_y I_{1z} I_{2z}^{(c)} s^2_{J3}\right] c^2_{J1} c^2_{J2}\right\}\xi_2$$

$$SI_3 \qquad \left\{\left[\begin{array}{l} -S_y^{(a)} c^3_{J3} \\ \\ +4\left(\begin{array}{l} S_y I_{1z} I_{2z}^{(c)} + S_y I_{1z} I_{3z} \\ + S_y I_{2z} I_{3z} \end{array}\right) c_{J3} s^2_{J3} \end{array}\right] c^3_{J1} c^3_{J2}\right\}\xi_2 \qquad 2.9$$

Where ξ_2 represents a proportionality constant depicting the dependence of the magnitude of the coherences on γ_S and:

- longitudinal relaxation of S between, during acquisition and after the relaxation delay (D_r)
- T_2 relaxation of S during the pulse sequence.

Therefore, the multiplets of breakthrough signals in the spectrum for CH_2 and CH_3 multiplicities, will exhibit multiplet anomalies. This serves as a convenient way of identifying small breakthrough of residual signals of these multiplicities.

2.4.2 Short-range coupled S nuclei that also exhibit long-range coupling to the selected proton

The effect of the pulse sequence upon these S coherences that exhibit short-range scalar

coupling and also long-range scalar coupling to the selected proton is presented here in a qualitative fashion so as to avoid lengthy product operator descriptions. The principles implicit in the description of the observable coherences due to these couplings have already been established by the treatments of the couplings given above.

The period τ_a causes evolution due to long-range scalar coupling while evolution due to chemical shift and short-range coupling is refocused at σ_1. The low-pass J-filter serves to further evolve coherences due to short-range couplings and chemical shift during τ_1, while the evolution of long-range couplings remain invariant. The number of I_z operators present in the product operators during the J-filter can give rise to a maximum of 6. This is because evolution of long-range scalar couplings during τ_a can involve a maximum of 3 protons since the proton selective pulse can only effect a maximum of 3 protons, i.e., a methyl group (assuming no spectral overlapping). Similarly, the maximum number of short-range coupled protons is also 3, i.e., 3 protons in a methyl group.

By analogy with exclusively short-range coupled coherence, P_7 causes odd-coupling order purging of the small magnitudes of residual coherence, which has survived the J-filter. Consequently, for short-range coupling multiplicities of SI_n, when $n>1$, residual coherences exhibit superposition's of in-phase and multiplet anomaly-causing coherences.

Evolution due to long-range scalar coupling occurs during the final evolution period τ_b, while the effects of short-range couplings and chemical shift are refocused at σ_5. For illustrative purposes, the product operator description of the observable residual coherences for SI_SI_L and $SI_{S2}I_{L2}$ are given below. Where SI_SI_L represents a doublet of doublets, according to short-range scalar coupling to one proton I_S and long-range scalar coupling to one proton I_L and $SI_{S2}I_{L2}$ represents a triplet of triplets.

The state of S coherence, which exhibits short-range scalar coupling and long-range scalar coupling to the selective proton is given by:

$$SI_SI_L \quad \left\{ + S_y c_{JbL} - 2S_x I_z s_{JbL} \right\} c_{JaL} c_{J1S} c_{J2S} \Big\}_{\sigma 2}$$

$$SI_{S2}I_{L2}\left\{\begin{bmatrix}+S_y c^2{}_{JbL}-2\left(S_x I_{1z} c_{JbL} s_{JbL}+S_x I_{2z} c_{JbL} s_{JbL}\right)\\-4S_y I_z I_z s^2{}_{JbL}\end{bmatrix} c^2{}_{JaL} c^2{}_{J1S} c^2{}_{J2S} c_{J3S}\right\}\xi_2$$

$$\left\{\begin{bmatrix}+4S_y I_{S1z} I_{S2z} c^2{}_{JbL}\\-8\left(S_x I_{S1z} I_{S2z} I_{L1z} c_{JbL} s_{JbL}+S_x I_{S1z} I_{S2z} I_{L2z} c_{JbL} s_{JbL}\right)\\+16S_y I_{S1z} I_{S2z} I_{L1z} I_{L2z} s^2{}_{JbL}\end{bmatrix} c^2{}_{JaL} c^2{}_{J1S} c^2{}_{J2S} s^2{}_{J3S}\right\}\xi_2$$

2.10

Where I_{Ln} represents the number n of long-range coupled I_L nuclei and I_{Sn} represents the number, n, of short-range coupled I_S nuclei. The functions e.g., $c^n{}_{JbL}$, represent the evolution during τ_b for long-range scalar coupling to nuclei I_L.

Residual S coherence, which exhibits long-range coupling to the selected proton is attenuated in the same manner as short-range coupled residual S coherence in PENDANT: the magnitude of the residual coherence is proportional to $c^n{}_{Ja}$ (the first evolution period), and the actual value of J as compared to the average value of <J> from which τ_a is set. As such the, level of suppression of residual coherence, which exhibits long-range scalar coupling to the selected proton as well as short-range scalar coupling will always be more efficient than residual coherence that exclusively exhibits short-range scalar coupling. This is due to the extra, $c^n{}_{JaL}$ function of the former.

2.4.3 S coherences that exhibit exclusive long-range scalar coupling to the selected proton: quaternary nuclei

Quaternary nuclei that exhibit long-range scalar coupling to the selected proton, experience the effect of the first purge pulse by analogy with that shown previously for coherence that exhibits long-range coupling to the selected proton and short-range coupling. Evolution of long-range scalar coupling during the short-range coupling optimised delay, τ_1, of the low-pass J-filter, is ineffective, while evolution due to chemical shift is effective.

The product operator transformation at σ_1 is not given here since it is identical in construction to that given for the PENDANT earlier (Chapter 1.2). P_1 causes the excitation of multiple quantum coherence of orders determined by the number n of I_z operators present in the product operators. The overall transformation up until σ_2 is given by:

$$S_z \xrightarrow{(\pi/2_S)_X + \pi J_{IS}\tau_a 2I_zS_z + (\pi_{1+S})_X} \sigma_1 \xrightarrow{\Omega S_z\tau_1 + (\pi/2_1)_X} \sigma_2 \qquad 2.11$$

$$P_2 \quad SI \quad \overbrace{+S_y c_{\Omega 1} c_{Ja} - S_x s_{\Omega 1} c_{Ja}}^{(a)} + 2\left(S_x I_y c_{\Omega 1} s_{Ja} + S_y I_y s_{\Omega 1} s_{Ja}\right)$$

$$SI_2 \quad \overbrace{+S_y c_{\Omega 1} c^2_{Ja} - S_x s_{\Omega 1} c^2_{Ja}}^{(a)} + 2\left(S_x I_{1y} c_{\Omega 1} c_{Ja} s_{Ja} + S_y I_{1y} s_{\Omega 1} c_{Ja} s_{Ja} + S_x I_{2y} c_{\Omega 1} c_{Ja} s_{Ja} + S_y I_{2y} s_{\Omega 1} c_{Ja} s_{Ja}\right) - 4S_y I_{1y} I_{2y} c_{\Omega 1} s^2_{Ja} + 4S_x I_{1y} I_{2y} s_{\Omega 1} s^2_{Ja}$$

$$SI_3 \quad \overbrace{+S_y c_{\Omega 1} c^3_{Ja} + S_x s_{\Omega 1} c^3_{Ja}}^{(a)} + \begin{pmatrix} x\ I_{1y} 2_{\Omega 1} c^2_{Ja} s_{Ja} + S_y I_{1y} s_{\Omega 1} c^2_{Ja} s_{J1} + S_x I_{2y} c_{\Omega 1} c^2_{Ja} s_{Ja} + S_y I_{2y} s_{\Omega 1} c^2_{Ja} s_{Ja} \\ S_x I_{3y} c_{\Omega 1} c^2_{Ja} s_{Ja} + S_y I_{3y} s_{\Omega 1} c^2_{Ja} s_{Ja} \end{pmatrix} - 4\begin{pmatrix} S_y I_{1y} I_{2y} c_{\Omega 1} c_{Ja} s^2_{Ja} - S_x I_{1y} I_{2y} s_{\Omega 1} c_{Ja} s^2_{Ja} + S_y I_{2y} I_{3y} c_{\Omega 1} c_{Ja} s^2_{Ja} - \\ S_x I_{2y} I_{3y} s_{\Omega 1} c_{Ja} s^2_{Ja} + S_y I_{2y} I_{3y} c_{\Omega 1} c_{Ja} s^2_{Ja} - S_x I_{2y} I_{3y} s_{\Omega 1} c_{Ja} s^2_{Ja} \end{pmatrix} - 8S_x I_{1y} I_{2y} I_{3y} c_{\Omega 1} s^3_{Ja} + S_y I_{1y} I_{2y} I_{3y} s_{\Omega 1} s^3_{Ja}$$

2.12

Therefore, by analogy with the proton polarisation exchange pulse in PENDANT, the pulse P_1 has caused the purging of all anti-phase coherences, which are long-range coupled to the selected proton(s)

During the short-range coupling optimised delay, τ_2, chemical shift evolution is refocused and evolution due to long-range scalar coupling is ineffective. All I coherences above are invariant to the y-phase pulse P_2 and thus remain trapped.

During τ_3, the residual coherences (terms (a)), which survived the low pass J-filter are refocused due to chemical shift that occurred during τ_1, since $\tau_1 = \tau_3$. The chemical shift of S single quantum coherence that had developed during τ_1, (which is now component to the

heteronuclear multiple quantum coherences) does not refocus due to chemical shift. This is because the chemical shift evolution of multiple quantum coherence is inherently different and only partial refocusing may occur [12] (Appendix A8.2.9.1). This has no bearing upon the experiment since these coherences remain unobservable.

S_y in-phase coherences (terms (a)) remain invariant to the y-phase polarisation exchange pulse P_7. Therefore, the transformation for in-phase single quantum coherence of S is given by:

$$\sigma_2 \xrightarrow{\pi J_{IS}\tau_2 2I_zS_z + (\pi/2_I)_y + (\pi_{I+S})_x} \sigma_3 \xrightarrow{\Omega S_z\tau_3 + (\pi/2_S)_y} \sigma_4 \qquad 2.13$$

Therefore, the residual observable coherence to pass the J-filter is given by:

$$\begin{array}{lll} \sigma_4 & SI & -S_y c_{Ja} \\ & SI_2 & -S_y c^2_{Ja} \\ & SI_3 & -S_y c^3_{Ja} \end{array} \qquad 2.14$$

It is demonstrated in subsequent sections that the purge pulse P_2 initiates polarisation transfer from the selected proton. The effect of the purge pulse, P_2, and the pulse, P_7, upon coherence that originates from insensitive nuclei are not entirely analogous to the effect of the polarisation exchange pulses in PENDANT. This is due to the fact that the two pulses are staggered: the chemical shift evolution of heteronuclear multiple quantum coherence during τ_3 necessitates only partial refocusing of that which occurred for S single quantum coherence during τ_1. The reverse transfer of polarisation from S to I is therefore different. However, polarisation transfer in the reverse sense is of no importance for selective PENDANT and it will be shown that polarisation transfer in the forward sense, i.e., from I to S (^{1}H to ^{13}C) is unaffected, which is of prime importance.

Evolution of the residual coherences due to long-range scalar coupling to the selected proton occurs during the final period τ_b, while evolution due to chemical shift is refocused.

$$\sigma_4 \xrightarrow{\pi J_{IS}\tau_b 2I_zS_z+(\pi_{I+S})_X} \sigma_5$$

$$\sigma_5 \quad SI \quad \left\{+S_y c_{Jb} - 2S_x I_z s_{Jb}\right\} c_{Ja} \xi_2$$

$$SI_2 \quad \left\{+S_y c^2{}_{Jb} - 2\left(S_x I_{1z} c_{Jb} s_{Jb} + S_x I_{2z} c_{Jb} s_{Jb}\right) - 4S_y I_z I_z s^2{}_{Jb}\right\} c^2{}_{Ja} \xi_2$$

$$SI_3 \quad \left\{\begin{bmatrix} +S_y c^3{}_{Jb} - 2\left(S_x I_{1z} c^2{}_{Jb} s_{Jb} + S_x I_{2z} c^2{}_{Jb} s_{Jb} + S_x I_{3z} c^2{}_{Jb} s_{Jb}\right) \\ -4\left(S_y I_{1z} I_{2z} c_{Jb} s^2{}_{Jb} + S_y I_{1z} I_{3z} c_{Jb} s^2{}_{Jb} + S_y I_{2z} I_{3z} c_{Jb} s^2{}_{Jb}\right) \\ +8S_x I_{1z} I_{2z} I_{3z} s^3{}_{Jb} \end{bmatrix} c^3{}_{Ja} \right\} \xi_2$$

2.15

Residual S coherence that originates from quaternary nuclei, which exhibit long-range coupling to the selected proton is attenuated in the same manner as short-range coupled residual S coherence in PENDANT: the magnitude of the residual coherence is proportional to $c^n{}_{Ja}$ (the first evolution period), and hence the actual value of J as compared to the average value of <J> from which τ_a is set. Due to the potentially large variation of long-range J-values the efficiency of purging and hence the level of attenuation can vary dramatically between quaternaries that share coupling with the selected proton. Consequently, in contrast to PENDANT, the effects of superposition of residual quaternary coherence that is coupled to the selected proton and coherence that originates from polarisation transfer from I can be of greater significance. The effects of the superposition are discussed later.

2.4.4 Polarisation transfer from I to S

The structure and phase cycling of the selective PENDANT pulse sequence enables the J-filter to act in a unique way, namely by performing the two centrally important functions for selective PENDANT:

- to render short-range heteronuclear coupled S coherence unobservable.
- To cause polarisation exchange and hence polarisation transfer from I to S.

As the principles implicit to the description of polarisation transfer from I to S are similar to that of PENDANT, only one IS coupling is considered in the product operator description up until σ_4.

The staggering of the selective pulse P_a with respect to the first S pulse P_4 by the amount τ_1, ensures that I coherence evolves due to long-range scalar coupling with S during the delay τ_c, while chemical shift and proton homonuclear scalar couplings are refocused prior to application of P_1. Refocusing of proton homonuclear coupling is achieved via the selective inversion pulse at the centre of τ_c [16] (Appendix A8.2.8.4).

$$I_Z \xrightarrow{\pi J_{IS}\tau_c 2I_zS_z + (\pi_{1+S})_X} \text{Prior to } P_1$$

$$\text{Prior to } P_1: \quad \overset{(a)}{+I_y c_{Jc}} - \overset{(b)}{2I_x S_z s_{Jc}} \qquad 2.16$$

The desired anti-phase single quantum coherence prepared for polarisation transfer (term (b)) remains invariant to the x-phase hard proton pulse, P_1, of the J-filter. This is achieved over the entire course of the experiment via the mutual phase cycling of P_a and P_1.

The entire transformation up until σ_2 is given by:

$$I_Z \xrightarrow{(\pi/2_{Isel})_X + \pi J_{IS}\tau_c 2I_zS_z + (\pi_{Isel})_X(\pi_S)_X + (\pi/2_1)_X} \sigma_2$$

where the subscript (sel) indicates selective pulses applied to I.

$$\sigma_2 \qquad IS \qquad \overset{(a)}{+I_z c_{Jc}} - \overset{(b)}{2I_x S_z s_{Jc}} \overset{(c)}{- I_y} \qquad 2.17$$

P_1 also serves to return in-phase I coherence to +Z (term a) that possess cosine modulations due to heteronuclear long-range scalar coupling during τ_c (term (a) in expression 2.16). Furthermore, P_1 causes the excitation of proton single quantum coherences of all other protons in the spin system (term (c)). If these proton coherences exhibit short-range scalar coupling to S, short-range scalar coupling evolution takes place during τ_2 while chemical shift is refocused:

$$\overset{(c)}{-I_y c_{J2}} + \overset{(d)}{2I_x S_z s_{J2}} \qquad 2.18$$

Meanwhile, long-range scalar coupling evolution of the selected proton(s) coherences, (term (b)) is ineffective during the short-range coupling optimised delay, τ_2, and evolution due to chemical shift is refocused prior to P_2. Application of P_2 creates longitudinal two-spin order from I coherence, which exhibited long-range scalar coupling to S (term (b) in expression 2.17) but also creates longitudinal two-spin order from I coherence that exhibited short-range scalar coupling (term (d) in expression 2.18) as described above:

$$\sigma_2 \xrightarrow{\pi J_{IS}\tau_2 2I_z S_z + (\pi_{I+S})_X + (\pi/2_I)_Y} \sigma_3$$

$$\overset{(a)}{-I_x c_{Jc}} - \overset{(b)}{2I_z S_z s_{Jc}} + \overset{(c)}{I_y} + \overset{(d)}{2I_z S_z s_{J2}} \qquad 2.19$$

P_2 has also served to convert I_z magnetisation to I_x coherence, which exhibits cosine modulations due to heteronuclear long-range scalar coupling that evolved during τ_c (term (a)). This coherence is not observable in the S spectrum and is omitted hereafter. I_y coherence (term(c)) evolves due to chemical shift and short-range heteronuclear scalar coupling during τ_3, but P_7 converts all anti-phase single quantum coherence to unobservable double quantum coherence. Similarly, this coherence is omitted hereafter. Furthermore, longitudinal two-spin order has been created by P_2 for protons that exhibit short-range scalar couplings (term (d)). The effect of this coherence is described later on.

As longitudinal spin-order (terms (b and d)) is invariant to evolution due to chemical shift and scalar coupling, this state is preserved until the application of P_7. Subsequently, the desired polarisation exchange is completed for nuclei that are long-range coupled to the selected proton (terms (b)):

$$\sigma_3 \xrightarrow{(\pi/2_S)_Y} \sigma_4 \qquad 2.20$$

σ_4 (term (b)) SI $2S_x I_z s_{Jc}$

$$SI_2 \qquad 2(S_x I_{1z} + S_x I_{2z}) s_{Jc}$$

$$SI_3 \qquad 2(S_x I_{1z} + S_x I_{2z} + S_x I_{3z}) s_{Jc} \qquad 2.21$$

Therefore, the pulses, P_2 and P_7 of the low-pass J-filter, which are staggered in time, do not jeopardise polarisation transfer in the forward sense, i.e., from I to S. The J-filter successfully achieves the dual function of purging residual coherences that exhibit short-range scalar coupling and causing selective polarisation transfer. Unlike INAPT, the proton polarisation transfer pulse, P_2, in selective PENDANT is not selective. It is envisaged that the accuracy of the non-selective proton pulse coupled with its shorter duration should minimise sensitivity losses due to adverse T_2 relaxation, which is inherent to longer selective pulses.

It was mentioned above that protons that exhibit short-range scalar coupling also attain a state of longitudinal two-spin order (expression 2.19). Therefore, P_7 has also facilitated polarisation transfer from I to S due to short-range scalar coupling. Consequently, these polarisation enhanced S coherences would contribute to the final spectrum thus rendering the experiment non-selective. To prevent these unwanted coherences from appearing in the spectrum, the phase of P_1 and the receiver is kept constant with respect to the phase of P_a, which is alternated every 8 transients (Appendix A13). This necessitates that, upon application of P_4, the polarisation transfer from I to S due to long-range heteronuclear scalar coupling is added and polarisation transfer that originates from short-range scalar coupling is cancelled over 16 transients.

During the final evolution period τ_b, S coherence evolves due to long-range coupling while evolution due to chemical shift is refocused in analogy with that described previously for PENDANT.

$$\sigma_5 \qquad SI \qquad \left\{\left(-2S_x I_z c_{Jb} - S_y s_{Jb}\right) s_{Jc}\right\} \xi_1$$

$$SI_2 \quad \left\{\left[\begin{array}{l}\left(-2S_xI_{1z}c^2{}_{Jb}-4S_yI_{1z}I_{2z}c_{Jb}s_{Jb}-S_ys_{Jb}c_{Jb}+2S_xI_{2z}s^2{}_{Jb}\right)+\\ \left(-2S_xI_{2z}c^2{}_{Jb}-4S_yI_{1z}I_{2z}c_{Jb}s_{Jb}-S_ys_{Jb}c_{Jb}+2S_xI_{1z}s^2{}_{Jb}\right)\end{array}\right]s_{Jc}\right\}\xi_1$$

SI_3 Overleaf

$$\left\{\left[\begin{array}{l}\left(-2S_xI_{1z}c^3{}_{Jb}-4S_yI_{1z}I_{2z}c^2{}_{Jb}s_{Jb}+8S_xI_{1z}I_{2z}I_{3z}c_{Jb}s^2{}_{Jb}-S_ys_{Jb}c^2{}_{Jb}\right.\\ \left.+2S_xI_{2z}c_{Jb}s^2{}_{Jb}-4S_yI_{2z}I_{3z}s^3{}_{Jb}\right)+\\ \left(-2S_xI_{2z}c^3{}_{Jb}-4S_yI_{2z}I_{3z}c^2{}_{Jb}s_{Jb}+8S_xI_{1z}I_{2z}I_{3z}c_{Jb}s^2{}_{Jb}-S_ys_{Jb}c^2{}_{Jb}\right.\\ \left.+2S_xI_{3z}c_{Jb}s^2{}_{Jb}-4S_yI_{3z}I_{1z}s^3{}_{Jb}\right)+\\ \left(-2S_xI_{3z}c^3{}_{Jb}-4S_yI_{2z}I_{3z}c^2{}_{Jb}s_{Jb}+8S_xI_{1z}I_{2z}I_{3z}c_{Jb}s^2{}_{Jb}-S_ys_{Jb}c^2{}_{Jb}\right.\\ \left.+2S_xI_{1z}c_{Jb}s^2{}_{Jb}-4S_yI_{1z}I_{2z}s^3{}_{Jb}\right)\end{array}\right]s_{Jc}\right\}\xi_1$$

2.22

Where ξ_1 represents a proportionality constant depicting the enhancement factor indicative of polarisation transfer from I to S, i.e., γ_I/γ_S, and the dependence of the magnitudes of the coherences on:

- the longitudinal relaxation of I between transients during acquisition and the relaxation delay (D_r).
- T_2 relaxation of I nuclei during τ_c, τ_1 and τ_2.
- T_2 relaxation of S nuclei during τ_b.

The descriptions of coherences that contribute to the selective PENDANT spectrum are given in the next section.

It is now possible to justify why the initial S pulse, P_4 is staggered in time, relative to the first selective proton pulse, P_a, by the amount τ_1 (Section 2.2). In order to facilitate optimum polarisation transfer from I, the first proton pulse, P_1, of the J-filter is situated at the end of the proton evolution delay τ_c so that chemical shift is refocused and the desired anti-phase proton coherence remains invariant to the phase of the first J-filter pulse P_1. Hence, the pulse, P_4, is staggered in time by the amount τ_1 in order to initiate the first element of the

low-pass J-filter without compromising the efficiency of polarisation transfer from I.

2.4.5 Quaternary nuclei that do not exhibit long-range scalar coupling to the selected proton or are completely isolated

The evolution of long-range scalar couplings for quaternary nuclei which are coupled to proton(s), other than those selected by the selective pulses, are refocused during τ_a and τ_b. It was mentioned previously (Section 2.2), that $\tau_1 = \tau_3$ in order to refocus chemical shift of quaternary coherence prior to the S polarisation transfer pulse, P_7.

During τ_1 the desired quaternary coherence that does not exhibit coupling to the selected proton or is devoid of coupling, has evolved due to chemical shift. As chemical shift evolution during τ_2 is refocused, τ_3 must be equal to τ_1 so as to refocus the evolution due to chemical shift that occurred during τ_1. If $\tau_1 \neq \tau_3$, the quaternary coherence would possess a chemical shift, proportional to τ_1- τ_3 and the effect of the S polarisation transfer pulse would be:

$$S_y c\Omega\tau_1 - \tau_3 - S_x s\Omega\tau_1 - \tau_3 \xrightarrow{(\pi/2)_y} S_y c\Omega\tau_1 - \tau_3 + S_z s\Omega\tau_1 - \tau_3$$

Application of P_7 would cause the partial return of the desired quaternary coherence to unobservable magnetisation, leaving observable quaternary coherence significantly attenuated by the factor $c\Omega\tau_1$-τ_3.

Quaternary nuclei that do not exhibit scalar coupling to the selected proton or are devoid of scalar coupling remain invariant to the low-pass J-filter and are refocused due to chemical shift prior to acquisition.

$$\sigma_5 \qquad + S_y \xi_2 \qquad 2.23$$

This state of coherence is also relevant for the description of S coherence of a field-frequency lock solvent (Appendix A4.3), e.g., $CDCl_3$, which has been homogeneously incorporated into the sample. The lock solvent signal appears in the spectrum with the same phase as the signals of quaternary nuclei that are not scalar coupled to the selected proton(s) or that are devoid of scalar coupling.

2.5 Observable coherences in the selective PENDANT spectrum

Residual coherences that exhibit short-range scalar coupling are significantly attenuated by the low-pass J-filter. The magnitudes of suppression being proportional to the choice of <J> used for τ_1 and τ_2, with respect to the actual J-values present. The strategy employed for the setting of τ_1 and τ_2 is described later on.

It is evident that the pulse sequence has been phase cycled so as to give a 'pseudo-edited' spectrum: coherences that originate from polarisation transfer, given in expression 2.22 appear anti-phase to those coherences that have not received polarisation transfer and have originated from S, given in expression 2.23. The pseudo-edited method of spectrum presentation is particularly powerful since assignment becomes trivial: S coherence of a field-frequency lock solvent, e.g., $CDCl_3$, which has been homogeneously incorporated into the sample, has identical phase properties as those quaternaries that have not received polarisation transfer.

If the sample does not possess a lock agent, which is observable in the S spectrum, assignment of each coherence type can be made by observing multiplet structure: nuclei that have received polarisation transfer possess multiplet anomalies, i.e., non-binomial intensity distribution of their component lines. Nuclei that have not received polarisation transfer exhibit multiplets with the intensities of component lines obeying a binomial distribution.

It is recommended that an off-resonance experiment is performed simultaneously, whereby the same experimental parameters are used while the selective pulses act upon a frequency region devoid of proton resonance's. The off-resonance spectrum, or 'control' spectrum, acts as a direct detect experiment for quaternary nuclei only, since the selective pulses are ineffectual but the low-pass J-filter still functions. Comparison to the pseudo-edited spectrum reveals those nuclei that have received polarisation transfer.

Spectra may contain low-levels of 'breakthrough' signals from nuclei, which exhibit short-range coupling, that were not entirely suppressed by the low-pass J-filter. However, breakthrough signals will have a constant phase and amplitude in both the on-resonance and off resonance spectrum, because the parameters of the low-pass J-filter remain unchanged in each. When the two spectra are compared for assignment purposes, the presence of identical breakthrough signals in both spectra will prevent incorrect assignments.

Comparison of on-resonance and off-resonance spectra can be implemented easily on most spectrometers using dual spectrum displays. A subtraction routine can also be employed whereby a new spectrum is displayed, which represents the difference between the two spectra, thus enabling rapid assignments.

The pseudo-edited method of detection is highly idealised. In order for pseudo-editing to work, all coherences that originate from polarisation transfer, regardless of their multiplicity and J-values, must exhibit the same phase. Coherences that originate from long-range polarisation transfer from I share the same trigonometric functions (expressions 2.22) that determine the sign of coherence in analogy with INEPT and PENDANT to achieve spectral editing (Chapter 1.2.3 and 1.2.4).

However, long-range J-values vary markedly. For example, ^{13}C-^{1}H long-range coupling constants in organic molecules can vary over the range 0 – 20Hz [10]. Consequently, it is rare that one is able to prescribe an average compromise value, <J>, from which the evolution delays, τ_c and τ_b are set, which encompasses the range of ^{13}C-^{1}H long-range J-values found in the molecule.

Therefore, in contrast to spectral editing, whereby, the phase of signals attributed to short-range scalar coupling multiplicity is influenced, and is more or less invariant to the choice of <J>, the phase, or sign, of coherences that exhibit long-range scalar couplings can not be easily influenced. As a result, the success of the pseudo-edited detection method relies largely upon the choice of <J>, the range of ^{13}C-^{1}H long-range J-values present, and hence the choice of τ_b.

Martin and Zexter [10], after considerable reviews of the literature and empirical data, advise 10Hz as a reasonable starting point from which to base the setting of long-range ^{13}C-^{1}H coupling evolution delays. Bax [16] has suggested that INAPT be used with a final evolution delay that does not exceed 0.025ms, excluding the length of selective pulses; since the length of selective pulses necessitates the simultaneous evolution of long-range scalar couplings.

The choice of long-range evolution delays and the strategy for their programming is due mainly to experience and is often a "hit-and-miss" affair. However, if one has knowledge of

the range of J-values in the molecule, a judicious choice of <J> and the evolution times τ_c and τ_b can be made to maximise polarisation transfer and optimum refocusing.

When knowledge and experience fails, experimenters tend to err on the side of caution, and program delays that are short, so as to prevent de-phasing of coherence and nulling of signals during the final evolution delays. Therefore, the final evolution delay τ_b in selective PENDANT was set to 1/8J, for J = 8Hz, which is a compromise between the recommendation by Bax, taking into account the length of selective pulses, and that recommended by Martin and Zexter, i.e., 10Hz as a starting point for the choice of J.

Investigative work has shown that the pseudo-edited spectrum works sufficiently well for assignment purposes. This was based upon the study of an organic compound which exhibits a typically wide range of ^{13}C-^{1}H long range J-values, with the delay τ_b set as described above. Should the pseudo-editing method fail, the ability to assign spectra is not compromised, since comparison to an off-resonance (quaternary only) spectrum reveals the nuclei that have received polarisation transfer.

2.5.1 Superposition of coherences

In exact analogy with normal PENDANT spectra, by default, selective PENDANT spectra also exhibit superpositions of coherence, i.e., residual coherence, which originates from S nuclei, and coherence, which originates from polarisation transfer from I. Due to the function of the low-pass J-filter, the effect of superposition is only important for quaternary nuclei that exhibit scalar coupling to the selected proton. This is because all other S nuclei that exhibit long-range coupling to the selected proton also exhibit short-range coupling, and consequently are largely suppressed from the spectrum.

It has already been shown that the effect of the superposition of residual coherence in PENDANT spectra of ^{13}C is very small for organic molecules, which exhibit a typical range of ^{13}C-^{1}H short-range couplings. This is because short-range couplings occur over a comparatively small range, so that the average <J> value used for the optimisation of the first evolution delay, gives rise to efficient purging of residual coherence by the polarisation exchange pulses. The magnitude of the observed signals, due to the superposition, is only slightly perturbed from that of the magnitude of signals that originate from polarisation transfer from I. (Chapter 1.5)

In selective PENDANT however this is not the case: the potential uncertainty in long-range J-values, may impose a significant effect due to the superposition of residual quaternary coherences that exhibit long-range couplings to the selected proton, and those which originate from polarisation transfer from I. The first evolution delays τ_c and τ_a for ^1H and ^{13}C respectively are set as usual to $1/2<J>_{LR}$ to initiate maximum polarisation transfer, where $_{LR}$ is long-range. When the actual long-range J-values significantly differ from <J>, from which the first evolution delays τ_c and τ_a are set, potentially very little polarisation transfer may take place. Equally, the magnitudes of the residual quaternary coherences will be comparatively large, since little purging is caused by first pulse of the J-filter P_1 (Section 2.4.2)

When the pulse sequence is phase cycled to provide spectra in the pseudo-edited mode, residual quaternary coherence is anti-phase to that which originates from polarisation transfer from I. Potentially large attenuation of the total signal intensity may occur for nuclei, which exhibit J-values far from <J> from which τ_a, τ_c and τ_b are set. This may impinge upon the interpretation of the spectrum only when the magnitude of coherence that has originated from polarisation transfer from I is less than the residual quaternary coherence that exists during detection: the signal would therefore exhibit a phase indicative of nuclei that have not received polarisation transfer. In this circumstance, comparison with a spectrum obtained for an off-resonance experiment would be necessary to make an assignment. The comparison would clearly show a reduction in intensity of the quaternary that is long-range coupled to the selected proton in comparison to the off-resonance spectrum and exhibit a multiplet structure indicative of polarisation transfer.

Coherences that are present during detection, i.e., stage: σ_5, were appended with an intensity scaling factor, ξ_1 or ξ_2, where ξ_1 represents a proportionality constant depicting the enhancement factor indicative of polarisation transfer from I to S, i.e., γ_I/γ_S and the dependence of the magnitudes of the coherences on:

- the longitudinal relaxation of I between transients during acquisition and the relaxation delay (D_r).
- T_2 relaxation of I nuclei during τ_c, τ_1 and τ_2.
- T_2 relaxation of S nuclei during τ_b

and ξ_2 represents a proportionality constant depicting the dependence of the magnitude of

residual coherences on γ_S and:

- longitudinal relaxation of S during acquisition and the relaxation delay (D_r)
- T_2 relaxation of S during the entire pulse sequence.

It is evident that the magnitudes of residual S coherences, differs significantly from S coherences that originate from polarisation transfer from I. This is unsurprising since coherences, which originate from polarisation transfer are a factor of γ_I/γ_S, greater than coherences that originate from S alone. For $^{13}C - {}^{1}H$ this corresponds to a factor of 4.

However, the relaxation times T_1 and T_2 of ^{1}H and ^{13}C significantly differ. For example, the T_1's of ^{1}H in organic molecules can vary between tens of milliseconds to seconds, compared to the T_1's of ^{13}C quaternary nuclei that can range from seconds to tens of seconds. In the extreme narrowing limit, the T_2 relaxation times of each will be comparable to their T_1 values (Appendix A6.5).

Selective long-range polarisation transfer experiments are inherently long. This is due to lengthy evolution delays, as a result of small J-values, and the inherent length of selective pulses (Appendix A10) to ensure good selectivity, i.e., narrow excitation bandwidths. Consequently, the sensitivity, i.e., the signal-to-noise ratios in spectra, are typically less than analogous short-range polarisation transfer experiments.

For example, based upon a square wave pulse, (which is the best case scenario for minimising pulse duration but poorest at achieving optimal selectivity (Appendix A10)) to encompass a 40Hz excitation bandwidth, which should sufficiently encompass the entire proton multiplet, the pulse duration is 1/40 = 0.025 seconds. For $\langle J \rangle$ = 8Hz with the evolution delays of selective PENDANT set to $\tau_a \approx \tau_c = 1/2J$ and $\tau_b = 1/8J$, this equates to a total experiment duration, neglecting D_r and taking into account all selective pulses applied to ^{1}H, of approximately 0.2 seconds.

Therefore, the duration of the pulse sequence represents a significant amount of time in which T_2 relaxation of ^{1}H and ^{13}C coherences can take place. Obviously, this length of time represents a more significant effect for ^{1}H's due to their much smaller T_2 values. However, selective PENDANT benefits from minimising the T_2 relaxation of ^{1}H during the first

evolution period, τ_a, in comparison to INAPT, since the latter utilises a selective polarisation transfer pulse. Selective PENDANT by comparison utilises a non-selective hard pulse of microseconds duration. Therefore, it is expected that selective PENDANT should benefit from greater magnitudes of coherence that originate from polarisation transfer from I in comparison to INAPT. Moreover, this should prove useful in selective PENDANT for polarisation transfer to quaternary nuclei: when the pseudo-edited method of detection is employed, the adverse effects of signal cancellation, which occur as a result of the superposition of coherences that originate from polarisation transfer from I, and residual quaternary coherences, are minimised.

2.5.2 Selective PENDANT using proton broadband de-coupling

In rare instances when the measurement of coupling constants is not required, selective PENDANT may be implemented with proton broadband decoupling during acquisition.
Broadband decoupling of protons causes S nuclei to experience a non-selective nuclear Overhauser enhancement (nOe). In the extreme narrowing limit, the magnitudes of the nOes at all S nuclei approaches the maximum steady-state theoretical two-spin value [24], i.e., $^{13}C\{^1H\}$ η_{max} = 1.99 (Appendix A7.2.6). However, acquisition times fall short of achieving steady-state and the nOe will vary between S nuclei, depending upon their individual longitudinal relaxation characteristics.

In general, short-range coupled S nuclei experience the largest enhancements, since their longitudinal relaxation is dominated by dipolar interactions with the directly bonded protons. Quaternary nuclei, on the other hand, receive comparatively less enhancement. This is due to the comparatively larger distances between quaternary nuclei and protons, and competition from relaxation sources other than dipolar relaxation with protons, which serves to reduce the nOe (Appendix A7.2.6). Nevertheless the enhancements at quaternaries are sizeable compared to their longitudinal recovery during acquisition and the relaxation delay, when proton broadband decoupling is not implemented.

Therefore, when selective PENDANT is implemented with proton broadband decoupling during acquisition and when <J> is significantly different from actual values, the magnitudes of residual quaternary coherences may start to approach those, which originate from polarisation transfer. Consequently, when selective PENDANT is implemented in the pseudo-edited mode, the increased magnitudes of residual quaternary coherence may

constitute a significant attenuation of signals that originate from polarisation transfer. Similarly, the greater potential for larger magnitudes of residual coherence, which exhibit short-range scalar couplings, necessitates that the low-pass J-filter functions efficiently in order to achieve optimal suppression.

When selective PENDANT is implemented using proton broadband decoupling during acquisition, employment of an alternative phase cycle that renders the experiment 'non-pseudo-edited' may be a viable option. In the 'non-pseudo-edited' mode, the superposition of residual coherences and those, which originate from polarisation transfer are additive. Of course, the utility of the 'non-pseudo-edited' mode is also highly idealised in analogy to the pseudo-edited method of detection. Coherences that exhibit long-range J-values far removed from <J>, may equally evolve so that they are once again anti-phase to residual quaternary coherences and hence lead to partial cancellation.

2.5.3 'Non-pseudo-edited' selective PENDANT

A π radians rotation of the phase cycle for the initial S pulse, P_4, gives rise to 'non-pseudo-edited' spectra. The implication of acquiring selective PENDANT spectra in this mode is that there is a less trivial matter of assignment, since all coherences possess the same phase. It would be necessary to obtain a spectrum of an off-resonance experiment for comparison.

2.6 The choice of evolution delays τ_1 and τ_2 in the low-pass J-filter

It has already been shown that limiting the breakthrough of residual coherence is dependent upon maximising the conversion of single quantum coherence that exhibits short-range coupling to various orders of multiple quantum coherence. Furthermore, those coherences that exhibit long-range scalar coupling to the selected proton, in addition to short-range coupling, will exhibit greater levels of suppression than coherence that exclusively exhibit the latter.

In terms of their product operators, the magnitudes of the residual coherence that exhibit short-range scalar coupling exclusively are summarised below.

Residual S coherence that exhibits short-range coupling only for SI

$$SI : c^{n}_{J1}c^{n}_{J2}c^{n}_{J3} \qquad 2.24$$

Residual S coherence that exhibits short-range coupling only for, SI_2 and SI_3

$$SI_2 : \quad c^{2}_{J1}c^{2}_{J2}c^{2}_{J3} + c^{2}_{J1}c^{2}_{J2}\left[1/2(1-c_{2J3})\right]$$

(In-phase + Multiplet anomaly coherence)

$$SI_3 : \quad c^{3}_{J1}c^{3}_{J2}c^{3}_{J3} + c^{3}_{J1}c^{3}_{J2}\left[1/2(1-c_{2J3})\right]c_{J3}$$

(In-phase + Multiplet anomaly coherence) 2.25

where $[1/2(1-c_{2J3})]$ has been substituted in for s^2_{J3} according to the trigonometric identity $[1/2(1-\cos 2A)] = \sin^2 A$.

The efficiency of suppression of each coherence type is directly proportional to minimisation of the product of the cosine functions present in the product operators. Judicious choice of the magnitudes of the evolution periods, τ_1 and τ_2 for a given set of typical J-values found in the molecule in question will suitably minimise the product of these functions and the residual coherences. As mentioned previously, the value of τ_3 is not open to variation in the same transient, since it must be the same as τ_1 to ensure the refocusing of chemical shift of quaternary coherence that originates from S, prior to P_7 (Section 2.3 and 2.4.4).

In organic molecules, the short-range J-values for CH_2 and CH_3 multiplicities typically fall in the range 120Hz – 140Hz and 140Hz -160Hz respectively, while CH multiplicities fall in the range 160Hz - 200Hz. It is not possible to simultaneously optimise the two evolution delays, τ_1 and τ_2 for the suppression of three different multiplicities. Therefore, it is proposed that the evolution period $\tau_1 = \tau_3$ will be optimised for the principal suppression of the CH_2 and CH_3 multiplicities and τ_2 will be optimised for the principal suppression of CH multiplicities. In order to implement this method the value of $\langle J \rangle$ for τ_1 is set to140Hz, i.e., the average of the linear combination of the two typical J-ranges for CH_2 and CH_3 multiplicities, and $\langle J \rangle$ for τ_2 is set to 180Hz i.e., the average of the typical J-range of CH multiplicities.

Justification of the use of this method is demonstrated by the experimental results obtained in the analysis of PENDANT spectra in chapter 1. The routine employment of PENDANT with

<J> = 145Hz, caused efficient purging of residual S coherences of the CH_2 and CH_3 multiplicities by the proton polarisation exchange pulse, which is tantamount to the first purge pulse in the J-filter. Furthermore, it was also proven that the efficiency of suppression of S residual coherences for the CH multiplicities is comparatively worse due to the increased difference in actual J-values as compared to <J>. Therefore, dedicating one evolution delay to suppression of the CH multiplicity seemed a logical decision.

Of course, should the short-range scalar couplings of the compound under study fall within a narrower J-range, judicious choice of the values of <J> for the optimisation of τ_1 and τ_2 will help to improve the efficiency of suppression.

2.7 Experimental

The analysis of the performance of the selective PENDANT pulse sequence is divided into the following sections:

- investigation into the efficiency of selective PENDANT for the suppression of short-range coupled coherences using the prescribed recommendation for the choice of τ_1 and τ_2 given previously (Section 2.6).

- Investigation into the performance of the selective PENDANT experiment and comparison of results to that predicted by the theoretical treatment given previously.

- Determination of the utility of the selective PENDANT experiment in direct comparison to the INAPT experiment, which is the appropriate 'benchmark'.

Before progressing to the experimental work that has been undertaken, a brief synopsis of the experimental methods used is given here.

Appendix A3 and A4 describes the standard experimental procedures for the preparation, acquisition of and processing of NMR spectra, which are valid for all experimental work undertaken. Appendix A4.5 provides information regarding pulse program language and spectrum acquisition parameters. All pulse programs pertaining to experiments reported herein are given in appendix A13.

2.7.1 Materials and Equipment

Experiments were performed using a sample of 60/40, vol/vol., ethyl-5-(chloromethyl)-2-

furan-carboxylate and duetero chloroform respectively, the latter providing field –frequency locking. Experiments were performed using a Bruker Avance 300MHz NMR spectrometer with a 5mm $^{13}C - {}^{1}H$ dual probe.

Ethyl-5-(chloromethyl)-2-furan-carboxylate was chosen because it exhibits an appropriate variety of $^{13}C - {}^{1}H$ short-range and long-range scalar coupling multiplicities with J-value ranges indicative of most common organic molecules. The molecule contains three quaternary carbon nuclei, which exhibit extensive long-range proton scalar couplings.

2.7.2 Selective pulses

For the excitation or refocusing of coherence, an entire series of experiments were performed using either DANTE (delays alternating with nutation for the tailored excitation), or shaped soft selective pulses. A description of the properties of these selective pulses is provided in appendix A10.

Unless otherwise stated, the selectivity or excitation bandwidth of all selective pulses was set to 40Hz to fully encompass the entire proton multiplet, which exhibits both heteronuclear long-range and homonuclear proton scalar coupling.

2.7.3 Selective excitation and refocusing using DANTE.

The excitation bandwidth in Hz implicit to the DANTE pulse train was calculated in the normal way [25] (Appendix A10), i.e., the excitation bandwidth is approximately equal to the inverse of the total duration of the DANTE pulse train $([\beta+t]N)^{-1}$. Where N is the number of delays/pulses in the train, t, is the length of the inter-pulse delay, and β is length of the pulse.

A hard proton pulse was calibrated following appropriate attenuation of the pulse power to give a $(\pi/2)$ pulse of 200 micrsosecond (μs) duration. To ensure the duration and hence the selectivity of the excitation and refocusing pulses remained the same, a 200 pulse train was used for each, with β = 1μs and 2μs respectively. The excitation sidebands implicit to DANTE, which occur at a frequency offset from the carrier of $\Delta v = k\pm/t$, where k is an integer, were approximately 8000Hz. Therefore, excitation sidebands did not interfere with other proton resonances in the spectrum. The duration of the DANTE pulse train is 0.025seconds.

2.7.4 Selective excitation and refocusing using shaped soft selective pulses

For proton selective excitation and refocusing, a SNEEZE pulse and a Gaussian cascade Q3 pulse (Appendix A10) were implemented, due to their pure-phase character and 'top-hat' excitation profile, which gives rise to high selectivity.

Pulse length and pulse power for both pulses for an excitation bandwidth of 40Hz, were determined using the standard software on the Bruker Avance 300MHz NMR spectrometer. The selective pulses were checked for phase coherence with hard proton pulses by the experimental method outlined in appendix A4.7. Both SNEEZE and the Gaussian cascade did not require additional phase correction.

The duration of the SNEEZE and Gaussian pulses cascade were 0.1454 seconds and 0.08628 seconds respectively, which by comparison to DANTE are approximately 6 and 3 times greater, respectively. Long durations are inherent to shaped pulses, and in comparison to DANTE, it is expected that the sensitivity of experiments that utilise these pulses may be slightly compromised due to greater adverse T_2 relaxation effects that occur during the pulse.

2.7.5 Acquisition parameters

All selective PENDANT experiments were performed in the following way unless otherwise stated:

- the long-range scalar coupling evolution delays, τ_c and τ_b were set to 1/2J and 1/8J respectively for J = 8Hz.
- SW was set to encompass the entire chemical shift range of the solute using TD = SI = 32K, which provided adequate digital resolution of 0.37Hz, to ensure correct representation of signal intensity and multiplet structure.
- Spectra were acquired at 300K without proton broadband decoupling during acquisition.
- The carrier frequency for ^{13}C was set at the centre of the solute chemical shift range. The carrier frequency for protons was set to the value specified by a frequency list prior to the particular pulse being executed. For example, prior to the selective pulse, the carrier frequency may be set on-resonance for the selected proton, while prior to execution of the J-filter element, the carrier frequency is set to the centre of the proton chemical shift range. This is to ensure optimum

purging of all short-range coupled protons by the minimisation of off-resonance effects (Appendix A1.8.3).

- 16 transient were collected using a 3 second relaxation delay.

2.7.6 Spectrum processing

All selective PENDANT spectra were phase corrected to the same phase constants and processed using line broadening of 1Hz. Unless otherwise stated, all spectra are presented in absolute intensity scaling mode for comparison purposes.

2.8 The efficiency of suppression of ^{13}C coherence that exhibits short-range scalar coupling with protons.

A selective PENDANT experiment was performed off-resonance, i.e., the proton carrier frequency upon application of the selective pulses is set far from the resonance frequencies of all protons. This yields a quaternary only spectrum and displays the breakthrough of residual short-range coupled signals that have survived the low-pass J-filter.

In one experiment the values of τ_1 and τ_2 were set according to the recommendation given earlier i.e., $\tau_1 = \tau_2 = 1/2J$ for J = 140Hz (CH_3, and CH_2 multiplicities) and 180Hz (CH multiplicities) respectively. Further experiments were performed using identical parameters with the exception of the controlled variation of either τ_1 or τ_2 in separate experiments, while the other remained constant:

- the value of τ_1 took values according to J for the range 120Hz – 160Hz in increments of 10Hz, while the magnitude of τ_2 remained constant due to the recommended value of J=180Hz.
- The value of τ_2 took values according to J for the range 160Hz – 200Hz in intervals of 10Hz, while the magnitude of τ_2 remained constant due to the recommended value of J=140Hz.

The separate variation of the delays τ_1 and τ_2 was designed to artificially emulate a typical variation in J between different molecules, for the corresponding multiplicities for which the delays are designed to encompass.

The breakthrough signals present in the off-resonance spectrum were integrated and then

compared to the corresponding signals in a direct-detect analogue of the selective PENDANT experiment. The integrated intensities of the signals in the direct-detect analogue spectrum were each normalised to 100%. The % suppression or breakthrough was calculated for the corresponding signals in the selective PENDANT experiment.

The direct-detect analogue is identical to the normal selective PENDANT experiment with the exception that all J-filter proton pulses are removed and replaced with delays equivalent to their durations. This ensures that the T_1 and T_2 relaxation of the ^{13}C nuclei in the direct-detect analogue closely emulates that in selective PENDANT so as to ensure appropriate comparison.

2.8.1 Results and Discussion

For illustrative purposes, figures 2.3 and 2.4 overleaf each display 3 spectra obtained for the variation of τ_1 and τ_2 respectively.

On inspection of figures 2.3 and 2.4, it is evident that the low-pass J-filter has been very successful for the suppression of short-range residual signals. The quaternary signals, **f**, **g** and **h** and solvent resonance are clearly visible.

The ^{13}C signals of the CH and CH_3 short-range scalar coupling multiplicities seem to be particularly invariant to a large variation in J for the setting of both τ_1 and τ_2 and are more or less completely suppressed in all spectra.

The ^{13}C signals of the CH_2 short-range scalar coupling multiplicities, signals **b** and **c**, clearly exhibit the poorest level of suppression. Upon comparison of the integrals of selective PENDANT to the direct-detect analogue, it is found that the maximum breakthrough is 7.0%, for signal **b** (CH_2) when J = 120Hz for the setting of τ_1. It is unsurprising that signal **b** for this J-value has been more poorly suppressed, because the actual J-value is 153Hz. Interestingly, it can be seen that the maximum suppression of signals **b** and **c** occurs when τ_1 and τ_2 are set to J = 140Hz and 200Hz respectively, which corresponds to complete suppression of **c** and 3% breakthrough of **b**.

Direct-detect using modified selective PENDANT

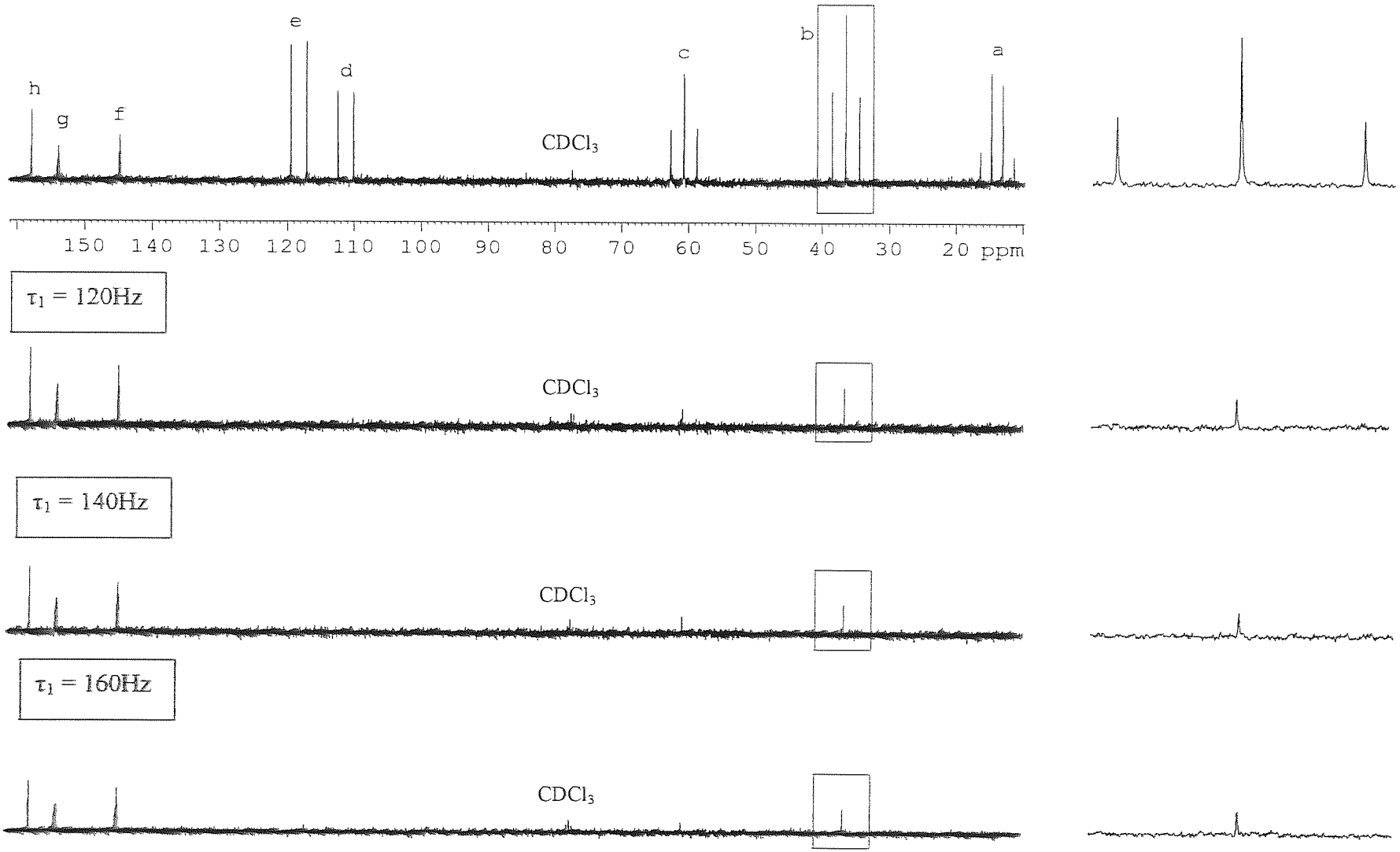

Figure 2.3 **Suppression of short-range scalar coupling residual signals. Area enclosed is shown expanded adjacently.**

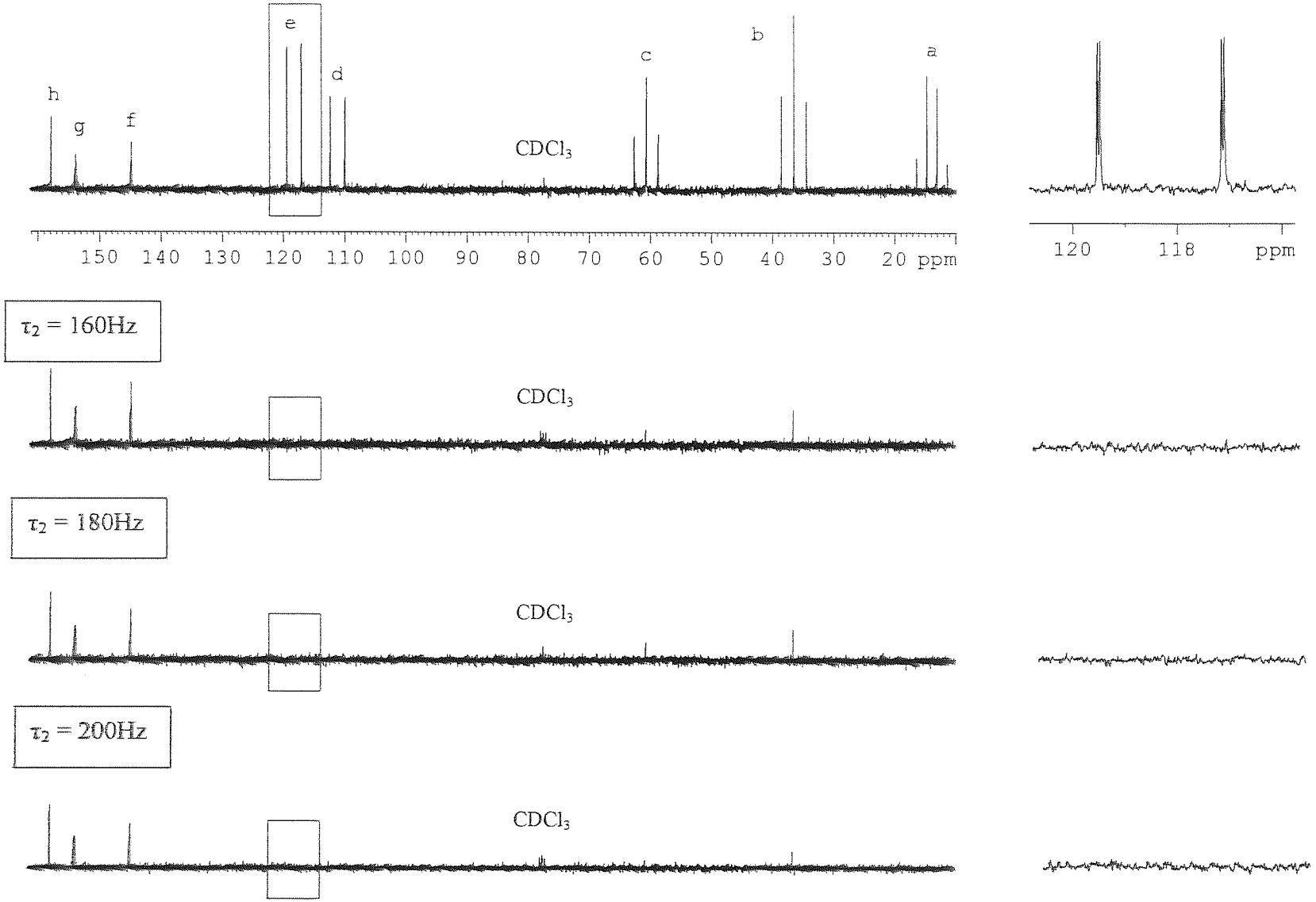

Figure 2.4 **Suppression of short-range scalar coupling residual signals. Area enclosed is shown expanded adjacently.**

Upon inspection of the expanded view of signal **b** adjacent to the spectra in figure 2.3, it can be seen that the CH_2 residual signals, clearly exhibit multiplet anomalies, which are predicted by the analysis of the experiment given previously (Section 2.4.1): the multiplet anomaly is caused by the superposition of residual in-phase coherence (S_y) and anti-phase multiplet anomaly-causing coherence ($4S_yI_zI_z$), created by the odd coupling-order selective purging effect of the S polarisation exchange pulse, P_7.

It is unknown why the ^{13}C signals of the CH_2 multiplicities are generally less well suppressed than the other scalar coupling multiplicities. Since, off-resonance effects, *r.f.* inhomogeneity effects and pulse imperfections presumably effect all coherences, it seems unlikely that these effects can be attributed to their poorer suppression. However, a brief investigation into these matters given in the next section would seem to suggest that these do play an important role in their less efficient suppression.

In summary, the recommended procedure of setting J to140Hz and 180Hz for τ_1 and τ_2 respectively, causes the complete suppression of ^{13}C signals for the CH and CH_3 multiplicities. Signals **b** and **c** were suppressed by 94.1% and 95.2% respectively, corresponding to breakthrough of 5.9% and 4.8%. The level of suppression achieved by the low-pass J-filter has been proven to be largely invariant to a range of short-range coupling constants that were emulated by variation of the evolution delays τ_1 and τ_2.

As mentioned previously (Section 2.4.1), the breakthrough of residual signals, i.e., for CH_2 multiplicities does not impact significantly upon the utility of selective PENDANT in comparison to INAPT. As the breakthrough signals inherently exhibit multiplet anomalies, their assignment is a trivial matter and does not cause ambiguity in assignment of signals due to long-range scalar coupling correlations. Furthermore, assignment of signals due to breakthrough is trivial when comparing on-resonance spectra to an off resonance spectrum, since the magnitude and phase of the breakthrough signals in each spectrum are identical.
The only unfortunate side-effect of the breakthrough of residual signals is a slight cosmetic degradation of the spectrum.

2.9 Investigation into off-resonance effects on the efficiency of suppression

Achieving maximum suppression of residual coherences in selective PENDANT, necessitates the attainment of accurate pulse lengths and phases in order that the J-filter functions

properly. Furthermore, subsequent pulses should not give rise to residual coherences that can breakthrough into the spectrum.

Beyond the ability of the spectrometer to produce accurate pulse lengths and phase shifts, the major source of inaccurate pulse angles and phases are due to *r.f.* inhomogeneities and off-resonance effects. *r.f.* inhomogeneities arise due to local variations in the intensity of the *r.f.* field. Ignoring sample dependent effects, the cause is in part related to the quality of transmitter coils and their orientation relative to the sample. The effect manifests itself by causing inaccurate nutation angles by analogy with pulse length miscalibration (Appendix A9).

Off-resonance effects (Appendix A1.8.3) are caused by the lack of uniformity of pulse power across the chemical shift range, inherent to the synthesis of square wave pulses. Off-resonance effects are manifested in nutation angle and phase discrepancies, which increase in severity with greater offset from the carrier.

Long-range polarisation transfer techniques like selective PENDANT, tend to magnify the effects of *r.f.* inhomogeneity and off-resonance effects due to the inherent length of the pulse sequences. Lengthy delays optimised for the evolution of long-range scalar couplings necessitate the longitudinal recovery of S (^{13}C) magnetisation between S pulses. Consequently, off-resonance effects serve to excite coherences that may exhibit short-range couplings and hence lead to further breakthrough in the spectrum. Refocusing pulses are the main culprits for these disadvantageous effects since they are more sensitive to nutation angle discrepancies (Appendix A1.8.3). The substitution of appropriate composite pulses for the normal hard pulses in a pulse sequence is often carried out for the compensation of off-resonance and *r.f.* inhomogeneity effects (Appendix A9).

It has been shown that the ^{13}C signals of the CH and CH_3 multiplicities in selective PENDANT are completely suppressed over a range of J-values. However, ^{13}C signals of the CH_2 multiplicities, although largely suppressed, do breakthrough and are reasonably invariant to a change in τ_2. It was surmised that off-resonance and *r.f.* inhomogeneity effects may aid in causing a large proportion of the signal breakthrough due to the number of pulses and duration of the selective PENDANT experiment. Indeed, the off-resonance and *r.f.* inhomogeneity effects may determine the maximum level of suppression that can be attained

by the selective PENDANT experiment for ^{13}C signals of the CH_2 multiplicities.

Therefore, in order to qualify the results obtained above, the following series of experiments were performed.

1. An off-resonance (control i.e. quaternary-only) selective PENDANT experiment was carried out in accordance with the recommended procedure for routine implementation, i.e., τ_1 = 140Hz and τ_2 = 180Hz, with the ^{13}C carrier frequency set to the centre of the ^{13}C chemical shift range. In addition another identical experiment was performed with the exception that the ^{13}C carrier frequency was set on the b (CH_2) signal.

2. Identical off-resonance selective PENDANT experiments as those carried out in experiment 1 were carried out with the exceptions;
   - all S refocusing pulses were substituted by one of the following composite pulses for the compensation of off-resonance effects:

   - $(90^\circ_x - 240^\circ_y - 90^\circ_x) = (\pi)_x$ = Composite pulse A
   - $(336^\circ_x - 246^\circ_{-x} - 10^\circ_y - 74^\circ_{-y} - 10^\circ_y - 246^\circ_{-x} - 336^\circ_x) = (\pi)_x$ = Composite pulse B

   - and the ^{13}C carrier frequency was only set to the centre of the ^{13}C chemical shift range.

Composite pulse A [23] gives rise to coherence phase shifts, however it receives widespread use in multiple pulse experiments for the purpose of chemical shift and scalar coupling refocusing. Composite pulse B more efficiently compensates for off-resonance effects over a wide frequency range and is apparently devoid of phase shift effects [22, 23]. Composite pulses A and B were chosen since each requires phase shifts in multiples of $\pi/2$ radians, making them suitable for implementation on all NMR spectrometers.

2.9.1 Results and discussion of experiment 1

The spectra of experiments 1 and 2 are presented in figure 2.5 and 2.6 respectively given overleaf, in addition to a spectrum of the direct detect analogue of the selective PENDANT experiment. All experiments were performed using identical acquisition parameters.

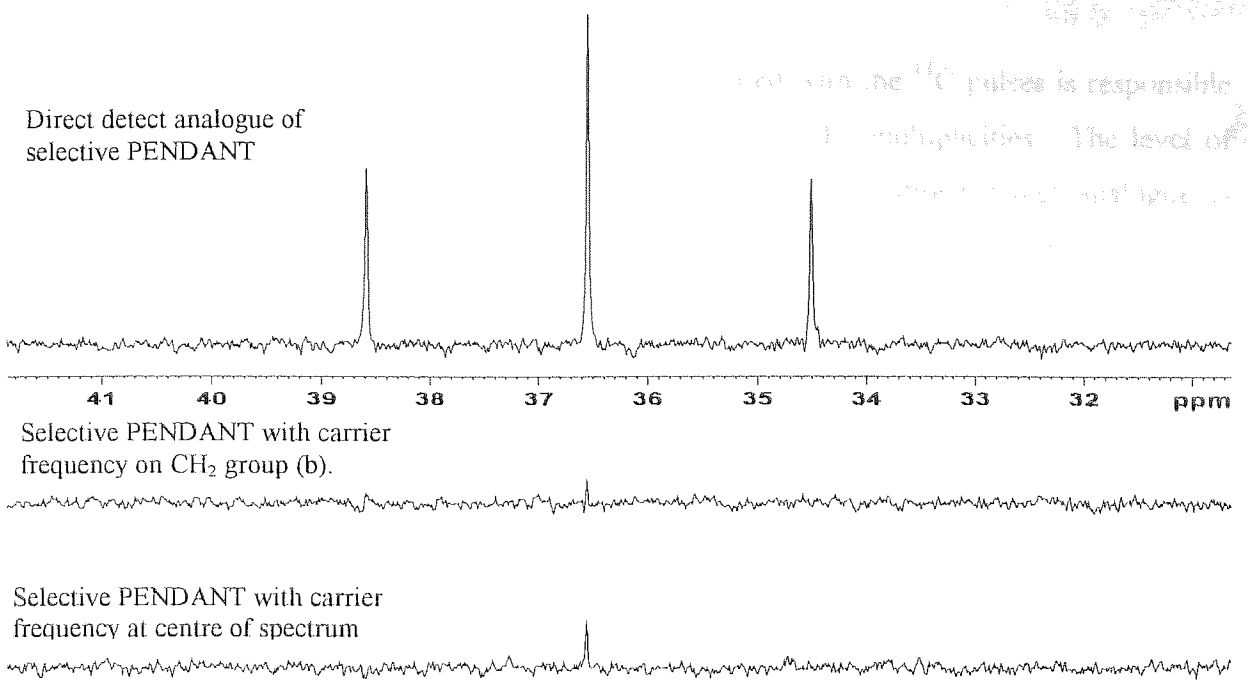

Figure 2.5 **Off-resonance effects upon the suppression of CH_2 multiplicity residual signals.**

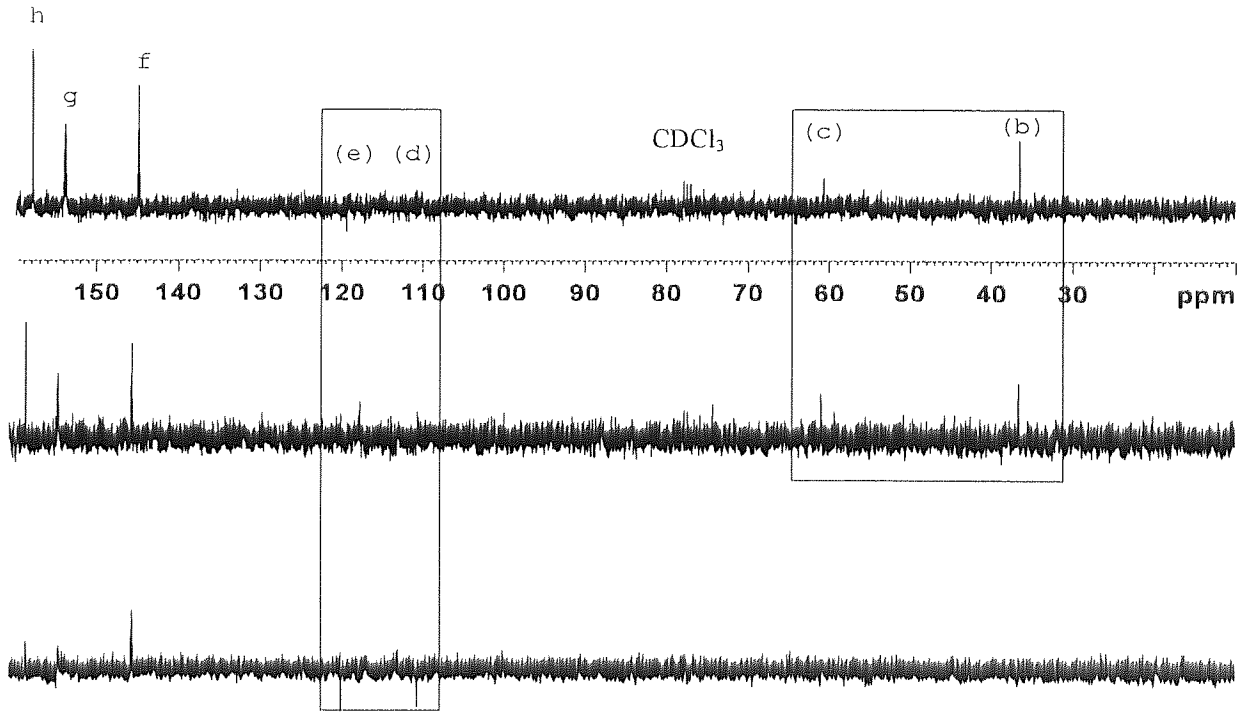

Figure 2.6 **Effect of composite pulses upon suppression of CH_2 multiplicity residual signals.**

From Top:
- **Selective PENDANT without composite pulses (16 transients).**
- **Selective PENDANT with composite pulse A ($90_x - 240_y - 90_x$) applied for S refocusing pulses (32 transients).**
- **Selective PENDANT with composite pulse B - ($336_x - 246_{-x} - 10_y - 74_{-y} - 10_y - 246_{-x} - 336_x$) applied for S refocusing pulses (16 transients).**

It is clearly evident that the off-resonance effect associated with the ^{13}C pulses is responsible for the majority of breakthrough of the ^{13}C signals of the CH_2 multiplicities. The level of breakthrough, calculated by integration and comparison to the direct-detect analogue is reduced to 1.8% as opposed to 5.9% when the carrier frequency is set to the centre of the ^{13}C chemical shift range.

2.9.2 Results and discussion of experiment 2

Figure 2.6 presents the spectra obtained for each of the selective PENDANT experiments, which separately utilise the composite pulses A and B for the refocusing of ^{13}C coherence. These are compared to the spectrum of a selective PENDANT experiment, obtained under identical conditions, utilising normal single hard ^{13}C refocusing pulses.

Due to the poor signal-to-noise ratio obtained, the selective PENDANT experiment utilising composite pulse A was acquired using 32 transients, as opposed to 16 transients. It is likely that this the poor signal-to-noise ratio is attributed to phase shifts inherent to this particular composite pulse, since further phase correction was required in comparison to the other spectra. Even with 32 transients accumulated, the signal-to-noise ratio of the quaternary nuclei are significantly attenuated in comparison to the standard selective PENDANT experiment. This is further illustrated by the absence of the solvent signal ($CDCl_3$).

In terms of suppression, the composite pulse A provides no advantages, since breakthrough of the ^{13}C signals of the CH multiplicity (**e**) has occurred. Furthermore, after appropriate scaling, to match the intensities of the quaternary nuclei in the standard selective PENDANT spectrum, the breakthrough of signals (**b**) and (**c**) would be of greater comparative intensity.

From inspection of figure 2.6 it is clearly evident that the performance of the composite pulse B is inappropriate for simple substitution for the ^{13}C refocusing pulses in selective PENDANT. The composite pulse has lead to an unacceptable loss of the signal-to-noise ratio and the inability to phase the signals of the quaternary nuclei.

It is unsurprising that the performance of the two composite pulses were inappropriate for the compensation of off-resonance effects. It is well known that some composite pulses do not perform well in some pulse sequences and, in general, pulse sequences of particular length [23]. It is always recommended that a set of investigative experiments be undertaken to test

the effectiveness of composite pulses in comparison to an uncompensated version.

2.10 Conclusions

The optimum suppression of residual coherence, which exhibits short-range scalar coupling is achieved using the normal uncompensated selective PENDANT pulse sequence when compared to the common composite pulses tested here. It has been proved that off-resonance effects due to ^{13}C pulses are the principal sources of increased levels of breakthrough of residual ^{13}C signals of the CH_2 multiplicities.

Should time have permitted, further investigation into the use of more suitable composite pulses for the compensation of off-resonance effects of ^{13}C pulses would have been undertaken. Similarly, a brief investigation into the use of composite pulses for the compensation of off-resonance and *r.f.* inhomogeneity effects of ^{1}H pulses would also have been undertaken. Although no evidence suggests that the latter played a significant role in the investigative work undertaken, it may become of greater importance for molecules that exhibit larger proton chemical shift ranges.

It is envisaged that the compensation of off-resonance and *r.f.* inhomogeneity effects of ^{1}H pulses may pose a significant task, because most $\pi/2$ composite pulses evoke phase shifts about the z-axis. [22, 26] However, Levitt [26] has proposed that such composite pulses should prove useful in the context of achieving excitation of heteronucelar multiple quantum coherence, upon which the J-filter of the selective PENDANT experiment relies. The issue remains however, that such composite pulses must not jeopardise polarisation transfer from I to S.

2.11 Experimental investigation into the performance of selective PENDANT

Six identical selective PENDANT experiments were performed, all of which were phase cycled to give a pseudo-edited spectrum, each differing only by the proton carrier frequency of the selective pulses: one off-resonance experiment was conducted as reference for the five remaining experiments, which were each set on-resonance for one of the five proton groups or nuclei of the solute molecule, i.e., **a**, **b**, **c**, **d** and **e**.

Acquisition and spectrum processing parameters were set according to those specified

previously. The carrier frequency, as usual, was set to the centre of the proton chemical shift range prior to the execution of the hard proton pulses in the low-pass J-filter.

In these initial investigative experiments, the shaped selective pulses described previously were utilised instead of DANTE. This was to ensure optimum selectivity in order to prevent unwanted excitation of heteronuclear short-range coupled protons via the proton satellites. DANTE is inherently less efficacious in this respect due to its excitation side lobes, which extend far from the principal excitation bandwidth (Appendix A10.3). This course of action was deemed prudent, since, excitation of the proton satellites with spurious phases may have caused unpredictable effects to the suppression of residual coherences. This is due to the fact that suppression is dependent upon heteronuclear multiple quantum coherences, which exhibit short-range scalar couplings, not being re-converted back into observable single quantum coherence by subsequent proton pulses.

2.12 Results and Discussion

Figures 2.7, and 2.8 overleaf present the spectra obtained for the on-resonance (when the proton(s) is selectively manipulated) experiments. Each figure is given on a separate page for increased ease of analysis and the maintenance of resolution of the spectra. Indeed this strategy where applicable is adopted throughout the remainder of the thesis. The adjacent molecular diagram of the solute in each of the figures indicates, by way of an arrow, the particular proton that has been manipulated (on-resonance) by the selective pulses. To the right of each figure is the off-resonance (no proton(s) manipulated by selective pulse) or 'control' spectrum for comparison purposes. Figure 2.7 also presents a reference spectrum for comparison, which is exactly that used in the analysis of suppression efficiencies: a direct detect analogue of selective PENDANT, i.e., without the proton purge pulses and the selective proton pulses set off-resonance.

The lower case letters adjacent to the peaks depict the ^{13}C nuclei that have received polarisation transfer from the selected proton. Quaternary signals that have not been labelled with their corresponding letters, i.e., **f**, **g** and **h**, are identical to the off-resonance experiment in terms of intensity and multiplet structure. Therefore, by definition they have not received polarisation transfer, and do not exhibit scalar coupling to the selected proton.

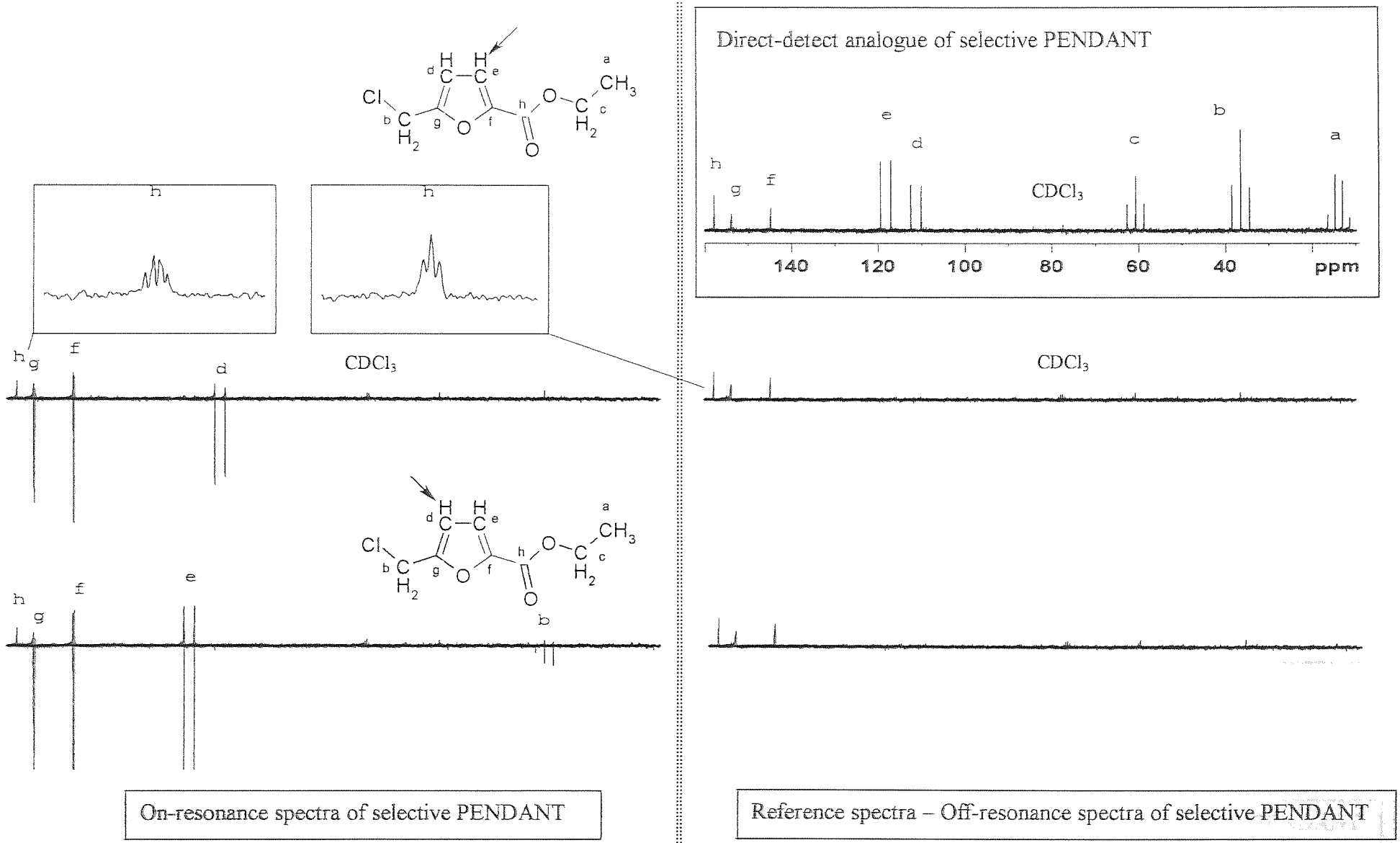

Figure 2.7 **Spectra of on-resonance selective PENDANT vs off-resonance for comparison. Lower case letters mark correlations to carbons, which exhibit long-range scalar coupling to selected proton (see text). Molecular diagram indicates selected proton**

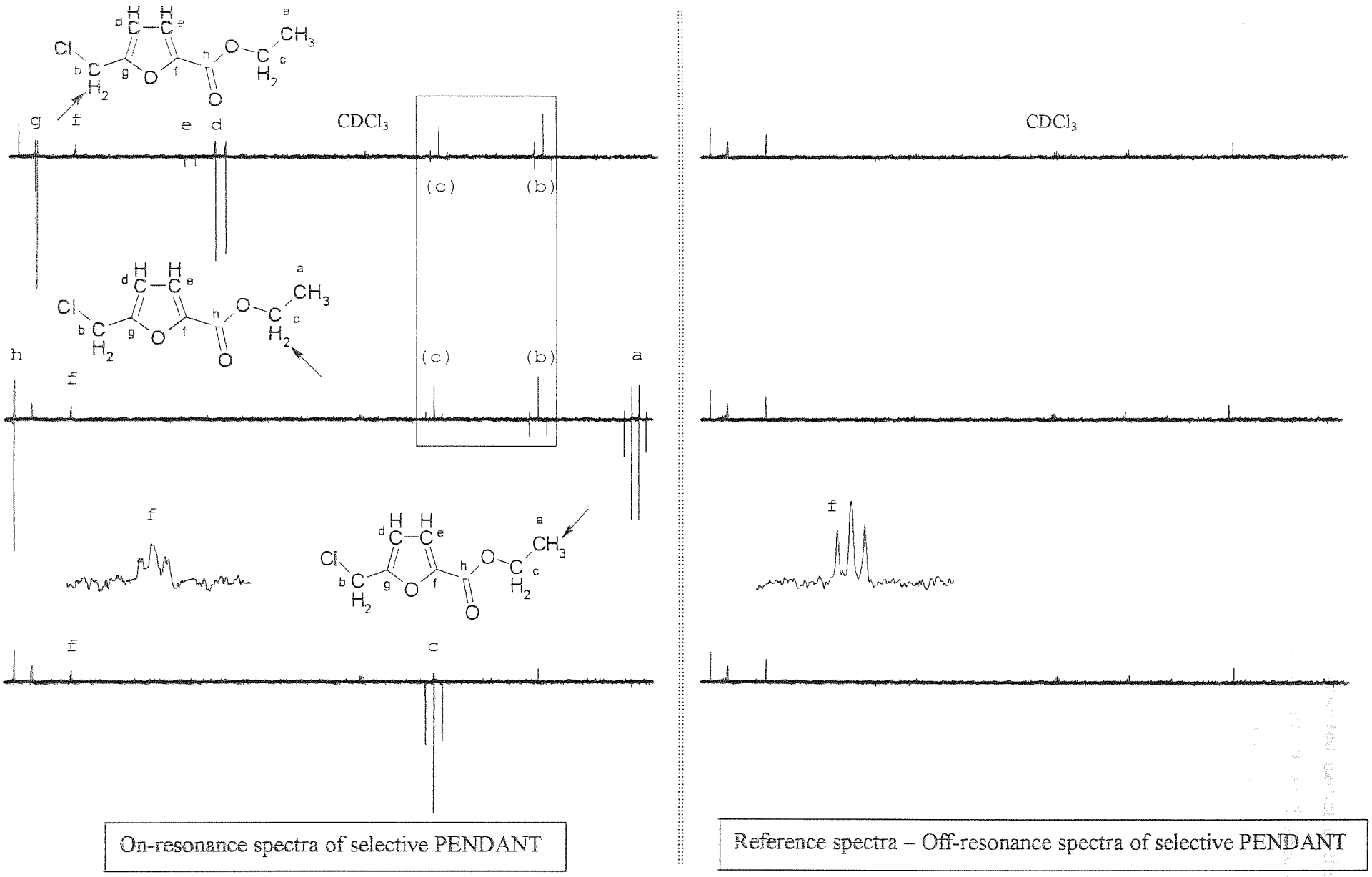

Figure 2.8 Spectra of on-resonance selective PENDANT vs off-resonance for comparison. Lower case letters mark correlations to carbons, which exhibit long-range scalar coupling to selected proton (see text). In the enclosed region with lower case letters in parentheses, the spectral changes are not attributed to correlations.

Figures 2.7 and 2.8 illustrate beautifully all of the factors presented earlier in the theoretical analysis of the selective PENDANT experiment. The selective PENDANT spectrum derived from selective manipulation of proton **e** in figure 2.7 is considered here in detail.

The ^{13}C nuclei, **h, g, f** and **d** have all received polarisation transfer from the selected proton. The signals **g, f** and **d** all appear anti-phase to the solvent resonance ($CDCl_3$) at 77ppm. This is also seen by comparison to the off-resonance spectrum, which has been phase corrected to the same parameters. This illustrates the successful function of the pseudo-edited detection method for these particular long-range scalar coupling correlations.

However, the exception to the total success of the 'pseudo edited' detection method is seen on inspection of the **h** quaternary signal. It has been shown that the observable coherence in selective PENDANT experiments are comprised of the superposition of coherences which originate from S (^{13}C) and those which originate from polarisation transfer from I (^{1}H) (Section 2.5.1). It was mentioned that in cases where the magnitude of the latter was smaller than the former, the resulting spectrum would exhibit attenuation of the S signal, and possess the same phase as if it had not received polarisation transfer. Indeed, this is the case for the **h** signal.

Comparison with the off-resonance spectrum illustrates clearly the attenuation of intensity and the change in multiplet structure indicative of polarisation transfer (see inset in figure 2.7). Therefore, as mentioned earlier (Section 2.5.1), the utility of selective PENDANT is not compromised by the failure of the pseudo edited detection method, since a trivial comparison to the off-resonance spectrum yields the assignment.

It is not surprising that the pseudo edited method of detection failed in this instance, because the J-value for long-range scalar coupling to the selected proton is 0.7Hz as compared to 8Hz from which the evolution delay τ_c is set.

2.13 Proof of the superposition of coherence for the attenuation of in-phase quaternary signals

A series of experiments were performed under identical conditions using the following modified selective PENDANT experiments in order to prove that the attenuation of the **h**

signal is due to the superposition of coherence as described earlier.

1. A selective PENDANT experiment with the first ^{13}C pulse (P_4) phase cycled to cancel all coherences that originate from ^{13}C.

2. A selective PENDANT experiment was performed with the first selective proton pulse executed off-resonance.

Experiment 1 necessitates the detection of coherence that originates purely from polarisation transfer from the selected proton. Experiment 2 necessitates the detection of coherences that originate purely from ^{13}C, as polarisation transfer from the proton does not occur due to the removal of the first selective proton pulse.

The superposition of both results is tantamount to a normal selective PENDANT experiment, i.e., the superposition of coherence that originates from polarisation transfer from I, and residual coherence from S. Consequently, one can appreciate the form of a normal slective PENDANT spectrum by the composition of these two elements.

2.13.1 Results and Discussion

Figure 2.9 presents the results of experiments 1 and 2. For comparison a normal selective PENDANT spectrum acquired under identical conditions, i.e., the spectrum of figure 2.7 for selected proton **e** examined previously. The insets in all figures, display a magnified view of the important multiplets for discussion.

The spectrum of figure 2.9a (Experiment 2) clearly demonstrates that the first J-filter pulse P_1 has efficiently purged quaternary coherences of **f** and **g**, which originate from ^{13}C as described previously. (Section 2.4.3 and 2.5) The efficiency of purging is high due to the fact that the J-value for long-range couplings of **f** and **g** to the selected proton is 8Hz, which is equivalent to that used for the setting of the evolution delays in these experiments.

Fig 2.9 (a) Result of experiment 2 (see text) – No signals from polarisation transfer . Signals from ^{13}C only.

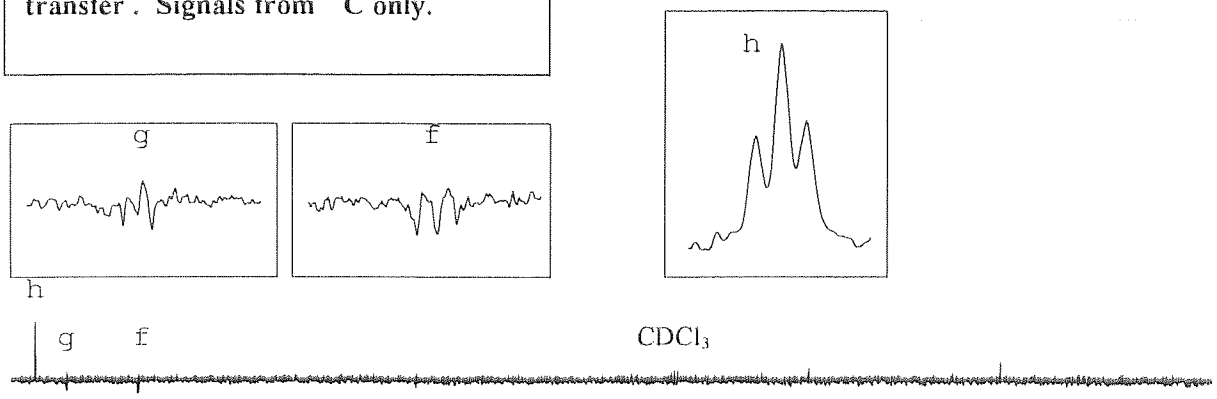

Fig 2.9 (b) Result of experiment 1 (see text) – Polarisation transfer from proton h only.

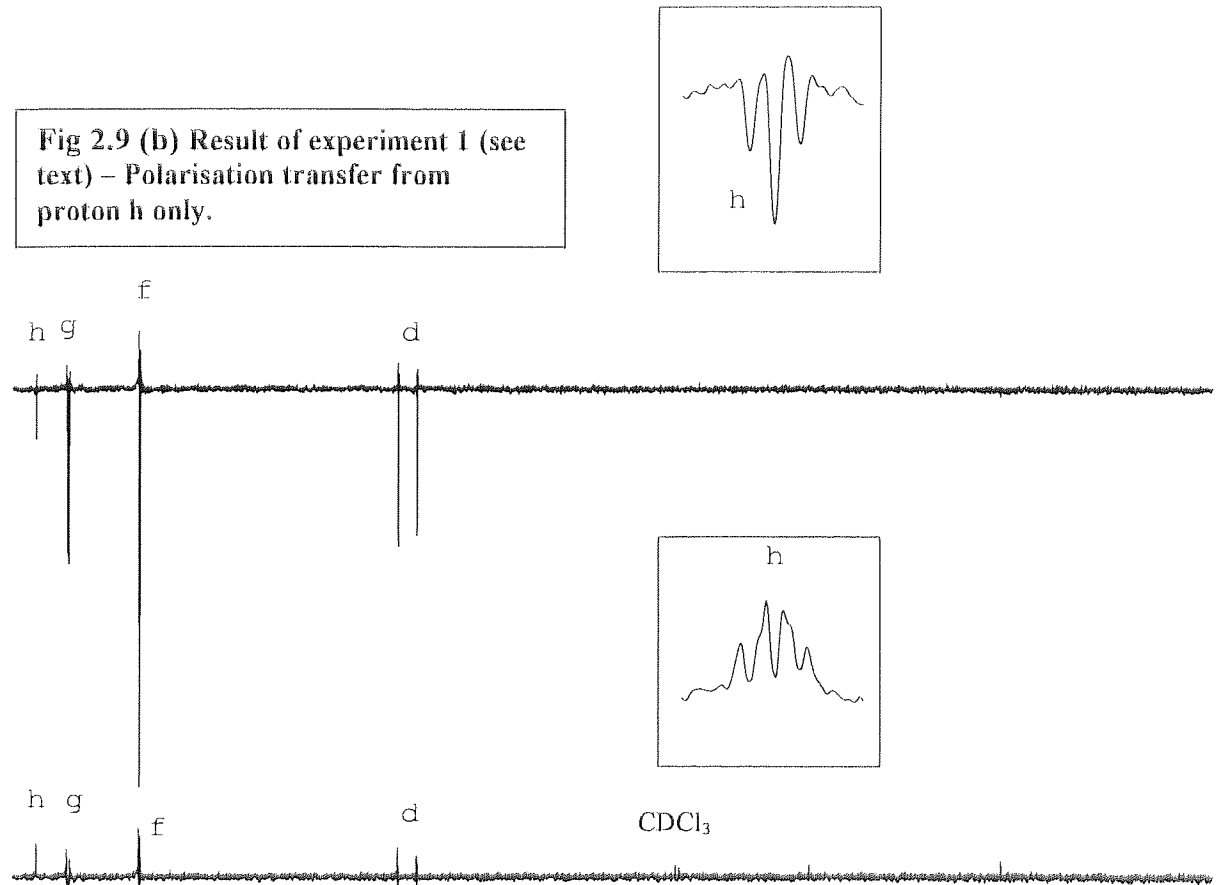

Fig 2.9 (c) Normal selective PENDANT spectrum taken from figure 2.7 (On -resonance for proton h)

Figure 2.9 Proof of the superposition of coherence for the attenuation of in-phase quaternary signals. Insets refer to labelled carbon

On the other hand, it can be seen in figure 2.9a, that much of the residual **h** quaternary coherence still exists due to the mismatch in J-values. Figure 2.9b, depicts coherence that originates purely from polarisation transfer from the selected proton. It can be seen that the superposition of the **h** signals from figures 2.9a and 2.9b, which are illustrated in the insets, results in the spectrum of figure 2.9c, i.e., the normal selective PENDANT experiment.

Although the **h** signal exhibits a phase indicative of signals that have not received polarisation transfer, it does differ in both magnitude and multiplet structure in comparison to the off-resonance spectrum. These observations are further demonstrated in figure 2.8 for the **f** quaternary. This demonstrates the necessity of performing an off-resonance experiment for comparison with on-resonance experiments for the routine use of selective PENDANT for the identification of long-range scalar coupling correlations.

In most cases, i.e., for samples of reasonably high solute concentrations, this does not represent a detrimental increase in experiment time, since it merely requires the rather trivial specification of an extra frequency list. For this small outlay, the experimenter is provided with a quaternary only spectrum of a quality closely resembling that of SEMUTGL^{+}(q) and a method of unambiguously determining long-range heteronuclear scalar coupling correlations.

When the multiplet structure of a quaternary signal is unresolvable and it exhibits a phase that suggests that polarisation transfer has not taken place, comparison to the off-resonance experiment in terms of signal intensity must be made. A pre-requisite for this kind of comparison, is that experiment stability is ensured, such that a change in intensity is truly attributable to the small magnitude of polarisation transfer.

Usually this constitutes using a strong field-frequency locking solvent, which possess high numbers of deuterium isotopes, e.g., DMSO $-D_6$, C_6D_6 etc, at reasonable concentrations. Additionally, it is wise to regulate the temperature of the sample. It has been demonstrated here that using a reasonably poor lock solvent, i.e., $CDCl_3$ at a constant sample temperature of 300K is more than adequate to maintain sufficient stability in order to make appropriate assignments using selective PENDANT. This can be readily seen in the spectrum of figure 2.7, where the residual signals of the CH_2 multiplicities **b** and **c** in the on resonance spectrum (selected proton **e**) are identical to those in the off-resonance spectrum. Similarly, in figure 2.8, quaternary resonances **g** and **h**, are identical in both the on-resonance spectrum (selected

proton **a**), and the off-resonance spectrum. This indicates their lack of scalar coupling to the selected proton or the complete mismatch of J-values used for the setting of the evolution delays. Of course, INAPT also suffers from the mismatch of J-values, but, does not benefit from the simultaneous identification of all quaternaries of the sample, which is the topic of discussion in the following section.

In figure 2.8, the enclosed areas of the on-resonance spectra (selected protons **b** and **c**) highlights a change that has occurred in the signals (**b**) and (**c**), (both CH_2 multiplets) which are not attributed to long-range heteronuclear couplings with the selected protons. These observations are one of the subjects for discussion in the next section.

2.14 Investigation into the utility of selective PENDANT with respect to INAPT

A series of INAPT experiments were performed on-resonance for each of the separate proton groups or nuclei. Where applicable, acquisition parameters and selective pulses that were identical to selective PENDANT were used.

As the INAPT experiment is designed to utilise a selective proton polarisation transfer pulse, a Gaussian Cascade Q5 pulse [23](Appendix A10) was used instead of another SNEEZE pulse and set to give an excitation bandwidth of 40Hz. This is due to SNEEZE being designed to act upon magnetisation and not coherence [23]. The Gaussian cascade is a universal pulse designed to work sufficiently on all initial states of coherence or magnetisation. The duration of the pulse was 0.214 seconds. Therefore, as mentioned previously (Section 2.5.2), the benefits of selective PENDANT in the context of invoking polarisation transfer from I to S using the hard pulses of the J-filter are apparent. The sensitivity of INAPT maybe compromised in comparison to selective PENDANT due to extra T_2 relaxation that occurs as a result of the duration of two selective pulses and the evolution delay.

2.14.1 Results and Discussion

The results of the INAPT experiments confirmed the long-range scalar coupling correlations made by the selective PENDANT experiment. Only three INAPT spectra are presented here for direct comparison with the same on-resonance selective PENDANT spectra, in order to illustrate the utility of the latter. The three experiments correspond to the separate selective

manipulation of protons **a**, **b** and **c**, which do not exhibit long-range coupling to all quaternary nuclei. The spectra are presented in figure 2.10 overleaf.

Quaternary nuclei invisible to INAPT are indicated by the asterisk in the selective PENDANT spectra. The INAPT technique successfully identifies the same long-range scalar couplings as selective PENDANT, however, it fails to identify the quaternary nucleus, **g**, in two experiments, as it does not exhibit long-range scalar coupling to protons **a** or **c**.

Identification of quaternary **g** only occurs when selective manipulation of protons **b**, **d** and **e** are undertaken. Therefore, quaternary **g** would go undetected in the INAPT experiment, if these protons had not been manipulated during the experiment.

It is evident that in circumstances when the identification of all quaternary nuclei in the molecule is not warranted, the INAPT experiment is clearly suitable. However, in circumstances when the molecule under scrutiny is larger and possess a greater number of quaternary nuclei, the INAPT experiment may fail to identify all of them. To ensure that all quaternary nuclei, had been identified by INAPT, presuming they exhibit coupling to protons, the INAPT experiment would have to be continued to manipulate all protons of the sample. Of course, the selective manipulation of all protons may be impossible as a result of proton spectral overcrowding, and even if it were not so, the performance of many other selective manipulations constitutes a significant extension of the experiment time. At this stage the utility of INAPT is lost and the experimenter would have to revert to alternative means of identifying all quaternary nuclei of the sample, which causes further extension to experiment time and greater inconvenience.

The selective PENDANT experiment provides an attractive alternative for the fast identification of all quaternary nuclei of the sample and long-range scalar coupling correlations should they exist. Of course, the utility of selective PENDANT for the identification of long-range couplings would be similarly compromised by proton spectral overcrowding, however, not before identifying all quaternary nuclei in the sample. Selective PENDANT should prove extremely useful for the routine study of novel organic compounds, which require the identification of all quaternary nuclei. As all quaternary nuclei of the sample are identified immediately, the experimenter is in a position to choose whether further selective assignments are required to prove the existence of long-range scalar couplings.

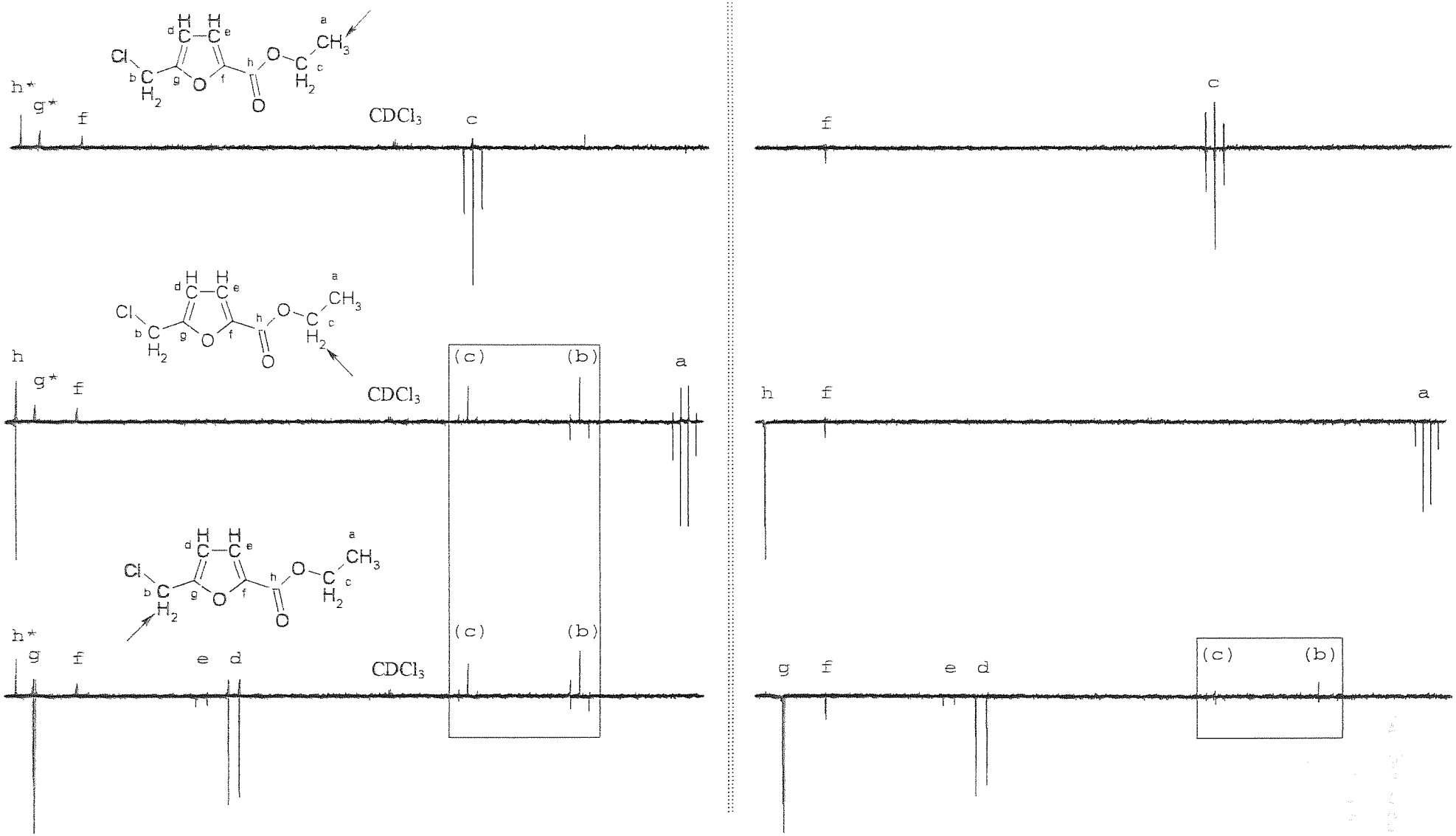

Figure 2.10 Selective PENDANT vs INAPT. Left of divide: Selective PENDANT spectra. Right of divide: INAPT spectra for same selected proton

Lower case letters mark correlations to carbons, which exhibit long-range scalar coupling to selected proton. In the enclosed region with lower case letters in parentheses, the spectral changes are not attributed to correlations.
Asterisk marks those quaternaries that are not long-range scalar coupled to the selected proton and are therefore invisible to INAPT.

Slight differences in the phase and multiplet structures exist between the selective PENDANT and INAPT experiment for nuclei that have received polarisation transfer from the selected proton(s). This is most likely caused by the use of a hard proton polarisation transfer pulse in selective PENDANT as opposed to the selective pulse used in INAPT, therefore invoking a slight timing difference between the two experiments in which scalar couplings evolve. The differences in phases are trivial and do not effect the utility of either experiment.

It was mentioned earlier (Section 2.5.1), that due to the use of a non-selective proton polarisation transfer pulse, the selective PENDANT experiment may exhibit a sensitivity advantage over INAPT, which uses a selective proton polarisation transfer pulse of longer duration: the comparatively much shorter non-selective polarisation transfer pulse in selective PENDANT reduces the disadvantageous effects of T_2 relaxation of the selected proton. However, the signal-to-noise ratios of the selective PENDANT experiment and INAPT experiment are comparable. The similarity in signal-to-noise ratios suggests that, for these experimental conditions, the selective PENDANT experiment utilising non-selective polarisation transfer pulses does not provide a genuine sensitivity advantage over INAPT. In circumstances when the T_2 of protons are short, selective PENDANT may prove advantageous for maximising sensitivity in comparison to INAPT.

2.14.2 Spurious breakthrough of non-long range coupled ^{13}C nuclei.

It was mentioned above, that the selective PENDANT spectra for selected protons **b** and **c**, in figure 2.8, reveals the simultaneous breakthrough of the ^{13}C (CH_2) signals **b** and **c**. On closer inspection of the INAPT spectrum in figure 2.10, a similar breakthrough of the **b** and **c** signal is observed (**b** and **c** in parentheses), however, the magnitudes in comparison to selective PENDANT are significantly smaller.

Figure 2.11 overleaf illustrates the proton spectrum of the solute molecule. The chemical shift between protons **b** and **c** is 97 Hz. Their respective short-range ^{13}C-^{1}H couplings, which are indicated by the ^{13}C satellites b′ and c′, are 153Hz and 148Hz respectively. It is evident that a selective pulse on-resonance for **b** and **c** with an excitation bandwidth of 40Hz, causes the 'partial' perturbation of one of the proton satellites of the other, i.e., **c′** and **b′** respectively.

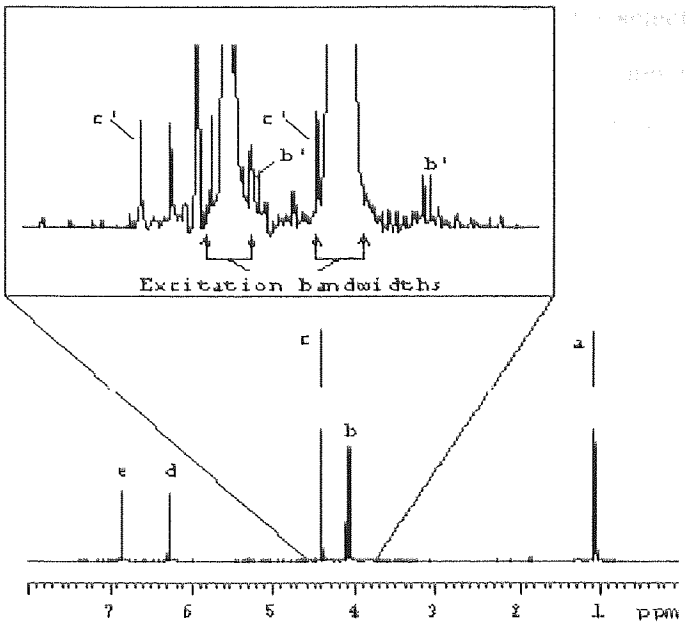

Figure 2.11 **Expanded region of proton spectrum for proton signals b and c in ethyl-5-(chloromethyl)-2-furan-carboxylate.**

When the proton satellite spin system is subjected to 'partial' perturbation by the selective inversion pulses, specific proton transitions attain a partial conversion to longitudinal two-spin order ($2I_zS_z$), with respect to the heteronuclear scalar coupling. This is analogous to that caused by selective population inversion (SPI) experiments [4], for the excitation of an entire spin multiplet.

Subsequent selective pulses and/or non-selective hard pulses can cause the excitation of short-range coupled heteronuclear multiple quantum coherences, in which the spin(s) associated with the transition(s) that were initially inverted by the selective pulse, are active in the coherence. Evolution of these heteronuclear multiple quantum coherences occurs in a similar way as those that were excited by the low-pass J-filter. Subsequently, components of these multiple quantum coherences are reconverted to observable single quantum coherences by remaining pulses in selective PENDANT and INAPT, i.e., the S polarisation transfer pulses, and/or selective and non-selective proton polarisation transfer pulses. Consequently, ^{13}C nuclei, which are short-range coupled to the perturbed proton, breakthrough into the spectrum.

Indeed, pulse sequences, which utilise a mixture of selective and non-selective pulses, have been used for the excitation of multiple quantum coherences ([27] pg 306 and references

therein) via the partial manipulation of spin transitions. In the selective PENDANT and INAPT experiments, partial manipulation of spin transitions was achieved accidentally by the unfortuitous relative positioning of the **b** and **c** ^{13}C satellites, **c′** and **b′** respectively.

Bax [16] indicated that, if the selective proton pulses affect the ^{13}C satellites of another proton, a small residual signal is seen in the INAPT spectrum for the associated short range coupled carbon. Bax did not suggest a reason for these observations, however the explanation given above seems a likely cause.

Breakthrough of a further residual ^{13}C signal occurs simultaneously in both INAPT and selective PENDANT spectra when an on-resonance experiment is performed for protons **b**. When protons **b** are on-resonance, breakthrough of the ^{13}C signal of **b** occurs. The ^{13}C satellites for **b** (**b′**), are far removed from the edge of the excitation bandwidth of the selective pulse, e.g., 56.5Hz. Therefore, one may deduce that the selective pulse does not cause direct perturbation of the ^{13}C satellites **b′**. Empirical evidence further substantiates this deduction by the absence of a ^{13}C residual signal for the methyl carbon **a** when protons **a** are selected: the short-range J-value of **a** (127Hz) is less than that of **b**, which necessitates the ^{13}C satellites, **a′**, are only 43.5Hz away from the edge of the excitation bandwidth.

If the breakthrough of the residual signal of **b** is not attributed to the direct perturbation of its ^{13}C satellites, **b′**, a mutual property must exist between the ^{13}C nuclei, **b**, and the 'satellite' protons **c′**. This supposition is based upon the fact that conceivably, the only protons that can be perturbed by the selective pulse applied at the frequency of **b** are:

- the **b** protons bonded to ^{12}C, which exhibit the desired long-range scalar coupling to ^{13}C and proton homonuclear coupling.
- One of the ^{13}C satellites of **c**, i.e., **c′**

For a mutual property to exist between the ^{13}C, nuclei, **b** and the proton satellites **c′**, there must be a ^{13}C **b** nucleus and ^{13}C **c** nucleus in the same molecule. However, the natural abundance of molecules, which possess two ^{13}C nuclei in the same molecule, is extremely low, and therefore the effect would hardly be observable. This phenomenon remains unexplained and would have been the subject of further investigation had time permitted.
The breakthrough of ^{13}C signals **b** and **c** are each present in the separate selective PENDANT

spectra of the selected protons **c** and **b** respectively. This observation in itself lends to the fact that a mutual property is mediating the effect that gives rise to the breakthrough.

Interestingly, the INAPT spectrum is devoid of breakthrough of signals **b** and **c** when protons, **c** are selected. Furthermore, the magnitude of the breakthrough signals is much greater in the selective PENDANT spectra compared to the INAPT spectrum. This suggests that the efficiency of excitation of multiple quantum coherence and re-conversion into single quantum coherence is more efficient in the selective PENDANT experiment.

As a means of preliminary investigation into the breakthrough of signals **b** and **c**, the following experiments were performed.

1. A INAPT experiment was modified so that the selective proton polarisation transfer pulse was substituted with a hard pulse to emulate the polarisation transfer conditions inherent in selective PENDANT. Two identical experiments were performed with either protons **b** or **c** selected. All other experimental parameters remained equivalent to those experiments detailed above.

2. The excitation bandwidth of the selective pulses in the normal selective PENDANT experiment, the modified INAPT experiment, detailed above, and the normal INAPT experiment, were reduced to 15Hz, to try to establish the dependence of the phenomenon on excitation bandwidth. This was conducted for protons **b** selected.

The results of experiment 1 are given in figure 2.12 overleaf. It is clearly evident that the magnitudes of the signals attributed to this phenomenon are at least, in part, related to the use of a hard pulse for polarisation transfer. Furthermore, the phenomenon is observable in both spectra (now when **c** is selected) of the modified INAPT experiment. Therefore, the selective PENDANT experiment is more sensitive to this phenomenon than the normal INAPT experiment.

The results of experiment 2 are given in figure 2.13 after figure 2.12. It is evident that upon the reduction of excitation bandwidth, the standard INAPT spectrum no longer exhibits the effects of breakthrough of the signals **b** and **c** when protons **b** are selected.

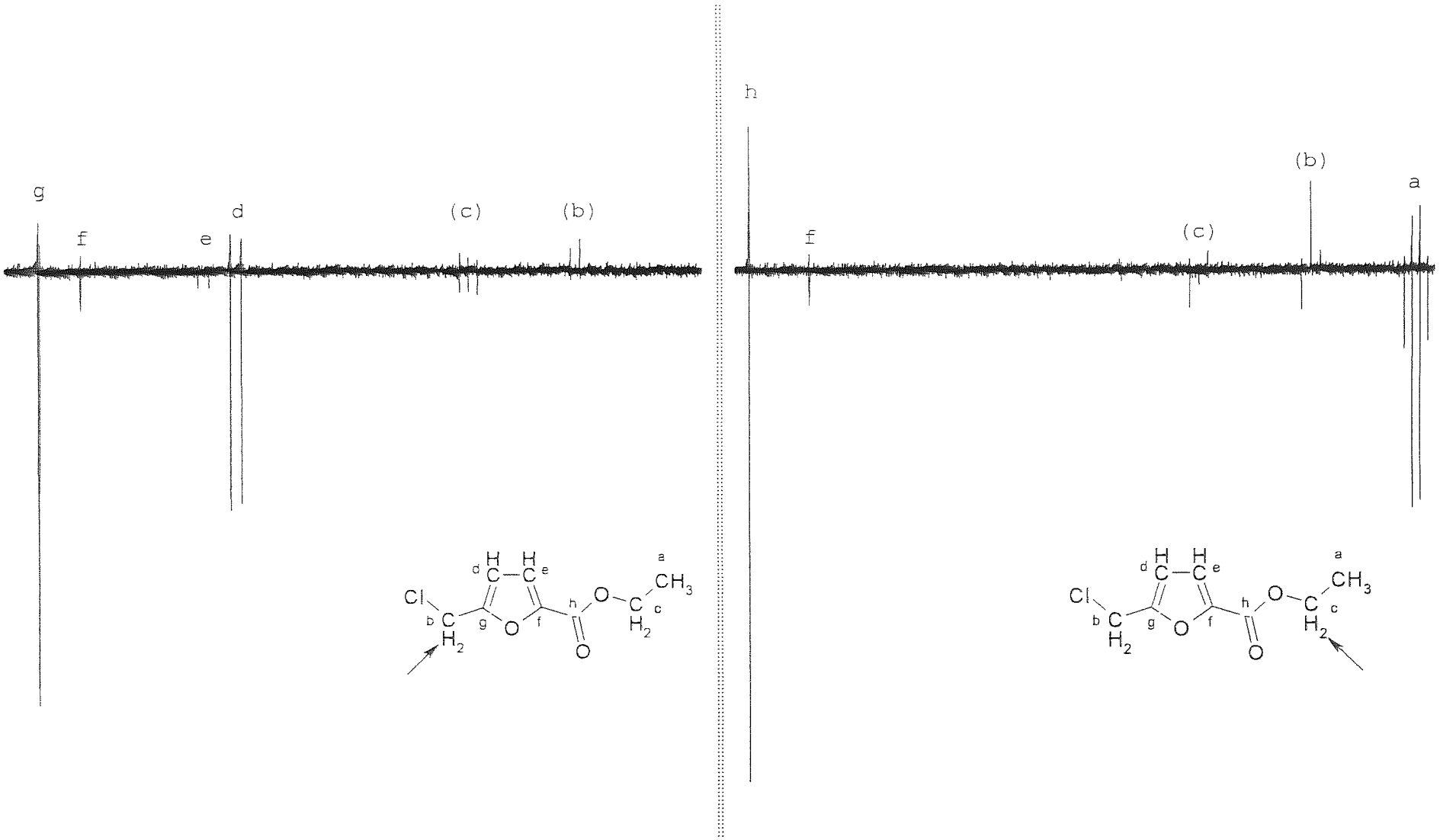

Figure 2.12 Results of experiment 1: Modified INAPT experiment: Selective proton polarisation transfer pulse replaced with non-selective (hard) proton pulse.

Lower case letters in parentheses, indicate spectral changes that are not attributed to correlations as described in text. Selected protons are indicated on molecular diagram.

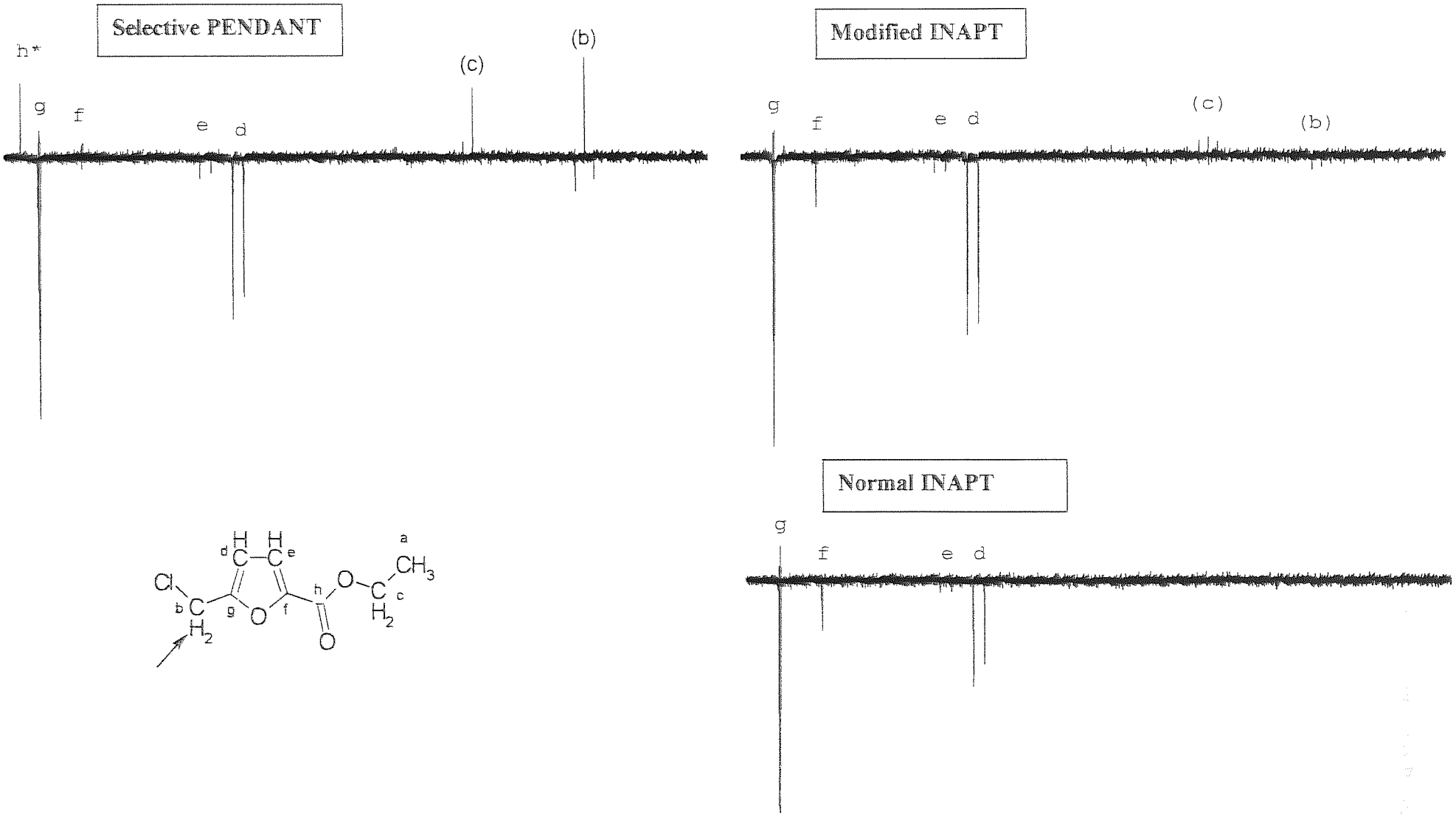

Figure 2.13 Results of experiment 2: Excitation bandwidth of all selective pulses in Selective PENDANT and INAPT experiments are set to 15Hz.

Protons, b, selected in all experiments

The modified INAPT spectrum does exhibit signals **b** and **c** when protons **b** are selected, but at significantly lower intensities, which are almost un-resolvable.

Figure 2.13 also demonstrates that the breakthrough of signals **b** and **c** in selective PENDANT are largely invariant to the change in selectivity if the phase changes are neglected.

A hypothesis for the sensitivity of selective PENDANT to the observation of the breakthrough signals **c** and **b** is as follows. Although the selective pulses give rise to high degrees of selectivity, small spurious frequency responses that modulate in phase and intensity exist at the periphery of the primary excitation bandwidth (Appendix A10 figure A10.3). Consequently, when the peripheral excitations cause the perturbations of the ^{13}C satellite transitions, the phases of subsequent coherences depend upon the spurious phase modulations caused by the selective pulse. As the J-filter is comprised of hard proton purge pulses of orthogonal phases, there is an increased chance that multiple quantum coherences of spurious phases will be re-converted back into observable single quantum coherences.

An investigation into the exact cause of the breakthrough of signals **b** and **c** is warranted for academic purposes. However, the presence of breakthrough signals does not impinge upon the utility of selective PENDANT. This is due to the fact that the INAPT experiment, on-resonance for protons **b,** similarly exhibits breakthrough of **b** and **c** in the spectrum when the excitation bandwidth is set to 40Hz. Decreasing the excitation bandwidth to less than 15Hz (a point at which breakthrough is eliminated from the INAPT spectrum) would not usually be implemented because it would significantly increase the likelihood of uneven perturbation of the multiplet for which even perturbation is desired for polarisation transfer.

2.14.3 Selective PENDANT using DANTE pulses

A series of identical selective PENDANT experiments were performed using DANTE for selective excitation and refocusing of proton coherence. These experiments were carried out in order to establish that the selective PENDANT pulse sequence is applicable for implementation on spectrometers without shaped pulse capabilities, one of the fundamental thrusts of this work.

The implementation of the DANTE pulse train is achieved via the execution of a loop in the

pulse sequence (Appendix A13.3 and Appendix A4.5.6), and necessitates that the S refocusing pulses are positioned either before or after the DANTE refocusing pulses. This is in contrast to selective PENDANT, in which the S refocusing pulses are positioned midway through the selective proton refocusing pulses.

In this investigation, the S refocusing pulses were positioned after the selective proton refocusing pulses and required that the first S pulse, P_4, be staggered such that it is positioned before the application of the first DANTE pulse, P_a, by the amount τ_1. Consequently, the final evolution period, τ_b, was extended by an amount equal to the duration of the DANTE pulse, i.e., 0.025 seconds, in order to facilitate refocusing of quaternary coherence ready for detection. All other experimental parameters were identical to those used in the selective PENDANT experiments reported earlier.

2.15 Results and Discussion

For means of comparison, figures 2.14 and 2.15 given overleaf present the results of the experiments for selected protons **a**, **b**, **c**, **d** and **e** of selective PENDANT using DANTE and selective PENDANT using shaped selective pulses.

The signal-to-noise ratios obtained from selective PENDANT that utilise DANTE pulses are comparable to the shaped selective pulse analogues. The differences attributed to the breakthrough of signals (b) and (c) are not surprising, since the excitation profile of each pulse differs significantly at the periphery of the excitation bandwidth. However, the excitation side lobes of DANTE clearly do not affect the suppression efficiencies of ^{13}C signals attributed to short-range scalar coupling. This is proven by the complete absence of CH and CH_3 signals and the similar breakthrough of CH_2 signals to a comparable level to that of selective PENDANT.

The results clearly show that selective PENDANT is applicable for routine implementation on NMR spectrometers without selective shaped pulse capability.

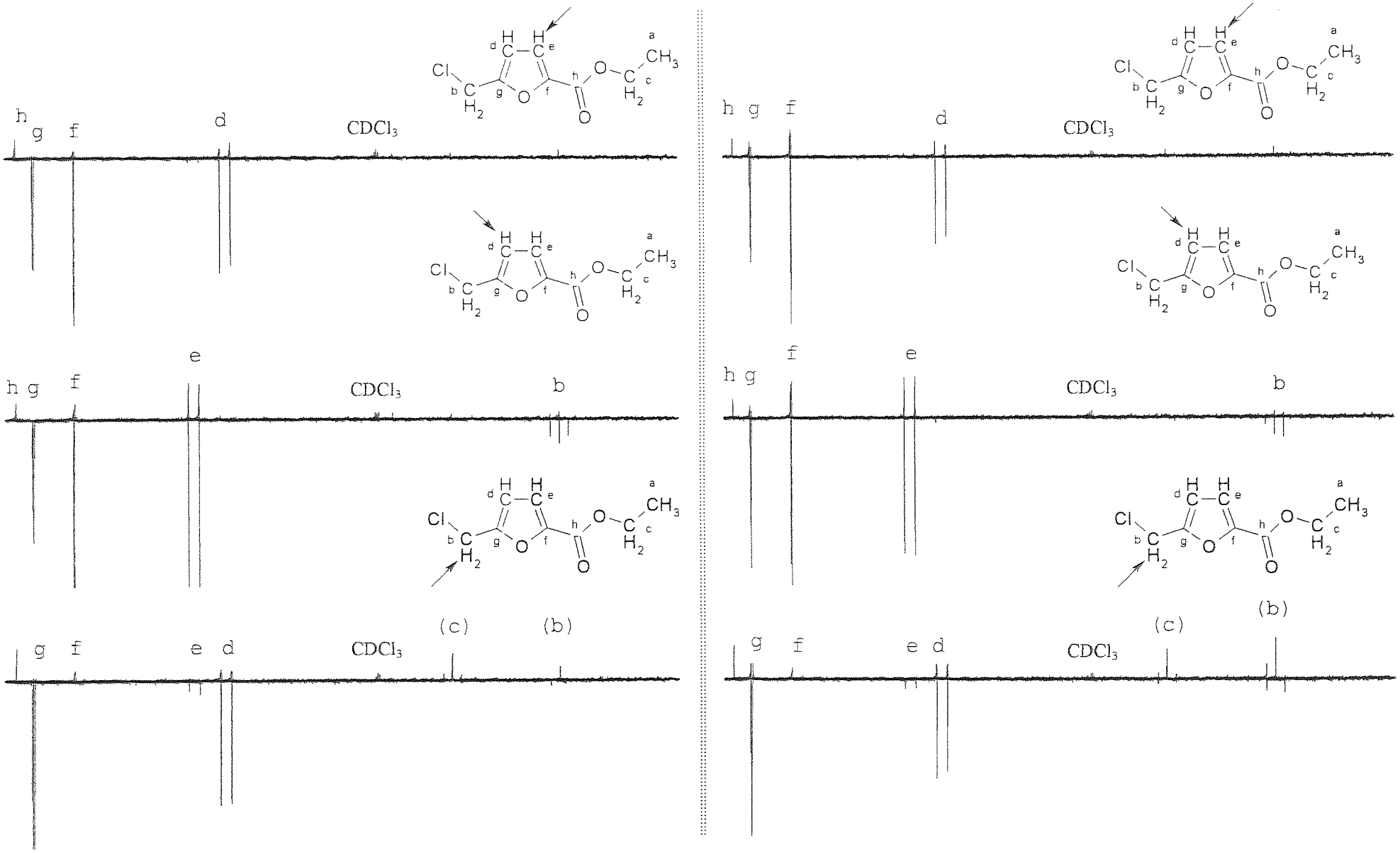

Figure 2.14 **Results of selective PENDANT using DANTE pulses vs Selective PENDANT us ing soft shaped pulses.**
Left of divide: Selective PENDANT using DANTE pulses. Right of divide: Selective PENDANT using soft shaped selective pulses as reported earlier.
Molecular diagram indicates proton(s) selected. Long-range scalar coupling correlations are indicated by lower case letters.
Letters in parentheses indicate breakthrough of signals not attributed to correlations as discussed earlier.

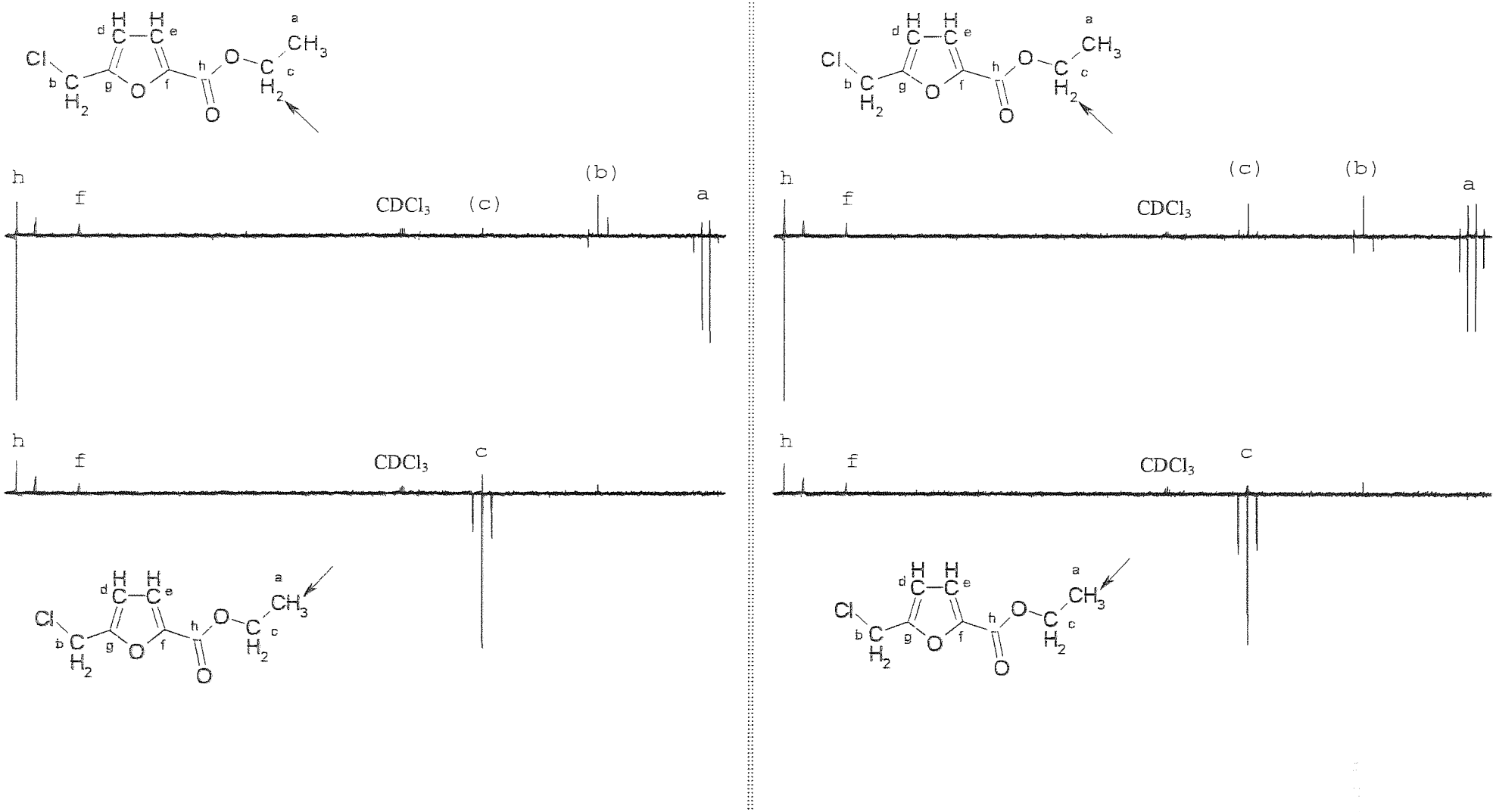

Figure 2.15 **Results of selective PENDANT using DANTE pulses vs Selective PENDANT using soft shaped pulses.**
Left of divide: Selective PENDANT using DANTE pulses. Right of divide: Selective PENDANT using soft shaped selective pulses as reported earlier.

Molecular diagram indicates proton(s) selected. Long-range scalar coupling correlations are indicated by lower case letters.
Letters in parentheses indicate breakthrough of signals not attributed to correlations as discussed earlier.

2.16 Conclusions

The selective PENDANT experiment successfully identifies all ^{13}C quaternary nuclei in the molecule under scrutiny, while simultaneously identifying ^{13}C long-range scalar coupling correlations to the selected proton by means of polarisation transfer (which is intrinsic with polarisation exchange).

The utility of selective PENDANT is realised when compared to the utility of INAPT. INAPT can only identify ^{13}C quaternaries that exhibit long-range scalar coupling to the selected proton. One can never be confident that all ^{13}C quaternaries in the sample have been identified, since spectral overcrowding may prevent selective perturbation of all protons. Consequently, a separate experiment must be performed that facilitates the detection of all other ^{13}C quaternary nuclei, e.g., PENDANT, DEPTQ, SEMUTGL^{+}(q). Ultimately, the performance of two separate experiments for the complete characterisation of the quaternary spin system is time consuming and represents increased inconvenience on behalf of the experimenter.

By analogy with INAPT, selective PENDANT identifies ^{13}C quaternary nuclei, which exhibit long-range scalar coupling to the selected proton while simultaneously identifying all other ^{13}C quaternary nuclei present in the sample. The attainment of an additional off-resonance experiment, for the accurate assignment of long-range scalar coupling correlations, is a trivial matter in comparison to the added inconvenience and investment of time involved in performing an additional experiment to identify all quaternary nuclei.

The incorporation of a low-pass J-filter into the selective PENDANT pulse sequence has enabled the efficient suppression of unwanted residual ^{13}C coherences that exhibit short-range scalar coupling. The excitation of such coherences is implicit to the detection of quaternary nuclei by PENDANT. It has been stated that the recommended procedure for the setting of the short-range coupling evolution delays, τ_1 and τ_2, in the J-filter to 140Hz and 180Hz respectively, causes excellent suppression. Indeed, it has been shown that ^{13}C signals, which exhibit CH and CH_3 short-range scalar coupling multiplicities are completely suppressed from the spectrum. It has also been demonstrated that the complete suppression of ^{13}C signals of the CH and CH_3 multiplicities is maintained when the choice of evolution delay, τ_1, is varied, which is tantamount to a range of typically encountered J-values.

The suppression of ^{13}C signals, which exhibit CH_2 short-range scalar couplings is very efficient. A suppression level of 94.1% was obtained when τ_1 and τ_2 were set to the recommended values as described above. It has been demonstrated that the level of suppression decreased to a maximum of 93% (7% breakthrough) when τ_1 was set according to a hypothetical J-value, which was approximately 30Hz less than the actual value of 153Hz. It has also been proven that off-resonance effects constitute the major proportion of breakthrough of ^{13}C signals of CH_2 multiplicities. It is thought that the compensation of off-resonance effects by the replacement of standard ^{13}C refocusing pulses with suitable composite pulses, will increase suppression efficiencies of the ^{13}C signals of CH_2 multiplicities further.

The presence of small magnitudes of breakthrough signals merely constitutes a slight cosmetic degradation of the spectrum but does not impinge upon the utility of the selective PENDANT experiment, when compared to an off-resonance spectrum.

The unique structure and positioning of the low-pass J-filter affords it a novel dual function, namely, to cause suppression of residual ^{13}C coherences, for which it is designed, and to cause polarisation exchange. At the time of writing, no examples have been found where J-filters have been incorporated into pulse sequences to perform a dual function.

The potentially large variation of long-range $^{13}C - {}^{1}H$ J-values in organic compounds sometimes necessitates the inefficient purging of coherence that originates from quaternary nuclei that exhibit long-range scalar coupling to the selected proton. The superposition of coherence that originates from these nuclei and that which originates from polarisation transfer sometimes necessitates the failure of the pseudo-edited detection method: quaternary nuclei that have received small magnitudes of polarisation transfer from the selected proton exhibit the same phase as quaternary's that have not received polarisation transfer. Consequently, it is recommended that an off-resonance (quaternary only) spectrum is performed in addition to on-resonance spectra as a means of comparison for assignment purposes. Armed with the off-resonance spectrum, assignment is a trivial matter by means of inspection of intensities and multiplet structures. The attainment of an off-resonance spectrum represents a trivial effort on behalf of the experimenter, by the simple inclusion of an extra proton frequency list.

Investigative work reported here has demonstrated that both INAPT and selective PENDANT spectra are subject to breakthrough of residual ^{13}C signals when the corresponding ^{13}C satellites in the proton spectrum are accidentally perturbed by the selective pulses. This phenomenon has been previously identified in INAPT spectra by Bax [16] although a suitable explanation for the occurrence was not given. A plausible explanation for the occurrence of these residual signals in both INAPT and selective PENDANT has been reported previously here (Section 2.14.2).

However, in comparison to INAPT, it was determined that the selective PENDANT experiment exhibits a greater sensitivity toward the breakthrough of residual ^{13}C signals that arise due to unintentional perturbation of the corresponding ^{13}C satellites. It has been proven that the increased sensitivity is due to the use of hard proton pulses in the low-pass J-filter element. Replacement of the selective proton pulses in INAPT with hard proton pulses revealed similar magnitudes of breakthrough.

In addition to the breakthrough of residual ^{13}C signals described above, a further residual ^{13}C signal was observed in the same spectrum for both INAPT and selective PENDANT (Section 2.14.2). At the time of writing this phenomenon remains unexplained, however, it is surmised that some kind of mutual scalar coupling effect exists between the ^{13}C nuclei involved in the unexpected breakthrough and the ^{13}C satellite protons that are perturbed accidentally by the selective pulses. Further investigation into this fascinating observation is warranted.

When proton (inverse) detected methods are not amenable to the experimenter and the proton spectrum of the molecule under scrutiny is devoid of spectral overcrowding, it has been demonstrated that the selective PENDANT experiment could be used for the routine characterisation of the entire ^{13}C quaternary spin system. In common with INAPT, selective PENDANT also identifies all long-range ^{13}C-^{1}H correlations other than those of quaternary nuclei in the same experiment.

Chapter 3 The combination of selective PENDANT and a selective transient nOe experiment

The complete elucidation of molecular structure, by liquid-state NMR, usually necessitates the analysis of, through-bond connectivities, by scalar couplings and through-space connectivities, by dipolar cross-relaxation effects. The latter facilitates the determination of internuclear distances, and so aids in the clarification of structural conformation.

When supplemented by heteronuclear scalar coupling data, the determination of inter-proton distances via proton homonuclear cross-relaxation experiments, e.g., the steady-state nOe experiment (Appendix A7) [24, 28], and the transient nOe (Appendix A7.3) experiment, NOESY [24, 29], are usually suitable for the elucidation of molecular structure. However, heteronuclear nOe experiments can prove useful when internuclear distances between insensitive nuclei, e.g., ^{13}C, and sensitive nuclei, e.g., ^{1}H, are required. This is particularly the case for the confirmation of the proton environment in proximity to quaternary nuclei, which provides importa provides importantarding the carbon 'back-bone' in organic molecules. Of course, the characterisation of dipolar relaxation and hence internuclear distance between directly bonded $^{13}C - ^{1}H$ nuclei is of little use.

When quantitative or semi-quantitative heteronuclear distance determinations are required, the transient nOe experiment, HOESY (Heteronuclear Overhauser Effect SpectroscopY) [30, 31, 32], is often implemented. HOESY is the heteronuclear equivalent of the homonuclear NOESY experiment and has received widespread use in a variety of fields [30, 31, 33, 34, 35].

The major disadvantage with transient nOe experiments is their lack of sensitivity, in terms of signal-to-noise ratios. However, for those users who are unable to perform the significantly more sensitive inverse (proton detected) HOESY [36] experiment, the traditional HOESY experiment suffers from a greater lack of sensitivity because of the following reasons:

- HOESY experiments utilise direct detection of insensitive nuclei.
- The very nature of, for example, quaternary nuclei that makes them interesting, i.e., their lack of direct bonding to protons, means that nOe experiment times are long

because:

- the greater distance over which cross-relaxation occurs between quaternary nuclei and distant protons causes slow nOe build-up rates.
- Quaternary nuclei are not directly bonded to protons, and as such their relaxation does not solely depend upon proton dipolar relaxation (Appendix A6). Consequently the observed nOe of quaternary nuclei are often reduced due to competitive relaxation mechanisms, including, spin-rotation relaxation and chemical shift anisotropy (Appendix A7.2.6).

HOESY experiments have received a great deal of attention in order to increase their sensitivity and reduce experiment times [37, 39]. One such study has revealed that the attainment of maximum nOes is ordinarily achieved when the mixing time (the time in which the transient nOe builds up) is set to approximately 1.5 times the T_1 (Appendix A6) of the proton [38, 32].

When the proton spectrum of the molecule under scrutiny is devoid of spectral overcrowding, the one-dimensional selective analogue of the HOESY experiment (1-D HOESY) is useful when only a small select number of assignments are required. The 1-D HOESY [32, 33, 34, 35] experiment facilitates a potentially large reduction in experiment time compared to a two-dimensional HOESY (2-D HOESY) experiment.

1-D HOESY experiments are performed in an analogous manner to heteronuclear selective long-range scalar coupling correlation experiments. The proton(s) bonded to ^{12}C are selectively perturbed (usually inverted), leaving all other protons bonded to ^{12}C unaffected. During the mixing time, the insensitive nuclei experience a transient nOe, which is largely attributed (see later) to dipolar cross-relaxation with the selected proton. (Appendix A7.3).

Heteronuclear nOe methods are usually supplemented by long-range scalar coupling correlation experiments. The results from each are used to build up an accurate picture of the through-bond and through-space $^{13}C - {}^{1}H$ environment.

A vast number of experimenters only have access to NMR spectrometers, that are not amenable to inverse methods, and hence the choice of long-range scalar coupling correlation experiment is limited to those that employ direct detection of the insensitive nucleus. When a

1-D HOESY experiment and a selective long-range scalar coupling correlation experiment (INAPT and more recently, selective PENDANT) have been deemed suitable for the elucidation of the ^{13}C - ^{1}H environment, the two experiments when performed sequentially, result in a significant overall experiment time. The 1-D HOESY experiment is the 'rate determining step' for the attainment of both sets of data, due to its comparative insensitivity.

The 1-D HOESY and selective long-range scalar coupling correlation experiments depend upon a common property, namely, the selective perturbation of proton(s) bonded to ^{12}C. Due to this similarity it was realised that there was potential for the two experiments to be combined into one, thereby delivering significant experimental time-savings in comparison to the sequential performance of each. A novel pulse sequence has been devised which combines sequentially, the selective PENDANT experiment and a 1-D HOESY experiment, hereafter referred to as selective PENDANT-1-D HOESY. It will emerge that the combination of the two experiments removes the need for the 1-D HOESY experiment to have a dedicated relaxation delay and nOe mixing time, thereby delivering significant experimental time-savings. This concept is schematised in figure 3.1.

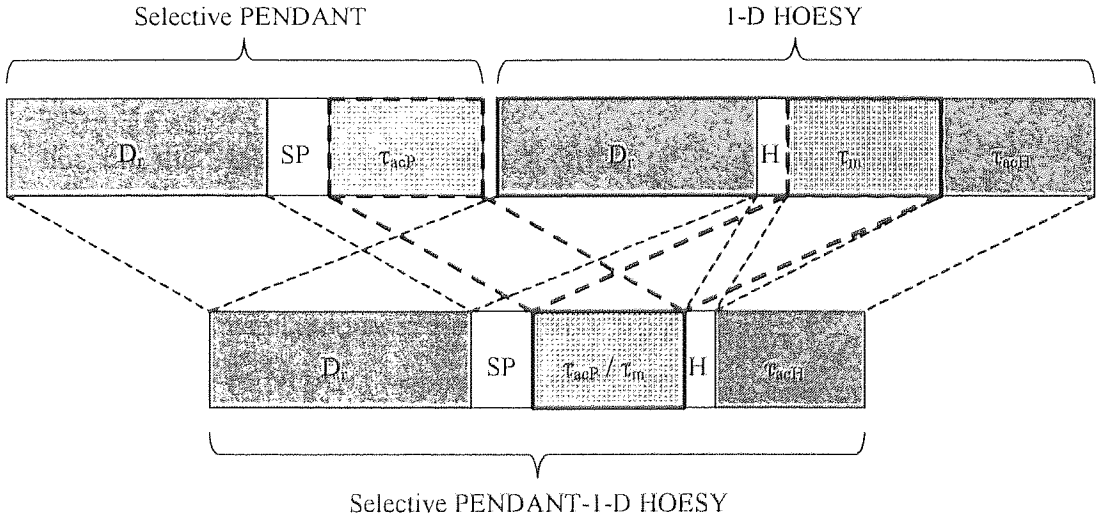

D_1	=	Relaxation delay for protons (^{12}C bonded))	H	=	1-D HOESY pulse sequence
SP	=	Selective PENDANT pulse sequence	τ_m	=	1-D HOESY mixing time
τ_{acP}	=	Selective PENDANT acquisition time	τ_{acH}	=	1-D HOESY acquisition time

Figure 3.1 Schematic diagram of selective PENDANT-1-D HOESY

The pulse sequence contains two signal acquisition periods. The first is dedicated to acquiring the selective PENDANT spectrum, τ_{acP} and the latter to acquiring the 1-D HOESY

spectrum, τ_{acH} . The acquisition period, τ_{acP}, has a dual purpose:

1. Acquiring the selective PENDANT free induction decay (FID).
2. Acting as the mixing time, τ_m, for the 1-D HOESY experiment.

The relaxation delay, D_r, preceding selective PENDANT serves as the relaxation delay of the protons bonded to ^{12}C for both selective PENDANT and 1-D HOESY.

From figure 3.1, it is easily seen that the new pulse sequence offers a reduction in experiment time of the sequential performance of the individual techniques. Since, the sensitivity of the HOESY experiment dictates the overall experiment time, the signal-to-noise ratios of the selective PENDANT spectra are excellent, therefore aiding assignment. Furthermore, the combination of both experiments provides greater convenience on behalf of the experimenter, whom is no longer required to separately set up and perform two independent experiments.

Apart from the similar dependence upon the selective perturbation of protons bonded to ^{12}C, it was the realisation of two fundamental concepts that allowed the integration of the two experiments:

- the 1-D HOESY experiment depends on the relaxation of protons bonded to ^{12}C and not on the lengthy longitudinal relaxation of insensitive nuclei. Moreover, the validity of the HOESY experiment depends on the consistent 'preparation' of the insensitive and proton spin system for each separate experiment before the mixing time begins. Justifications of these remarks are given later.
  The selective PENDANT experiment and its proton relaxation delay, which precedes 1-D HOESY, necessitate the consistent preparation of the spin systems.

- To ensure maximum sensitivity, the mixing time in HOESY experiments is nominally set to around 1.5 T_1 of the protons, which in typical organic molecules for de-oxygenated samples, is of the order 1-3 seconds. This corresponds to the typical signal acquisition periods of selective PENDANT, and similarly INAPT, for a ^{13}C spectrum encompassing the full chemical shift range of a typical organic molecule with adequate digital resolution of scalar coupling multiplicities. Therefore, the selective PENDANT acquisition time, τ_{acP}, can simultaneously serve as the mixing

time, τ_m, in 1-D HOESY ($\tau_{acP} = \tau_m$).

It is evident that the concepts for the incorporation of a selective 1-D HOESY experiment into selective PENDANT are also valid for other selective long-range heteronuclear scalar coupling correlation experiments, e.g., INAPT. Indeed, when the identification of all quaternary nuclei is not required, the integration of INAPT and 1-D HOESY is more suitable. This is because the selective PENDANT experiment may require the acquisition of an off-resonance experiment, which, by comparison to an INAPT-1-D HOESY experiment, constitutes an extension to experimental time. Furthermore, an off-resonance experiment provides no useful data for the 1-D HOESY experiment.

3.1 The use of HOESY experiments

HOESY experiments have been used for quantitative internuclear distance determinations [33, 34, 35, 39]. However, in most circumstances only tentative determinations can be made [34]. This is due to the unique properties of the development of heteronuclear transient nOes.

3.2 The development of heteronuclear transient nOes.

The selectively perturbed protons not only take part in cross-relaxation with insensitive nuclei, but also take part in cross-relaxation with protons. Subsequently this causes the development of transient nOes at insensitive nuclei to be comprised of both direct and indirect effects, e.g., $^1H_{sel} \rightarrow {}^{13}C$ and $^1H_{sel} \rightarrow {}^1H \rightarrow {}^{13}C$ respectively, where $^1H_{sel}$ represents the selected proton. These indirect effects are analogous to those encountered in steady-state nOe experiments, which were described in appendix A7.2.3.1. Indeed, negative nOes attributed to indirect effects are often observed in HOESY spectra [32, 40, 33-35].

As a result of indirect effects, the development of the transient nOe in HOESY experiments is not simply attributed to direct cross-relaxation with the selected proton. To determine the cross-relaxation rate constant, σ, and hence internuclear distances, the experimentally derived curves are fitted to theoretically derived curves. Theoretical nOe build-up curves are derived from the results of calculations using modified relaxation equations. The parameters of the relaxation equations are determined from a mixture of relaxation measurements and theoretical modelling of the direct and indirect relaxation rate constants. Due to the level of uncertainty in the relaxation measurements and the assumptions employed in the relaxation models, only tentative distance determinations can be made [33-35].

Due to the inherent complexity and rigours of quantitative distance determinations, HOESY spectra are usually analysed to give a qualitative interpretation of internuclear distances. For example, it can be said that one proton is more proximate to a ^{13}C nucleus than another proton, due to it invoking a greater magnitude of transient nOe. Although indirect effects complicate the determination of quantitative internuclear distances, their very nature makes them particular useful for the qualitative determination of internuclear distance. By analogy with steady-state experiments, described previously in appendix A7.2.3.1, negative nOes can often be used to confirm the conformation of proton structure around ^{13}C quaternary nuclei.

3.3 The utility of the selective PENDANT-1D HOESY experiment.

An unfortunate consequence of the selective PENDANT-1-D HOESY experiment is that it is not amenable to use for the determination of quantitative internuclear distances. The acquisition period, τ_{acP}, of selective PENDANT, which is the mixing time, τ_m, of the 1-D HOESY experiment, would have to be changed in a set of successive experiments in order to produce a nOe build-up curve (Appendix A7.3.2 and A7.3.6). Even if this were possible, without degrading the digital resolution of spectra, there is no need to collect more than one set of selective PENDANT spectra. Therefore, the selective PENDANT-1-D HOESY experiment is restricted to the use of the 1-D HOESY results for the qualitative determination of $^{13}C - {}^{1}H$ internuclear distances. However, because HOESY results are usually used for qualitative distance determinations, the utility of the selective PENDANT-1-D HOESY experiment is realised. The experimenter derives qualitative data from 1-D HOESY, while simultaneously acquiring selective PENDANT spectra, in a significantly reduced experiment time.

The next section describes in more detail the theoretical basis of the selective PENDANT-1D HOESY experiment.

3.4 The preparatory requirements of the 1-D HOESY experiment

It is often remarked in the literature, quite misleadingly, that a 'relaxation delay' is required to attain or approach thermal equilibrium, prior to the next transient in a pulse sequence experiment. The realisation of this erroneous concept was first reported by Sweeting [41], in the context of T_1 measurements involving ^{13}C nuclei, and later embraced by Andersen et al [42], where it was highlighted that; more correctly, the spin system should be suitably

prepared during a preparation time, or delay, in a known and reproducible manner.

The requirement of a delay, which is solely devoted to relaxation, is simply not required for a large number of important experiments. Indeed, this is the case for 1-D HOESY experiments, where the relaxation of protons bonded to ^{12}C is important, but, the relaxation of insensitive nuclei is unimportant. Rather, the proton and ^{13}C spin system prior to the mixing time in 1-D HOESY should be suitably and consistently prepared during a preparation delay (PD). The preparation delay or period can be comprised of any number or types of elements, e.g., pulses and delays, as long as the preparation delay functions appropriately.

The validity of the 1-D HOESY experiment is maintained, when the following criteria for the preparation of the heteronuclear spin system are satisfied:

1. The state of ^{13}C magnetisation prior to the mixing time for each separate selective experiment is constant.
2. The perturbation of each of the selected proton(s), relative to the remaining protons bonded to ^{12}C is constant for each experiment.

With respect to statement 1: 1-D HOESY experiments have been performed, in which all ^{13}C (insensitive (S)) nuclei are broadband decoupled prior to the mixing time [34-35]. This ensures a consistent preparation of the ^{13}C spin system prior to the mixing time, i.e., the magnetisation of all ^{13}C nuclei, is zero ($M_z^S = 0$).

Selective perturbation of protons in 1-D HOESY experiments, usually constitutes complete inversion, i.e., $-M_{z\,sel}^I$, where (sel) indicates the selected proton(s). After inversion, recovery of ^{13}C magnetisation occurs due to longitudinal relaxation processes, which includes cross-relaxation with the selected proton(s), should mutual dipolar coupling exist between them. When the experiment is repeated off-resonance, and the selective pulse is applied at a frequency away from the proton spectrum, longitudinal relaxation of ^{13}C occurs without the contribution from dipolar cross-relaxation with the selected proton.

After the mixing time, the magnetisations of the ^{13}C nuclei in each experiment are observed by a $\pi/2$ 'read' pulse. Subtraction of the off-resonance spectrum from the on-resonance

spectrum yields the absolute transient nOe corresponding to dipolar cross-relaxation with the selected proton(s) (Appendix A7.3.3)

With respect to statement 2: ideally, all protons bonded to ^{12}C should be at thermal equilibrium, i.e., the preparation delay, PD, should be set to establish a state that satisfies the condition: 5.3 x T_1 of the slowest relaxing proton nucleus. However, for qualitative distance determinations, a relaxation delay approaching the T_1 [27] of the slowest relaxing nucleus is sufficient, which is close to the value that is routinely employed in polarisation transfer experiments such as selective PENDANT.

In order to maintain true selectivity of the transient nOe, the selected proton(s) should be perturbed by the same amount for each different on-resonance experiment, while the remaining protons bonded to ^{12}C within the same molecule are required to remain invariant.

Furthermore if it is assumed that the molecule under scrutiny is not isotopically enriched with ^{13}C, the state of the proton spin system for protons bonded to ^{13}C is unimportant in selective heteronuclear nOe experiments. This is due to the low natural isotopic abundance of insensitive nuclei: the probability of finding a ^{13}C nucleus adjacent to another in the same molecule, which is dipolar coupled to the selected proton(s) is very low. Over the entire molecular ensemble, a transient nOe at the ^{13}C nucleus, resulting from perturbation of protons directly bonded to the adjacent ^{13}C nucleus, is insignificant.

In summary, the validity of the 1-D HOESY experiment is maintained for all on-resonance experiments when the heteronuclear spin system is prepared in a consistent manner:

$$\mathbf{M_z^I{}_{sel} \neq M_0^I = constant} \qquad \mathbf{M_z^S = constant} \qquad \mathbf{M_z^I{}_{unsel} = or \approx M_0^I = constant} \tag{3.1}$$

Where $M_z^I{}_{unsel}$ represents the magnetisations of all unselected protons bonded to ^{12}C.
The selective PENDANT experiment, which is comprised of pulses and delays, serves as the preparation delay (PD), for the 1-D HOESY experiment in the selective PENDANT-1-D HOESY experiment. The relaxation delay, D_r, serves to restore a constant state of $M_z^I{}_{sel}$ and $M_z^I{}_{unsel}$ for the selective PENDANT experiment, which subsequently prepares the spin

system for 1-D HOESY according to condition 3.1 given previously. In order that the selective PENDANT experiment satisfies the preparatory requirements of the 1-D HOESY experiment, modification of the selective PENDANT pulse sequence was required.

3.5 Modification of the selective PENDANT pulse sequence

Prior to acquisition in selective PENDANT, the state of the heteronuclear spin system is very similar to that described in the treatment of SNARE given later (Chapter 4). Consequently, the magnetisations of insensitive nuclei S (^{13}C) and sensitive nuclei I (^{1}H) are close to zero, $M_z^S \approx M_z^I \approx 0$, because the selective PENDANT pulse sequence utilises non-selective $\pi/2$ pulses applied to ^{13}C nuclei and protons, the latter occurring during the low-pass J-filter.

Deviations from the condition $M_z^S \approx 0$ are due to, for example, pulse imperfections, *r.f.* inhomogeneity effects and off-resonance effects, the latter being significantly different for all insensitive nuclei in the spectrum. According to these effects, the individual magnitudes of M_z^S, from one transient to another, will remain constant; as long as ^{13}C steady-state has been attained by performing a suitable number of dummy scans (Appendix A4.5.2).

However, between different on-resonance experiments, the value of M_z^S will change when ^{13}C nuclei exhibit long-range scalar couplings to the selected proton(s). The J-values of long-range couplings to the selected proton(s) may be different for all ^{13}C nuclei, which necessitates that varying magnitudes of in-phase coherence exists prior to every ^{13}C pulse. When the ^{13}C pulses are applied, the residual M_z^S components for each ^{13}C nucleus will be significantly different prior to the 1-D HOESY mixing time, i.e., the selective PENDANT acquisition time. The M_z^S components will exhibit magnitudes, which depend on; the severity of the off-resonance effects etc, and the J-value of the long-range coupling to the selected proton. Such a description neglects the fact that during the pulse sequence, differing levels of M_z^S build-up as a result of the differing longitudinal relaxation times (T_1) of individual ^{13}C nuclei (Appendix A6). When subject to the same off-resonance effects, etc, as those described above, variation of M_z^S can occur prior to the mixing time.

A consequence of the selective PENDANT experiment, is that the entire proton spin system receives near equivalent perturbation. The action of the low-pass J-filter, i.e., the application of non-selective $\pi/2$ proton purge pulses, causes the populations of the all the proton spin-energy levels, including, protons bonded to ^{12}C, to be more or less equalised ($M_z^I \approx 0$).

Therefore, the action of the low-pass J-filter in selective PENDANT completely negates the selectivity of perturbation required for the 1-D HOESY experiment.

In conclusion, the normal selective PENDANT experiment does not function as a suitable preparatory device for 1-D HOESY. Therefore, changes were made to selective PENDANT in order for it to act as an appropriate preparatory device, while maintaining its rudimentary function. The changes to the selective PENDANT pulse sequence are summarised below. Detailed descriptions of the impact of the changes upon the selective PENDANT experiment have been deferred to later sections.

3.5.1 Summary of the changes made to selective PENDANT

The selective PENDANT- 1-D HOESY pulse sequence is given in figure 3.2 overleaf and corresponding pulse program given in appendix A14. The low-pass J-filter element and the preparation element (pulse and Z-gradient cascade) are highlighted for ease of comparison to selective PENDANT and are discussed below. Pulse phases are given in parentheses adjacent to the pulses and correspond to the first transient in the phase cycle. The labels σ_n indicate the various points at which the pulse sequence is analysed in the following sections.

The re-structure and its repositioning of the low-pass J-filter to the beginning of the selective PENDANT pulse sequence causes perturbation of protons bonded to ^{13}C only, while leaving those protons bonded to ^{12}C unaffected. The latter is achieved by appropriate phase cycling of the component pulses of the J-filter, and is described later in section 3.8.1. As the J-filter need only affect the protons directly bonded to ^{13}C nuclei, the function of the J-filter is maintained. Moreover, the perturbation of protons bonded to ^{13}C is unimportant in HOESY experiments. Therefore, selective pulses applied to proton(s) directly bonded to ^{12}C causes the desired selective polarisation transfer, while providing the necessary selectivity for the 1-D HOESY experiment.

Figure 3.2 Selective PENDANT-1-D HOESY pulse sequence

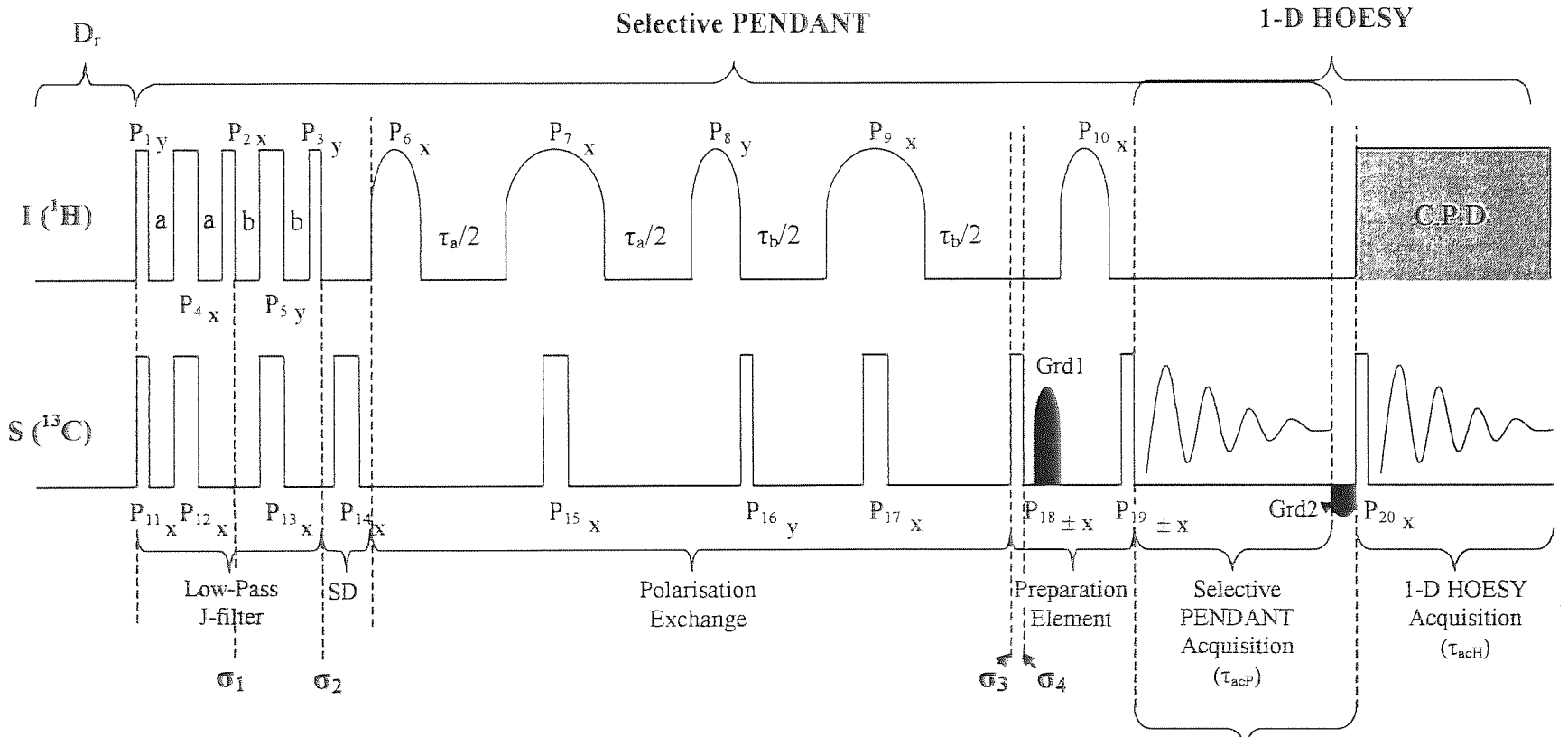

D_r = Normal Proton relaxation delay
SD = Power switching delay for selective pulse
Grdn = Gradient pulse
a = $\tau_1/2$
b = $\tau_2/2$

Pulse length:

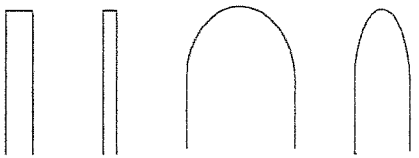

In order to achieve a consistent and constant preparation of the ^{13}C and selected proton(s) spin system, a pulse and homo-spoil (Z-gradient) cascade, hereafter called the preparation element, was implemented prior to the acquisition period of selective PENDANT, i.e., the 1-D HOESY mixing time. The preparation element has the function of de-phasing ^{13}C coherence and attaining the condition $M_z^S = 0$ and $M_z^I{}_{sel} = 0$, by analogy with that achieved in standard 1-D HOESY experiments via ^{13}C decoupling. Additionally, the selective proton pulse achieves a state of constant perturbation of the desired protons. Both aspects are explained in more detail in section 3.9.9. Therefore, the state of the entire spin system prior to the mixing time of 1-D HOESY (τ_m) i.e., the selective PENDANT acquisition period, τ_{acP}, is:

$$\mathbf{M_z^I{}_{sel} = M_z^S = 0} \qquad \textbf{and} \qquad \mathbf{M_z^I{}_{unsel} \approx M_0^I = constant} \qquad 3.2$$

Where $M_z^I{}_{unsel}$ are the magnetisations for all other protons bonded to ^{12}C.

It is evident that the perturbation of the selected proton(s) I_{sel}, relative to the unselected protons, I_{unsel}, bonded to ^{12}C is equal to 'half-inversion', i.e., $M_z^I{}_{sel} = 0$, as opposed to full inversion, $-M_z^I{}_{sel}$, which is attained in normal 1-D HOESY experiments. This difference in relative perturbations of the selected and unselected protons impacts upon the rate of build-up of the transient nOe.

3.6 The nOe intensities in 1-D HOESY experiments

When the initial rate approximation is valid, for a given mixing time, τ_m, the magnitude of the transient nOe in 1-D HOESY, depends on the relative perturbation of the selected proton(s) compared with all other protons bonded to ^{12}C (Appendix A7.3.1).

For total inversion of the selected proton(s) relative to all other protons bonded to ^{12}C, which are at thermal equilibrium, the rate of transient nOe build-up is given by twice the cross-relaxation rate, $2\sigma_{IS}$, between the selected proton(s), I, (^1H) and insensitive nuclei, S (^{13}C), respectively.

The selective PENDANT-1-D HOESY experiment attains a relative perturbation of 'half-inversion', giving rise to a nOe build up rate of σ_{IS}, which is half of that achieved by normal 1-D HOESY experiments. Attaining a state of 'half-inversion' is inherent to the selective

PENDANT experiment, since execution of a selective $\pi/2$ pulse is required for optimal polarisation transfer. The relative perturbation achieved in selective PENDANT-1-D HOESY is the same as a 2-D transient nOe experiment, i.e., the nOe build up rate is half that of the selective analogue version (Appendix A7.3.4).

When the initial rate approximation is valid, the magnitudes of the observed nOe in selective PENDANT- 1-D HOESY will be half that of the 1-D HOESY experiment.
However, this does not detract from the utility of the experiment, since a selective PENDANT experiment is simultaneously performed in the time it takes to perform a 1-D HOESY experiment. Moreover, the added convenience of obtaining two sets of data in the same experiment is a further advantage.

3.7 The performance of the selective PENDANT – 1-D HOESY experiment

The observed absolute transient nOes in 1-D HOESY experiments are determined by measuring the difference between the spectra of the on-resonance and off-resonance experiments. The conventional way of obtaining difference spectra is to interleave the off-resonance (control) and the on-resonance experiments, by employing a simple phase cycling scheme: by alternating the phase of the receiver by π radians on every other transient, the spectrum of each experiment is automatically subtracted from the other, and the resulting spectrum is representative of the absolute transient nOe. Interleaving the control and on-resonance experiments reduces the effects of slow drifts in spectrometer stability, which can give rise to spurious results [24, 43].

The implications of this method of for 1-D HOESY is that the selective PENDANT experiment should also be subject to interleaved, off-resonance and on-resonance experiments. Unlike the HOESY experiment, the selective PENDANT off-resonance and on-resonance acquisitions must be added so as to maintain the addition of signals originating from quaternary nuclei and nuclei that have received polarisation transfer, for which the pulse sequence is designed. Therefore, the true off-resonance spectrum will be the coherent addition of all off-resonance transients collected, i.e., with the selective pulse off-resonance. However, the 'on-resonance' spectrum will be comprised of the addition of an equal number of 'true' on-resonance spectra (selective pulse manipulates desired proton) and off-resonance spectra, i.e., **'on-resonance' = (off-resonance/2 + on-resonance/2).**

The affect of this method of acquisition on the selective PENDANT experiment is as follows.

- When conducted in the 'pseudo edited' mode, the phase of the quaternary coherences in the off-resonance experiment are in opposition to those which exhibit scalar coupling to the selected proton in the on-resonance experiment. Therefore, the signal-to-noise ratios of those nuclei that receive polarisation transfer from the selected proton(s) are diminished. However, this does not detract from the utility of the selective PENDANT experiment, since comparison to the off-resonance spectrum still facilitates the unambiguous identification of scalar coupling. Moreover, the signal-to-noise ratios found in selective PENDANT spectra is large, due to the number of transients collected being determined by the comparatively less sensitive 1-D HOESY experiment.

- ^{13}C quaternary coherences that do not exhibit scalar coupling to the selected proton possess the same phase in both the control and on-resonance experiment. Similarly, small magnitudes of residual coherence, which pass the low-pass J-filter have identical phases in the control and on-resonance experiment. Both of these coherences benefit from coherent addition.

It has been shown that the interleaved acquisition of the selective PENDANT spectrum has no detrimental effect on performance, in terms of making accurate assignments.

It is evident however, that the incorporation of the preparation element into INAPT would prove more advantageous when the identification of all quaternary nuclei of the sample is not required. This is because the INAPT experiment would not suffer from the ill effects of the superposition of signals that originate from ^{13}C nuclei when the off-resonance spectrum is added. Furthermore, the experiment time is reduced due to the fact that an off-resonance experiment is not required.

3.8 Analysis of the selective PENDANT-1-D HOESY experiment

The analysis of the selective PENDANT- 1-D HOESY experiment is given in a more descriptive format as opposed to the rigorous product operator treatment given earlier for selective PENDANT. This is because intelligible similarities exist with the selective PENDANT experiment, which allows interpretation to be made without the need to resort to lengthy product operator expressions. Therefore, the product operator description is limited

to the explanation of those important aspects of the pulses sequence, which are more difficult to conceptualise when compared to selective PENDANT. In these circumstances, derivations are kept to a minimum and the pertinent transfer functions are given for complete comparison.

In common with the description of the selective PENDANT experiment, the following assumptions hold for the description of the selective PENDANT-1-D HOESY experiment.

- All selective pulses (Appendix A10) are pure-phase pulses acting over the entire proton multiplet, i.e., to encompass long-range heteronuclear couplings and proton homonuclear couplings, with uniform phase and intensity.
- All selective pulses are phase-coherent with hard pulses, i.e., a selective x-phase pulse corresponds exactly to a x-phase hard pulse.
- Relaxation during the selective pulse is assumed to be negligible and evolution due to scalar coupling during this time is also assumed to be zero.
- All hard pulse lengths are accurately calibrated.

The selectivity or excitation bandwidth of the selective pulses were set to ensure perturbation of the protons that are bonded to ^{12}C only.

The selective PENDANT-1-D HOESY pulse sequence is analysed in chronological order according to its component elements as shown in figure 3.2 given previously.

3.8.1 Modified low-pass J-filter element

The function of the modified low-pass J-filter, now situated at the beginning of the pulse sequence is two fold, of which function 1 is identical to that required in selective PENDANT:

1. To cause the purging of ^{13}C coherence, which exhibits short-range scalar coupling. To pass ^{13}C quaternary coherence, which exhibits long-range coupling or no scalar coupling.
2. All proton coherence that originates from protons directly bonded to ^{12}C to is returned to +Z magnetisation. Subsequent selective perturbation of the desired proton maintains selectivity of the 1-D HOESY experiment ($M_z^I{}_{unsel} \approx M_0^I$) and facilitates

polarisation transfer in the normal way.

Figure 3.3 shows the composition of the J-filter taken from figure 3.2. For comparison the structure of the low-pass J-filter in normal selective PENDANT is shown also.

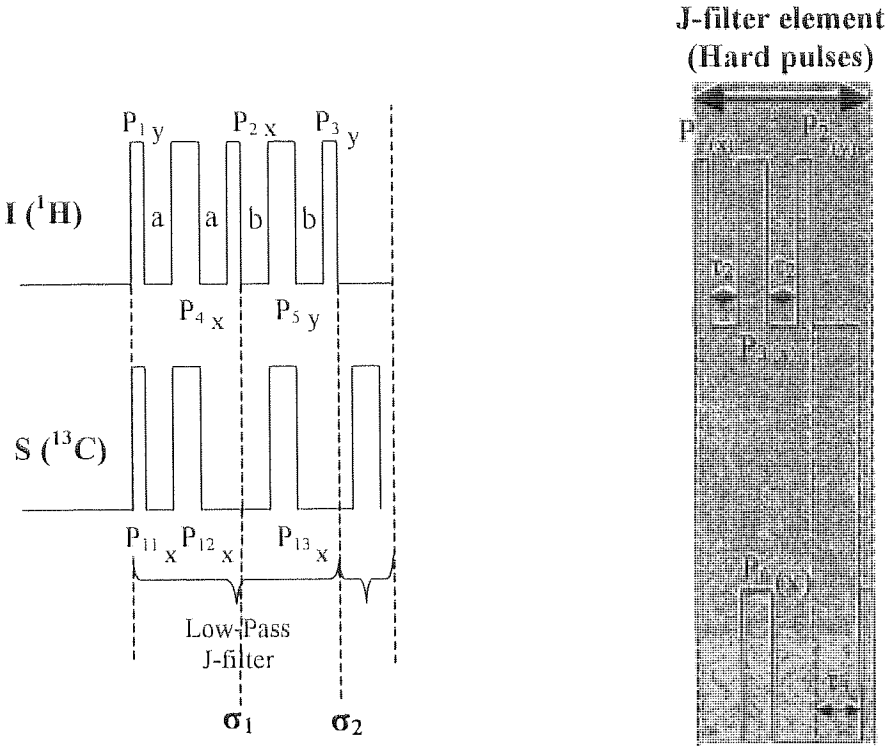

Figure 3.3 **Left: Low pass J-filter in selective PENDANT-1-D HOESY**
Right and highlighted: Low-pass J-filter in normal selective PENDANT

In order to satisfy criteria 2 given above, an additional hard proton $\pi/2$ pulse, P_1, has been inserted at the very beginning of the pulse sequence, with a phase that is orthogonal to P_2 and parallel to P_3. The phase of P_3 ensures the conversion to +Z magnetisation of coherence, which is attributed to protons directly bonded to ^{12}C. At most, protons bonded to ^{12}C may experience proton homonuclear and long-range heteronuclear coupling, so that their evolution during the short-range coupling evolution delays of the J-filter can be considered insignificant. Therefore, the initial state of magnetisation of protons bonded to ^{12}C at the beginning of the J-filter is largely re-established at the end of the J-filter.

Furthermore, an extra hard proton refocusing pulse, P_4, has been inserted at the midpoint of τ_1 to refocus chemical shift of proton coherence prior to the application of P_2. Without, P_4, proton coherence would be reconverted into +Z magnetisation by P_2 with a magnitude that is

modulated according to the individual chemical shift evolution of each proton during τ_1, i.e., $+M_z^I\Omega\tau_1$. This condition would negate the consistent preparation of all protons bound to ^{12}C before the acquisition of selective PENDANT (HOESY mixing time, τ_{acH}), i.e., $M_{z\,unsel}^I \neq M_0^I$.

The insertion of P_4 necessitated the inclusion of an extra ^{13}C refocusing pulse, P_{11}, at the midpoint of τ_1. P_4 causes the continued evolution of ^{13}C coherence, which exhibits short-range scalar coupling, during the second half of τ_1 in readiness for purging by the proton pulse P_2.

In selective PENDANT, the J-filter had the secondary function of causing polarisation exchange. In selective PENDANT-1-D HOESY, polarisation exchange is caused by a selective proton pulse, P_8 and ^{13}C pulse, P_{16}.

In selective PENDANT, the ^{13}C polarisation transfer pulse at the end of τ_3, had the simultaneous effect of causing odd-coupling order (SI_n where n = 1, 3) purging of short-range coupled coherence, which had previously passed the J-filter. Only multiplet anomaly coherences ($4S_yI_zI_z$), and in-phase (S_y) coherences survived (Chapter 2.4.1).

The ^{13}C polarisation transfer pulse, P_{16}, in the selective PENDANT-1-D HOESY experiment, does not have the same effect, because at this stage in the experiment, any residual S coherence that has passed the J-filter has been refocused due to short-range scalar coupling: the selective proton refocusing pulses after the J-filter, do not serve to further evolve short-range coupling.

The placement of the J-filter in selective PENDANT-1-D HOESY has been shown in investigative experiments not to significantly impact upon the efficiency of suppression. In common with selective PENDANT, of more importance to the efficiency of suppression, are the detrimental effects caused by off-resonance effects from subsequent ^{13}C refocusing pulses. The new structure of the low-pass J-filter necessitates a greater number of ^{13}C pulses and increase in pulse sequence length, which further increases the potential for breakthrough of ^{13}C coherence caused by off-resonance effects.

3.9 The product operator description of the selective PENDANT section of the selective PENDANT-1-D HOESY experiment

It is assumed that pulse nutation angles and phases are perfect and that *r.f.* inhomogeneity and off-resonance effects are ineffective. The product operator representations for the description of coherences present at the key numbered stages (σ_n) in the pulse sequence are given.

For means of clarity the following notations will be used to describe the various product operator coefficients.

$$c_{Jn} = \cos \pi J_{IS} \tau_n$$
$$s_{Jn} = \sin \pi J_{IS} \tau_n$$

It is assumed that all spins I (^{1}H) involved in short-range coupling to S (^{13}C) are magnetically equivalent and the cosine (cos) and sine (sin) terms do not discriminate between the I spins involved, to save unnecessary lengthening of the terms.

3.9.1 Protons which exhibit short-range heteronuclear coupling

Proton homonuclear coupling and long-range heteronuclear coupling are considered ineffective during the J-filter delays, which are optimised for short-range coupling. The effective transformation up until σ_2 is given by:

$$I_z \xrightarrow{(\pi/2_1)_y\, \pi J_{IS}\tau_1\, 2I_zS_z\, +(\pi_{1+S})_x\, +(\pi/2_1)_x} \sigma_1 \xrightarrow{\pi J_{IS}\tau_2\, 2I_zS_z\, +(\pi_{1+S})_{y,x}\, +(\pi/2_1)_y} \sigma_2$$

$$\sigma_1 = I_x c_{J1} + \overset{(2)}{2I_zS_z} s_{J1} \qquad 3.3$$
$$\sigma_2 = + \overset{(1)}{I_z} c_{J1} c_{J2} - \overset{(3)}{2I_xS_z} c_{J1} s_{J2}$$

Term (1) essentially emulates the behaviour of coherence of protons bound to ^{12}C, i.e., they do not evolve due to scalar coupling evolution during the delays optimised for short-range coupling evolution and therefore, are re-converted to +Z at σ_2.

Longitudinal spin order (term (2)) remains invariant to the selective proton pulses for the remainder of the pulse sequence, however, the non-selective ^{13}C polarisation transfer pulse,

P_{16}, causes polarisation transfer to S coherence. The action of the J-filter to cause polarisation transfer for short-range $^{13}C - {}^{1}H$ coupling, is a property shared by the J-filter in selective PENDANT. To prevent the breakthrough of these unwanted signals into the spectrum, P_1 and P_2 are mutually phase cycled in relation to the receiver to cause cancellation over 8 transients (Appendix A14.1).

Anti-phase single quantum coherence of I (term (3)) remains invariant to subsequent selective proton pulses and is converted to unobservable heteronuclear double quantum coherence by the ^{13}C polarisation exchange pulse, P_{16}.

3.9.2 Coherence which originates from Quaternary nuclei

At σ_2, quaternary coherence is refocused due to chemical shift evolution and it is considered that evolution due to long-range coupling has been ineffective during the short J-filter delays, which are optimised for short-range coupling evolution. Therefore, the state of coherence at the end of the J-filter is given by:

$\sigma_2 \qquad -S_y$

3.9.3 S coherence which exhibit short-range scalar coupling

Chemical shift is refocused during τ_1 while short-range scalar coupling evolves. Coherence that is anti-phase with respect to scalar coupling is converted to heteronuclear multiple quantum coherence by P_2, and this remains 'trapped' and unobservable for the remainder of the experiment.

By exact analogy with selective PENDANT, those coherences that did not evolve to their maximum order during τ_1, prior to conversion to multiple quantum coherence, will evolve due to passive spin-couplings during τ_2. These coherences are subsequently converted to higher orders of multiple quantum coherence by P_3 and remain unobservable for the remainder of the experiment.

During τ_2, residual in-phase coherence that passed the first stage of the filter, subsequently evolves due to short-range scalar coupling, while chemical shift is refocused.
The state of coherence at the end of the J-filter is given by:

$$\sigma_2 \quad SI \quad \left[-\overset{(a)}{S_y} c_{J2} - 2 S_x I_y s_{J2} \right] c_{J1}$$

$$SI_2 \quad \left[\begin{array}{l} -\overset{(a)}{S_y} c^2_{J2} \\ -2\left(S_x I_{1y} c_{J2} s_{J2} + S_x I_{2y} c_{J2} s_{J2} \right) \\ +4 S_y I_{1y} I_{2y} s^2_{J2} \end{array} \right] c^2_{J1}$$

$$SI_3 \quad \left[\begin{array}{l} -\overset{(a)}{S_y} c^3_{J2} \\ -2\left(\begin{array}{l} S_x I_{1y} c^2_{J2} s_{J2} + S_x I_{2y} c^2_{J2} s_{J2} \\ +S_x I_{3y} c^2_{J2} s_{J2} \end{array} \right) \\ +4\left(S_y I_{1y} I_{2y} c_{J2} s^2_{J2} + S_y I_{2y} I_{3y} c_{J2} s^2_{J2} + S_y I_{2y} I_{3y} c_{J2} s^2_{J2} \right) \\ -8 S_x I_{1y} I_{2y} I_{3y} s^3_{J2} \end{array} \right] c^3_{J1}$$

3.4

For the remainder of the experiment, only single quantum coherence, i.e., terms (a) remain observable. The rest of the pulse sequence utilises selective proton pulses to achieve selective polarisation transfer and refocusing. Consequently, no further evolution due to short-range scalar coupling occurs for terms (a) due to the S refocusing pulses at the midpoint of the remaining evolution delays. Therefore, the S polarisation transfer pulse, P_{16}, has no effect upon the residual S coherence, as it is of the same phase as that of the desired quaternary coherence.

The transfer function depicting the magnitudes of potential residual S coherences prior to the preparation element are given by:

$$\sigma_3 \quad SI \quad \left\{ \left[+\overset{(a)}{S_y} c_{J2} \right] c_{J1} \right\} \xi_2$$

$$SI_2 \quad \left\{ \left[+\overset{(a)}{S_y} c^2_{J2} \right] c^2_{J1} \right\} \xi_2$$

$$SI_3 \quad \left\{\left[+\overset{(a)}{S_y}c^3{}_{J2} \right]c^3{}_{J1}\right\}\xi_2 \qquad 3.5$$

Where ξ_2 represents a proportionality constant depicting the dependence of the magnitude of the coherences on γ_S and:

- longitudinal relaxation of S during acquisition and the relaxation delay (D_r)
- T_2 relaxation of S during the pulse sequence.

The change in sign of the coherence is a consequence of the remaining S inversion pulses prior to the preparation element. Therefore, for all coupling multiplicities, residual signals, which originate from coherence that exhibits short-range scalar coupling, should give a multiplet structure indicative of a binomial distribution of intensities. This is in contrast to selective PENDANT, where for example, the residual coherences of ^{13}C nuclei for CH_2 multiplicities, is comprised of a superposition of in-phase and mulitplet anomaly-causing coherence, which gives rise to multiplet anomalies (Chapter 2.4.1 and 2.5.1).

For comparison with the transfer functions given above, those pertaining to selective PENDANT are given below.

$$SI \quad \left\{\left[-\overset{(a)}{S_y} \right]c_{J1}c_{J2}\right\}\xi_2$$

$$SI_2 \quad \left\{\left[-\overset{(a)}{S_y}c^2{}_{J3} + 4\overset{(c)}{S_y I_{1z} I_{2z}} c_{J3}s^2{}_{J3} \right]c^2{}_{J1}c^2{}_{J2}\right\}\xi_2$$

$$SI_3 \quad \left\{\left[\begin{array}{l} -\overset{(a)}{S_y}c^3{}_{J3} \\ \\ +4\left(\overset{(c)}{\begin{array}{l} S_y I_{1z} I_{2z} + S_y I_{1z} I_{3z} \\ + S_y I_{2z} I_{3z} \end{array}}\right) c_{J3}s^2{}_{J3} \end{array} \right] c^3{}_{J1}c^3{}_{J2}\right\}\xi_2$$

3.6

In selective PENDANT the residual observable in-phase coherence is further attenuated by a $\cos^n(I_n)$ function invoked by the final J-filter evolution period τ_3.

3.9.4 The function of the polarisation transfer element

The action of the J-filter facilitates the return of protons bonded to ^{12}C to +Z. After the J-filter, the selective proton pulse, P_6, causes excitation of coherence of the selected proton, while leaving unaffected, all other protons bonded to ^{12}C. During the execution of P_6, ^{13}C quaternary coherence continues to evolve due to chemical shift and long-range scalar coupling. Therefore, an extra ^{13}C refocusing pulse, P_{14}, has been inserted to refocus evolution that had occurred during the power switching delay (pl0) in preparation for the selective pulse, P_6 (Appendix A4.5). As mentioned previously, the unfortunate consequence of extra ^{13}C refocusing pulses, is to increase the potential for off-resonance effects causing the breakthrough of residual ^{13}C signals in the spectrum.

The remainder of the polarisation transfer element is easily recognisable and gives rise to polarisation exchange and refocusing of coherence in a manner analogous to normal PENDANT. The evolution delays, τ_a and τ_b, are set to 1/2J and 1/8J respectively in accordance with normal implementation of selective PENDANT (Chapter 2.6).

3.9.5 S coherence which exhibits long-range scalar coupling to the selected proton: Quaternary nuclei

During the delays of the J-filter, which are optimised for short-range coupling evolution, long-range scalar coupling evolution is considered ineffective and chemical shift is refocused. During the delay τ_a, evolution due to long-range scalar coupling occurs and chemical shift is refocused. The selective proton polarisation transfer pulse, P_6, converts the ^{13}C coherences, which are anti-phase with respect to long-range scalar coupling to the selected proton, to heteronuclear multiple quantum coherences. By analogy with the proton polarisation transfer pulse in PENDANT, the selective proton pulse has caused the similar purging of residual ^{13}C coherences that exhibit long-range coupling to the selected proton. So after P_{16}:

$$SI \qquad -S_y^{(a)} c_{Ja} + 2S_z^{(b)} I_x s_{Ja}$$

$$SI_2 \quad -S_y \overset{(a)}{c^2}_{Ja} - + 2\left(S_z I_{1x} c_{Ja} s_{J1} \overset{(b)}{+} S_z I_{2x} c_{Ja} s_{Ja}\right) + - 4 S_y \overset{(c)}{I_{1x}} I_{2x} s^2_{Ja}$$

$$SI_3 \quad \begin{aligned} & -S_y \overset{(a)}{c^3}_{Ja} + 2\left(S_z I_{1x} c^2_{Ja} s_{Ja} + S_z I_{2x} \overset{(b)}{c^2}_{Ja} s_{Ja} + S_z I_{3x} c^2_{Ja} s_{Ja}\right) \\ & -4\left(S_y I_{1x} I_{2x} c_{Ja} s^2_{Ja} + S_y I_{1x} \overset{(c)}{I_{3x}} c_{Ja} s^2_{Ja} + S_y I_{2x} I_{3x} c_{Ja} s^2_{Ja}\right) \\ & -8 S_z I_{1x} \overset{(d)}{I_{2x}} I_{3x} s^3_{Ja} \end{aligned}$$

3.7

By analogy with PENDANT and selective PENDANT, the ^{13}C polarisation transfer pulse, P_{16}, causes the conversion of odd coupling-order (n = 1, 3 (SI_n)) heteronuclear multiple quantum coherence into homonuclear quantum coherences (terms (d)) and inverse polarisation transfer to I single quantum coherence (terms (b)). Even-coupling order (n = 2, (SI_n)) heteronuclear multiple quantum coherence remains invariant to P_{16} (terms (c)).

During the final evolution delay τ_b, the remaining residual in-phase single quantum coherences (terms (a)) evolve due to long-range scalar coupling to the selected proton, while all other long-range couplings are refocused.

The state of coherence prior to the preparation element is given by:

$$\sigma_3 \quad SI \quad \left\{\left[+ S_y c_{Jb} - 2 S_x I_z s_{Jb}\right] c_{Ja}\right\} \xi_2$$

$$SI_2 \quad \left\{\left[+ S_y c^2_{Jb} - 2\left(S_x I_{1z} c_{Jb} s_{Jb} + S_x I_{2z} c_{Jb} s_{Jb}\right) - 4 S_y I_z I_z s^2_{Jb}\right] c^2_{Ja}\right\} \xi_2$$

$$SI_3 \quad \left\{\left[\begin{aligned} & + S_y c^3_{Jb} - 2\left(S_x I_{1z} c^2_{Jb} s_{Jb} + S_x I_{2z} c^2_{Jb} s_{Jb} + S_x I_{3z} c^2_{Jb} s_{Jb}\right) \\ & - 4\left(S_y I_{1z} I_{2z} c_{Jb} s^2_{J2} + S_y I_{1z} I_{3z} c_{Jb} s^2_{Jb} + S_y I_{2z} I_{3z} c_{Jb} s^2_{Jb}\right) \\ & + 8 S_x I_{1z} I_{2z} I_{3z} s^3_{Jb} \end{aligned}\right] c^3_{Ja}\right\} \xi_2$$

3.8

The product operator representation of quaternary coherence that originates from ^{13}C (S) and that exhibits long-range scalar coupling to the selected proton, is identical to that given in the

analysis of the selective PENDANT experiment. Here the assumption is made that the selective pulses are ideal, i.e., they exhibit pure-phase character and relaxation during the selective pulses is ineffective. In reality, this is of course not the case, and the purging effect caused by P_6, described above, will no doubt be different from that which is similarly achieved by a non-selective hard pulse in the J-filter of selective PENDANT (Chapter 2.4.3).

3.9.6 S coherence which exhibits short-range scalar coupling and long-range scalar coupling to the selected proton

In contrast to the selective PENDANT experiment, the effect upon ^{13}C coherence, which exhibits short-range scalar coupling and long-range scalar coupling to the selected proton, is far simpler. This is due to the repositioning of the low-pass J-filter at the beginning of the pulse sequence and the lack of a final evolution delay τ_3, which is integral to the J-filter in selective PENDANT.

In selective PENDANT, the S polarisation transfer pulse causes even-order selective purging of S coherence, for SI_2 and SI_3 short-range scalar couplings, which have evolved during the final evolution delay of the J-filter, τ_3 (Chapter 2.4.1). Remaining residual coherence is a superposition of in-phase and multiplet anomaly coherence, which subsequently evolves due to long-range scalar coupling during the final delay, τ_b.

The J-filter in the selective PENDANT-1-D HOESY pulse sequence necessitates that remaining residual coherence is purely in-phase. Subsequently, by analogy with that described above for quaternary coherence (3.8.7), the evolution and purging of long-range scalar coupling by the I and S polarisation transfer pulses, P_8 and P_{16}, leave only in-phase coherence remaining for all scalar coupling multiplicities. This is represented by the following product operator representation.

$$SI_{Sn}I_{Ln} \left\{ S_y c^n{}_{J1S} c^n{}_{J2S} c_{JaL} \right\}_{\tau_2} \qquad 3.9$$

Where I_{Ln} represents the number n of long-range coupled I_L nuclei and I_{Sn} represents the number, n, of short-range coupled I_S nuclei. The functions e.g., $c^n{}_{JbL}$, represent the evolution during τ_b for long-range scalar coupling to nuclei I_L and functions e.g., $c^n{}_{J1S}$, represent the evolution due to short-range scalar coupling to n I nuclei during τ_1.

The observable coherences for ^{13}C nuclei, which exhibit short-range scalar coupling and long-range scalar coupling to the selected proton, after evolution during the final evolution delay are given by:

$$\sigma_3 \quad SI \quad \left\{\left[+S_y c_{Jb} - 2S_x I_z s_{Jb}\right] c_{JaL} c^n{}_{J1S} c^n{}_{J2S}\right\}\xi_2$$

$$SI_2 \quad \left\{\left[+S_y c^2{}_{Jb} - 2\left(S_x I_{1z} c_{Jb} s_{Jb} + S_x I_{2z} c_{Jb} s_{Jb}\right) - 4S_y I_z I_z s^2{}_{Jb}\right] c_{JaL} c^n{}_{J1S} c^n{}_{J2S}\right\}\xi_2$$

$$SI_3 \quad \left\{\left[\begin{array}{l} +S_y c^3{}_{Jb} - 2\left(S_x I_{1z} c^2{}_{Jb} s_{Jb} + S_x I_{2z} c^2{}_{Jb} s_{Jb} + S_x I_{3z} c^2{}_{Jb} s_{Jb}\right) \\ -4\left(S_y I_{1z} I_{2z} c_{Jb} s^2{}_{J2} + S_y I_{1z} I_{3z} c_{Jb} s^2{}_{Jb} + S_y I_{2z} I_{3z} c_{Jb} s^2{}_{Jb}\right) \\ +8S_x I_{1z} I_{2z} I_{3z} s^3{}_{Jb} \end{array}\right] c^3{}_{JaL} c^n{}_{J1S} c^n{}_{J2S}\right\}\xi_2$$

3.10

In common, with selective PENDANT, residual coherence, which exhibits long-range scalar coupling to the selected proton and short-range coupling, is attenuated to a greater extent than residual coherence, which exhibits short-range coupling exclusively.

Therefore in common with selective PENDANT, should breakthrough of residual coherence occur in the selective PENDANT-1-D HOESY spectrum, it will be of greater magnitude for residual coherences, which exhibit short-range scalar coupling exclusively.

3.9.7 Quaternary nuclei that do not exhibit J-Coupling

These coherences will be refocused due to chemical shift at σ_3, with the same phase as those residual in-phase S coherences that have originated from S nuclei exhibiting long-range coupling.

$$\sigma_3 \quad +S_y\xi_2 \qquad 3.11$$

3.9.8 S coherences which originates from selective long-range polarisation transfer from I

Only coherence that exists prior to the preparation element (σ_3) is given here to avoid repetition of what has already been described in the analysis of selective PENDANT.

$$\sigma_3 \qquad SI \qquad \left\{\left(-2S_x I_z c_{Jb} - S_y \overset{(a)}{s}_{Jb}\right) s_{Ja}\right\}\xi_1$$

$$SI_2 \qquad \left\{\left[\begin{array}{l}\left(-2S_x I_{1z} c^2_{Jb} - 4S_y I_{1z} I_{2z} c_{Jb} s_{Jb} - S_y \overset{(a)}{s}_{J2} c_{Jb} + 2S_x I_{2z} s^2_{Jb}\right) + \\ \left(-2S_x I_{2z} c^2_{Jb} - 4S_y I_{1z} I_{2z} c_{Jb} s_{Jb} - S_y \overset{(a)}{s}_{J2} c_{J2} + 2S_x I_{1z} s^2_{Jb}\right)\end{array}\right] s_{Ja}\right\}\xi_1$$

$$SI_3$$

$$\left\{\left[\begin{array}{l}\left(\begin{array}{l}-2S_x I_{1z} c^3_{Jb} - 4S_y I_{1z} I_{2z} c^2_{Jb} s_{Jb} + 8S_x I_{1z} I_{2z} I_{3z} c_{Jb} s^2_{Jb} - S_y \overset{(a)}{s}_{Jb} c^2_{Jb} \\ +2S_x I_{2z} c_{Jb} s^2_{Jb} - 4S_y I_{2z} I_{3z} s^3_{Jb}\end{array}\right) + \\ \left(\begin{array}{l}-2S_x I_{2z} c^3_{Jb} - 4S_y I_{2z} I_{3z} c^2_{Jb} s_{Jb} + 8S_x I_{1z} I_{2z} I_{3z} c_{Jb} s^2_{Jb} - S_y \overset{(a)}{s}_{Jb} c^2_{Jb} \\ +2S_x I_{3z} c_{Jb} s^2_{Jb} - 4S_y I_{3z} I_{1z} s^3_{Jb}\end{array}\right) + \\ \left(\begin{array}{l}-2S_x I_{3z} c^3_{Jb} - 4S_y I_{2z} I_{3z} c^2_{Jb} s_{Jb} + 8S_x I_{1z} I_{2z} I_{3z} c_{Jb} s^2_{Jb} - S_y \overset{(a)}{s}_{Jb} c^2_{Jb} \\ +2S_x I_{1z} c_{Jb} s^2_{Jb} - 4S_y I_{1z} I_{2z} s^3_{Jb}\end{array}\right)\end{array}\right] s_{Ja}\right\}\xi_1$$

3.12

Where ξ_1 represents a proportionality constant depicting the enhancement factor indicative of polarisation transfer from I to S, i.e., γ_I/γ_S and the dependence of the magnitudes of the coherences on:

- the longitudinal relaxation of I between transients during acquisition and the relaxation delay (D_r).
- T_2 relaxation of I nuclei during τ_a, , and τ_2
- T_2 relaxation of S nuclei during τ_b.

In common with selective PENDANT, the pulse sequence is phase cycled to give the idealised pseudo-edited spectrum: those signals that originate from polarisation transfer are in anti-phase to quaternary nuclei that have not received polarisation transfer.

3.9.9 The preparation element for 1-D HOESY: The Z-gradient and pulse cascade

The preparation element for 1-D HOESY is shown in figure 3.4, which is taken from figure 3.2 given previously. The description given here is presented in a chronological order of events.

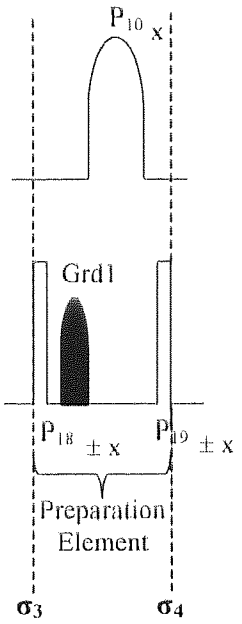

Figure 3.4 Preparation element for 1-D HOESY

1. The $\pi/2$ pulse, P_{18}, converts all ^{13}C coherence, which are required for acquisition of the selective PENDANT spectrum, into Z magnetisation, so that it remains invariant to the Z-gradient pulse (Appendix 11). P_{18} also causes conversion of residual ^{13}C magnetisation to single quantum coherence, which exist as a result of off-resonance effects that have a J-dependence as described previously (Section 3.5). In addition, small amounts of ^{13}C magnetisation to have built up are converted to coherence that is subsequently de-phased by the Z-gradient.

2. The Z-gradient de-phases all ^{1}H and ^{13}C coherences that remain after P_{18} and those that have been converted to single quantum coherences by P_{18} (see next section). De-phasing of coherence is essential for the consistent preparation of the spin system in readiness for 1-D HOESY. When the coherences have been de-phased, they can no longer give rise to magnetisations, which have J-dependent magnitudes caused by the last ^{13}C pulse, P_{19}, in the preparation element. The Z-gradient pulse is applied with an

appropriate amplitude and duration to cause de-phasing of coherence, for which an explanation of the function of Z-gradients is given in appendix 11.

3. Application of the $\pi/2$ selective pulse, P_{10}, causes the desired condition $M_z^{I}{}_{sel} = 0$ for the consistent preparation of the 1-D HOESY experiment.

By analogy with the description given earlier in section 3.5 for the variable state of M_z^{S} prior to the preparation element, the state of $M_z^{I}{}_{sel}$ can potentially vary for different selected proton(s). Each selected proton potentially has a different long-range J –value, which necessitates a different magnitude of in-phase coherence prior to each selective pulse in the pulse sequence. If the selective pulses are inaccurate, the magnitude of $M_z^{I}{}_{sel}$ can vary in proportion to J prior to the preparation element and mixing time thus negating true selectivity. The Z-gradient de-phases all remaining proton coherence of the selected proton and the selective proton pulse P_{10} causes the desired condition $M_z^{I}{}_{sel} = 0$ for each separate on-resonance experiment.

4. The effects caused by the $\pi/2$ ^{13}C pulse, P_{19}, are two fold:
    - coherence that had been converted to magnetisation, via the $\pi/2$ pulse, P_{18}, (point 1), is reconverted back to observable single quantum coherence, to enable detection of the selective PENDANT F.I.D.
    - The populations across the spin-energy levels of all S nuclei are equalised to complete the desired preparatory condition for 1-D HOESY: $M_z^{I}{}_{sel} = M_z^{S} = 0$ and $M_z^{I}{}_{unsel} \approx M_0^{I}$ (Expression 3.2 section 3.5).

3.9.10 Longitudinal relaxation during the Z-gradient

Execution of a Z-gradient by a NMR spectrometer usually requires the performance of the following functions.

- Preparation of the Z-gradient pulse, e.g., the power levels and pulse length are set.
- Application of the Z-gradient pulse.
- A delay to enable recovery of the field-frequency locking system, and other specific hardware functions (Appendix 11 and A4.5.6).

The total duration of the Z-gradient process varies between NMR spectrometers. Modern

spectrometers can execute all of the gradient functions in a few hundred milliseconds (ms), while for older spectrometers, the whole process can take longer than 1 second.

^{13}C nuclei undergo longitudinal relaxation during both the Z-gradient process and the execution of the selective proton pulse, P_{10}. The longitudinal relaxation of quaternary nuclei during this time is likely to be negligible because of their comparatively large T_1s. However, ^{13}C nuclei directly bonded to protons, which have much shorter T_1s may develop a small magnetisation, which would be 'read' by the last ^{13}C pulse, P_{19}, in the preparation element. Therefore, ^{13}C nuclei that have not received polarisation transfer during the selective PENDANT part of the experiment will appear in the selective PENDANT spectrum as breakthrough signals.

In order to prevent the breakthrough of signals as a result of the build-up of magnetisation, the ^{13}C pulse, P_{19}, in the preparation element is phase-alternated by π radians with respect to a constant receiver phase. Therefore, over two transients the coherences due to relaxation are cancelled. The synchronous phase alternation of P_{18} with P_{19} ensures that over two transients, the coherences detected for selective PENDANT are added. Therefore, P_{18} has the effect of returning the desired in-phase ^{13}C coherence (Statement1 given previously) to +Z and –Z on concurrent transients. The latter condition will have little effect upon the desired quaternary coherences due to their inherently large T_1s in comparison to the length of both the Z-gradient and the selective proton pulse.

3.9.11 The effect of the preparation element upon observable coherence in the selective PENDANT spectrum

As described previously, in-phase ^{13}C coherence is converted to Z magnetisation by P_{18} in order that it is preserved during the Z-gradient for later detection in the selective PENDANT acquisition period, τ_{acP}. However, P_{18} also causes purging of ^{13}C coherence, which is anti-phase with respect to long-range coupling to the selected proton. The following explanation deals with this effect for ^{13}C coherence, which originates from polarisation transfer. However, the same principles apply for residual coherence, which exhibit long-range coupling(s) to the selected proton(s).

The effect of the ^{13}C pulse, P_{18}, upon coherence that is anti-phase due to long-range scalar

coupling at σ_3 (expression 3.12), is given by:

$$\sigma_4 \qquad SI \qquad \{(-2S_x I_z c_{Jb})s_{Ja}\}\xi_1$$

$$SI_2 \qquad \left\{2\left[\left(-2S_x I_{1z} c^2{}_{Jb} - 4S_z I_{1z} \overset{(a)}{I_{2z}} c_{Jb} s_{Jb} + 2S_x I_{2z} s^2{}_{Jb}\right) + \right] s_{Ja}\right\}\xi_1$$

$$SI_3 \qquad \left\{3\left[\left(\begin{array}{l} -2S_x I_{1z} c^3{}_{Jb} - 4S_z I_{1z} \overset{(a)}{I_{2z}} c^2{}_{Jb} s_{Jb} + 8S_x I_{1z} I_{2z} I_{3z} c_{Jb} s^2{}_{Jb} \\ +2S_x I_{2z} c_{Jb} s^2{}_{Jb} - 4S_z I_{2z} \overset{(a)}{I_{3z}} s^3{}_{Jb} \end{array}\right) + \right] s_{Ja}\right\}\xi_1$$

3.13

P_{18} causes even-coupling order (n = 0, 2 (SI_n)) excitation of longitudinal spin order, i.e., terms (a), while all other odd-coupling order (n = 1, 3 (SI_n)) (S_x) single quantum coherences remain invariant. The latter along with all other single quantum coherences are subsequently de-phased by the Z-gradient, while the longitudinal spin order remains invariant. Application of the selective proton pulse, P_{10}, in the preparation element, converts the longitudinal spin order ($-4S_zI_zI_z$) to proton double quantum coherence ($-4S_zI_yI_y$).

Application of the final ^{13}C pulse, P_{19}, 'reads' the Z-magnetisation for detection in the selective PENDANT spectrum, which corresponds to the desired in-phase coherence that was converted into Z-magnetisation by P_{18}. Furthermore, P_{19} causes the conversion of proton double quantum coherence, given above, to heteronuclear triple quantum coherence ($4S_yI_yI_y$), which remains unobservable for the remainder of the experiment. Therefore, the preparation element has purged all ^{13}C coherences, which were anti-phase with respect to long-range scalar coupling to the selective proton at σ_3 at σ_4. Consequently, the selective PENDANT spectrum of ^{13}C nuclei, which exhibit long-range coupling to the selected proton, will have multiplets, which have component lines with intensities obeying a binomial distribution.

However, if there is a pulse nutation angle error of the selective pulse, P_{10}, i.e., $\theta \neq \pi/2$ radians, residual longitudinal spin-order may still persist and exhibit a pulse angle dependency ($-4S_zI_zI_z\cos\theta$). P_{19} would cause the conversion of residual longitudinal spin

order to observable multiplet anomaly-causing coherence ($-4S_yI_zI_z\cos\theta$). Therefore, when selective pulses do not give rise to accurate nutation angles, the possibility exists for a superposition of a small amount of multiplet anomaly-causing coherence and the desired in-phase ^{13}C coherence, which is re-excited for detection. This does not impact upon the identification of long-range scalar coupling correlations, however, it may explain the presence of unexpected multiplet anomalies. Investigative experimental work reported here, has proven that the accuracy of the selective pulses is sufficient to prevent the appearance of signals with multiplet anomalies.

3.10 Observable coherence during the selective PENDANT acquisition period (1-D HOESY mixing time)

The 'on-resonance' selective PENDANT-1-D HOESY spectrum is comprised of the addition of an equal number of 'true on-resonance' and off-resonance experiments, which is required to obtain the absolute transient nOe for 1-D HOESY (Section 3.7).

The selective PENDANT-1-D HOESY experiment is phase cycled in the pseudo-edited mode, therefore, quaternary nuclei that do not exhibit scalar coupling appear anti-phase to those ^{13}C nuclei that experience polarisation transfer from the selected proton.

Residual ^{13}C coherences that pass the low-pass J-filter should appear with multiplet structure indicative of a binomial distribution (Section 3.9.5).

In the selective PENDANT spectrum of the 'true on-resonance' experiment, ^{13}C nuclei that exhibit long-range coupling to the selected proton will have multiplets, which have component lines with intensities obeying a binomial distribution (Section 3.9.9).

In common with selective PENDANT, signals of ^{13}C nuclei, which exhibit long-range scalar coupling to the selected proton are comprised of a superposition of residual coherence and coherence that originates from polarisation transfer from the selected proton.

3.10.1 Acquisition of the selective PENDANT F.I.D.: The mixing time for 1-D HOESY

At the beginning of the acquisition time, τ_{acP}, the spin system has been prepared in the

consistent way as described previously. During the acquisition time the free induction decay (F.I.D.) of the selective PENDANT experiment is recorded. Simultaneously, ^{13}C nuclei relax from their prepared state, $M_z^S = 0$, due to longitudinal relaxation, which may also include cross-relaxation with the selected proton, should mutual dipolar coupling exist. After acquisition, the selective PENDANT F.I.D. is stored in a separate memory area so that the subsequent acquisition of the 1-D HOESY F.I.D. does not overwrite it (Appendix A14 and A4.5.7).

3.10.2 Acquisition of the 1-D HOESY F.I.D.

Directly after the 1-D HOESY mixing time, τ_{acH}, i.e., the Selective PENDANT acquisition period, τ_{acP}, another Z-gradient is applied to de-phase residual coherence that remains after the acquisition of the selective PENDANT F.I.D. Therefore, only pure magnetisation that built-up from longitudinal relaxation during the mixing time exists. The final ^{13}C $\pi/2$ pulse, P_{20}, 'reads' this magnetisation for acquisition under proton broadband decoupling.

3.11 Experimental

Investigative experimental work was undertaken to determine the utility of the selective PENDANT-1-D HOESY experiment with respect to the following factors.

1. To determine whether the selective PENDANT-1-D HOESY experiment is successful in providing 1-D HOESY spectra that can be used for qualitative distance determinations.
    - The results of the 1-D HOESY experiment obtained using selective PENDANT-1-D HOESY were compared to a standard 1-D HOESY experiment.

2. To determine whether the utility of the selective PENDANT experiment is maintained in comparison to normal selective PENDANT as a result of the integration with 1-D HOESY.
    - A series of selective PENDANT spectra, which were simultaneously obtained with the 1-D HOESY spectra using selective PENDANT-1-D HOESY, were compared to spectra obtained using normal selective PENDANT.

Unfortunately it was not possible to perform the complete fully automated selective PENDANT-1-D HOESY pulse program given in appendix A14 and so obtain data simultaneously for selective PENDANT and 1-D HOESY as originally designed. This seems to be a result of the inability of the pulse programmer to properly execute the sequential acquisitions, i.e., the selective PENDANT acquisition followed by the 1-D HOESY acquisition in the current pulse program. In order to facilitate sequential acquisitions in the same pulse programme, a specific set of pulse program statements are used to define the selective PENDANT acquisition. These statements and their function are given in appendix A4.5.7, which have been directly taken from the relevant pulse programming manual for the Bruker Avance NMR spectrometer and established example programs. Furthermore the syntax of the selective PENDANT-1-D HOESY pulse programme, which is based upon this information, has also been verified by Bruker UK. Consequently, the selective PENDANT 1-D HOESY pulse program has been modified in order to emulate the performance of the fully automated experiment had it functioned properly. This was achieved by the following amendments:

- the 1-D HOESY acquisition period, τ_{acH}, was removed and replaced with a time delay, d30, equal, to its duration (d30 = τ_{acH}) (Appendix A14.1). Consequently, with the exception of a data acquisition period, which has been replaced by an equivalent delay, the selective PENDANT experiment remains the same. Therefore, the modified selective PENDANT pulse sequence experiment is performed in the same way as that which would have been undertaken for the fully automated selective PENDANT-1-D HOESY experiment. Consequently the modified selective PENDANT experiment should yield the same results as the latter.
- To obtain an equivalent 1-D HOESY data set, the selective PENDANT acquisition was removed from the selective PENDANT-1-D HOESY pulse program (Appendix A14) and similarly replaced with a delay, d30, equal to its duration (d30 = τ_{acP}) (Appendix A14.2).

With respect to the criterion 1 and 2 given above, the following properties were analysed using the two pulse programs:

- suppression levels of residual signals obtained using the modified selective PENDANT-1-D HOESY experiment (A14.1) in comparison to normal selective PENDANT. The effectiveness of the low-pass J-filter and impact of it being placed

at the beginning of the pulse sequence was determined.

- Consistency of assignments of long-range scalar coupling correlations in comparison to normal selective PENDANT. Analysis reveals the effect on spectra for modified selective PENDANT-1-D HOESY being a summation of 'true on-resonance' and off-resonance experiments.
- Analysis of multiplet structures of residual signals. Analysis reveals that, if residual signals exhibit multiplets that display binomial intensities of component lines as predicted by theory given previously (Section 3.9.5).
- Analysis of multiplet structures of ^{13}C signals for nuclei that are long-range coupled to the selected proton. Analysis reveals that, if the signals exhibit multiplets that display binomial intensities of component lines (as a result of the purging function of the preparation element) predicted by theory given previously (Section 3.9.11).

3.11.1 Materials and Equipment

Experiments were performed using the same composition of sample as used previously in the selective PENDANT experiments for comparison: 60/40, vol/vol., ethyl-5-(chloromethyl)-2-furan-carboxylate and duetero chloroform ($CDCl_3$) respectively, the latter providing field – frequency locking.

In common with the performance of most transient nOe experiments, the sample was de-gassed to reduce the levels of dissolved molecular oxygen, which serves to reduce the transient nOes [23]. Degassing was performed using three freeze-pump-thaw cycles, in accordance with the procedure given in appendix A4.3.2.1.

Experiments were performed using a Bruker Avance 300MHz NMR spectrometer with 5mm ^{13}C – ^{1}H dual probe.

3.11.2 Selective pulses

With the exception of the SNEEZE pulse (Appendix A10), experiments were performed using the same soft shaped pulses as those used in previous selective PENDANT and INAPT experiments. All selective pulses were set to the same excitation bandwidth of 40Hz.

Pulse P_6 and P_{10}: SNEEZE pulse of duration 0.1454 seconds = Excitation

Pulse P_7 and P_9: Gaussian Cascade Q3 of duration 0.08628 seconds = Refocusing

Pulse P_8: Gaussian Cascade Q5 pulse of duration 0.214 seconds = Excitation (Polarisation transfer)

3.11.3 Gradient pulses

Gradient pulse 1 (Preparation element)

Duration: 1.5milliseconds

Type: Shaped Gradient : sine wave (Power of gradient is varied over time according to the shape function used)

Power: 70% of maximum power

Phase: Positive.

Gradient pulse 2 (Pre-HOESY acquisition)

Duration: 1.5milliseconds

Type: Shaped Gradient : sine wave

Power: 30% of maximum power.

Phase: Negative.

The power and phase of gradient 2 were changed with respect to gradient 1, in line with recommended procedures [43] to prevent fortuitous refocusing of coherence that was de-phased by gradient 1 (Appendix 11).

3.11.4 Acquisition parameters for selective PENDANT-1-D HOESY

The acquisition parameters given below were relevant to all experiments performed.

- The long-range scalar coupling evolution delays in selective PENDANT, τ_a and τ_b were set to 1/2J and 1/8J respectively for J = 8Hz.
- SW was set to encompass the entire ^{13}C chemical shift range of the solute using TD = SI = 32K, which provided adequate digital resolution of 0.37Hz to ensure correct representation of signal intensity and multiplet structure.
- The carrier frequency for ^{13}C was set at the centre of the solute chemical shift range. The carrier frequency for protons was set to the value specified by the values in a frequency list. The values in the frequency list (fq1:f2) (Appendix A14.1 and A14.2 and A4.5.6) were set so that the carrier frequency was alternated on every other transient between, on-resonance and off-resonance, for each selected proton. Therefore, the desired interleaving of the experiments, which is a

requirement of the 1-D HOESY acquisition was maintained (Appendix A3.1). The proton carrier frequency was set to the centre of the proton chemical shift range, by subsequent pulse program statements, for J-filtering and composite pulse decoupling when applicable.

- 16 dummy scans were executed to achieve steady state for ^{13}C magnetisation.
- To ensure long-term stability of the transient nOe measurements, the sample temperature was maintained at 300K, and the field-frequency lock system was set to optimum sensitivity in order to better adjust for drifts in $\mathbf{B}_0$ inhomogeneity.
- The relaxation delay prior to selective PENDANT was set at 3 seconds.
- The default selective PENDANT acquisition time τ_{acP}, which corresponds to the 1-D HOESY mixing time, τ_m, was set at 1.47 seconds. In the pulse programs A14.1 and A14.2 the simulated acquisition period τ_{acP} is given by d30 =1.47 seconds.

3.11.5 The standard 1-D HOESY experiment

The results of a 1-D HOESY experiment, similar to that routinely employed by Canet et al [33-35], which was mentioned previously (Section 3.4), was used as a 'control' for comparison to the results of the 1-D HOESY experiment in selective PENDANT-1-D HOESY. The 1-D HOESY experiment employed by Canet et al (figure 3.5) prepares the heteronuclear spin system in an identical fashion to selective PENDANT-1-D HOESY, with the exception of inverting the selected proton.

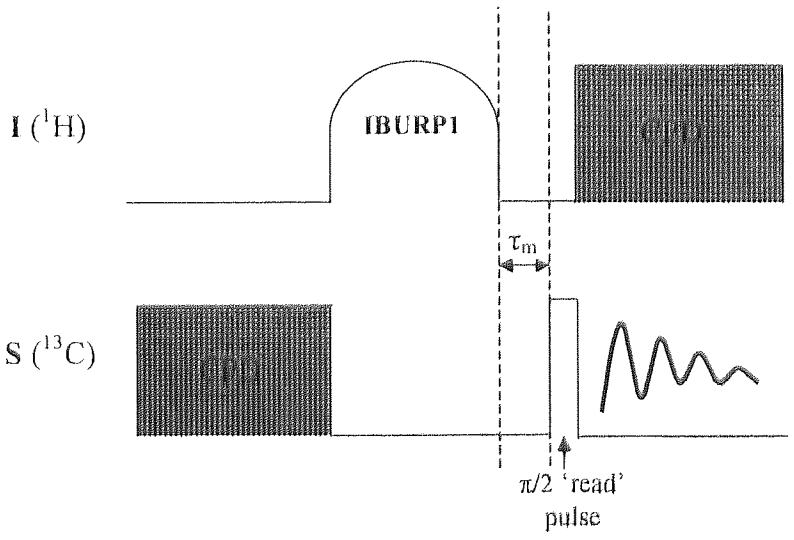

Figure 3.5 Standard (control) 1-D HOESY experiment

$-M_z^I{}_{sel}$ and $M_z^S = 0$ and $M_z^I{}_{unsel} \approx M_0^I$ = constant: 1-D HOESY

$M_z^I{}_{sel} = 0$ and $M_z^S = 0$ and $M_z^I{}_{unsel} \approx M_0^I$ = constant: selective PENDANT-1-D HOESY

3.11.6 Acquisition parameters for 1-D HOESY 'control' experiment

In contrast to the DANTE-Z selective inversion pulse [44] used by Canet et al, a IBURP1 [23] shaped selective inversion pulse with an excitation bandwidth of 40Hz, and duration 0.08996 seconds, was used for selective inversion of the selected proton.

All other acquisition parameters were identical to the corresponding parameters in selective PENDANT-1-D HOESY: the relaxation delay for the protons bonded to ^{12}C that remain unperturbed, which also corresponds to the ^{13}C (CPD) composite pulse decoupling time, was set to 3 seconds. WALTZ-16 [22, 23] CPD was used to ensure a high degree of broadband decoupling across the entire ^{13}C chemical shift range. The mixing time, τ_m, was set equal to the mixing time in selective PENDANT-1-D HOESY, i.e., the selective PENDANT acquisition time $\tau_{acP} = 1.47$ seconds.

3.11.7 Spectrum processing

All spectra were phase corrected to the same phase constants and processed using line broadening of 1Hz. All spectra are presented in absolute intensity scaling mode for comparison.

3.11.8 The efficiency of suppression of ^{13}C coherence, which exhibits short-range scalar coupling to protons

For comparison purposes, the same strategy that was previously employed to test the efficiency of suppression achieved with selective PENDANT was also used for testing the selective PENDANT 1-D HOESY experiment.

The selective PENDANT spectrum in the selective PENDANT 1-D HOESY experiment is comprised of 'true on-resonance' and off-resonance experiments. However, the function of selective PENDANT experiment necessitates that the residual signals, (i.e., those that also do not exhibit scalar coupling to the selected proton) have a consistent phase and magnitude in each of the on-resonance and off-resonance spectra, so that comparisons can be made between spectra for assignment purposes. Therefore, it is valid to compare the levels of

suppression achieved with the modified selective PENDANT experiment, with the levels of suppression achieved in the normal selective PENDANT experiment when both have been conducted off-resonance.

In common with the analysis of normal selective PENDANT, the levels of suppression for the modified selective PENDANT experiment in selective PENDANT 1-D HOESY were calculated by comparison to a direct-detect analogue. The direct-detect analogue is identical to the modified selective PENDANT pulse sequence, with the exception of the removal of all proton pulses in the J-filter, and their replacement with delays equivalent to their durations. This ensures that the T_1 and T_2 relaxation of the ^{13}C nuclei in the direct-detect analogue, closely emulates that in selective PENDANT, to ensure appropriate comparison.

To maintain comparison to normal selective PENDANT, the same strategy for the variation of the J-filter evolution delays, τ_1 and τ_2, was employed. The variation of J emulates a range in J-values of the scalar coupling multiplicities for which, τ_1 and τ_2 are designed to encompass, i.e., τ_1 for CH_2 and CH_3 and τ_2 for CH. A total of 16 transients were collected for each τ value:

- the value of τ_1 (1/2J) took values of J for the range 120Hz – 160Hz in intervals of 10Hz, while τ_2 (1/2J) remained constant and set to the recommended value of J=180Hz.
- The value of τ_2 (1/2J) took values of J for the range 160Hz – 200Hz in intervals of 10Hz, while τ_1 (1/2J) remained constant and set to the recommended value of J=140Hz.

The integrated intensities of the signals in the direct-detect analogue spectrum were each normalised to 100%. The % suppression or breakthrough was calculated for the corresponding signals in the modified selective PENDANT experiment.

3.11.9 Results and Discussion

For illustrative purposes, figures 3.6 and 3.7 overleaf each display 3 spectra obtained for the variation of τ_1 and τ_2 respectively. For the range of τ_1 and τ_2 evolution delays tested, which were designed to emulate a variation in J-values, it is evident that the low-pass J-filter successfully purges ^{13}C residual coherences associated with the CH and CH_3 multiplicities.

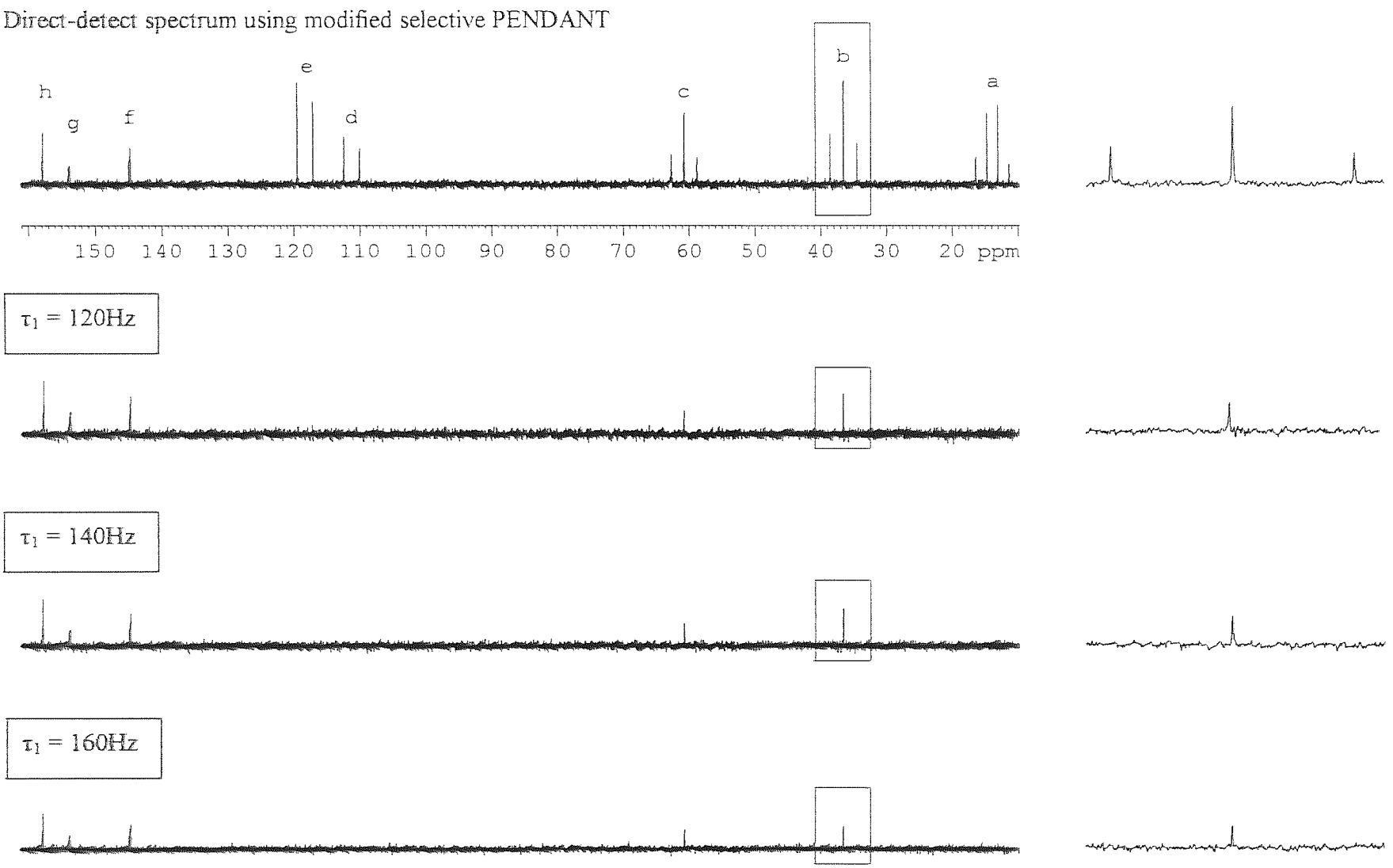

Figure 3.6 Suppression efficiencies of residual signals as a function of τ_1 in the selective PENDANT spectra of the simulated selective PENDANT 1-D HOESY experiment. Area enclosed is shown expanded adjacently.

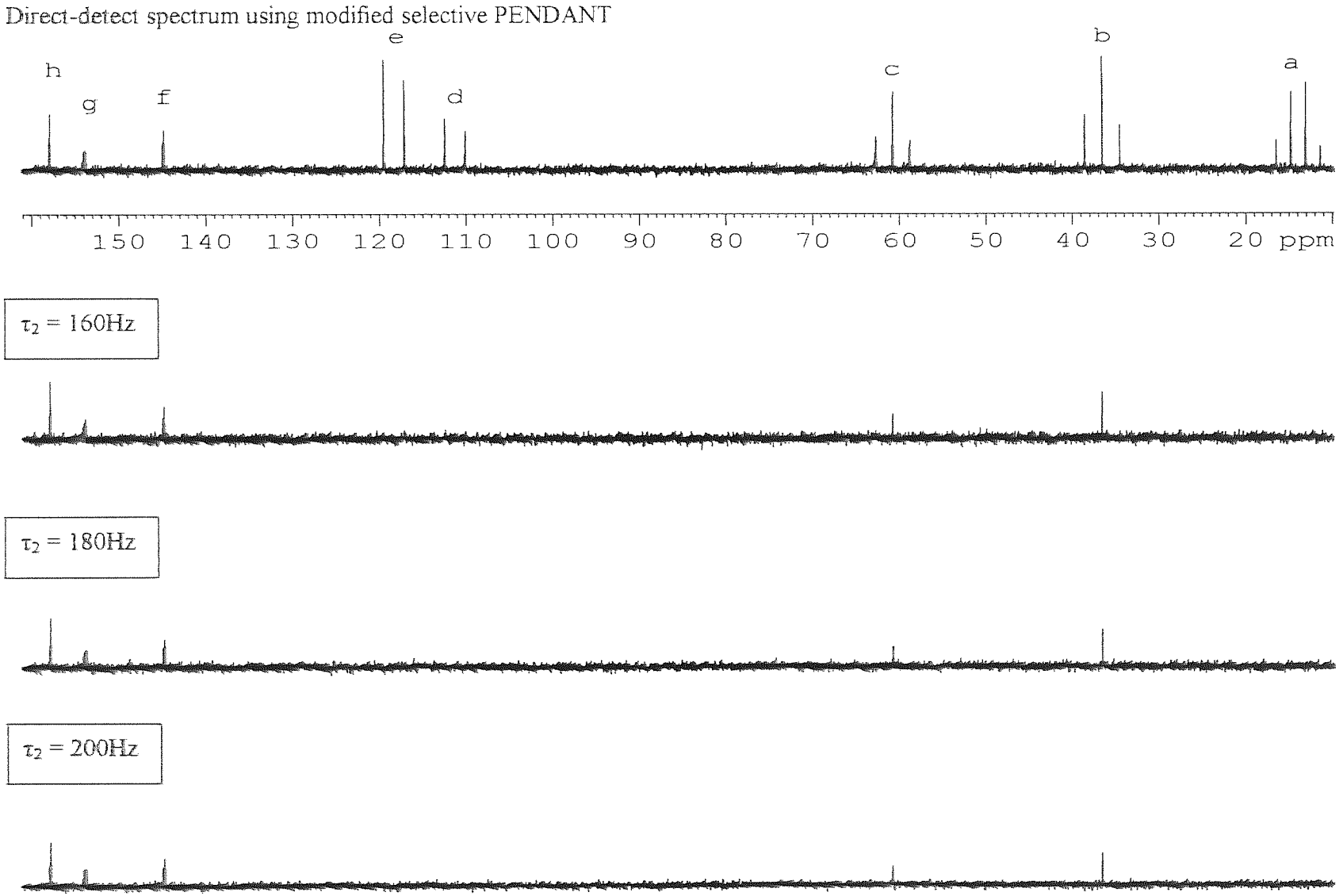

Figure 3.7 **Suppression efficiencies of residual signals as a function of τ_2 in the selective PENDANT spectra of the simulated selective PENDANT 1-D HOESY experiment.**

In common with normal selective PENDANT, which also exhibits the same purging efficiencies of the CH and CH_3 coherences, breakthrough of signals associated with the CH_2 multiplicities has occurred.

In figure 3.6, with respect to the direct-detect analogue spectrum, the CH_2 (**b**), signal exhibits 83%, 84% and 88% suppression for the τ_1 values, 120Hz, 140Hz and 160Hz respectively. Not surprisingly, the best suppression efficiency is attained when τ_1 is set according to 160Hz, which is closest to the actual J-value of 153Hz. Interestingly, in common with the results observed for the normal selective PENDANT experiments, the efficiency of suppression for the CH_2 signals decreases, as J increases from 160Hz to 200Hz, for setting τ_2. One would not expect this to happen, since the J-values diverge further from the actual value of 153Hz.

In comparison with selective PENDANT, the efficiency of suppression of the ^{13}C signals of the CH_2 multiplicities has reduced, on average, by 10% for the entire range of J-values tested. In common with the investigative experiments performed for the analysis of selective PENDANT, a simple experiment was performed to determine the effect of off-resonance effects on the efficiency of suppression of the ^{13}C signals of the CH_2 multiplicities.
An experiment was performed with τ_1 and τ_2 set with the recommended values of J = 140Hz and 180Hz respectively, with the exception that the ^{13}C carrier frequency was set on-resonance for the CH_2 (**b**) multiplet. The level of suppression achieved was 96%, in comparison to 84% when the ^{13}C carrier frequency is set to the middle of the ^{13}C chemical shift range. Therefore, in common with normal selective PENDANT, further investigation into the compensation of off-resonance effects associated with the ^{13}C pulses is warranted.

The utility of the modified selective PENDANT experiment is not compromised by the breakthrough of residual $^{13}CH_2$ signals, since comparison to the off-resonance spectrum confirms their true origin. However, the cosmetic degradation of the spectrum is more serious in comparison to the normal selective PENDANT experiment

It was mentioned previously (Section 3.8.5) that the multiplets of breakthrough signals, from residual coherences that pass the J-filter, should exhibit a binomial distribution of the intensities of their component lines. However, upon inspection of the residual $^{13}CH_2$ signals **b** and **c** in all spectra of figures 3.6 and 3.7, it is evident that this is not the case, and in fact

the signals exhibit multiplet anomalies. It is unknown why this is so and warrants further research.

The restructuring of the low-pass J-filter, in order to convert coherence from protons bonded to ^{12}C into + Z magnetisation, has not compromised the suppression of residual coherences of the CH and CH_3 multiplicities. However, the repositioning of the low-pass J-filter to the beginning of the modified selective PENDANT experiment necessitated the inclusion of extra ^{13}C refocusing pulses. Furthermore the length of the pulse sequence is increased in comparison to selective PENDANT. Seemingly a combination of these two factors has lead to greater sensitivity to off-resonance effects associated with ^{13}C refocusing pulses, which causes greater breakthrough of ^{13}C signals of the CH_2 multiplicities.

3.12 Experimental investigation into the performance of selective PENDANT in selective PENDANT 1-D HOESY

The total number of transients collected for the selective PENDANT experiment (Appendix A14.1) (of the selective PENDANT-1-D HOESY experiment) is necessarily controlled by the number of transients that are required to build-up sufficient signal-to-noise ratios for the considerably less sensitive 1-D HOESY experiment. In this investigation, 1600 transients were collected for the off-resonance experiment and each of the on-resonance experiments for protons, **a**, **b**, **c**, **d** and **e**. It is seen later that this provides adequate signal-to-noise ratios of the 1-D HOESY spectra. The total experiment time was 24 hours.

Spectra are presented in figures 3.8, 3.9 and 3.10 overleaf where the selected proton is indicated in the adjacent molecular diagrams by way of an arrow. The off-resonance spectrum is presented at the top right-hand side in each figure for comparison purposes. Normal selective PENDANT spectra taken from Chapter 2 for the same selected proton are shown adjacently (to the left of the divide) for comparison. The correlation assignments, which are indicated as usual by lower case letters, have been made in the normal way: those nuclei which have received polarisation transfer are indicated with signals that point downward, i.e., the pseudo-edited method. Those that have received polarisation transfer but exhibit a positive phase (where the pseudo-edited method has failed) have been assigned by comparison to the off-resonance spectrum by means of signal amplitude differences. As usual the term 'on-resonance' refers to the selective pulse manipulating the said proton.

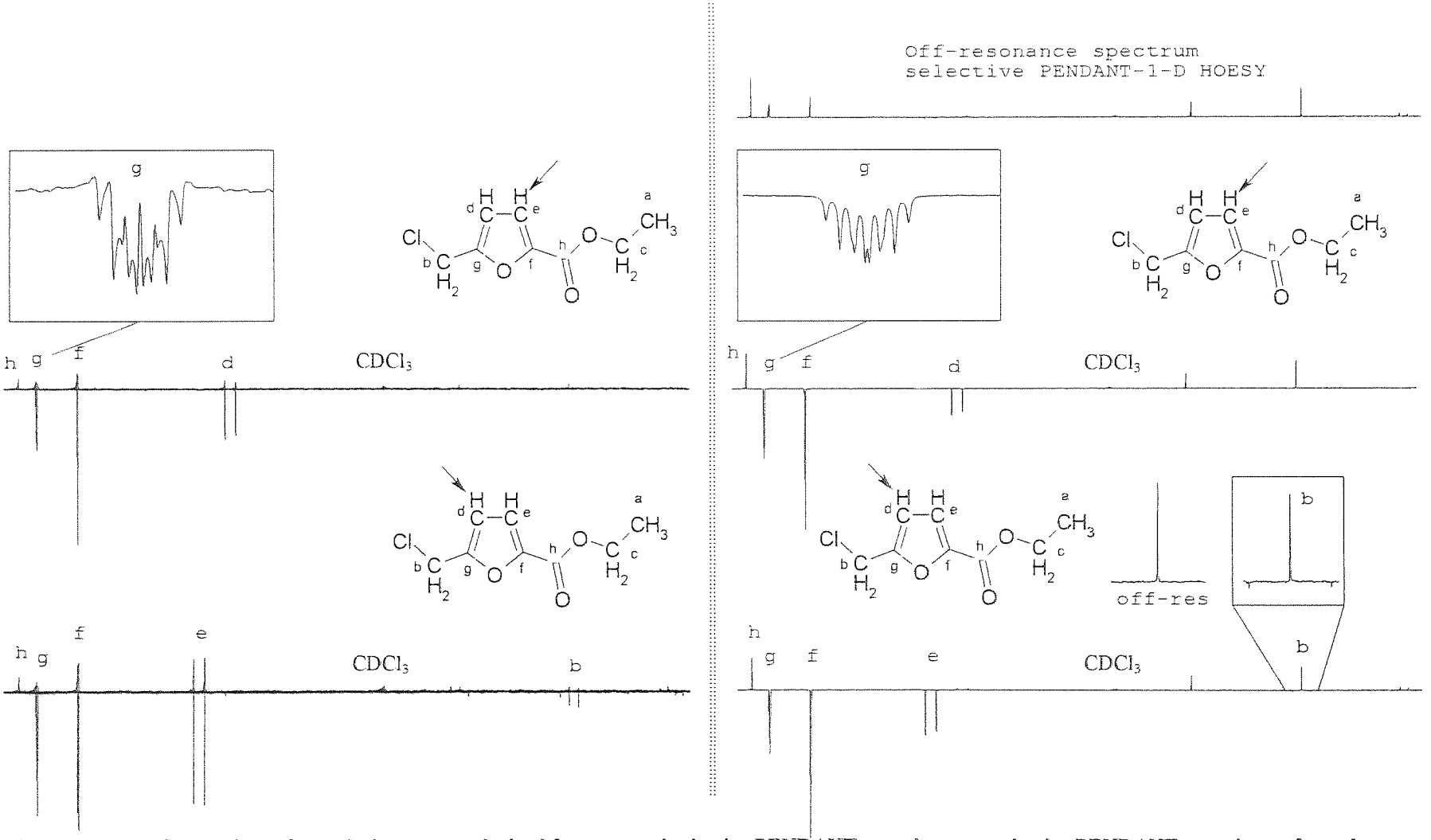

Figure 3.8 Comparison of correlation spectra derived from normal selective PENDANT experiment to selective PENDANT experiment from the simulated selective PENDANT-1-D HOESY experiment. (see text)

Left of divide: Normal selective PENDANT spectra for selected proton.
Right of divide: Selective PENDANT spectra from simulated selective PENDANT-1-D HOESY experiment.
Selected proton is shown in molecular diagram by way of an arrow.
Carbons which exhibit long-range scalar coupling correlations with selected proton are indicated by lower case letters (see text)

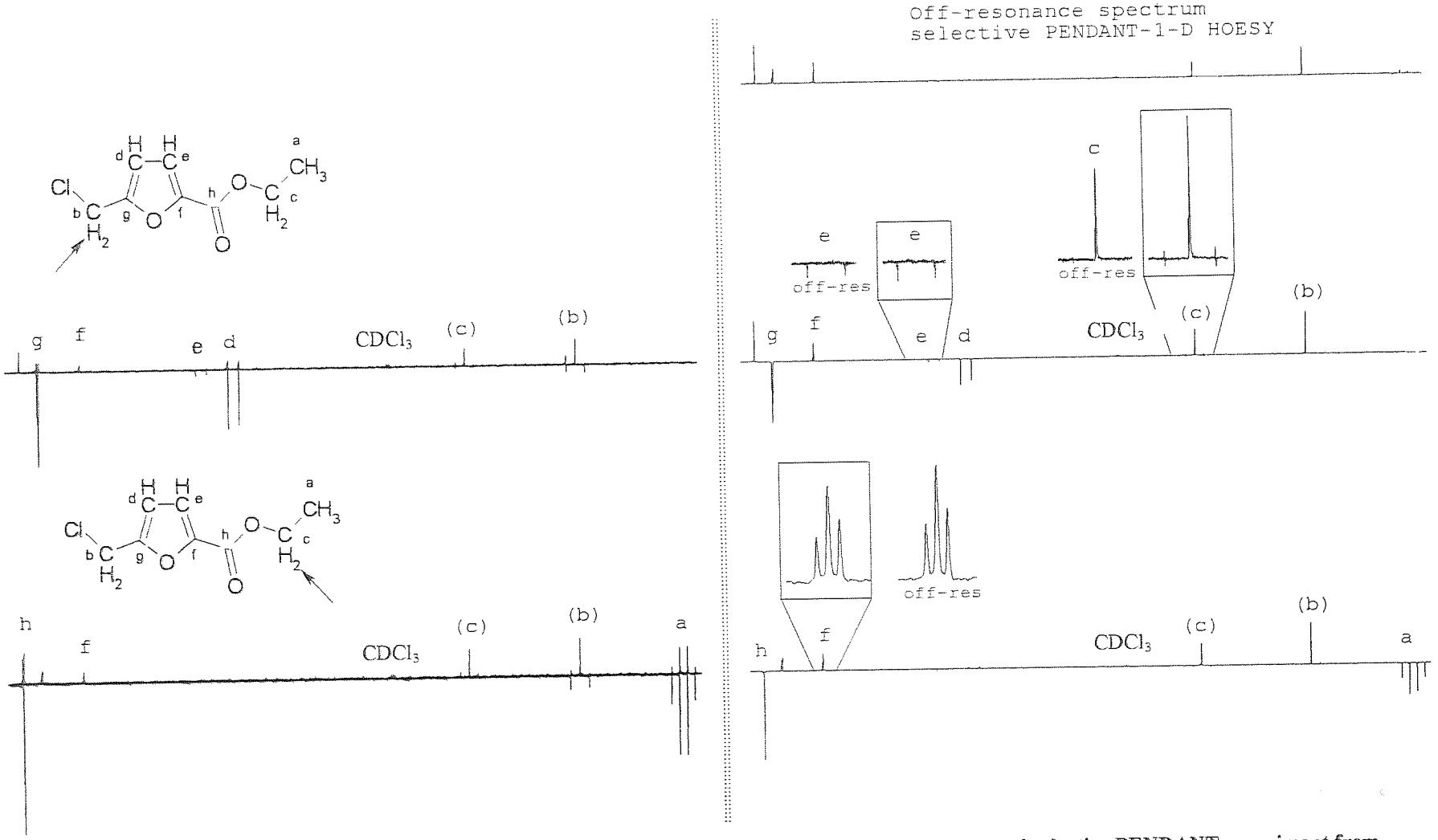

Figure 3.9 Comparison of correlation spectra derived from normal selective PENDANT experiment, and selective PENDANT experiment from the simulated selective PENDANT-1-D HOESY experiment. (see text)

Left of divide: Normal selective PENDANT spectra for selected proton. Right of divide: Selective PENDANT spectra from simulated selective PENDANT-1-D HOESY for same selected proton as shown adjacently.

Selected proton is shown in molecular diagram by way of an arrow. Carbons which exhibit long-range scalar coupling correlations with selected proton are indicated by lower case letters (see text). Lower case letters in parentheses indicate changes that are not attributed to correlations (see text).

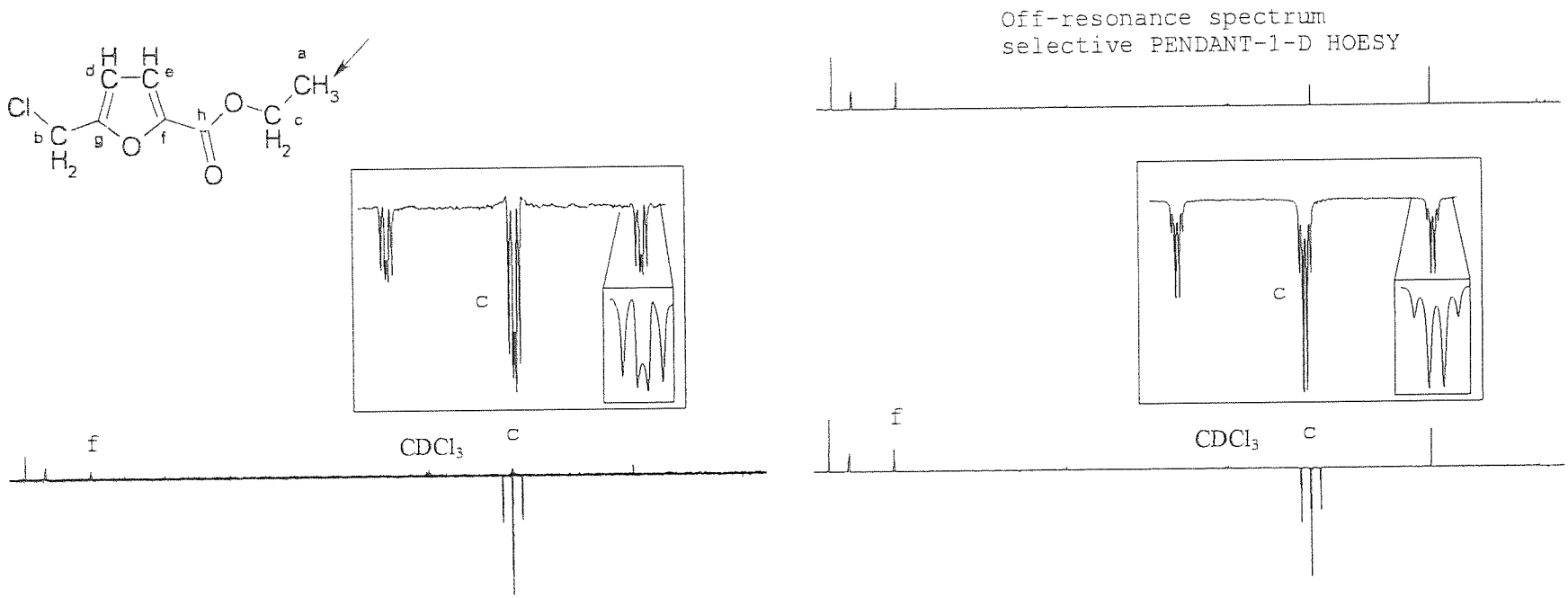

Figure 3.10 Comparison of correlation spectrum derived from normal selective PENDANT experiment to selective PENDANT experiment from the simulated selective PENDANT-1-D HOESY experiment. (see text)

Left of divide: Normal selective PENDANT spectra for selected proton.
Right of divide: Selective PENDANT spectra from simulated selective PENDANT-1-D HOESY experiment.
Selected proton is shown in molecular diagram by way of an arrow.
Carbons which exhibit long-range scalar coupling correlations with selected proton are indicated by lower case letters (see text).

Upon inspection of all spectra it is evident that the correlations derived from normal selective PENDANT spectra are emulated by the spectra of selective PENDANT experiment from the simulated selective PENDANT-1-D HOESY experiment.

By analogy with normal selective PENDANT, comparison to the off-resonance spectrum is required in order to assign a correlation when the idealised pseudo-edited method fails. For example, in figure 3.9, the on-resonance experiments of CH_2 protons, **b**, and CH_2 protons, **c**, each show a long-range scalar coupling with ^{13}C nuclei **e** and **f**. The correlation to the ^{13}C nucleus **e** in the on-resonance experiment of protons **b** is seen by the small magnitude difference with the **e** signal in the off-resonance experiment. This is shown for convenience by the insert labelled (off-res), which appears adjacent to the expanded views of **e** and is taken from the off-resonance experiment shown in the top left hand corner. Similarly the correlation to ^{13}C signal **f** in the on-resonance experiment of protons **c** is realised by the small intensity difference with the off-resonance experiment (off-res inset).

Fortunately a pre-requisite of transient nOe experiments like HOESY, is that every effort is made to ensure the long-term stability of $\mathbf{B_0}$, by optimising the field-frequency lock system (Appendix A4.3). Subsequently, fine assignments of correlations can be made, since small differences in signal intensities between the on-resonance and the off-resonance spectra will less likely be attributed to magnetic field-drifts.

An illustration of the unfortunate magnitude of breakthrough of residual signals that occurs for the ^{13}C signals of the CH_2 multiplicities is illustrated in the on-resonance experiment of proton **d** in figure 3.8. The normal selective PENDANT spectrum yields a correlation with the ^{13}C nucleus of the CH_2 multiplicity **b.** This is identified by the weak signal, which exhibits severe multiplet anomalies in anti-phase to **h**. However, in the selective PENDANT spectrum derived from the simulated selective PENDANT-1-D HOESY experiment, it is not clearly evident that a correlation with carbon **b** exists. However, on closer inspection, the outer lines of signal **b**, (shown in the expanded region) can be seen to have phases that are indeed indicative of polarisation transfer, i.e., in anti-phase to quaternaries that have not received polarisation transfer.

Unfortunately, the superposition of the residual signal, and that which has originated from polarisation transfer, has cancelled the centre line of the triplet. Therefore, one would only

make a tentative assignment. This observation further demonstrates the need to find a method of compensating for the off-resonance effects that give rise to breakthrough of ^{13}C signals of the CH_2 multiplicities.

3.12.1 The purging effect of the preparation element

In figure 3.8 it can be seen that the quaternary nucleus **g** exhibits a correlation with proton **e**. Quaternary **g** is shown expanded and enhanced in the inset of both the normal selective PENDANT spectrum and the selective PENDANT spectrum derived from the simulated selective PENDANT-1-D HOESY experiment. Similarly in figure 3.10, the CH_2 multiplicity **c** is shown to exhibit a correlation with protons **a**, and is also shown expanded and enhanced in an inset in both spectra. Both insets show clearly the purging effect of the preparation element (Section 3.9.11) in selective PENDANT-1-D HOESY. Multiplets **g** and **c** in the selective PENDANT spectra obtained from the simulated selective PENDANT-1-D HOESY experiment are devoid of both phase and multiplet anomalies. The action of the ^{13}C pulse, P_{18}, at the beginning of the preparation element, removes phase anomalies, and the selective proton pulse, P_{10}, during the preparation element, removes multiplet anomalies (Section 3.9.11).

In contrast, the multiplets **g** and **c** in the normal selective PENDANT spectra, exhibit the usual phase and multiplet anomalies, which are inherent to polarisation transfer and subsequent refocusing of coherence during the final evolution delay, τ_b.
The purging effects of the ^{13}C pulse, P_{18}, and the selective proton pulse, P_{10}, in the preparation element are demonstrated in two separate experiments:

1. One experiment was performed with the selective proton pulse, P_{10}, in the preparation element present.
2. One experiment was performed with the selective proton pulse, P_{10}, in the preparation element removed. To compensate for the difference in timing, a delay of equal duration to the selective pulse was substituted in its place.

16 transients were collected for each experiment while all other acquisition parameters reported above remained constant. Figure 3.11 a and b overleaf presents spectra for experiments 1 and 2 conducted with CH_2 protons **b** on-resonance. Quaternary **g** is shown expanded in each spectrum.

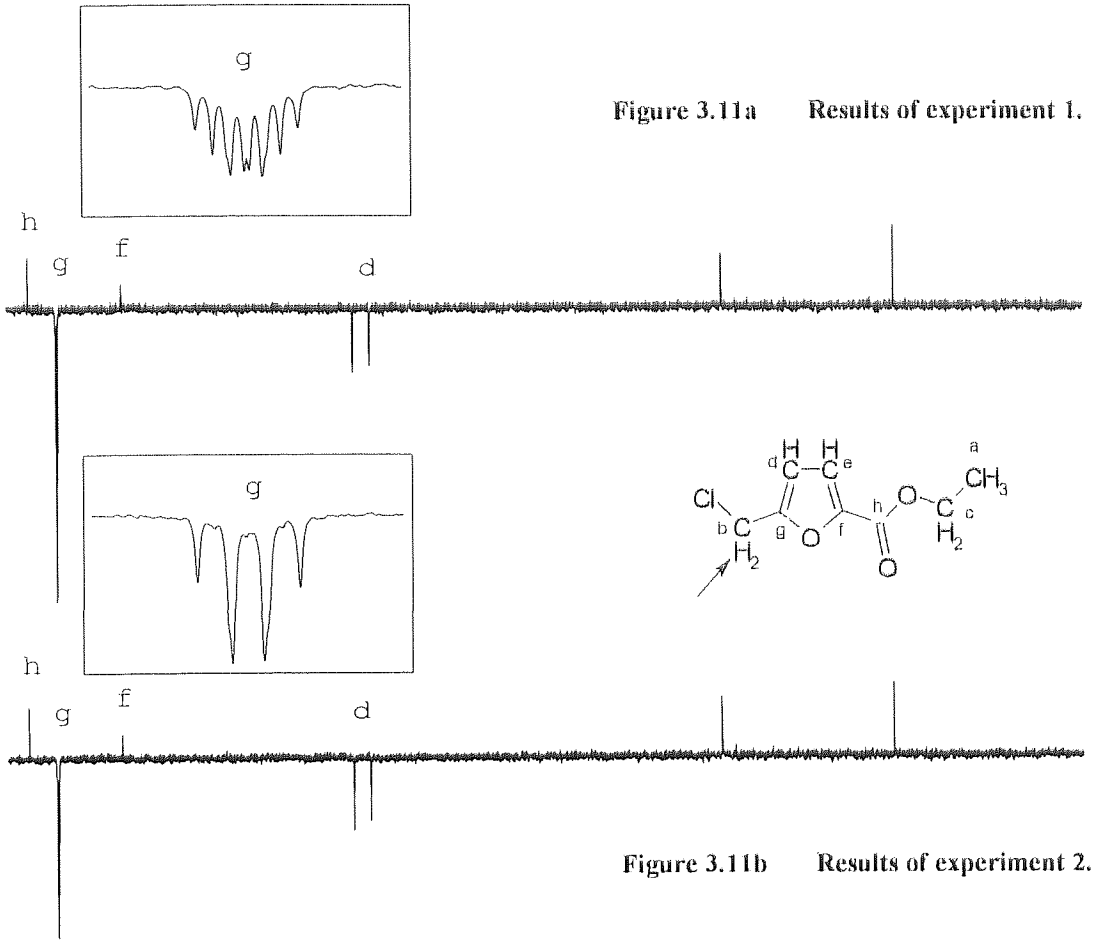

Figure 3.11a Results of experiment 1.

Figure 3.11b Results of experiment 2.

Figure 3.11 Purging effect of preparation element in selective PENDANT-1-D HOESY experiment.

It is evident that the first ^{13}C pulse, P_{18}, in the preparation element successfully purges phase anomalies, as the component lines of the multiplets are free from dispersive contributions (Section 3.9.11). Figure 3.11a illustrates the purging effect of, P_{10}, which has restored the binomial distribution of intensities and the full coupling pattern of the multiplet. Figure 3.11b clearly demonstrates the presence of multiplet anomalies due to the omission of the selective proton pulse, P_{10}, in the preparation element.

3.12.2 Spurious breakthrough of ^{13}C signals **b** and **c**

Rather interestingly, a feature that was common to both INAPT and selective PENDANT spectra (Chapter 2.14.2) has appeared in the selective PENDANT spectra of the simulated selective PENDANT-1-D HOESY experiment. In figure 3.9 the unexplained breakthrough of ^{13}C signals (**b**) and (**c**), has once again occurred for the on-resonance experiments of protons **b** and **c**. This can be seen by the positive intensity change in comparison to the off-resonance spectrum and slight change in multiplet pattern. Both aspects are illustrated in the insets for ^{13}C signal (**c**). Although of far less severity than that exhibited by normal selective PENDANT, it is nevertheless a rather puzzling observation. Indeed the presence of such breakthrough signals may contradict a theory, which was presented for the explanation of their appearance in selective PENDANT and INAPT spectra (Chapter 2.14.2).

It was thought that the breakthrough of one signal was attributed to the excitation of multiple quantum coherence by the accidental perturbation of the ^{13}C proton satellites by the selective pulses. At later times it was thought that the multiple quantum coherences were converted to observable single quantum coherence by the hard proton and ^{13}C pulses in the low-pass J-filter. It was proven, by modification to INAPT, that the phenomenon was more sensitive to hard proton pulses, when the selective proton polarisation transfer pulse was replaced by a hard pulse. The simultaneous appearance of signal **b** and **c** in the on-resonance experiments of protons **b** and **c** respectively remains unexplained. This is because the selective proton pulses are far removed from each of the ^{13}C proton satellites, which correspond to the signals **b** and **c**. Seemingly, there does not seem to be a mechanism by which a scalar coupling effect can be relayed between the affected proton satellites and the ^{13}C nuclei **b** and **c** in the same molecule.

In the selective PENDANT-1-D HOESY experiment, the application of a Z-gradient in the preparation element should cause the de-phasing of all orders of heteronuclear multiple

quantum coherence. Consequently, there should be no possibility of conversion of multiple quantum coherence to observable single quantum coherence by the application of the $\pi/2$ 'read' pulse P_{19}, and the selective proton pulse, P_{10}, during the preparation element. The appearance of these breakthrough signals may suggest that: the Z-gradient, either on its own or in combination with the pulses of the preparation element, does not cause sufficient de-phasing of heteronuclear multiple quantum coherence from which the breakthrough coherences may originate.

Although, pulses are known to refocus the effects of de-phasing due to gradients [43], it seems unlikely that one ^{13}C $\pi/2$ pulse and a single selective proton pulse can cause this to happen. Furthermore, even though the efficiency of de-phasing of heteronuclear zero quantum coherence by the Z-gradient is the worst of all the various orders of multiple quantum coherence that can later give rise to observable signals, it seems unlikely that this prevails. Heteronuclear zero quantum coherence de-phases at the difference of the chemical shifts of the protons and the carbons, which are active in the coherence. This equates to approximately ¾ the sensitivity of de-phasing of proton homonuclear single quantum coherence (Appendix 11 and A8.2.9.1). Due to the fact that gradients of the duration and amplitude that are used in the preparation element are used to successfully de-phase the latter in homonuclear experiments, it seems unlikely that heteronuclear multiple quantum coherence survives.

If time had permitted, an investigation into the effect of varying the gradient duration, phase and amplitude upon the breakthrough signals would have been carried out. Such an investigation would reveal if the phenomenon was indeed related to the survival of residual multiple quantum coherences that are potentially re-converted to observable single quantum coherences by the pulses of the preparation element.

The phenomenon of simultaneous breakthrough from the ^{13}C signals **b** and **c** for the on-resonance experiments of protons **b** and **c**, remains unexplained and demands further research. Since the phenomenon is also inherent to INAPT, which is comparatively simple in construction and manipulation of the spin-system, preliminary investigations should probably be focused on using INAPT.

3.13 Analysis of the 1-D HOESY results from selective PENDANT-1-D HOESY

Figures 3.12 and 3.13 overleaf present the absolute transient nOes, which are attained by the interleaving of the on-resonance and off-resonance experiments as described earlier (Section A3.7). The spectra to the left-hand side of each figure are obtained from the 1-D HOESY 'control' experiment. Immediately to the right of the divide are the corresponding 1-D HOESY spectra derived from the simulated selective PENDANT-1-D HOESY experiment (A14.2) for the same selected proton. The selected proton is indicated by way of an arrow on the molecular diagram adjacent to the spectra.

From simple inspection of the spectra it is evident that the signal-to-noise ratios of the 1-D HOESY spectra approach half that of the conventional 1-D HOESY spectra. This is not surprising as the relative inversion of the selected proton with respect to all other protons bonded to ^{12}C is half that in the selective PENDANT-1-D HOESY experiment in comparison to the conventional 1-D HOESY experiment (Section 3.6). The important aspect to determine is whether the inclusion of 1-D HOESY into the selective PENDANT experiment has invalidated the results of the former in comparison to a conventional 1-D HOESY spectrum. As the 1-D HOESY experiment in selective PENDANT-1-D HOESY is intended to be used in a purely qualitatively manner (Section 3.3), a simple comparison of the relative intensities of peaks within each spectrum, compared with the relative intensities of each peak in the conventional 1-D HOESY spectrum suffices.

By means of simple inspection it is possible to see that relative intensities of the signals closely correlates with those in the conventional 1-D HOESY spectra, which validates the use of selective PENDANT-1-D HOESY for the qualitative determination of 1-D ^{13}C-^{1}H transient nOes. The only exceptions to the complete success of the 1-D HOESY experiment, in the simulated selective PENDANT-1-D HOESY experiment, is seen upon inspection of the relative intensities of quaternary signals, **g** and **h** due to proton **e**.

In the conventional 1-D HOESY spectrum, **h** is more intense than **g** by approximately 1/3 of the total unit intensity of **g**. In the 1-D HOESY spectrum from selective PENDANT-1-D HOESY, the quaternaries **g** and **h** have approximately equal intensities. It is unknown why this result was the only exception.

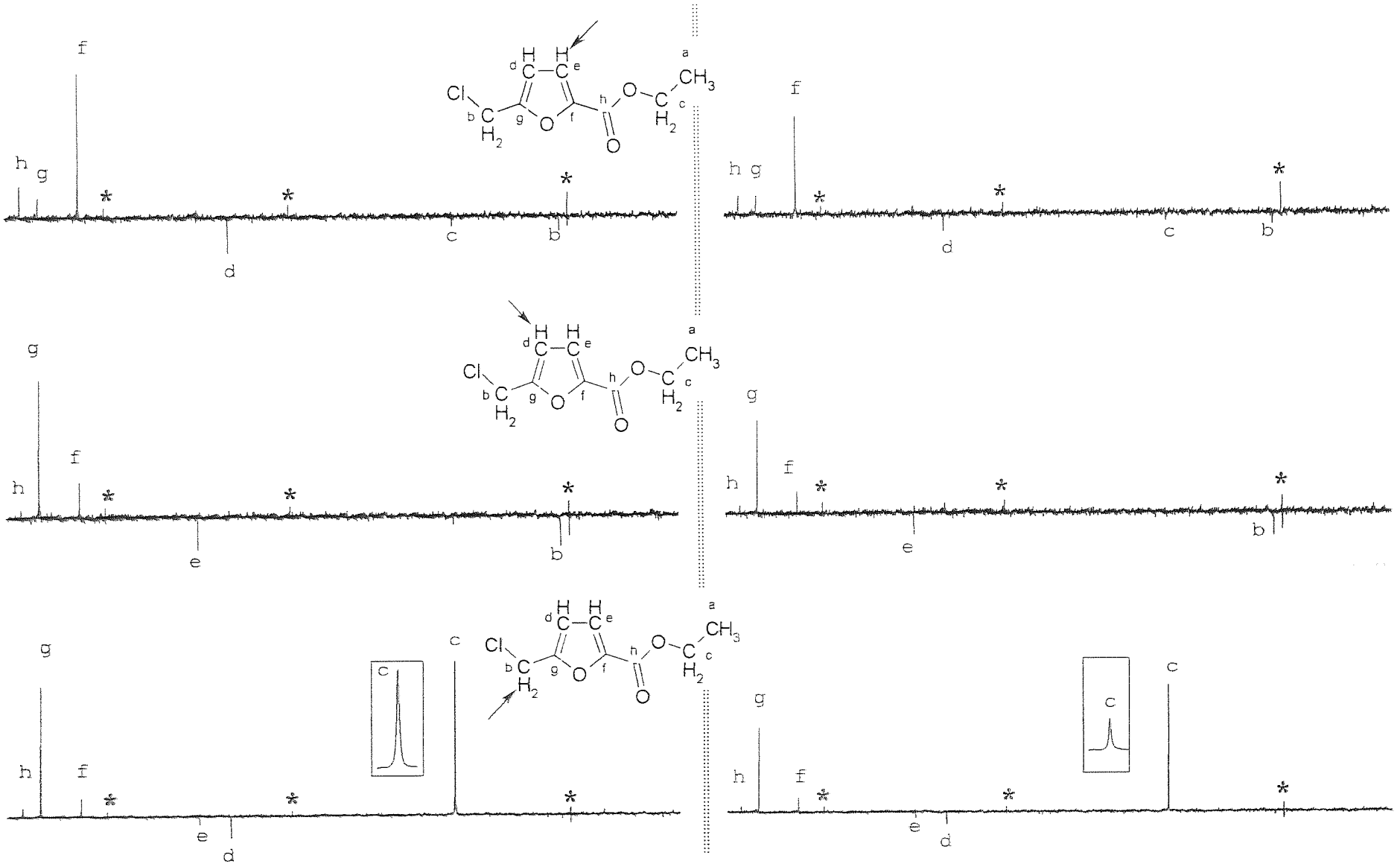

Figure 3.12 Comparison of 1-D HOESY 'control' spectra (left of divide) to 1-D HOESY spectra from simulated selective PENDANT-1-D HOESY (right of divide).
Selected proton is indicated on molecular diagram by way of an arrow. (*) Indicates artefact or impurity (see text)
On resonance spectrum of proton b is displayed at ½ intensity.

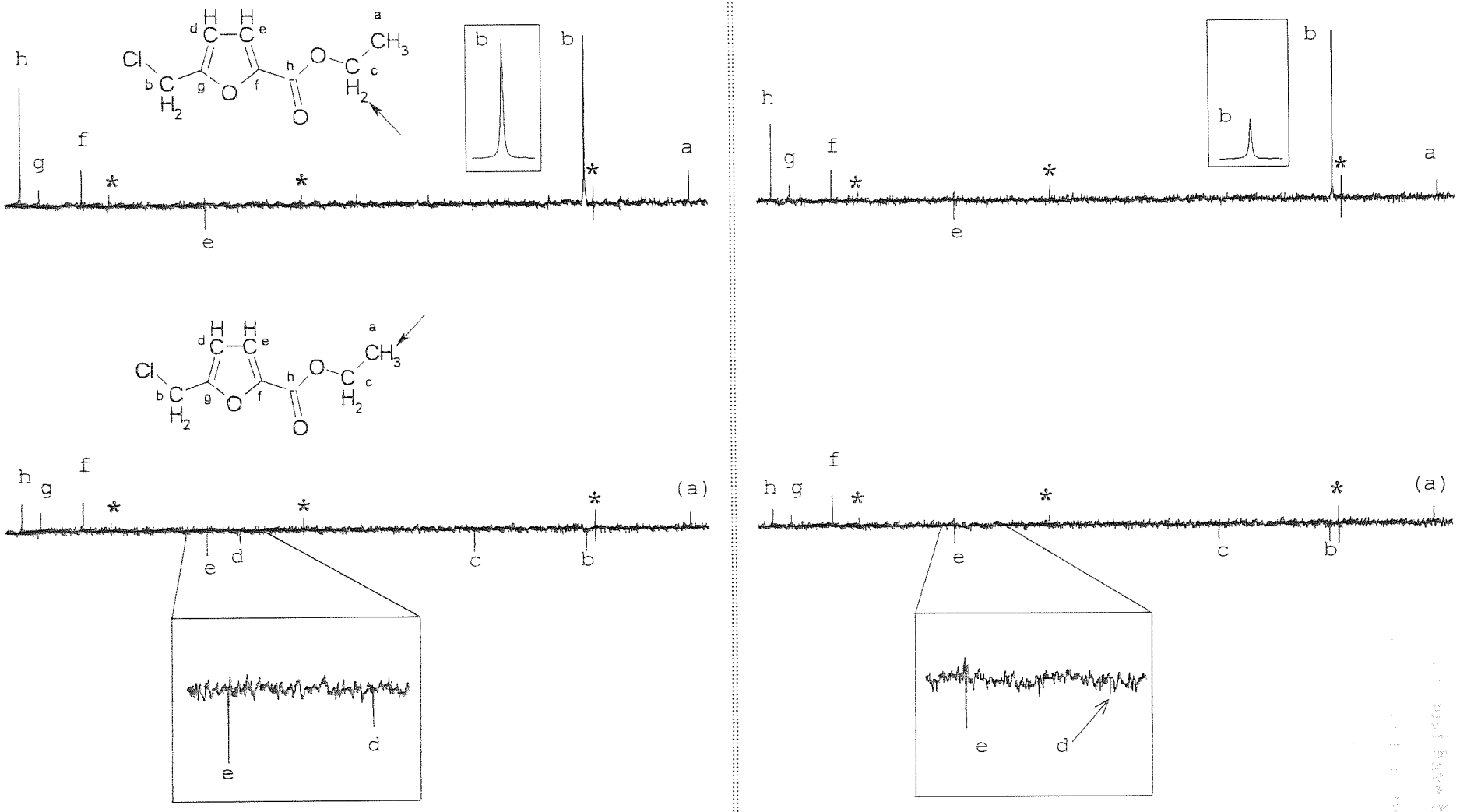

Figure 3.13 Comparison of 1-D HOESY 'control' spectra (left of divide) to 1-D HOESY spectra from simulated selective PENDANT-1-D HOESY (right of divide).

Selected proton is indicated on molecular diagram by way of an arrow. (*) Indicates artefact or impurity (see text)

If time had permitted, a conventional 1-D HOESY experiment would have been performed utilising the same $\pi/2$ selective proton pulse (SNEEZE (P_{10}), which is used to provide selective perturbation in selective PENDANT-1-D HOESY. Consequently, this may immediately reveal a deficiency when using a particular type of selective pulse or adverse T_1 relaxation effects of the selected proton. The former seems unlikely as no other results prove this to be the case.

From a purely academic point of view, the 1-D HOESY spectra exhibit indirect effects (negative nOes), which are often manifested in HOESY spectra (Section 3.2). Indeed at least one indirect effect is observed in each spectrum. There are also a large number of artefacts in the spectra, which are marked by the asterisks and in most instances appear in complete or partial dispersion. It is likely that these are attributed to the interleaving of on-resonance and off-resonance F.I.Ds and subsequent subtraction via phase cycling.

In the on-resonance spectra of protons **b** and **c** breakthrough of ^{13}C signals **c** and **b** have occurred respectively. This is most likely caused by a similar phenomenon as that described earlier in chapter 2.14.2 for similar breakthrough. The periphery of the excitation bandwidth of the selective pulse P_{10} excites one of the ^{13}C proton satellites of the adjacent proton resonance. Consequently the ^{13}C satellite spin energy levels attain an uneven population perturbation similar to that invoked by selective population inversion experiments (SPI). The ^{13}C pulse P_{20} completes polarisation transfer rendering an uneven anti-phase and enhanced signal for the corresponding ^{13}C nuclei. Due to the uneven nature of the polarisation transfer, proton broadband decoupling does not entirely cancel the signal and breakthrough into the spectrum occurs.

3.13.1 Conclusions

It has been shown that a 1-D HOESY experiment has been successfully combined with a selective PENDANT experiment. The utility of the 1-D HOESY experiment is limited to the determination of qualitative internuclear distance determinations as a result of the integration of the HOESY mixing time into the signal acquisition period of the selective PENDANT experiment.

Comparison of the relative intensities of the signals of the transient nOes within each 1-D HOESY experiment compared to a conventional 1-D HOESY experiment reveals the success

of selective PENDANT-1-D HOESY for providing consistent assignments for qualitative purposes. One exception to the complete success of the technique is observed for two quaternary nuclei that exhibit near equal nOe intensities. According to the conventional 1-D HOESY experiment, the relative intensities should have been approximately 1:1.33. Since all other results suggest a good agreement with the conventional 1-D HOESY experiment, it would be unfair to say at this early stage that the selective PENDANT-1-D HOESY experiment has failed in the assignment of these particular nOes. Further investigation into this result is warranted.

The majority of results suggest that the re-structuring and re-positioning of the J-filter and the effect of the preparation element, does indeed lead to the consistent preparation of the heteronuclear spin system in readiness for the 1-D HOESY experiment.

It has been shown that the repositioning of the low-pass J-filter to the beginning of the selective PENDANT pulse sequence does not adversely affect the efficiency of suppression of residual ^{13}C coherences, which are implicit to the detection of quaternary nuclei. Indeed, the low pass J-filter has been shown once again to be remarkably invariant to a range in J-values, which were tested by controlled variation of the evolution delays τ_1 and τ_2.

The recommended procedure for setting the evolution delays of the J-filter, i.e., $\tau_1 = 1/2J$ for $J = 140Hz$ and $\tau_2 = 1/2J$ for $J = 180Hz$ has been proven to completely suppress ^{13}C signals of the CH and CH_3 multiplicities, while the CH_2 multiplicities breakthrough to a level of 16% (84% suppression) for the compound under scrutiny. The poor level of suppression of the ^{13}C signals of the CH_2 multiplicities, by analogy with normal selective PENDANT, is largely dependent on off-resonance effects associated with the ^{13}C pulses. For the same experimental parameters, the level of suppression achieved for the ^{13}C signal of the CH_2 b multiplicity was increased to 96% when the ^{13}C carrier frequency was set on resonance for this signal. Further work is warranted to compensate for off-resonance effects in order to obtain more efficient levels of suppression.

The relative increase in sensitivity to breakthrough of the ^{13}C signals of the CH_2 multiplicities, as compared to normal selective PENDANT, is no doubt attributed to the increase in the number of ^{13}C refocusing pulses and the inherent length of the pulse sequence. Both were necessitated by the restructuring of the low-pass J-filter and its repositioning to the

beginning of the pulse sequence. The increase in pulse sequence length is due to the fact that one of the J-filter pulses no longer has the secondary function of acting as the proton polarisation transfer pulse. Consequently the pulse sequence is lengthened by the inclusion of a dedicated selective polarisation transfer pulse like that inherent to INAPT.

The preparation element in selective PENDANT-1-D HOESY causes the efficient purging of multiplet and phase anomaly-causing coherences for nuclei that exhibit long-range scalar coupling to the selected proton. An unfortunate side-effect caused by purging is a decrease in signal intensity. Consequently, careful comparison with the off-resonance spectrum is required in order to make long-range scalar coupling correlation assignments for signals experiencing poor polarisation transfer efficiencies. However, as spectrometer stability is maximised for the performance of 1-D HOESY (simulated acquisition in this work), small differences in intensity between the off-resonance and on-resonance spectra can be resolved.

It has been shown that the combination of selective PENDANT with 1-D HOESY is successful and provides the experimenter with a convenient method for the qualitative analysis of selective transient nOes. Furthermore, from the same experiment the user is provided with long-range ^{13}C-^{1}H scalar coupling correlation data with the added advantage of the detection of all ^{13}C quaternary nuclei of the system. The principles inherent to selective PENDANT combined with 1-D HOESY are also valid for INAPT. In fact, when the identification of all ^{13}C quaternary nuclei is unimportant, the integration of 1-D HOESY with INAPT, would prove more useful. This is because there is no need to collect an additional off-resonance experiment, which reduces experiment time in comparison to selective PENDANT-1-D HOESY.

Unfortunately execution of the fully automated version of selective PENDANT-1-D HOESY (Appendix A14) has not been possible. However, the design of experiments to simulate the effect of the working pulse program (Appendix A14.1 and A14.2) has proven the validity of the concept of selective PENDANT-1-D HOESY. A major thrust of work detailed in this thesis is to produce novel pulse sequences that are amenable to use on NMR spectrometers of lesser specification, specifically those, which cannot perform inverse (proton detected) experiments. Indeed the selective PENDANT-1-D HOESY pulse sequence can be programmed on such instruments, which are equipped with less sophisticated pulse programmers. The major difference would be in the use of homospoil pulses (Appendix

A11) in contrast to the more modern Z-gradient pulses, which have dedicated gradient coils in the NMR probe. Aside from the issues pertaining to the formation of eddy currents (Appendix A11), conveniently, the length of the 1-D HOESY mixing time, i.e., selective PENDANT acquisition time is long enough to accommodate the necessary recovery in the field-frequency lock system.

Chapter 4 A semi-theoretical and practical investigation into the development of SNARE

The spectral signal-to-noise ratios (S/N) of insensitive nuclei, e.g., ^{13}C in spectra derived from polarisation transfer experiments, like INEPT and DEPT and their derivatives, and more recently, the polarisation exchange experiment PENDANT, largely depend upon the longitudinal relaxation of protons between transients. Relaxation delays between transients constitute a large proportion of overall experiment time, particularly when the T_1's of protons are large and when a high number of transients are required as a result of low concentrations of the insensitive nuclei under scrutiny.

The demand for NMR spectroscopy coupled with its intrinsic financial cost, often requires that experimental time is minimised, sometimes at the expense of poorer S/N. Conversely, if demand permits, a greater financial outlay is required to achieve better S/N by extending experiment times. Therefore, methods of reducing the T_1 of protons in order to shorten relaxation delays and hence reduce experimental time can be useful.

The most popular method of reducing T_1, is achieved by doping analytical samples with paramagnetic relaxation agents [49]. However, this course of action is often chemically undesirable. The application of ultrasound to samples to reduce T_1's is experimentally complex and may not be amenable to the chemical system under scrutiny [45], and therefore is often declined.

To this end, a pulse sequence was proposed by Homer and Perry [45] which invokes sensitive-nucleus accelerated relaxation for enhancement (SNARE) of the spectral S/N of the insensitive nucleus during a given experimental time. In essence, SNARE causes the accelerated longitudinal relaxation of sensitive (I) nuclei, i.e., protons, through inverse polarisation transfer from insensitive (S) and usually dilute nuclei, e.g., ^{13}C, which have been subject to nuclear Overhauser enhancement during their detection.

Pulse sequence experiments like INEPT, DEPT and PENDANT, are routinely performed using proton broadband decoupling during acquisition. During the acquisition time, τ_{ac}, the insensitive nuclei are subject to all normal modes of longitudinal relaxation including nuclear

Overhauser enhancement (nOe) (Appendix A7.2.6) from dipolar cross-relaxation with the decoupled protons. At the end of acquisition and the removal of proton broadband decoupling, the longitudinal magnetisation of the S nuclei (M_z^S) has recovered to an extent, which is largely dependent upon the length of τ_{ac}.

The pulse sequence used for SNARE, which is inserted directly after acquisition, causes the inverse polarisation transfer of M_z^S to protons via short-range scalar coupling, in a manner consistent with that employed in inverse spectroscopy [4, 10, 15]. Furthermore, the anti-phase single quantum coherence of I is refocused and converted to +Z magnetisation, which consequently 'step-jump accelerates' the longitudinal recovery of the proton magnetisation (M_z^I) toward their equilibrium magnetisations M_0^I. The SNARE pulse sequence is appended to the polarisation transfer or exchange pulse sequence experiments, to either entirely replace, or significantly reduce, the usual relaxation delay D_r.

Experimental time-savings in excess of 30% for a given S/N have been reported for the use of SNARE in a PENDANT (S-PENDANT) experiment, over that of a normal PENDANT experiment performed on the same analytical sample.

The advantages of implementing SNARE for accelerating the T_1 relaxation of protons over those methods described previously are:

- no need for chemical perturbation of the sample
- No extra experimental complexity involved
- Easily implemented by means of simple insertion of the SNARE pulse sequence
- Is 'inert' in terms of the manipulation of spin systems, so not causing detrimental effects to the experiment to which it is attached

The pre-requisites for the implementation of SNARE, as interpreted from the original publication [45] are:

1. The experiment to which SNARE is appended, must utilise proton broadband decoupling during acquisition of the insensitive (S) nuclei to build-up the desired nOe.
2. The gyromagnetic ratios (γ) of both I and S must be the same sign. (γ_I and $\gamma_S > 0$)

3. The S nuclei are short-range scalar coupled to I nuclei upon which inverse polarisation transfer depends.

Work reported in this chapter addresses the potential for the use of SNARE when γ_I and γ_S have opposite signs, namely $\gamma_I > 0$ and $\gamma_S < 0$. According to the original publication (statement 2), it was initially thought that negative nOes inherent to S nuclei with $\gamma_S < 0$ would reduce the recovery of S during τ_{ac} such that there is insufficient magnetisation, M_z^S for inverse polarisation transfer to I. An illustrative experiment presented here provides evidence to the contrary. Furthermore, general theoretical comments regarding the viability of SNARE with S nuclei with negative γ is given in order to provide a basis for further research should it continue in this field.

The theoretical comments are focused upon the longitudinal relaxation characteristics and typical J-values of ^{15}N and ^{29}Si, which are arguably the most popularly studied nuclei in organic chemistry, which have negative γ. Furthermore, general theoretical comments are given for the general improvement of SNARE applied to arbitrary nuclei I and S. Before progressing, to novel work, a general overview of the theoretical basis of SNARE is given as interpreted from the original publication.

4.1 Theoretical basis of SNARE for γ_I and $\gamma_S > 0$ (^1H and ^{13}C)

The SNARE pulse sequence is appended to the end of a pulse sequence (INEPT, PENDANT etc) replacing entirely or in series with a reduced relaxation delay, D_r. The theory of SNARE as communicated in the original publication was based on the following assumptions with respect to the state of the ^{13}C (S) and ^1H (I) spin system prior to, during, and after acquisition for the pulse sequence experiment to which SNARE is appended.

1. At the start of acquisition, S and I magnetisation is considered to be zero ($M_z^S = M_z^I = 0$). A polarisation transfer or exchange pulse sequence like INEPT, DEPT and PENDANT, necessitates the equalisation of the S (^{13}C) and I (^1H) spin-energy level populations as a result of the application of non-selective $\pi/2$ pulses applied to both S and I. Therefore, it can be considered that $M_z^S = 0$ at the start of acquisition, neglecting small amounts of longitudinal relaxation, which may occur during the comparatively small short-range scalar coupling evolution delays of the pulse sequence.

2. During acquisition of S, proton broadband decoupling necessitates that proton (I) magnetisation is zero ($M_z^I = 0$).
3. During acquisition longitudinal relaxation of S takes place, and is also subject to nOe. The latter builds up toward the maximum theoretical nOe, η_{max}, which is $\gamma_I/2\gamma_S + 1$ times the equilibrium magnetisation of S (M_0^S). (Appendix A7.2.6)
4. After proton broadband decoupling is turned off, it is assumed that $M_Z^S \leq 3$, i.e., equal to or less than the theoretical maximum enhancement for $^{13}C\{^1H\}$.
5. Before the start of SNARE, a fraction of longitudinal recovery of protons (I) is assumed to have taken place as a result of power-switching delays implicit to moving from proton decoupling to normal hard pulsing ($M_z^I > 0 << M_0^I$). This is considered inconsequential on modern NMR instruments, which require only a few tens of microseconds to perform power-switching functions.

4.1.1 The development of the heteronuclear nOe

During proton broadband decoupling the steady-state nOe at an insensitive nucleus (S), e.g., ^{13}C, due to protons (I), is given by [24] (Appendix A7.2.6):

$$f_S\{I\} = \sum_I \frac{\gamma_I}{2\gamma_S} \frac{\sigma_{IS}}{R^S_{DD}} = \eta_{max} = \frac{\gamma_I}{2\gamma_S} \qquad 4.1$$

Where R^S_{DD} is the intramolecular dipolar relaxation rate constant for dipolar relaxation between S and I exclusively.

Therefore, for S nuclei directly bonded to I, which by definition exhibit mutual short-range scalar coupling, M_z^S approaches the maximum values of enhanced magnetisation $\eta_{max} + 1$ times M_0^S upon broadband decoupling of I. This is because the longitudinal relaxation of nuclei that are directly bonded to protons is dominated by dipolar relaxation with the directly bonded proton. Empirical findings have shown that, during proton broadband decoupling and the attainment of steady-state, the observed nOe at ^{13}C, which are directly bonded to protons, is often very close to η_{max}, regardless of bonding multiplicity. Consequently, proton broadband decoupling during acquisition of insensitive nuclei generates sizeable magnitudes of M_z^S, which can be inverse polarisation transferred to I via the mutual short-range scalar coupling. Of course, the actual magnitudes depend upon the length of the acquisition time, which typically ranges between 1 and 3 seconds to encompass the entire S, e.g., ^{13}C chemical

shift range, and on the transfer functions. Steady-state will never be achieved during the acquisition time. However, the nOe will not be far short of its maximum magnitude.

Exceptions to achieving η_{max} can occur for nuclei that have efficient sources of longitudinal relaxation other than dipolar relaxation with the decoupled protons. In particular, the longitudinal relaxation of isolated S nuclei, e.g., quaternary ^{13}C nuclei, which are not directly bonded to protons, can be largely influenced by spin-rotation relaxation (SRR) and at greater magnitudes of $\mathbf{B}_0$, chemical shift anisotropy relaxation (CSA) (Appendix A6.4.5 and A6.4.6). Both SRR and CSA, serve to effectively reduce the empirical nOe and are referred to as 'leakage' relaxation sources, (Appendix 7.2.2) which are represented by the rate constant ρ_S^*. Therefore, the total relaxation rate constant for S (R_S) is given by $R_S = R^S_{DD} + \rho_S^*$ and under steady-state conditions, during proton broadband decoupling, R^S_{DD} is better replaced with R_S, to describe the empirical nOe of isolated nuclei.

The effect of leakage relaxation must be considered for all insensitive nuclei that maybe utilised for SNARE. Ultimately the proportion of leakage relaxation will determine the viability of that nucleus for providing reasonable magnitudes of M_z^S for reverse polarisation transfer to I.

Assuming single-exponential longitudinal relaxation of I (and S), the normal relaxation of I during the relaxation delay, D_r, of the pulse sequence to which SNARE is appended, is given by:

$$M_z^I = M_0^I\left[1 - \mathbf{exp}\left(-D_r / T_1^I\right)\right] \qquad 4.2$$

During the acquisition time, τ_{ac}, under proton broadband decoupling, S magnetisation recovers due to all modes of longitudinal relaxation and dipolar cross-relaxation (nOe) with I, which is given by:

$$M_z^S = M_0^S(\eta_{max} + 1)\left[1 - \mathbf{exp}\left(-t_{ac} / T_1^S\right)\right]. \qquad 4.3$$

Assuming SNARE were able to cause inverse polarisation transfer of M_z^S to I, then the

magnetisation of the latter after the same D_r reaches:

$$M_{zS}^{\ I} = M_0^I\left[1-\exp\left(-D_r/T_1^I\right)\right]+\exp\left(-D_r/T_1^I\right)M_0^S(\eta+1)\left[1-\exp\left(-t_{ac}/T_1^S\right)\right]\gamma_I/\gamma_S \quad 4.4$$

where T_1^S and T_1^I are the longitudinal relaxation times of S and I respectively and M_{zS}^I represents the magnetisation of I, which has recovered due to SNARE and D_r.

In general, for a given τ_{ac} and D_r, the percentage enhancement (E) of I magnetisation that may be obtained using SNARE, relative to that achieved by normal longitudinal relaxation of I during, D_r, is given by, if $M_0^I = M_0^S(\gamma_I/\gamma_S)^2$:

$$E = \frac{100\left[1-\exp\left(-t_{ac}/T_1^S\right)\right](\eta_{max}+1)\gamma_S}{\left[\exp\left(D_r/T_1^I\right)-1\right]\gamma_I}. \quad 4.5$$

From this the theoretical maximum values of E corresponding to typical values of T_1 of I and S, τ_{ac} and D_r can be given. Alternatively, for a given ^{13}C S/N, the percentage reduction in D_r and hence overall experiment time can be calculated for comparison.

The treatment given above, (in the original publication) indicates the idealised maximum value of M_{zS}^I and the maximum value of E, which can be obtained with the assumption that complete and maximal inverse polarisation transfer of M_z^S to I (M_z^I) has occurred.

In real experiments, SNARE will be implemented on molecules that contain a variety of short-range scalar coupling multiplicities, which exhibit a range of J-values. Therefore, the efficiency of inverse polarisation transfer and hence the magnitude of M_{zS}^I, will depend greatly upon the scalar coupling evolution delays and the ability of the pulse sequence to invoke inverse polarisation transfer.

4.1.2 Inverse polarisation transfer

In principal, any polarisation transfer sequence performed in the inverse mode would be suitable for use for SNARE, e.g., inverse (reverse) INEPT [1, 4], and inverse (reverse) DEPT [51]. In the original publication, a PENDANT-like sequence was favoured, for which a justification will be given later on. It will be shown later on that in fact reverse INEPT and

inverse DEPT would prove useful in most circumstances for the implementation of SNARE. The SNARE pulse sequence is given by:

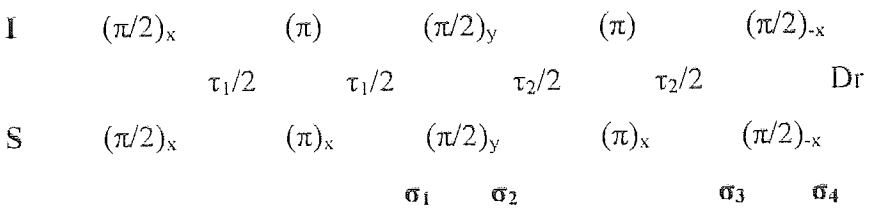

where σ_n represent the key stages of the pulse sequence which will be analysed.

In contrast to reverse INEPT and DEPT, the pulse sequence structure at the beginning of PENDANT does not require inversion. Reverse polarisation transfer is implicit to PENDANT (Chapter 1) due to its inherent symmetry, and the simultaneous $\pi/2$ pulses applied to I and S at the beginning of the pulse sequence. The final $\pi/2_{-x}$ pulse applied to I nuclei, necessitates the conversion of in phase I coherence to +Z magnetisation M_{ZS}^{I}. The final $\pi/2_x$ pulse applied to S nuclei causes the conversion of quaternary S coherence, which was created from +Z magnetisation by the first S pulse, back into +Z magnetisation. Therefore, the SNARE pulse sequence leaves essentially unaffected, quaternary magnetisation that had built-up during acquisition due to longitudinal relaxation and nOe. This is important when SNARE is appended to PENDANT so that the detection of quaternary nuclei is maintained. The optimisation of the short-range scalar coupling evolution delays τ_1 and τ_2 are discussed later on.

The effect of the SNARE pulse sequence upon the inverse polarisation transfer of M_Z^S to I, is identical to that for employing reverse INEPT. The product operator description of coherences present at the numbered stages σ_n is given here.

To maintain simplicity and clarity, the following assumptions have been made:

- all spins I involved in short-range coupling to S are magnetically equivalent.
- All pulses are assumed to be perfect, i.e., on-resonance, of correct length (hence causing correct nutation angles), of the correct phase and do not suffer from the adverse effects of *r.f.* inhomogeneity.
- Off-resonance effects are ineffective.

To save unnecessary lengthening of the product operator terms, the following notations are used to describe the various product operator coefficients:

$$c_{Jn} = \cos \pi J_{IS} \tau_n$$
$$s_{Jn} = \sin \pi J_{IS} \tau_n$$

The cosine (cos) and sine (sin) terms above do not discriminate between the magnetically equivalent I spins involved in the coupling multiplicity SI_n, e.g., $^{13}CH_2$. In order to convey the relevant points, it is assumed that the average value of <J> used invokes the condition $\tau_1 \neq 1/2J$ for all heteronuclear short-range scalar coupling multiplicities. It is assumed that quaternary coherence does not evolve due to long-range coupling during the short-range coupling optimised delays.

The overall transformation of the pulse and delay cascade up until σ_1, is to refocus chemical shift evolution due to τ_1, and to cause evolution of scalar coupling:

$$S_Z \xrightarrow{(\pi/2_{I+S})_x \, \pi J_{IS} \tau_1 \, 2I_z S_z \, (\pi_{I+S})_x}$$

σ_1

$$S \qquad +S_y \quad \text{Quaternary coherence}$$

$$SI \qquad +S_y c_{J1} - 2S_x I_z s_{J1}$$

$$SI_2 \qquad +S_y c^2_{J1} - 2\left(S_x I_{1z} c_{J1} s_{J1} + S_x I_{2z} c_{J1} s_{J1}\right) - 4S_y I_z I_z s^2_{J1}$$

$$SI_3 \qquad \begin{aligned} &+S_y c^3_{J1} - 2\left(S_x I_{1z} c^2_{J1} s_{J1} + S_x I_{2z} c^2_{J1} s_{J1} + S_x I_{3z} c^2_{J1} s_{J1}\right) \\ &-4\left(S_y I_{1z} I_{2z} c_{J1} s^2_{J1} + S_y I_{1z} I_{3z} c_{J1} s^2_{J1} + S_y I_{2z} I_{3z} c_{J1} s^2_{J1}\right) + 8S_x I_{1z} I_{2z} I_{3z} s^3_{J1} \end{aligned}$$

4.6

The effect of the polarisation transfer pulses upon the coherences is given by:

$$I_1 \xrightarrow{(\pi/2_{,})} I_2$$

σ_2 S $+\overset{(1)}{S_y}$ Quaternary coherence

SI $+\overset{(1)}{S_y}c_{J1} - 2S_z\overset{(2)}{I_x}s_{J1}$

SI_2 $+\overset{(1)}{S_y}c^2{}_{J1} - 2\left(S_zI_{1x}c_{J1}s_{J1} + \overset{(2)}{S_z}I_{2x}c_{J1}s_{J1}\right) + 4\overset{(3)}{S_y}I_{1x}I_{2x}s^2{}_{J1}$

SI_3 $+\overset{(1)}{S_y}c^3{}_{J1} - 2\left(S_zI_{1x}c^2{}_{J1}s_{J1} + \overset{(2)}{S_z}I_{2x}c^2{}_{J1}s_{J1} + S_zI_{3x}c^2{}_{J1}s_{J1}\right)$
$+4\left(S_yI_{1x}I_{2x}c_{J1}s^2{}_{J1} + \overset{(3)}{S_y}I_{1x}I_{3x}c_{J1}s^2{}_{J1} + S_yI_{2x}I_{3x}c_{J1}s^2{}_{J1}\right)$
$+8\overset{(4)}{S_z}I_{1x}I_{2x}I_{3x}s^3{}_{J1}$

4.7

Terms (3) and (4) represent unobservable double and triple quantum coherence respectively which cannot be re-converted to single quantum coherence by the remainder of SNARE and therefore do not contribute to $M_{zS}{}^{I}$. Similarly, residual S in-phase single quantum coherences, which include quaternary coherences, terms (1), are converted to +Z magnetisation. As such, terms (1), (3) and (4) are omitted from the following product operator transformations.

Only anti-phase single quantum coherences of I terms (2) which have arisen due to inverse polarisation transfer from S contribute to $M_{zS}{}^{I}$. Chemical shift is refocused during τ_2 while scalar coupling continues to evolve. Only in-phase I coherence, which contributes to $M_{zS}{}^{I}$ is presented:

$\sigma_2 \xrightarrow{\pi J_{IS}\tau_2 2I_zS_z} \sigma_3$

σ_3 $(IS) = +I_ys_{J2}s_{J1}$
$(I_2S) = +2I_ys_{J2}s_{J1}c_{J1}$
$(I_3S) = +3I_ys_{J2}s_{J1}c^2{}_{J1}$

4.8

The in-phase $+I_y$ coherences are subsequently converted to $+I_z$, and hence M_{zS}^I by the final I $(\pi/2)_{-x}$ pulse. Expression 4.8 represents the transfer function implicit to inverse polarisation transfer from S to I using the SNARE pulse sequence, which is also applicable to the use of reverse INEPT. Therefore, the empirical value of M_{zS}^I is more appropriately represented by the incorporation of the transfer function with expression 4.4, so reflecting the dependence of M_{zS}^I on the <J> values employed in the chosen pulse sequence. For example, for a ^{13}CH short-range scalar coupling multiplicity, the empirical value of M_{zS}^I is given by:

$$\text{IS} \qquad M_{ZS}^I = \begin{bmatrix} M_0^I\left[1-\exp\left(-D_e/T_1^I\right)\right]+ \\ \exp\left(-D_r/T_1^I\right)M_0^S(\eta+1)\left[1-\exp\left(-t_{ac}/T_1^S\right)\right]\gamma_I/\gamma_S \end{bmatrix} s_{J1}s_{J2} \qquad 4.9$$

Although the dependence upon <J> was implied in the original publication, conveyance of this fact was not communicated in the convenient form of a transfer function as given above. However, the transfer function is still idealised, since it neglects the effects of T_2 relaxation of I and S during the evolution delays τ_1 and τ_2, which serves to reduce M_{ZS}^I.

4.1.3 The setting of the evolution delays in SNARE

To optimise inverse polarisation transfer for the short-range scalar coupling multiplicities SI, SI_2 and SI_3, τ_1 should obviously be set to, 1/2J, 1/4J and 1/5J respectively. The evolution delay for the SI_3 multiplicity is a compromise since the $s_{J1}c^2_{J1}$ cannot be refocused using a single fixed delay [46, 4]. To optimise refocusing of in-phase proton coherence for conversion to M_{zS}^I, the evolution delays for the above multiplicities should all be set to 1/2J.

Obviously the range in J-values and SI multiplicities found in organic molecules, for which INEPT, DEPT and PENDANT are implemented, necessitates that the effect of SNARE cannot be optimised for all protons. Consequently, the S/N enhancement is uneven across the J and multiplet range. When SNARE is used for polarisation transfer experiments, the evolution delays in SNARE can be optimised for a particular coupling multiplicity or J-value. Similarly, the evolution delays in the pulse sequence, e.g., INEPT, DEPT or PENDANT etc, can be optimised to give maximum enhancement of the other multiplicities or J-values. Therefore, for a given experiment time, the enhancement of S/N is more evenly spread across the range of multiplicities and/or J-values present. SNARE has been invoked in a 'semi-selectively' way by judicious choice of the evoluti the evolution are contingent to

maximising inverse polarisation transfer and refocusing for the accelerated relaxation of a proton with a particular scalar coupling multiplicity or J-value.

Used in this way, a S-PENDANT experiment performed on ethylbenzene, which is indicative of most commonly encountered J-ranges in typical organic compounds, gave a 25% reduction in overall experiment time for a given ^{13}C S/N as compared with a standard PENDANT experiment.

4.1.4 General attributes of SNARE

When SNARE is implemented in series with a reduced D_r, it has been proven that S/N improvements are better when the length of D_r is small. This is because the relative effect of SNARE is less, since the sensitive nuclei are closer to attaining thermal equilibrium with long D_r's. When the length of τ_{ac} is larger, the enhancements produced by SNARE are larger due to the closer approach of η_{max}.

Actual S/N enhancements seen as a result of implementing SNARE are in general larger than that predicted by theory. It is thought that this is attributed to a multiexponential recovery of S during τ_{ac} rather than the assumed single exponential recovery. The former facilitates a larger value of M_z^S build-up during τ_{ac} for inverse transfer to I.

4.2 SNARE applied to I and S when $\gamma_S < 0$.

Other **I** = ½ insensitive nuclei commonly found in organic and inorganic molecules of interest to the chemist are ^{15}N and ^{29}Si, which have γ of -2.71 and –5.32, and natural isotopic abundances of 0.37% and 4.70% respectively. ^{15}N is of particular importance to the full characterisation of peptide linkages, base pair interactions and on a smaller scale, amino acid residues etc [47]. ^{29}Si on the other hand finds uses in the organic fields of surfactant chemistry and speciality polymer applications and information regarding their bonding environments are often sought after [48].

The low natural isotopic abundance of ^{15}N and ^{29}Si compared with ^{13}C, necessitates their detection, in most circumstances, via polarisation transfer or exchange techniques like, INEPT, DEPT and PENDANT. The INEPT experiment has received popular use for their routine study [47-49]. This is particularly so because the nOe cannot always be relied on to provide polarisation enhancement for detection. This is because nuclei of $\gamma < 0$, exhibit

negative nOes, (Appendix A7.2.6.2) which can potentially significantly reduce, or even cancel their signals entirely. In some circumstances the empirical nOe enhancement is either, equal to, or close to, $\eta_{max} = -1$, such that the enhancement factor given by, $\eta_{max} + 1$, is close to or equal to zero. When probed by polarisation transfer and exchange techniques, the generation of negative nOes at these nuclei is insignificant, as the S/N of the insensitive nucleus depends entirely on the relaxation of the sensitive (proton) nuclei, from which polarisation transfer originates.

However, in the extreme narrowing limit, in comparison to $^{13}C\{^1H\}$ where $\eta_{max} = 1.998$, for $Si^{29}\{^1H\}$, $\eta_{max} = -2.51$ and for $^{15}N\{^1H\}$, $\eta_{max} = -4.94$, which are 25% and 250% larger respectively. Both theoretical enhancements represent potential for the accelerated relaxation of protons, which share short-range scalar coupling to ^{29}Si and ^{15}N.

In the original publication of SNARE it was stated that the sign of γ for I and S must be the same because it was thought that negative nOes would oppose the recovery of M_z^S during τ_{ac} such that there would be insufficient magnetisation for inverse polarisation transfer to I. However, this is not the case. Indeed, a trivial modification of SNARE facilitates the use of negative nOes from nuclei with negative γ.

The realisation that negative nOes can be used for SNARE stems from the recognition of the state of magnetisations of insensitive nuclei prior to acquisition and hence proton broadband decoupling. The negative nOe builds up from an idealised state of zero S magnetisation ($M_z^S = 0$) as described previously, which is inherent to heteronuclear polarisation transfer or exchange pulse sequences. This is due to the non-selective $\pi/2$ pulses used to invoke the various conversions of magnetisations to coherence. Consequently, the negative nOe, $-M_z^S$, can be inverse polarisation transferred to I in exactly the same way as if it had been positive. The only exception is that the phase of the first S pulse is inverted i.e., it becomes $(\pi/2)_{-x}$ as opposed to $(\pi/2)_x$.

Inversion of the phase of the first S pulse accommodates the conversion of enhanced magnetisation ($-M_z^S$) to single quantum coherence with a phase that after polarisation exchange allows the final I pulse to convert in-phase coherence to $+M_{zS}^I$. The phase inversion was necessary to account for the opposite nutation angle dependence invoked by nuclei of $\gamma < 0$ in comparison to nuclei of $\gamma > 0$. This is simply a consequence of the

opposite sign of Larmor frequency and the subsequent opposite precessional sense of the magnetic moments in $\mathbf{B_0}$. Therefore, all nuclei of $\gamma < 0$ interact with the opposite phase of one of the two contra-rotating magnetic field components of $\mathbf{B_1}$, in contrast to nuclei of $\gamma > 0$.

4.3 An illustrative experiment for SNARE using ^{29}Si

An amount of triphenylsilane ($HSi(Ph)_3$) was dissolved in $CDCl_3$ for field-frequency locking purposes to give a 10mM solution. The modified SNARE pulse sequence was appended to a normal PENDANT experiment, and the S/N of the ^{29}Si signal was compared via integration to that obtained using a normal PENDANT pulse sequence with identical acquisition parameters as described below.

4.3.1 Acquisition parameters

The scalar coupling evolution delays in SNARE and PENDANT were optimised to 1/2J for the short-range ^{29}Si-^{1}H coupling constant. SNARE was appended in series with a 0.5 second relaxation delay (D_r) for PENDANT. The PENDANT acquisition time was 3 seconds using the composite pulse decoupling sequence MLEV16. The T_1 of ^{29}Si and ^{1}H were determined by normal inversion recovery methods and were 12 seconds and 1.3 seconds respectively in the non-degassed sample. 16 transients were collected for both S-PENDANT and normal PENDANT at a constant sample temperature of 300K. Experiments were performed on a Bruker AC300 NMR spectrometer with a10mm broadband probe, tuned to ^{29}Si.

4.3.2 Results and Discussion.

The results of both experiments are presented in figure 4.1 overleaf. SNARE has caused a 15% increase in S/N of the ^{29}Si signal attained using PENDANT, which is a modest improvement. However, this improvement was obtained by careful optimisation of the component evolution delays in both SNARE and PENDANT to ensure optimum polarisation transfer and refocusing. Furthermore, complete optimisation of these delays was made possible due to the exclusivity of a single ^{29}Si-^{1}H short-range scalar coupling in this simple compound.

It is noted that the experiment was performed on a sample that had not been de-gassed such that competition from leakage relaxation due to dissolved molecular oxygen may be reasonably efficient. Consequently the nOe may not be the maximum attainable during the PENDANT acquisition. A degassed sample was not used because it is rare that one would

perform degassing prior to a routine polarisation transfer experiment.

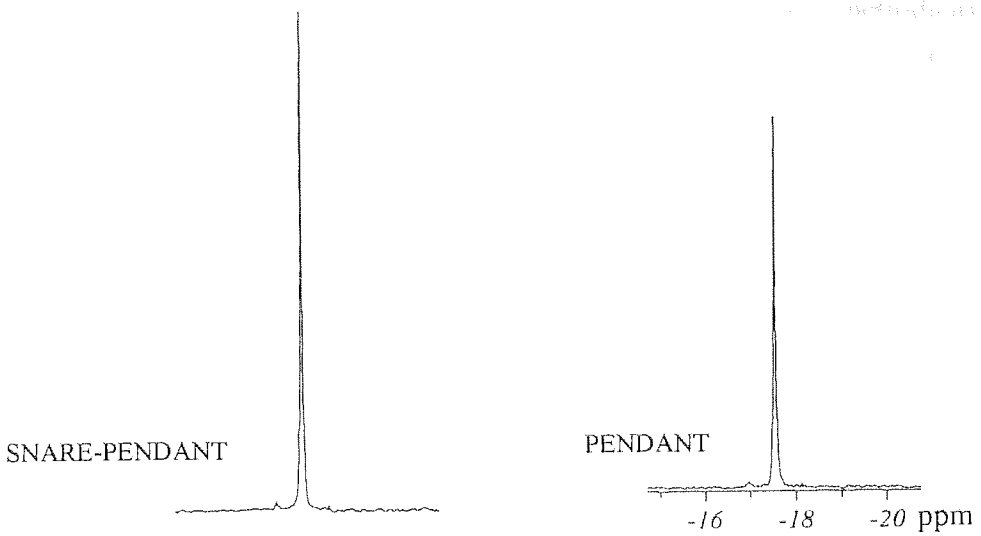

Figure 4.1 SNARE-PENDANT vs PENDANT for ^{29}Si-^{1}H

4.3.3 Conclusions.

It has been proved, by means of an illustrative experiment, that the use of nuclei, which have $\gamma < 0$, i.e., in the case of ^{29}Si, is possible for the sensitive nucleus accelerated relaxation for enhancement (SNARE) of the S/N of the insensitive nucleus during a given experimental time. This was facilitated by a trivial modification to the SNARE pulse sequence, i.e., the simple phase inversion of the first $\pi/2$ S pulse ($\pi/2_{-x}$). However, careful optimisation of the evolution delays to ensure optimum polarisation transfer and subsequent refocusing was required. When one is faced with more than one coupling and multiplicity with a potential range in J-values, the routine implementation of SNARE would become difficult when one has no knowledge of the J-values present in the molecule.

The efficiency of SNARE depends upon the transfer function given in expression 4.9 (for SI only (^{13}CH)), i.e., the ability of the pulse sequence to accommodate a range of short-range J-values, and the magnitude of the empirical nOe. The latter is dependent on the length of τ_{ac} and more importantly the efficiency of 'leakage' relaxation mechanisms. The viability of the use of ^{29}Si and ^{15}N for SNARE are discussed below with respect to both aspects.

4.3.4 The viability of using ^{29}Si for SNARE

^{29}Si shares similar bonding attributes to ^{13}C as they share the same periodicity. However, ^{29}Si will in general be involved in less direct bonding with protons in favour of direct bonding with carbon and other heteroatoms. It is common to find R-Si-H and R-Si-R environments, where R can be an aliphatic group i.e., $(CH_3)_3C$- for carbosilanes or oxygen in the case of siloxanes or N in the case of silazanes etc.

Therefore, ^{29}Si will in most cases be primarily involved in long-range scalar coupling with protons although not exclusively and their longitudinal relaxation will be mostly dominated by dipolar relaxation with protons over more than one chemical bond. As such, the potential for leakage relaxation is high, and as eluded to above, the complete or near cancellation of ^{29}Si due to the negative nOe often occurs [48]. Therefore, in most circumstances, the use of ^{29}Si will be of little use for the relaxation enhancement of scalar coupled protons, apart from in those circumstances when the experimenter can be reasonably confident that leakage relaxation is minimal.

4.3.5 The transfer function: Dependence upon the variation of J for Si-H

Unfortunately, scalar coupling constants for short-range coupling of ^{29}Si vary over a much wider range than that of analogous ^{13}C chemical environments, typically, 140-420Hz [50]. Therefore, in molecules containing an array of structurally unique ^{29}Si-H environments, it is unlikely that the polarisation transfer efficiency would be good enough for SNARE. Optimisation of τ_1 and τ_2 would simply not be possible to encompass the likely range of J-values encountered. Instead, SNARE may have to be invoked 'selectively' for a particular proton in a given ^{29}Si-^{1}H environment, for which the experimenter knows the exact J-value. Alternatively, a 'semi-selective' approach maybe taken where, ^{29}Si-^{1}H couplings that exhibit similar J-values can be exploited by judicious choice of J for setting of τ_1 and τ_2.

Therefore, in compounds containing more than one chemically distinct ^{29}Si environment, SNARE will tend not to be amenable by means of 'routine' implementation, due to the variation in J-values and the high possibility of poor magnetisations M_z^S, which are close to zero. Instead, some prior knowledge of the J-values and relaxation dependencies of ^{29}Si will be required such that SNARE can be appropriately optimised, or employed selectively or semi-selectively.

4.3.6 The viability of using ^{15}N for SNARE

$^{15}N\{^1H\}$ nOes are often peculiar with respect to their large variations in magnitude in apparently similar chemical structure environments. This is more than likely, attributed to a combination of unique factors exclusive to the chemical nature of ^{15}N and its usual bonding environments. ^{15}N, unlike ^{13}C, and ^{29}Si, is more often found at the periphery of molecules increasing potential for more efficient sources of intermolecular dipolar relaxation, which forms the basis of the largest contribution to leakage relaxation with respect to attaining η_{max}.

The lone pair of electrons also serve as efficient sources of potential relaxation causing interactions with; paramagnetic species, protons involved in exchange or hydrogen bonding, or any other species involved in time dependent interactions. Therefore intermolecular dipolar relaxation and scalar coupling relaxation serve to further reduce the potential attainment of η_{max} [47]. Furthermore, when ^{15}N is involved in dative bonding to some arbitrary species, it becomes cationic, i.e., R_4N^+, which serves as another potential site for interaction and hence relaxation. It is thought that spin rotation relaxation often plays a significant role for the reduction of empirical ^{15}N nOes [24].

Seemingly, it is the apparent unpredictability of the empirically nOe that is the greatest barrier for the confident use of ^{15}N for SNARE. However, the sheer magnitude of η_{max} ascribes enough potential benefit to warrant the use of ^{15}N in SNARE. Since the natural isotopic abundance is so poor i.e., 0.37%, any potential increase in ^{15}N S/N via SNARE for a given experiment time is a significant advantage. In some systems the experimenter will intuitively know if the nOe is likely to approach η_{max} due to the knowledge of the system under scrutiny and its associated impact on leakage relaxation.

4.3.7 The transfer function: Dependence upon the variation of J for N-H

^{15}N-^1H short-range J-values in typical organic molecules range from 60-140Hz [50], which is approximate to the total range over which ^{13}C-^1H short-range scalar couplings vary, i.e., approximately 80Hz. Consequently, the optimisation of τ_1 and τ_2 takes much the same strategy as that employed for SNARE in $^{13}C\{^1H\}$ systems and therefore, reasonable inverse polarisation transfer efficiencies can be achieved. Furthermore, benefits of using SNARE can also be achieved when used in a selective or semi-selective way as described previously.

4.3.8 The applicability of reverse INEPT and reverse DEPT as pulse sequences for SNARE

In the original publication it was noted that a reverse INEPT pulse sequence could be used to invoke the necessary reverse polarisation transfer. A point unmade in this treatment, was the applicability of reverse DEPT [51] to achieve the same aims. The employment of SNARE over that of reverse INEPT in the original publication, was validated when the experimental method to which SNARE is appended, necessitates the detection of isolated insensitive nuclei i.e., quaternary nuclei. In this circumstance, the use of SNARE (which is based on PENDANT) is ideal, as it leaves essentially unaffected the +Z magnetisation of the quaternary nuclei that build-up during the acquisition time.

When the detection of quaternary nuclei is unimportant, the use of reverse INEPT or reverse DEPT pulse sequences are viable options. A reverse INEPT pulse sequence can be modified by the incorporation of a ($\pi/2$) I pulse (with an appropriate phase) to convert the in-phase I coherence at the end of the final evolution period to +Z magnetisation (M_{zS}^{I}). The transfer functions for reverse INEPT, which are identical to that given earlier for SNARE, would be subject to the same dependencies on the compromise values of $<J>$ and τ_1 and τ_2.

If reverse DEPT were implemented with nutation angles of the final S pulse set to $\pi/4$, all I_nS multiplicities appear in-phase after refocusing and thus can be readily converted to +Z ($+M_{zS}^{I}$) by inclusion of a suitably phased ($\pi/2$) pulse applied to I. Therefore, reverse DEPT in theory should invoke comparable accelerated relaxations of the I nuclei when utilised with a $\pi/4$ pulse applied to S.

Reverse DEPT may also be used in a 'selective' sense due to its pulse angle dependence. Setting the final S pulse to $\pi/2$ suppresses all other multiplicities except IS (except due to J-cross-talk[3]) and so maximising accelerated relaxation of protons with IS multiplicity. Reverse DEPT, unlike PENDANT and reverse INEPT, is 'absolutely selective' since PENDANT and reverse INEPT can only ever be semi-selective: when the evolution delays are optimised for a particular multiplicity, e.g., IS, the other S nuclei with greater scalar coupling multiplicities (I_2S and I_3S) also receive partial relaxation enhancement, as it is impossible to discriminate entirely by means of J-values.

Reverse DEPT can be implemented with the flip angle of the final S pulse set to $\pi/1.33$. This is inappropriate since it causes the spectral editing of the groups IS and I_3S anti-phase to that of I_2S. The final ($\pi/2$) I pulse would necessitate that one of the two combinations will attain the condition $-M_{zS}^{I}$. This would severely reduce the recovery of I toward thermal equilibrium for that particular multiplicity when used in combination with D_r.

4.3.9 General theoretical improvements to SNARE: Further Work

The following theories for the general improvements to SNARE are implicit to an arbitrary system I and S regardless of the signs of γ. If time had permitted each of the proposals would have been investigated and are therefore considered as possibilities for further work.

4.3.10 Compensation of off-resonance effects and *r.f.* inhomogeneity

The empirical value of M_{zS}^{I} is in part dependent upon the efficiency of reverse transfer, which is depicted by the transfer function and hence the range of J-values encountered. However additional factors namely, *r.f.*inhomogeneity, pulse mis-calibration and off-resonance effects may diminish the efficiency of reverse transfer and hence the maximum attainable value M_{zS}^{I}.

In particular off-resonance effects (Appendix A1.8.3) can be a major source of pulse nutation angle and phase errors, the combined effect of which could cause a loss of in-phase I coherence from which M_{zS}^{I} is derived. Therefore, it is recommended, that SNARE (and indeed any other pulse sequence used for inverse polarisation transfer) should be compensated for these effects by the substitution of appropriate composite pulses for the normal I and S pulses [22] (Appendix A9). Preferably, the composite pulses employed should simultaneously compensate for off-resonance and *r.f.* inhomogeneity effects. However, as always, care should be taken with their selection, as some composite pulses invoke inappropriate Z-phase shifts, which may subsequently detriment inverse polarisation transfer (Appendix A9).

4.3.11 Broadband SNARE

The efficiency of SNARE is largely dependent upon the optimisation of the evolution delays in the chosen pulse sequence, with respect to the scalar coupling multiplicities present, and the range of J-values encountered. As the evolution delays cannot be chosen to simultaneously invoke optimum reverse polarisation transfer and refocusing for all

multiplicities, inevitably, the efficiency of SNARE differs between protons. It has been shown that SNARE can be performed semi-selectively: the evolution delays comprising SNARE can be set to induce maximum efficiency for a selected multiplicity(s). Meanwhile, the evolution delays of the pulse sequence to which it is appended can be set to favour the enhancement of the S/N of the other multiplicities. Consequently, a more even enhancement of the S/N of all multiplicities is achieved in a given experimental time.

In order to invoke SNARE in the semi-selective way detailed above, effort on behalf of the experimenter is required to fashion the length of the delays inherent to both pulse sequences. In this case the general applicability of using SNARE as a routine method is lost, since the user incurs a time penalty when optimising the delays, which may not be a trivial exercise.
It would be particularly desirable to be able to invoke SNARE so that more even enhancement of protons of all short-range coupling multiplicities was achieved without the need to customise the component evolution delays of each pulse sequence.

The problem of optimising the evolution of scalar couplings over a given J range is common to all polarisation transfer experiments, whether it be for the purpose of maximising polarisation transfer or refocusing. For example, to attain optimal inverse polarisation transfer, the anti-phase coupling condition represented by e.g., $2I_xS_z$ in the product operator formalism is desired. This corresponds to an evolution of the coupling through an angle $\theta = \pi/2$ radians about the internal scalar coupling Hamiltonian ($\pi J I_z S_z \tau$), which is contingent to an evolution delay of $1/2J$, where J is the actual coupling constant. Achieving this optimal condition for a range of J-values for different multiplicities is not possible using fixed evolution delays.

To this, end composite pulses have been successfully integrated into a refocused INEPT experiment: in the same way that composite pulses compensate for a range in θ in terms of nutation angle discrepancies, these composite pulses, invoke composite rotations [22], which compensate for a range of θ, which has been caused by a range of J. This experiment is referred to as the "Broadband INEPT experiment" [46] because the bandwidth or range of scalar couplings is extended beyond that amenable in normal refocused INEPT.

The bandwidth over which the compensatory properties of composite pulses are effective, i.e., in this case the maximum range of J-values, is determined by its composition by exact

analogy with composite pulses compensating for *r.f.* inhomogeneity (Appendix A9).
It would be a trivial matter to substitute the composite pulses into SNARE or simply to implement broadband INEPT in the reverse mode.

It was found that the broadband INEPT experiment provides significant compensation over a range in J of 120Hz –200Hz for the optimisation of the anti-phase condition, e.g., $2S_xI_z$ for inverse polarisation transfer. It was shown that using an evolution delay optimised for SI_2, coupling i.e., 1/4J, and assuming all the J-values to be constant, that the increase in unit intensity as compared to that of standard INEPT for the couplings IS, I_2S and I_3S was 7%, 5% and 33% respectively. The broadband INEPT pulse sequence is three times longer than a normal refocused reverse INEPT experiment and consequently did not work well for the refocusing of proton coherence due to the interference of proton homonuclear couplings.
Therefore in principle, the implementation of a modified inverse broadband INEPT or *Broadband SNARE* pulse sequence may significantly benefit the magnitude of reverse polarisation transfer of M_z^S to M_z^I and more evenly distribute the effect of proton accelerated relaxation for nuclei of all short-range scalar coupling multiplicities and J-values.

Chapter 5 Thesis Conclusions

Until now the presence and effect of *residual* single quantum coherences originating from the insensitive nuclei, e.g., ^{13}C, which are inherent to the detection of isolated (quaternary) nuclei by PENDANT have been neglected [6, 8]. Residual coherences, as they have been named in this thesis, refer to those single quantum coherences that originate from insensitive nuclei, e.g., ^{13}C that exhibit short-range scalar coupling with protons.

It has been shown in investigative work detailed in chapter 1, that the polarisation exchange pulses in PENDANT are responsible for the effective purging of a large proportion of the residual coherences prior to acquisition. In PENDANT spectra of ^{13}C nuclei, the superposition of the remaining residual coherences with those that originate from polarisation transfer from protons, is reasonably inconsequential. The superposition of residual coherences is additive, and benefits the development of signal-to-noise ratio by approximately 4 % over that which would be theoretically obtained in refocused INEPT under identical experimental conditions. This was demonstrated for ^{13}C nuclei, in ethyl-5-(chloromethyl)-2-furan-carboxylate, which exhibit a typical range of short-range J-values and multiplicities encountered in commonly studied organic ^{13}C-^{1}H spin systems. The investigative work was based upon the use of PENDANT in the way recommended by the original authors, Homer and Perry, [6, 8] for routine use, i.e., for $\langle J \rangle$ = 145Hz with τ_1 and τ_2 set to 1/2J and 5/4J respectively.

It has also been shown theoretically that pulses A and B, situated after the polarisation exchange pulses in a modified PENDANT experiment by Homer and Perry [8], do not effect the removal of phase anomaly-causing coherences. However, by analogy with DEPT$^+$, the exclusive effect of the y-phase π pulse situated just prior to acquisition, i.e., pulse C, in the original publication, effects the removal of phase-anomaly coherence on every second transient.

It has been demonstrated by experiments in chapter 1 that, contrary to the publication by Homer and Perry [8], specification of an x-phase proton purge pulse, in what is now known as PENDANT$^+$, is critical for the purging of phase and multiplet anomaly-causing coherences. The specification of a x-phase pulse in PENDANT$^+$ is due to the unique symmetric structure of the PENDANT pulse sequence and its phase cycling, which enables

the simultaneous detection of quaternary nuclei. This feature of the PENDANT experiment necessitates the excitation of heteronucelar triple quantum coherence that originates from residual S coherences, by the polarisation exchange pulses. Consequently, the phase of these coherences necessitates the use of a x-phase purge pulse to prevent their subsequent re-conversion to multiplet anomaly-causing coherence prior to acquisition.

The more detailed characterisation of the PENDANT experiment, which has been facilitated by this investigative work, has enabled its successful use in the development of novel pulse sequences, which are the subject of chapters 2 and 3.

The investigative work detailed in chapter 2 demonstrates the utility of the novel pulse sequence, selective PENDANT. Selective PENDANT successfully identifies all ^{13}C quaternary nuclei in the sample, while simultaneously identifying ^{13}C long-range scalar coupling correlations to the selected proton by means of polarisation exchange.

The utility of selective PENDANT is realised when compared to the utility of the analogous pulse sequence experiment, selective INEPT or INAPT [16]. INAPT can only identify ^{13}C quaternaries that exhibit long-range scalar coupling to the selected proton. Consequently, INAPT is incapable of identifying truly isolated nuclei, i.e., those that do not exhibit resolvable long-range scalar couplings. Furthermore, when molecules exhibit regions of proton spectral overcrowding selective perturbation is prevented. This leads to the inability of both selective PENDANT and INAPT in the identification of long-range scalar coupling correlations of insensitive nuclei to protons in those regions. Consequently, INAPT may fail to identifying all quaternary nuclei if some exist in the molecule that are only exclusively scalar coupled to those protons in the crowded spectral regions. Therefore a separate experiment must be performed that facilitates the detection of all other ^{13}C quaternary nuclei, e.g., PENDANT, DEPTQ, SEMUTGL^{+}(q) etc. Consequently, the performance of two separate experiments for the complete characterisation of the quaternary spin system represents a significant increase in experimental time and inconvenience on behalf of experimenter.

In contrast to INAPT, selective PENDANT necessitates the detection of all quaternary nuclei in addition to identifying their scalar coupling correlations. Consequently, selective PENDANT can at least identify all quaternary nuclei of the sample, which may prove useful

in these circumstances.

In order to suppress residual coherences inherent to selective PENDANT a low-pass J-filter was incorporated into the selective PENDANT pulse sequence. This enabled the total suppression of ^{13}C residual coherences of CH and CH_3 multiplicities and efficient suppression of CH_2 multiplicities for a typical range of J-values. However, it was proved that further work is necessary to combat the small amounts of breakthrough of the latter, which seemingly are a result of off-resonance effects.

Therefore, for selective PENDANT, the attainment of an additional off-resonance experiment for the accurate assignment of long-range scalar coupling correlations is usually necessary. Simple comparison to an off-resonance spectrum (i.e., when no protons have been selectively perturbed) yields a quaternary-only spectrum with identical levels of breakthrough of any residual signals. Comparison to the on-resonance (correlation spectra) spectra facilitates a rapid assignment of genuine correlation signals, which is aided by multiplet characteristics of the residual signals that are inherent to their suppression. Such a comparison is of very little consequence when compared to the potential added inconvenience and investment of time involved in identifying all quaternary nuclei, when using INAPT. The presence of small magnitudes of breakthrough signals merely constitutes a slight cosmetic degradation of the spectrum but does not impinge upon the utility of the selective PENDANT experiment.

The unique structure and positioning of the low-pass J-filter affords it a novel dual function, namely, to cause suppression of residual ^{13}C coherences, for which it is designed, and to cause polarisation exchange. At the time of writing, no examples have been found where J-filters have been incorporated into pulse sequences to perform a dual function.

Investigative work has demonstrated that both INAPT and selective PENDANT spectra are subject to breakthrough of residual ^{13}C signals when the corresponding ^{13}C satellites in the proton spectrum are accidentally perturbed by the selective pulses. This phenomenon has been previously identified in INAPT spectra by Bax [16] although a suitable explanation for the occurrence was not given. A plausible explanation for the occurrence of these residual signals in both INAPT and selective PENDANT has been reported here. However, in comparison to INAPT, it was determined that the selective PENDANT experiment exhibits a greater sensitivity toward the breakthrough of residual ^{13}C signals that arise due to

unintentional perturbation of the corresponding ^{13}C proton satellites. It has been proven that the increased sensitivity is due to the use of hard proton pulses in the low-pass J-filter element. Replacement of the selective proton pulses in INAPT with hard proton pulses revealed similar magnitudes of breakthrough.

In addition to the breakthrough of residual ^{13}C signals described above, a further residual ^{13}C signal was observed in the same spectrum for both INAPT and selective PENDANT. At the time of writing this phenomenon remains unexplained. Further investigation into this observation is required.

Therefore, when proton (inverse) detected methods are not amenable to the experimenter and the proton spectrum of the molecule under scrutiny is devoid of spectral overcrowding, it has been demonstrated that the selective PENDANT experiment could be used for the routine characterisation of the entire ^{13}C quaternary spin system. In common with INAPT, selective PENDANT also identifies all long-range ^{13}C-^{1}H correlations other than those of quaternary nuclei in the same experiment.

It has been demonstrated by investigative work detailed in chapter 3 that a 1-D HOESY experiment has been successfully combined with a selective PENDANT experiment to give the new pulse sequence selective PENDANT-1-D HOESY. Therefore, significant experimental time-savings are realised when one wishes to perform both sets of experiments for investigative work. Furthermore, the combination of the two experiments reduces added experimental inconvenience associated with setting up and running of two separate experiments.

Using selective PENDANT-1-D HOESY one should be able to obtain long-range ^{13}C scalar coupling correlations while simultaneously obtaining useful qualitative ^{13}C transient nOe data. The latter is particularly useful for the confirmation of molecular structure and the determination of structural conformation. Unfortunately the fully automated pulse program did not function as intended such that at the time of writing, the proof of the function of the experiment was undertaken using modifications of the original experiment that appropriately simulate its entire effect. It is unknown why the fully automated pulse sequence does not function, because the pulse programming has been confirmed to be correct.

It has been shown that the repositioning of the low-pass J-filter to the beginning of the selective PENDANT-1-D HOESY pulse sequence does not adversely affect the efficiency of suppression of residual ^{13}C coherences, which are implicit to the detection of quaternary nuclei. The poorer level of suppression of the ^{13}C signals of the CH_2 multiplicities, by analogy with normal selective PENDANT, is largely dependent on off-resonance effects associated with the ^{13}C pulses.

The relative increase in sensitivity to breakthrough of the ^{13}C signals of the CH_2 multiplicities, as compared to normal selective PENDANT, is no doubt attributed to the increase in the number of ^{13}C refocusing pulses and the inherent length of the pulse sequence. Both were necessitated by the restructuring of the low-pass J-filter and its repositioning to the beginning of the pulse sequence.

The principles inherent to selective PENDANT combined with 1-D HOESY are also valid for INAPT. In fact, when the identification of all ^{13}C quaternary nuclei is unimportant, the combination of 1-D HOESY with INAPT, would prove more useful. This is because there is no need to collect an additional off-resonance experiment, which reduces experiment time in comparison to selective PENDANT-1-D HOESY.

Finally an investigative experiment detailed in Chapter 4 proves that in fact nuclei of $\gamma < 0$ can in fact be used for the accelerated longitudinal relaxation of protons using SNARE. In the original publication [45] it was mentioned that this would not be the case. Theoretical proposals for the development of SNARE have been given. In particular it has been suggested that a *Broadband SNARE* pulse sequence can be used to reduce the sensitivity of inverse polarisation transfer to a range of J-values upon which accelerated relaxation depends.

References

[1] S. Braun, H. O. Kalinowski, S. Berger, "100 NMR and More Basic NMR Experiments. A practical Course", VCH, Weinheim, 1996

[2] H. Bildsoe, S, Donstrup and H.J. Jakobsen, "Subspectral Editing Using a Multiple Quantum Trap: Analysis of *J* Cross-Talk.", J. Magn. Reson., **53**, 154-162, 1983.

[3] O.W. Sorensen and S Donstrup, H Bildsoe and H.J. Jacobsen, "Suppression of *J* Cross-Talk in Subspectral Editing. The SEMUT GL Pulse Sequence.", J. Magn. Reson., **55**, 347-354, 1983.

[4] Richard R. Ernst, Geoffrey Bodenhausen and Alexander Wokaun, "Principles of Nuclear Magnetic Resonance in One and Two Dimensions", Clarendon Press, Oxford, 1994.

[5] D. M. Doddrell, D. T. Pegg and M. R. Bendall, "Distortionless Enhancement of NMR Signals by Polarisation Transfer", J. Magn. Reson., **48**, 323-327, 1982.

[6] John Homer and Michael C. Perry, "New Method for NMR Signal Enhancement by Polarisation Transfer and Attached Nucleus Testing", J. Chem. Soc., Chem. Commun., 373-374, 1994.

[7] R. Burger and P. Bigler, "DEPTQ: Distortionless Enhancement by Polarisation Transfer Including the Detection of Quarternary Nuclei", J. Magn. Reson., **135**, 529-534, 1998.

[8] John Homer and Michael C. Perry, "Enhancement of the NMR Spectra of Insensitive nuclei using PENDANT with Long-range Coupling Constants", J. Chem. Soc. Perkin Trans., **2**, 533-536, 1995.

[9] Stuart A Palfreyman, "Sonically Induced Narrowing of the NMR lines of Solids and other novel NMR techniques", Ph.D Thesis, Aston University, 1996.

[10] Gary E. Martin and Andrew S. Zexter, "Two-Dimensional NMR Methods for Establishing Molecular Connectivity. A Chemist's Guide to Experiment Selection, Performance, and Interpretation", VCH, New York, 1988.

[11] Horst Kessler, Matthias Gehrke and Christian Griesinger, "Two-Dimensional NMR spectroscopy: Background and Overview of the Experiments", Angew. Chem. Int. Ed. Engl., **27**, 490-536, 1988.

[12] O.W. Sorensen, G.W. Eich, M.H. Levitt, G. Bodenhausen and R. R. Ernst, "Product operator Formalism for the Description of NMR Pulse Experiments", Prog. NMR. Spectr., **16**, 163-192, 1983.

[13] O.W. Sorensen and R.R. Ernst, "Elimination of Spectral Distortion in Polarisation Transfer Experiments. Improvements and Comparison of Techniques.", J. Magn. Reson., **51**, 477-489, 1983.

[14] U.B. Sorensen, H. Bildsoe and H.J. Jakobsen, "Purging Sandwiches and Purging Pulses in Polarisation Transfer Experiments. The equivalence of DEPT and Refocused INEPT with a Purging Sandwich.", J. Magn. Reson., **58**, 517-525, 1984.

[15] H. Kessler, C. Griesinger, J. Zarbock and H. R. Loosli, "Assignment of Carbonyl Carbons and Sequence Analysis in Peptides by Heteronuclear Shift Correlation via Small Coupling Constants with Broadband Decoupling in t_1 (COLOC)", J. Magn. Reson., **57**, 331-336, 1982.

[16] Ad Bax, "Structure Determination and Spectral Assignment by Pulsed Polarization Transfer via Long-Range ^{1}H-^{13}C Couplings", J. Magn. Reson., **57**, 314-318, 1984.

[17] Geoffrey A. Cordell and A. Douglas Kinghorn, "One-Dimensional Proton-Carbon Correlations for the Structure Determination of Natural Products", Tetrahedron, **47**, No 22, 3521-3534, 1991.

[18] G. A. Nagana Gowda, "One-dimensional pulse techniques for detection of quarternary carbons", Magn. Reson. Chem., **39**, 581-585, 2001.

[19] H. Bildsoe, S, Donstrup and H.J. Jakobsen and O.W. Sorensen, "Editing of Proton-Coupled ^{13}C NMR Spectra", J. Magn. Reson., **65**, 222-238, 1985.

[20] Ad Bax and Susanta K. Sarka, "Elimination of Refocusing Pulses in NMR Experiments", J. Magn. Reson., **60**, 170-176, 1984.

[21] K.V. Schenker and W. Von Philipsborn, "Off-Resonance Effects and Their Compensation in Multiple-Pulse Sequences INEPT, DEPT, and INADEQUATE", J. Magn. Reson., **66**, 219-229, 1986.

[22] M. H. Levitt, "Composite Pulses", Progress in NMR Spectroscopy, **18**, 61-122, 1986.

[23] Timothy. D. W Claridge, "High-resolution NMR Techniques in Organic Chemistry", Pergamon, Oxford, 1999.

[24] David Neuhaus and Michael Williamson, "The Nuclear Overhauser Effect in Structural and Conformational Analysis", VCH, New York, Cambridge and Weinheim, 1989.

[25] G.A.Morris and R. Freeman, "Selective Excitation in Fourier Transform Nuclear Magentic Resonance.", J. Magn. Reson., **29**, 433-462, 1978.

[26] R. Tycko, H.M. Cho, E. Schneider, and A. Pines, "Composite Pulses without Phase Distortion.", J. Magn. Reson., **61**, 90-101, 1985.

[27] T. J. Norwood, "Multiple-Quantum NMR Methods", Prog. NMR. Spectr., **24**, 4, 295-375, 1992.

[28] Noggle, J.H. and Schirmer, R. E. "Nuclear Overhauser Effect" Academic Press, London, 1971.

[29] S. Macura and R. R. Ernst, "Elucidation of cross relaxation in liquids by two-dimensional N.M.R. spectroscopy", Mol. Phys., **41**, No 1, 95-117, 1980.

[30] Chin Yu and George C. Levy, "Two-Dimensional Heteronuclear (HOESY) Experiments: Investigation of Dipolar Interactions between Heteronuclei and Nearby Protons", J. Am. Chem. Soc., **106**, 6533-6537, 1984.

[31] Peter L. Rinaldi, "Heteronuclear 2D-NOE Spectroscopy", J. Am. Chem. Soc., **105**, 5167-5168, 1983.

[32] Katalin E. Kover and Gyula Batta, "Theoretical and Practical Aspects of One- and Two-Dimensional Heteronuclear Overhauser Experiments and Selective ^{13}C T_1-Determination of Heteronuclear Distances", Prog. NMR. Spectr., **19**, 223-266, 1987.

[33] N. Mahieu, P. Tekely, and D Canet, "Heteronuclear Overhauser Effect Measurements in Surfactant Systems. 3. Average Location of Water with Respect to Surfactant Polar Head in Micellized Sodium Octonoate and Sodium Dodecanoate", J. Phys. Chem., **97**, 2764-2766, 1993.

[34] P. Palmas, P. Tekely, P. Mutzenhardt, and D. Canet, "Heteronuclear Overahauser effect measurements in surfactant systems. IV. Direct and remote correlations with alkyl chains", J. Chem. Phys., **99**, 4775-4785, 1993.

[35] A. Belmajdoub, N. Mahieu, P. Tekely, and D Canet, "Heteronuclear Overhauser Effect Measurements in Surfactant Systems. 2. Evidence of Solvent Penetration into Micelles in an Nonaqueous medium", J. Phys. Chem., **96**, 3, 1992.

[36] W. Bauer, "Pulse Field Gradient 'inverse' HOESY applied to the isotope pairs H-1 , P-31 and H-1, Li-7", Magn. Reson. Chem., **34**, 7, 532-537, 1996.

[37] Peter Bigler and Chrisitan Muller, "Superior Pulse Sequence for Two-Dimensional Heteronuclear Overhauser Spectroscopy", J. Magn. Reson., **79**, 45-53, 1988.

[38] Katalin E. Kover and Gyula Batta, "The Role of Mixing Time in 2D Heteronuclear NOE Experiments", J. Magn. Reson., **69**, 344-349, 1986.

[39] Katalin E. Kover, Gyula Batta and Zoltan Madi, "Quantitative 2D Heteronuclear NOE Spectroscopy Application to a Rigid Molecule", J. Magn. Reson., **69**, 538-541, 1986.

[40] Katalin E. Kover and Gyula Batta, "Detection of Indirect, Negative Effects in Heteronuclear 2D NOE Spectroscopy with Pure Absorption Phase", J. Magn. Reson., **69**, 519-522, 1986.

[41] Linda M. Sweeting, "The Recovery-Preparation time in Pulsed FT NMR experiments", J. Magn. Reson., **48**, 311-313, 1982.

[42] Niels H. Andersen, Khe T. Nguyen, Cynthia J. Hartzell, "Rapid Acquisition of NOE Difference Spectra. The Relative Merits of Transient versus Driven Experimental Protocols", J. Magn. Reson., **74**, 195-211, 1987.

[43] Ray Freeman, "A Handbook of Nuclear Magnetic Resonance, 2nd Edition", Longman, Singapore, 1997.

[44] Timothy A. Flood, "1D Analogues of Homonuclear 2D NMR By DANTE-Selective Pulses", Concepts of Magnetic Resonance ., **8-2**, 119-138, 1996.

[45] John Homer, Michael C. Perry and Stuart A. Palfreyman, "Accelerated Relaxation of Sensitive Nuclei for Enhancement of Signal-to-Noise with Time", J. Magn. Reson., **125**, 20-27, 1997.

[46] S. Wimperis and G. Bodenhausen, "Heteronuclear Coherence Transfer over a Range of Coupling Constants. A Broadband-INEPT Experiment.", J. Magn. Reson., **69**, 264-282, 1986.

[47] Gerard J. Martin, Maryvonne L. Martin, Jean-Paul Gousenard, "NMR, ^{15}N-NMR Spectroscopy", Springer-Verlag, Berlin, **18**, 1981.

[48] H. Masmann, "NMR, Basic Principles and Progress, ^{29}Si-NMR spectroscopic Results", Springer-Verlag, Berlin, **17**, 1981.

[49] J. W. Akitt, "NMR and Chemistry. An Introduction to Modern NMR Spectroscopy, Third Edition", Chapman and Hall, London, 1992.

[50] C. Brevard and P. Granger, "Handbook of High Resolution Multi nuclear NMR", Wiley-Interscience, USA, 1981.

[51] M. Robin Bendall, David T. Pegg, David M. Doddrell, and James Field, "Inverse DEPT sequence. Polarisation Transfer from Spin-½ Nucleus to n-Spin-½ Heteronuclei via Correlated Motion in the Doubly Rotating Reference Frame", J. Magn. Reson., **51**, 520-526, 1983.

[52] Malcolm H. Levitt, "Spin Dynamics. Basics of Nuclear Magnetic Resonance", Wiley, Chichester, England, 2001.

[53] C. P. Slichter, "Principles of Magnetic Resonance. Third Edition", Springer-Verlag, USA, 1990.

[54] A. Abragam, "The Principles of Nuclear Magnetism", Clarendon press, Oxford, 1961

[55] Alan G. Marshall and Francis R. Verdun, "Fourier Transforms in NMR, Optical and Mass Spectroscopy. A User's Handbook", Elsevier, Amsterdam, 1990.

[56] S. W. Homans, "A Dictionary of Concepts in NMR. Revised Edition", Clarendon Press, Oxford, 1992.

[57] P. J. Hore, "Nuclear Magnetic Resonance", Oxford Science Publications, New York, 1998.

[58] Robin K Harris, "Nuclear Magnetic Resonance Spectroscopy", Longman Scientific and Technical, England, 1986.

[59] N. Bloembergen, "Nuclear Magnetic Relaxation", W. A. Benjamin, inc., New York, 1961.

[60] Levy, Lichter, Nelson, "Carbon-13 Nuclear Magnetic Resonance Spectroscopy", Second Edition, Wiley-Interscience, Canada, 1980.

[61] I. Solomon, "Relaxation Processes in a System of Two Spins", Phys Rev., **99**, 2, 559-565, 1959.

[62] Larry Werbelow, "Frequency Dependence of Relaxation Rates and Nuclear Overhauser Effects. Coupled Nuclei with Gyromagnetic Ratios of Opposite Sign", J. Magn. Reson., **47**, 331-338, 1982.

[63] Larry G. Werbelow, "Nuclear Magnetic Relaxation for Coupled Spins of Oppositely Signed Magnetic Moments", J Chem. Soc., Faraday Trans. 2, 1987, **83**, 897-904.

[64] H. Kessler, H. Oschkinat and C. Griesinger and W. Bermel, "Transformation of Homonuclear Two-Dimensional Techniques Using Gaussian Pulses", J. Magn. Reson., **70**, 106-133, 1986.

[65] Jan Friedrich, Simon Davies and Ray Freeman, "Shaped Selective Pulses for Coherence-Transfer Experiments", J. Magn. Reson., **75**, 390-395, 1987.

[66] C. Bauer, R.Freeman, T. Frenkiel, J. Keeler, and J. Shaka, "Gaussian Pulses" , J. Magn. Reson., **58**, 442-457, 1984.

[67] Daniel Canet, "Radiofrequency field gradient experiments", Prog. NMR. Spectr., **30**, 101-135, 1997.

[68] Teodor Parella, "Pulsed field gradients: a new tool for routine NMR", Magn. Reson. Chem., **36**, 467-495, 1998.

Bibliography

O.W. Sorensen, M.H.Levitt and R.R. Ernst, "Uniform Excitation of Multiple-Quantum Coherence: Application to Multiple Quantum Filtering.", J. Magn. Reson., **55**, 104-113, 1983.

S. Wimperis and G. Bodenhausen, "Criteria for the Accuracy of Composite Pulses in Multiple-Quantum NMR.", J. Magn. Reson., **71**, 355-359, 1987.

V. Rutar and T.C. Wong, "Effects of Long-Range and Homonuclear Couplings on Bilinear Rotation Pulses.", J. Magn. Reson., **71**, 75-82, 1987.

Ping. Xu, Xi-Li Wu, and R. Freeman, "User-Friendly Selective Pulses." , J. Magn. Reson., **99**, 308-322, 1992.

Helen Green and Ray Freeman, "Band-Selective Radiofrequency Pulses", J. Magn. Reson., **93**, 93-141, 1991.

Xi-Li Wu, Ping Xu and Ray Freeman, "A New Kind of Selective Excitation Sequence", J. Magn. Reson., **83**, 404-410, 1989.

David G. Donne and David G. Gorenstein, "Pictorial Representation of Product Operator Formalism: Non-Classical Vector Diagrams for Multidimensional NMR", Biophysical Society Online NMR textbook.

Ad Bax, Ray Freeman, Stewart P. Kempsell, "Investigation of ^{13}C-^{13}C Long-Range Couplings in Natural-Abundance Samples", J. Magn. Reson., **41**, 349-353, 1980.

J. Brondeau, C. Millot and D. Canet, "Assignment of Carbon-13 Resonances from Homonuclear Polarisation Tranfer by Semiselective Excitation. Improved Elimination of Unwanted Signals", J. Magn. Reson., **57**, 319-323, 1984.

Martin Billeter, Werner Braun and Kurt Wuthrich, "Sequential Resonance Assignments in Protein ^{1}H Nuclear Magnetic Resonance Spectra", J. Mol. Biol., **155**, 321-346, 1982.

Gy Batta and K.E. Kover, "Easy Implementation of Homonuclear 1D Correlation NMR techniques. Applications to Oligosaccharides", Tetrahedron, 47, No 22, 3535-3544, 1991.

Dagmar Stresinkova and Norbert Muller, "Improved Heteronuclear Long-Range Coherence Transfer in the Presence of Homonuclear Coupling", J. Magn. Reson Ser A., **111**, 220-224, 1984.

V. Rutar and Tuck C. Wong, "Effects of Long-Range and Homonuclear Couplings on Bilinear Rotation Pulses", J. Magn. Reson., **71**, 75-82, 1987.

V. Blechta and J. Schraml, "Product Operator Formalism Applied to Large Spin Systems, with INEPT and DEPT Examples", J. Magn. Reson., **69**, 293-301, 1987.

Alex D. Bain, "Coherence Levels and Coherence Pathways in NMR. A simple Way to Design Phase Cycling Procedures", J. Magn. Reson., **56**, 418-427, 1984.

Geoffrey Bodenhausen, Herbert Kogler and R. R. Ernst, "Selection of Coherence-Transfer Pathways in NMR Pulse Experiments" J. Magn. Reson., **58**, 370-388, 1984.

C. Muller and P Bigler, "2D Heteronuclear NOE Spectroscopy. Theoretical Comparison of Improved Methods", J. Magn. Reson., **84**, 585-590, 1989.

Christopher Bauer, Ray Freeman and Stephen Wimperis, "Long-Range Carbon-Proton Coupling Constants", J. Magn. Reson., **58**, 526-532, 1984.

George H. Weiss, James A. Ferretti and R. Andrew Byrd, "Accuracy and Precision in the Estimation of Peak Areas and NOE Factors. II. The Effects of Apodization", J. Magn. Reson., **71**, 97-105, 1987.

Michael P. Williamson and David Neuhaus, "Symmetry in NOE Spectra", J. Magn. Reson., **72**, 369-375, 1987.

Jozef Kowalewski and Gareth Morris, "A rapid Method for Spin-Lattice Relaxation Time on Low Magnetogyric Ratio Nuclei: Inept Signal Enhancment", J. Magn. Reson., **47**, 331-338, 1982.

J. Mark Bulsing, William M. Brooks, James Field, and David M. Doddrell, "Polarisation Transfer via Intermediate Multiple-Quantum State of Maximum Order"
J. Magn. Reson., **56**, 167-173, 1984.

David T. Pegg, David M Doddrell, and M. Robin Bendall, "Correspondence between INEPT and DEPT Pulse Sequences for Coupled Spin-Half Nuclei", J. Magn. Reson., **51**, 264-269, 1983.

M. Robin Bendall, David T. Pegg, and David M Doddrell, "Polarisation Transfer Pulse Sequences for Two-Dimensional NMR by Heisenberg Vector Analysis",
J. Magn. Reson., **45**, 8-29, 1981.

Katalin E. Kover and Gyula Batta, "Sensitivity-Enhanced 2D Heteronuclear NOE Spectroscopy. Two-to Threefold Improved S/N Ratio at Quarternary Carbons in the MIEMI experiment", J. Magn. Reson., **79**, 206-210, 1988.

Katalin E. Kover and Gyula Batta, "Selective and Biselective ^{13}C Spin-Lattice Relaxation Experiments for the Determination of Carbon-Proton Distances. Misleading Indirect Effects", J. Magn. Reson., **73**, 512-515, 1987.

Andreas Dolle, "Orientational Dynamics of the Model Compound 1,2,3,4-Tetrahydro-5,6-dimethyl-1,4-methanonapthalene in Neat Liquid from Temperature-Dependent ^{13}C Nuclear Magnetic Relaxation Data: Spectral Densities and Correlation Functions", **106**, 48, 11683-11694, 2002.

Catherine Zwahlen, Pascale Legault, Sebastien J.F. Vincent, Jack Greenblatt, Robert Konrat and Lewis E. Kay, "Methods for Measurement of Intermolecular NOEs by Multinuclear NMR Spectroscopy: Application to a Bacteriophage λ N-Peptide/*boxB* RNA Complex", J. Am. Chem. Soc., 119, 6711-6721, 1997.

Reinhold Kaiser, "Intermolecular Nuclear Overhauser Effect in Liquid Solutions", J. Chem. Phys., 42, 1838-1839, 1965.

R. A. Bell and J. K. Saunders, "Correlation of the intramolecular nuclear Overhauser effect with internuclear distance", Canadian Journal of Chemistry, 48, 1114-1122, 1970.

Andreas Dolle, "Interpretation of ^{13}C Magnetic Relaxation Data for the Quarternary Carbon Atoms in Liquid 1,2,3,4-Tetrahydro-5,6-dimethyl-1,4-methanonapthalene", J. Magn. Reson Series A., **114**, 258-260, 1995.

Katherine Stott, James Keeler, Que N. Van, and A. J. Shaka, "One-Dimensional NOE Experiments Using Pulsed Field Gradients", J. Magn. Reson., **125**, 302-324, 1997.

Luzineide Wanderley Tinoco and Jose Daniel Figueroa-Villar, "Determination of Correlation Times from Selective and Non-Selective Spin Lattice Relaxation Rates and their Use in Drug-Drug and Drug-Albumin Interaction Studies", J. Braz. Chem.Soc., **10**, No 4, 281-286, 1999.

Michael P. Williamson and David Neuhaus, "Symmetry in NOE spectra", J. Magn. Reson., 72, 369-375, 1987.

Hugh L. Eaton and Niels H. Andersen, "Computer Simulation of Transient NOE Experiments with Short Preparatory Delays", J. Magn Reson., 74, 212-225, 1987.